AD_____

AWARD NUMBER: W81XWH-05-1-0211

TITLE: Combinations of Novel Histone Deacetylase and Bcr-Abl Inhibitors in the Therapy of Imatinib Mesylate-Sensitive and –Refractory Bcr-Abl Expressing Leukemia

PRINCIPAL INVESTIGATOR: Kapil Bhalla, M.D.

CONTRACTING ORGANIZATION: Medical College of Georgia Cancer Center
Augusta, GA 30904

REPORT DATE: December 2008

TYPE OF REPORT: Final

PREPARED FOR: U.S. Army Medical Research and Materiel Command
Fort Detrick, Maryland 21702-5012

REPORT DOCUMENTATION PAGE

Form Approved
OMB No. 0704-0188

1. REPORT DATE	2. REPORT TYPE	3. DATES COVERED
1 December 2008	Final	1 Mar 2005 – 28 Nov 2008

4. TITLE AND SUBTITLE

Combinations of Novel Histone Deacetylase and Bcr-Abl Inhibitors in the Therapy of Imatinib Mesylate-Sensitive and –Refractory Bcr-Abl Expressing Leukemia

5a. CONTRACT NUMBER

5b. GRANT NUMBER
W81XWH-05-1-0211

5c. PROGRAM ELEMENT NUMBER

6. AUTHOR(S)

Kapil Bhalla, M.D.

E-Mail: kbhalla@mcg.edu

5d. PROJECT NUMBER

5e. TASK NUMBER

5f. WORK UNIT NUMBER

7. PERFORMING ORGANIZATION NAME(S) AND ADDRESS(ES)

Medical College of Georgia Cancer Center
Augusta, GA 30904

8. PERFORMING ORGANIZATION REPORT NUMBER

9. SPONSORING / MONITORING AGENCY NAME(S) AND ADDRESS(ES)
U.S. Army Medical Research and Materiel Command
Fort Detrick, Maryland 21702-5012

10. SPONSOR/MONITOR'S ACRONYM(S)

11. SPONSOR/MONITOR'S REPORT NUMBER(S)

12. DISTRIBUTION / AVAILABILITY STATEMENT
Approved for Public Release; Distribution Unlimited

13. SUPPLEMENTARY NOTES

14. ABSTRACT

Overall, our findings demonstrate that the novel Bcr-Abl kinase inhibitors nilotinib or the dual Bcr-Abl/Src kinase inhibitor dasatinib synergistically interact with pan-HDAC inhibitors vorinostat or panobinostat to deplete Bcr-Abl and inhibit its downstream signaling through STAT5 and AKT. This is associated with growth arrest and apoptosis of CML cells. Significantly, our findings also demonstrate that treatment with the pan-HDAC inhibitor vorinostat or panobinostat depletes the levels of unmutated and mutant forms of Bcr-Abl, as well as induces growth arrest and apoptosis of CML cells with unmutated and mutant forms of Bcr-Abl. Additionally, our findings indicate that combined treatment with vorinostat or panobinostat with nilotinib, dasatinib or MK-0457 exerts synergistic anti-Bcr-Abl activity against imatinib-sensitive and resistant CML cells. Collectively, these findings support the rationale to test the in vivo efficacy of the combination of vorinostat or panobinostat with nilotinib, dasatinib or MK-0457 against imatinib-sensitive and imatinib-resistant CML.

15. SUBJECT TERMS
Nilotinib, LHB589, Bcr-Abl, dasatinib, chronic myelogenous leukemia (CML)

16. SECURITY CLASSIFICATION OF:			17. LIMITATION OF ABSTRACT	18. NUMBER OF PAGES	19a. NAME OF RESPONSIBLE PERSON
a. REPORT	b. ABSTRACT	c. THIS PAGE			USAMRMC
U	U	U	UU	107	19b. TELEPHONE NUMBER *(include area code)*

Table of Contents

	Page
Introduction……..…..	**1**
Body……..	**2**
Key Research Accomplishments……..	**6**
Reportable Outcomes……	**6**
Conclusion……	**8**
References……	**8**
Appendices……	**(none)**

Introduction:

Although anti-Bcr-Abl tyrosine kinase (TK) inhibi tor, imatinib, is effective therapy in newly diagnosed patients with CML, resistance to imatinib commonly occur s in patie nts wit h accelerated and blastic phase of CML. AMN107 (n ilotinib) and dasatinib are more potent anti-Bcr-Abl TK inhibitor, which al so inhibits the commonly encount ered mutant forms of Bcr-Abl known to confer resistance against imatin ib. MK-0457 (VX-680) is a pan-Aurora kinase inhibitor, which has also been shown to inhibi t the activity of Bcr-Abl. Panobinostat (PS , LBH589) and vorinostat are potent pan-histone deace tylase (HDAC) inhibitor (HDI), which depletes the levels of Bcr-Abl, by inhibiti ng the heat shock prot ein 90 (hsp90) chaperone function toward Bcr-Abl. The overall purpose of the studies performed during the funded period of this project was to dete rmine the combined effects of PS or vorinostat and nilotinib, dasatinib or MK-0457 on unmutated and mutant forms of Bcr-Abl and its downstream signaling proteins. Additionally , these studies wer e des igned to determine the effect of this drug combination on cell growth and apoptosis of Bcr-Abl-containi ng cultured mouse and human leukemia cells and primary human CML cells.

Body:

Based on the rationale described above, we first determined the effect of co-treatment with panobinostat and nilotinib or dasatinib and vorinostat on imatinib-sensitive or refractory human CML cells with expression of unmutated or mutant forms of Bcr-Abl.

Combined effects of novel tyrosine kinase inhibitor AMN107 (Nilotinib) and histone deacetylase inhibitor LBH589 (Panobinostat) against Bcr-Abl-expressing human leukemia cells. Nilotinib (AMN107, Novartis Pharmaceuticals, Basel, Switzerland) has potent in vitro and in vivo activity against the unmutated and most common mutant forms of Bcr-Abl. Treatment with the histone deacetylase inhibitor LBH589 (Novartis) depletes Bcr-Abl levels. We determined the effects of AMN107 and/or LBH589 in Bcr-Abl-expressing human K562 and LAMA-84 cells, as well as in primary chronic myelogenous leukemia (CML) cells. AMN107 was more potent than imatinib mesylate (IM) in inhibiting Bcr-Abl tyrosine kinase (TK) activity and attenuating p-STAT5, p-AKT, Bcl-x(L), and c-Myc levels in K562 and LAMA-84 cells. Co-treatment with LBH589 and AMN107 exerted synergistic apoptotic effects with more attenuation of p-STAT5, p-ERK1/2, c-Myc, and Bcl-x(L) and increases in p27 and Bim levels. LBH589 attenuated Bcr-Abl levels and induced apoptosis of mouse pro-B BaF3 cells containing ectopic expression of Bcr-Abl or the IM-resistant, point-mutant Bcr-AblT315I and Bcr-AblE255K. Treatment with LBH589 also depleted Bcr-Abl levels and induced apoptosis of IM-resistant primary human CML cells, including those with expression of Bcr-AblT315I. As compared with either agent alone, cotreatment with AMN107 and LBH589 induced more loss of cell viability of primary IM-resistant CML cells. Thus, cotreatment with LBH589 and AMN107 is active against cultured or primary IM-resistant CML cells, including those with expression of Bcr-AblT315I.

Cotreatment with vorinostat (suberoylanilide hydroxamic acid) enhances activity of dasatinib (BMS-354825) against imatinib mesylate-sensitive or imatinib mesylate-resistant chronic myelogenous leukemia cells. We determined the effects of vorinostat [suberoylanilide hydroxamic acid (SAHA)] and/or dasatinib, a dual Abl/Src kinase (tyrosine kinase) inhibitor, on the cultured human (K562 and LAMA-84) or primary chronic myelogenous leukemia (CML) cells, as well as on the murine pro-B BaF3 cells with ectopic expression of the unmutated and kinase domain-mutant forms of Bcr-Abl. Following exposure to dasatinib and/or vorinostat, apoptosis, loss of clonogenic survival, as well as the activity and levels of Bcr-Abl and its downstream signaling proteins were determined. Treatment with dasatinib attenuated the levels of autophosphorylated Bcr-Abl, p-CrkL, phospho-signal transducer and activator of transcription 5 (p-STAT5), p-c-Src, and p-Lyn; inhibited the activity of Lyn and c-Src; and induced apoptosis of the cultured CML cells. Combined treatment of cultured human CML and BaF3 cells with vorinostat and dasatinib induced more apoptosis than either agent alone, as well as synergistically induced loss of clonogenic survival, which was associated with greater depletion of Bcr-Abl, p-CrkL, and p-STAT5 levels. Cotreatment with dasatinib and vorinostat also attenuated the levels of Bcr-AblE255K and Bcr-AblT315I and induced apoptosis of BaF3 cells with ectopic expression of the mutant forms of Bcr-Abl. Finally, cotreatment of the primary CML cells with vorinostat and dasatinib induced more loss of cell viability and depleted Bcr-Abl or Bcr-AblT315I, p-STAT5, and p-CrkL levels than either agent alone. Therefore, this preclinical in vitro activity of vorinostat and dasatinib against cultured and primary CML cells

supports the in vivo testing of the combination in imatinib mesylate-sensitive and imatinib mesylate-resistant CML cells.

As described below, the Principal Investigator also participated in determining the clinical efficacy of nilotinib in patients with imatinib-resistant CML and Philadelphia chromosome-positive AML. The findings of these studies are summarized in the two following sections.

Nilotinib in imatinib-resistant CML and Philadelphia chromosome-positive ALL. Resistance to imatinib mesylate can occur in chronic myelogenous leukemia (CML). Preclinical in vitro studies have shown that nilotinib (AMN 107) is more potent than imatinib against CML cells by a factor of 20 to 50. In a phase 1 dose-escalation study, we assigned 119 patients with imatinib-resistant CML or acute lymphoblastic leukemia (ALL) to receive nilotinib orally at doses of 50 mg, 100 mg, 200 mg, 400 mg, 600 mg, 800 mg, and 1200 mg once daily and at 400 mg and 600 mg twice daily. Common adverse events were myelosuppression, transient indirect hyperbilirubinemia, and rashes. Of 33 patients with the blastic phase of disease, 13 had a hematologic response and 9 had a cytogenetic response; of 46 patients with the accelerated phase, 33 had a hematologic response and 22 had a cytogenetic response; 11 of 12 patients with the chronic phase had a complete hematologic remission. Our conclusions are that nilotinib has a relatively favorable safety profile and is active in imatinib-resistant CML.

Nilotinib is effective in patients with Philadelphia chromosome–positive CML in chronic phase (CP) following imatinib resistance and intolerance: Nilotinib, an orally bioavailable, selective Bcr-Abl tyrosine kinase inhibitor, is 30-fold more potent than imatinib in pre-clinical models, and overcomes most imatinib resistant BCR-ABL mutations. We participated in a phase 2 open-label study in which 400 mg of nilotinib was administered orally twice daily to 280 patients with Philadelphia chromosome–positive (Ph+) CML-CP after imatinib failure or intolerance. Patients had at least 6 months of follow-up and were evaluated for hematologic and cytogenetic responses, as well as for safety and overall survival. At 6 months, the rate of major cytogenetic response (Ph ≤35%) was 48%: complete (Ph = 0%) in 31%, and partial (Ph = 1%-35%) in 16%. The estimated survival at 12 months was 95%. Nilotinib was effective in patients harboring BCR-ABL mutations associated with imatinib resistance (except T315I), and also in patients with a resistance mechanism independent of BCR-ABL mutations. Adverse events were mostly mild to moderate, and there was minimal cross-intolerance with imatinib. Grades 3 to 4 neutropenia and thrombocytopenia were observed in 29% of patients; pleural or pericardial effusions were observed in 1% (none were severe). In summary, nilotinib is highly active and safe in patients with CML-CP after imatinib failure or intolerance.

Most studies test for mutations in the kinase domain of the *abl* gene in chronic myeloid leukemia (CML) using peripheral blood (PB) cells. However, frequently, progression of the disease manifests with increased blasts in bone marrow (BM) and not in PB. Therefore, we also performed and reported studies that showed that the circulating plasma mRNA is a reliable alternative to BM mRNA for detecting ABL mutations, as described below.

Heterogeneity in detecting Abl kinase mutations and better sensitivity using circulating plasma RNA. Simultaneous analysis of plasma, PB cells and BM cells from 41 imatinib-resistant CML patients showed mutations in 63% of PB cells and 68% of plasma or BM cells (P = 0.04). In discordant patients, 13 mutations were detected in plasma, 11 in BM cells and 9 in PB cells. The T315I mutation was detected in plasma and BM but not PB cells in one patient. We detected no mutations in the plasma of 45 previously untreated CML patients, but two of these patients showed mutations in plasma and not cells by 9 months on therapy. Circulating plasma mRNA is a reliable alternative to BM mRNA for detecting ABL mutations.

We also determined whether the effect of anti-CML blast crisis activity of pan-HDAC inhibitor such as panobinostat and LAQ824 also involves targeting of other deregulated epigenetic mechanisms besides the increased activity of histone deacetylases and histone deacetylation. We foucused on the SET domain-containing histone methyltransferase EZH2 and the multiprotein polycom be repressive complex, PRC2, in which EZH2 performs the catalytic activity and functions as the histone methltransferase. Our novel and highly interesting findings are described below.

Histone deacetylase inhibitors deplete enhancer of zeste 2 and associated polycomb repressive complex 2 proteins in human acute leukemia cells. Human enhancer of zeste 2 (EZH2) protein belongs to the multiprotein polycomb repressive complex 2, which also includes suppressor of zeste 12 (SUZ12) and embryonic ectoderm development (EED). The polycomb repressive complex 2 complex posseses histone methyltransferase activity mediated by the Su(var)3-9, enhancer of zeste, and trithorax domain of EZH2, which methylates histone H3 on lysine (K)-27 (H3K27). In the present studies, we determined that treatment with the hydroxamate histone deacetylase inhibitor LBH589 or LAQ824 depleted the protein levels of EZH2, SUZ12, and EED in the cultured (K562, U937, and HL-60) and primary human acute leukemia cells. This was associated with decreased levels of trimethylated and dimethylated H3K27, with concomitant depletion of the homeobox domain containing HOXA9 and of MEIS1 transcription factors. Knockdown of EZH2 by EZH2 small interfering RNA also depleted SUZ12 and EED, inhibited histone methyltransferase activity, and reduced trimethylated and dimethylated H3K27 levels, with a concomitant loss of clonogenic survival of the cultured acute myelogenous leukemia (AML) cells. EZH2 small interfering RNA sensitized the AML cells to LBH589-mediated depletion of EZH2, SUZ12, and EED; loss of clonogenic survival; and LBH589-induced differentiation of the AML cells. These findings support the rationale to test anti-EZH2 treatment combined with hydroxamate histone deacetylase inhibitors as an antileukemia epigenetic therapy, especially against AML with coexpression of EZH2, HOXA9, and MEIS1 genes.

It had been previously reported that BCR-ABL induces the activity of STAT5 transcription factor, which upregulates the levels of the antiapoptotic Bcl-xL protein thereby conferring a survival advantage on BCR-ABL expressing CML cells. Therefore we determined the effect of dasatinib on STAT5 signaling and determined whether high intracellular levels of STAT5 activity would confer relative resistance against dasatinib. Findings of this study are described below.

Dasatinib inhibits Stat5 si gnaling associated w ith apoptos is in chronic my elogenous leukemia cells: Dasatinib is a novel, oral, potent, mult i-targeted kinase inhibitor of B cr-Abl and Src family kinases (SFK) and is a promisi ng cancer therapeutic agent. Dasatinib is 325-fold more potent than imatinib against cells ex pressing wild-type Bcr-Abl, and that dasatinib is active against 18 of 19 Bcr-Abl mutations known to cause imatinib resistance. In the present study, we first confir med that dasatinib inhibits tyrosine phosphorylation of SFKs, including Src, Hck, and Lyn, in K562 human CML cells. Significantly , downstream signa l transducer and activator of transcription 5 (Sta t5) signaling was determined to be blocked by dasatinib as shown by decreases in levels of phosphorylated Stat 5 and Stat5 DNA-binding activities. In addition, treatment with dasatinib down- regulated express ion of Stat5 target genes, including Bcl-x, Mcl-1, and cyclin D1. Consis tent with these results, b lockade of Stat5 signaling by dasatinib was accompanied by inhibi tion of cell prolifer ation and induction of apoptosis. Surprisingly, Stat5 D NA-binding ac tivities were enhanced with increasin g cell density, which is associated with resistance to apoptosis by dasatinib. These findings indicate that inhibition of Stat5 signaling downstream of Bcr-Abl/SF Ks contributes to the action of dasatinib, and, conversely, that incr easing cell dens ity up-regulates Stat5 activation and confers resistance to dasatinib. Moreover, the level of phosphorylated Stat5 in CML cells represents a mechanistically rele vant biomarker for monitoring i nhibition of Bcr-Abl sign aling by dasatinib in CML patients using convenient immunocytochemical assays.

Ex-vivo studies have suggested t hat imatinib-resistance in chr onic myeloid leukemia (CML) patients occurs despite adequate suppressi on of BCR-ABL activi ty. Whether BCR-ABL phosphorylation levels differ between imatinib-sens itive and -resistant patients is not known. We probed this issue by comparing t he autophosphorylation and downstream si gnaling activity of BCR-ABL in CML cells derived fr om patients who had been untreated or exhibited imatinib-refractory progressive CML. Additi onally, we also developed a novel immunolog ic assay to estimate the plasma levels of circul ating BCR-ABL protein as well as to determine its activity by estimating the level of BCR- ABL phosphorylation. This technique would be useful in monitoring patient s with chronic myeloid leukemia (CML) or acute lymphoblastic leukemia (ALL), and the same approach c an be us ed in other translocations and has the potential of multiplexing. The findings of these two important studies are described below.

Phosphorylation levels of BCR- ABL, CrkL, AKT and ST AT5 in imatinib-resistant chronic myeloid leukemia cells implicate alternative pathw ay usage as a survival strategy: We compared the phosphorylation of B CR-ABL in 54 previo usly untreated CML patients and 62 imatinib-resistant CML patients with progressive disease. Resistant pa tients had significantly lower levels of BCR-ABL, CrkL and AKT phosphorylati on t han previously untreated patients, but STAT 5 phosphorylation showed no diffe rence. These observations suggest that imatinib- resistance is not necessa rily dependent on higher activity in BCR-ABL-dependent pathways, but is likely due to the activation of other pathways.

An immunological method for th e detection of BCR-ABL fusi on protein and monitoring its activation: We have developed a simplified s andwich immunoassay to measure free circulating total and p-BCR-AB L protein in patients with t he t(9;22)(q34;q11) chromosomal translocation. The as say is bas ed on im munoprecipitating BCR-ABL protein usin g beads

coated with anti-BCR antibody and detecting the fusion protein with anti-ABL antibody and flow cytometry. We show that this method allows the quantification of this protein in the plasma and may allow the measurement of tumor load. This method also allows the measurement of the level of phosphorylation of the immunoprecip itated BCR-ABL using antibodies agains t phosphorylated ABL protein, wh ich can be used for monitori ng of therapy with kinas e inhibitors. The sensitivity of this immunoassay was comparable to the sensitivity of reverse transcription-polymerase chain reaction (RT-PCR) assay.

It is now w ell recognized that novel BCR-ABL ty rosine kinase inhibitors, such as nilotinib and dasatinib, do not inhibit the activity of BCR-ABL T315I mutation, which is seen in approximately 10% of patients with CML refractory to imatinib. A preliminary report suggested that the Aurora kinase inhibitor, MK-047 (VX-680) also inhibits the activity of BCR-ABL and its mutant versions, including BCR-ABLT315I. Based on this, we performed the following studies.

Cotreatment w ith vorinostat enhances activity of MK-0457 (VX-680) against acute and chronic m yelogenous leukemia cells. We determined the effects of vorinostat (suberoylanalide hydroxamic acid) and/or MK-0457 (VX-680), an Aurora kinase inhibitor on the cultured human (HL-60, OCI-AM L3, and K562) and primary acute my elogenous leukemia (AML) and chronic myelogenous leukemia (CML), as well as on the murine pro-B BaF3 cells with ectopic expression of the unmutated and mutant forms of B cr-Abl. Following exposure to MK-0457 and/or vorinostat, apoptosis, loss of viability, as well as activity and levels of Aurora kinase and Bcr-Abl proteins were determined. Treatment w ith MK-0457 decreased the phosphorylation of Aurora kinase substrates including serine (S)10 on histone H3 and survivin, and led to aberrant mitosis, DNA endoreduplication as well as apoptosis of the cultured human acute leuk emia HL-60, OCI-AML3, and K562 cells . Combined treatment with vorinostat and MK-0457 resulted in greater att enuation of Aurora and Bcr-Abl (in K562) kinase activity and levels as well as synergistically induced apopt osis of OCI-AML3, HL- 60, and K562 cells. MK-0457 plus vorinostat also induced synergistic apoptosis of BaF3 cells with ectopic overexpression of wild-type or mutant Bcr-Abl. Finally, cotreatment with MK-0457 and vorinostat induced more loss of viability of primary AML and imatinib -refractory CML than treatment with either agent alone, but exhibited minimal toxic ity to normal CD34+ progenitor cells. These findings demonstrate that comb ined in vitro treatment with MK-0457 and vorinostat is highly active agains t cultured and primary leukemia cells. These findings merit in vivo testing of the combination against human AML and CML cells, especially against im atinib mesylate-resistant Bcr-AblT315I-expressing CML Cells.

Based on our findings that panobinostat depletes EZ H2 levels and induces growth arrest in apoptosis of CML blast crisis ce lls (BC), we extended these studies to determine the effects of combined treatment w ith panobinostat and DNMT1 inhibitor dec itabine on CML-BC cells. Our studies and findings are described below.

Panobinostat treatment deplet es EZH2 and DNM T1 levels and enhances deci tabine mediated de-repression of JunB and loss of survival of human acute leukemia cells: The PRC2 complex protein EZ H2 is a histone methyltransferase that is known to bind and recruit DNMT1 to the DNA to modulate DNA meth ylation. Here, we determined that the pan-HDAC inhibitor panobinostat (LBH589) treatment depletes DNMT1 and EZH2 prot ein lev els,

disrupts the interaction of DNMT1 with EZH2, as well as de-represses Jun B in human acute leukemia cells. Similar to treatment with the hsp90 inhibitor 17- DMAG, treatment with panobinostat also inhibited the chaperone associ ation of heat shock protein 90 with D NMT1 and EZ H2, which pr omoted the proteasomal degradation of DNMT1 and EZH2. Unlik e treatment with the DNA methyltr ansferase inhibitor decitabine, which demethylates JunB promoter D NA, panobinostat treatm ent mediated chromatin alterati ons in the JunB promoter. Combined treatment with panobinostat and decit abine caused greater attenuation of DNMT1 and EZH2 levels than either agent alone, which was acco mpanied by more JunB de-repression and loss of clonogenic survival of the C ML-BC K562 cells. Co-treatment with panobinostat and dec itabine als o caused more loss of viability of primary CML-BC but not normal CD34+ bone marrow progenitor cells. Collec tively, these findings indic ate that co-treatment with panobinostat and dec itabine targets multiple ep igenetic m echanisms to de-repress JunB and exerts antileukemia activity against human CML-BC cells.

Key research accomplishments:

- Combined treatment with the histone deacetylase inhibitor, LBH58 9, and nilotinib (AMN107) exerts synergistic cytotox icity against Bcr-Abl positiv e human acute leukemia cells.

- LBH589 and nilotinib combination exer ts superior activity against imatinib-resistant mutants of Bcr-Abl, i.e., Bcr-AblE255K and Bcr-AblT315I.

- Histone deacetylase inhibitors deplete enhancer of zeste 2 and associated polycomb repressive complex 2 proteins in human acute leukemia cells.

- Circulating plasma mRNA is a relia ble alternative to BM mRNA for detecting ABL mutations.

- Nilotinib is effective in patients wit h Philadelphia chromosome–positive CML in chronic phase (CP) following imatinib resistance and intolerance

- A simplified sandwic h immunoassay to measure free circulating total and p-BCR-ABL protein in patients with the t(9;22)(q34;q11) chromosomal translocation.

- Phosphorylation levels of BCR-ABL, CrkL, AKT and STAT5 in imatinib-resistant chronic myeloid leukemia cells implicate alternative pathway usage as a survival strategy.

- Dasatinib inhibits Stat5 signaling associated with apoptosis in chronic myelogenous leukemia cells.

- Cotreatment with vorinostat enhances ac tivity of MK -0457 (VX-680) against acute and chronic myelogenous leukemia cells.

- Panobinostat treatment depletes EZH2 and DNMT1 levels and enhances decitabine mediated de-repression of JunB and loss of survival of human chronic myelogenous leukemia cells.

Reportable Outcomes:

1. Fiskus W, Pranpat M, Bali P, Balasis M, Kumaraswamy S, Boyapalle S, Rocha K, Wu J, Atadja P, Manley P, and Bhalla K. Combined effects of novel tyrosine kinase inhibitor AMN107 and histone deacetylase inhibitor LBH589 against Bcr-Abl expressing human leukemia cells. Blood. 2006;108:645-52

2. Kantarjian H, Giles F, Wunderle L, Bhalla K, O'Brien S, Wassmann B, Tanaka C, Manley P, Rae P, Mietlowski W, Bochinski K, Hochhaus A, Griffin JD, Hoelzer D, Albitar M, Dugan M, Cortes J, Alland L, Ottmann OG. Nilotinib in imatinib-resistant CML and Philadelphia chromosome-positive ALL. N Engl J Med. 2006; 354: 2542-51.

3. Fiskus W, Pranpat M, Balasis M, Bali P, Estrella V, Kumaraswamy S, Rao R, Rocha K, Herger B, Lee F, Richon V, Bhalla K. Co-treatment with vorinostat (suberoylanilide hydroxamic acid, SAHA) enhances activity of dasatinib (BMS-354825) against imatinib mesylate sensitive or resistant chronic myelogenous leukemia cells. Clin Cancer Res. 2006;12: 5869-78

4. Fiskus W, Pranpat M, Balasis M, Bali P, Estrella V, Kumaraswamy S, Herger B, Rao R, Rocha K, Chinnaiyan AM, Atadja P and Bhalla K. Histone deacetylase inhibitors deplete enhancer of zeste 2 and associated polycomb repressive complex 2 proteins in human acute leukemia cells. Mol Cancer Ther. 2006; 5: 3096-104.

5. Ma W, Kantarjian H, Jilani I, Gorre M, Bhalla K, Ottmann O, Giles F, Albitar M. Heterogeneity in detecting Abl kinase mutations and better sensitivity using circulating plasma RNA. Leukemia. 2006; 20: 1989-91.

6. Nam S, Vultur A, Bhalla K and Jove R. Dasatinib (BMS-354825) inhibits STAT5 signaling associated with apoptosis in chronic myelogenous leukemia cells. Mol Cancer Ther. 2007; 6: 1400-5.

7. O'Brien S, Berman E, Bhalla K, Copelan EA, Devetten MP, Emanuel PD, Erba HP, Greenberg PL, Moore JO, Przepiorka D, Radich JP, Schilder RJ, Shami P, Smith BD, Snyder DS, Soiffer RJ, Tallman MS, Talpaz M, Wetzler M; National Comprehensive Cancer Network: Chronic myelogenous leukemia. J Natl Compr Canc Netw. 2007; 5: 474-96.

8. Kantarjian HM, Giles F, Gattermann N, Bhalla K, Alimena G, Palandri F, Ossenkoppele GJ, Nicolini F, O'Brien SG, Hochhaus A, Litzow M, Bhatia R, Cervantes F, Haque A, Shou Y, Rest DJ, Weitzman A, le Coutre P. Nilotinib (formerly AMN107), a highly selective BCR-ABL tyrosine kinase inhibitor, is effective in patients with Philadelphia

chromosome-positive chronic myelogenous leukemia in chronic phase following imatinib resistance and intolerance. Blood. 2007; 110: 3540-6

9. Jilani I, Kantarjian H, Gorre M, Cortes J, Ottmann O, Bhalla K, Giles FJ, Albitar M . Phosphorylation levels of BCR-ABL, CrkL, AKT and STAT5 in im atinib-resistant chronic myeloid leukemia cells implicate alternative pathway usage as a survival strategy. Leuk Res. 2008; 32: 643-9.

10. Jilani I, Kantarjian H, Faraji H, Gorre M, Cortes J, Ottmann O, Bhalla K, O'Brien S, Giles F, Albitar M. An immunological method for the detection of BCR-ABL fusion protein and monitoring its activation. Leuk Res. 2008; 32: 936-43.

11. Fiskus W, Wang Y, Joshi R, Rao R, Yang Y, Chen J, Kolhe R, Balusu R, Eaton K, Lee P, Ustun C, Jillella A, Buse r CA, Peiper S, Bhalla K. Co-treatment with vorinostat enhances activity of MK-0457 (VX-680) agai nst acute and chronic myelogenous leukemia cells. Clin Cancer Res. 2008; 14: 6106-15.

12. Fiskus W, Buckley K, Rao R, Mandawat A, Yang Y, J oshi R, Wang Y, Balusu R, Chen J, Koul S, Joshi A, Upadhyay S, Atadja P, Bhal la K. Panobinost at treatment depletes EZH2 and DNMT1 levels and enhances decitabine mediated de-repression of JunB and loss of survival of human acute leukemia cells. Cancer Biol Ther. In press.

Conclusions: Overall, our findings demons trate that the novel Bc r-Abl kinase inhibitors nilotinib or the dual Bcr-Abl/Src kinase inhibito r dasatinib synergistica lly interact with pan-HDAC inhibitors vorinostat or panobinostat to deplete Bcr-Abl and inhibit its downstream signaling through ST AT5 and AKT. This is asso ciated with growth arrest and apoptosis of CML cells. Significantly, our findings also dem onstrate that treatment with the pan-HDAC inhibitor vorinostat or panobinost at depletes t he levels of unmutated and mutant forms of Bcr-Abl, as well as induces growth arrest and apoptosis of CML ce lls with unmutated and mutant forms of Bcr-Abl. Additionally, our fi ndings indicate that co mbined treatment with vorinostat or panobinostat with nilotinib, dasa tinib or MK-0457 exerts synergistic anti-Bcr-Abl activity against imatinib-sens itive and resist ant CML cells. Collectively, these findings support the rationale to te st the in vivo efficacy of the combination of vorinostat or panobinostat with nilotinib, dasatinib or MK -0457 against imatinib-s ensitive and imatinib-resistant CML.

References:

1. Ren R. Mechanisms of BCR-ABL in the pathogenesis of chronic myelogenou s leukaemia. Nat Rev Cancer. 2005;5:172-183.

2. Hoover RR, Gerlach MJ, Koh EY, Daley GQ. Cooperative and redundant effects of STAT5 and Ras signaling in BCR/ABL transformed hematopoietic cells. Oncogene. 2001;20:5826-5835.

3. Aichberger KJ, Mayerhofer M, Krauth MT, et al. Low-level expression of proapoptotic Bcl-2-interacting mediator in leukemic cells in patients with chronic myeloid leukemia: role of BCR/ABL, characterization of underlying signaling pathways, and reexpression by novel pharmacologic compounds. Cancer Res. 2005;65:9436-9444.

4. Shah NP, Nicoll JM, Nagar B, et al. Multiple Bcr-Abl kinase domain mutations confer polyclonal resistance to the tyrosine kinase inhibitor imatinib (STI571) in chronic phase and blast crisis chronic myeloid leukemia. Cancer Cell. 2002;2:117-125.

5. Hochhaus A, La Rosee P. Imatinib therapy in chronic myelogenous leukemia: strategies to avoid and overcome resistance. Leukemia. 2004;18:1321-1331.

6. Michor F, Hughes TP, Iwasa Y, et al. Dynamics of chronic myeloid leukaemia. Nature. 2005;435:1267-1270.

7. Golemovic M, Verstovsek S, Giles F, et al. AMN107, a novel aminopyrimidine inhibitor of Bcr-Abl, has in vitro activity against imatinib-resistant chronic myeloid leukemia. Clin Cancer Res. 2005;11:4941-4947.

8. Weisberg E, Manley PW, Breitenstein W, et al. Characterization of AMN107, a selective inhibitor of native and mutant Bcr-Abl. Cancer Cell. 2005;7:129-141.

9. O'Hare T, Walters DK, Stoffregen EP, et al. In vitro activity of Bcr-Abl inhibitors AMN107 and BMS-354825 against clinically relevant imatinib resistant Abl kinase domain mutants. Cancer Res. 2005;65:4500-4505.

10. Bhalla KN. Epigenetic and chromatin modifiers as targeted therapy of hematologic malignancies. J Clin Oncol. 2005;23:3971-3993.

11. Lindemann RK, Gabrielli B, Johnstone RW. Histone-deacetylase inhibitors for the treatment of cancer. Cell Cycle. 2004;3:779-788.

12. Nimmanapalli R, Fuino L, Stobaugh C, Richon V, Bhalla K. Cotreatment with the histone deacetylase inhibitor suberoylanilide hydroxamic acid (SAHA) enhances imatinib-induced apoptosis of Bcr-Abl-positive human acute leukemia cells. Blood. 2003;101:3236-3239.

13. Nimmanapalli R, Fuino L, Bali P, et al. Histone deacetylase inhibitor LAQ824 both lowers expression and promotes proteasomal degradation of Bcr-Abl and induces apoptosis of Imatinib Mesylate-sensitive or -refractory chronic myelogenous leukemia-blast crisis cells. Cancer Res. 2003;63:5126-5135.

14. George P, Bali P, Annav arapu S, et al . Combination of the histone deacetylas e inhibitor LBH589 and the hsp90 inhibitor 17- AAG is highly active against human CML-BC cells and AML cells with activating mutation of FLT-3. Blood. 2005;105:1768-1776.

15. Bali P, Pranpat M, Bradner J, et al. Inhibition of histone deacetylase 6 acetylates and disrupts the chaperone func tion of heat shock protei n 90: a novel basis for antileukemia activity of histone deacetyl ase inhibitors. J Biol Chem. 2005;280:26729-26734.

16. Shah NP, Tran C, Lee FL, Chen P, Norri s D, Sawyers CL. Overriding imatinib resistance with a novel ABL kinase inhibitor. Science. 2004;305:399-401.

17. Nimmanapa lli R, O'Bryan E, Bhalla K. Geldanamycin and its analogue 17-allylamino-17-demothoxygeldanamycin (17-AAG) lowers Bcr-Abl level and induces apoptosis and differentiation of Bcr-Abl posit ive human leukemic blasts. C ancer Res. 2001;61:1799-1804.

18. Gambacorti-Passerini C, Gasser M, Ahmed S, Assouline S, Scapozza L. Abl inhibitor BMS354825 binding mode in Abels on kinase revealed by molecular docking studies. Leukemia. 2005;19:1267-1269.

19. Burgess MR, Skaggs BJ, Shah NP, Lee FY , Sawyers CL. Comparative analysis of two clin ically active BCR-A BL kinase inhibitors reveals the role of conformation-specific binding in resistance. Proc Natl Acad Sci U S A. 2005;102:3395-3400.

20. Keen N, Taylor S. Aurora -kinase inhibitors as anticancer agents. Nat Rev Canc er 2004; 4:927-36.

21. Fu J, Bian M, Jiang Q, Zhang C. Ro les of Aurora kinases in mitosis and tumorigenesis. Mol Cancer Res 2007; 5:1-10.

22. Schmit TL, Ahmad N. Regul ation of mitosis via mitoti c kinases: new op portunities for cancer management. Mol Cancer Ther 2007; 6:1920-31.

23. Zhang Y, Ni J, Huang Q, Ren W, Yu L, Zhao S. Identificat ion of the auto-inhibitory domains of Aurora-A kinase. Biochem Biophys Res Commun 2007; 357:347-52.

24. Carvajal RD, Tse A, Schwartz GK. Auro ra kinases: new target s for cancer therapy. Clin Cancer Res 2006; 12:6869-75.

25. Harrington EA, Bebbington D, Moore J, et al. VX-680, a potent and selective small-molecule inhibitor of the Au rora kinases, suppresses tumor growth in vivo. Nat Med 2004; 10:262-7.

26. Young MA, Shah NP, Chao LH, et al. Structure of the kinase domain of an imatinib-resistant Abl mutant in complex with the Aurora kinase inhibitor VX-680. Cancer Res 2006; 66:1007-14.

27. Cheetham GM, Charlton PA, Golec JM, Pollard JR. Structural basis for potent inhibition of the Aurora kinases and a T315I multi-drug resistant mutant form of Abl kinase by VX-680. Cancer Lett 2007; 251:323-9.

28. Giles FJ, Cortes J, Jones D, Bergstrom D, Kantarjian H, Freedman SJ. MK-0457, a novel kinase inhibitor, is active in patients with chronic myeloid leukemia or acute lymphocytic leukemia with the T315I BCR-ABL mutation. Blood 2007; 109:500-2.

29. Dokmanovic M, Clarke C, Marks PA. Histone deacetylase inhibitors: overview and perspectives. Mol Cancer Res 2007; 5:981-9.

30. Glozak MA, Seto E. Histone deacetylases and cancer. Oncogene 2007; 26:5420-32.

31. Fiskus W, Pranpat M, Balasis M, et al. Cotreatment with vorinostat (suberoylanilide hydroxamic acid) enhances activity of dasatinib (BMS-354825) against imatinib mesylate-sensitive or imatinib mesylate-resistant chronic myelogenous leukemia cells. Clin Cancer Res 2006; 12:5869-78.

32. Park JH, Jong HS, Kim SG, et al. Inhibitors of histone deacetylases induce tumor-selective cytotoxicity through modulating Aurora-A kinase. J Mol Med 2007; Sep 13; [Epub ahead of print] DOI 10.1007/s00109-007-0260-8.

33. Weisberg E, Manley PW, Cowan-Jacob S, et al. Second generation inhibitors of BCR-ABL for the treatment of imatinib-resistant chronic myeloid leukemia. Nat Rev Cancer 2007; 7:345-358.

34. Deininger MW. Optimizing therapy of chronic myeloid leukemia. Exp Hematol 2007; 35:144-54.

35. Chu S, Xu H, Shah NP, et al. Detection of BCR-ABL kinase mutations in CD34+ cells from chronic myelogenous leukemia patients in complete cytogenetic remission on imatinib mesylate treatment. Blood 2005; 105:2093-8.

36. Peng C, Brain J, Hu Y, et al. Inhibition of heat shock protein 90 prolongs survival of mice with BCR-ABL-T315I-induced leukemia and suppresses leukemic stem cells. Blood 2007; 110:678-85.

37. Yu H, Jove R. The STATs of cancer: new molecular targets come of age. Nat Rev Cancer 2004;4:97–105.

38. Moriggl R, Sexl V, Kenner L, et al. Stat5 tetramer formation is associated with leukemogenesis. Cancer Cell 2005;7:87–99.

39. Shah NP, Tran C, Lee FY, et al. CL Overriding imatinib resistance with a novel ABL kinase inhibitor. Science 2004;305:399–401.

40. Nam S, Kim D, Cheng JQ, et al. Action of the Src family kinase inhibitor, dasatinib (BMS-354825), on human prostate cancer cells. Cancer Res 2005;65:9185–9.

Combined effects of novel tyrosine kinase inhibitor AMN107 and histone deacetylase inhibitor LBH589 against Bcr-Abl–expressing human leukemia cells

Warren Fiskus, Michael Pranpat, Purva Bali, Maria Balasis, Sandhya Kumaraswamy, Sandhya Boyapalle, Kathy Rocha, Jie Wu, Francis Giles, Paul W. Manley, Peter Atadja, and Kapil Bhalla

AMN107 (Novartis Pharmaceuticals, Basel, Switzerland) has potent in vitro and in vivo activity against the unmutated and most common mutant forms of Bcr-Abl. Treatment with the histone deacetylase inhibitor LBH589 (Novartis) depletes Bcr-Abl levels. We determined the effects of AMN107 and/or LBH589 in Bcr-Abl–expressing human K562 and LAMA-84 cells, as well as in primary chronic myelogenous leukemia (CML) cells. AMN107 was more potent than imatinib mesylate (IM) in inhibiting Bcr-Abl tyrosine kinase (TK) activity and attenuating p-STAT5, p-AKT, Bcl-x_L, and c-Myc levels in K562 and LAMA-84 cells. Cotreatment with LBH589 and AMN107 exerted synergistic apoptotic effects with more attenuation of p-STAT5, p-ERK1/2, c-Myc, and Bcl-x_L and increases in p27 and Bim levels. LBH589 attenuated Bcr-Abl levels and induced apoptosis of mouse pro-B BaF3 cells containing ectopic expression of Bcr-Abl or the IM-resistant, point-mutant Bcr-AblT315I and Bcr-AblE255K. Treatment with LBH589 also depleted Bcr-Abl levels and induced apoptosis of IM-resistant primary human CML cells, including those with expression of Bcr-AblT315I. As compared with either agent alone, cotreatment with AMN107 and LBH589 induced more loss of cell viability of primary IM-resistant CML cells. Thus, cotreatment with LBH589 and AMN107 is active against cultured or primary IM-resistant CML cells, including those with expression of Bcr-AblT315I. (Blood. 2006;108:645-652)

Introduction

The deregulated activity of the Bcr-Abl tyrosine kinase (TK) encoded by the *bcr-abl* oncogene remains a therapeutic target in all phases of chronic myelogenous leukemia (CML).[1-3] Bcr-Abl activates diverse progrowth and prosurvival mechanisms, which confer resistance to apoptosis.[1,3] These include increased phosphorylation and transactivation by STAT-5 (signal transducer and activator of transcription), which leads to increased expression of the antiapoptotic Bcl-x_L and Pim-2 protein,[4-6] and increased Ras/Raf/MEK/ERK1/2, AKT, and NFκB activity.[1,3,7,8] Bcr-Abl TK activity also leads to depletion of the cyclin-dependent kinase-2 inhibitor p27 and the BH3 domain-only–containing proapoptotic Bim protein.[9-11] Collectively, these molecular perturbations promote cell proliferation and survival and contribute to Bcr-Abl–mediated leukemia transformation of normal bone marrow progenitor cells (NBMCs).[1,3] Although highly active in inducing clinical and cytogenetic complete remissions, resistance to imatinib mesylate (IM; Gleevec) is a common clinical problem in CML, especially in the accelerated phase and blast crisis (BC) of CML.[12] The mechanisms of resistance to IM include mutations in the kinase domain of *BCR-ABL*, amplification of the *BCR-ABL* gene, as well as Bcr-Abl–independent mechanisms of resistance.[13-16] Approximately 40 different point mutations have been described in the kinase domain of Bcr-Abl.[17] On the basis of the known crystal structure of Abl complexed with STI571, the mutations are of 2 broad categories: those that directly interfere with the ability of IM to bind to the kinase domain (eg, T315I) and those that impair the ability of Bcr-Abl from achieving the inactive conformation required for binding to IM, for example, those in the P loop (eg, E255K).[13,14,18] Bcr-Abl mutations impart varying degrees of resistance to IM, including some that remain susceptible to higher concentrations of IM.[13-15] Mutations that interfere directly with Bcr-Abl in binding IM are the most resistant to inhibition by IM.[13-15] Polyclonal resistance in a single patient represented by 2 or more distinct mutations in Bcr-Abl has also been described in 35% of patients.[13-15] These observations emphasize the need to develop and test novel anti–Bcr-Abl agents that are more potent than IM and/or are able to override the resistance to IM because of either mutations or amplifications of Bcr-Abl.[15] AMN107 (Novartis Pharmaceuticals Inc, Basel, Switzerland) is a rationally designed Bcr-Abl TK inhibitor, which binds to the ATP-binding site of the kinase in its inactive conformation.[19] AMN107 is approximately 10- to 20-fold more potent than IM in inhibiting the activity of the unmutated Bcr-Abl and induces growth inhibition and apoptosis of Bcr-Abl–transformed cells.[20,21] AMN107 is also able to inhibit the activity of mutant Bcr-Abl, with mutations in the P loop and activation loop but not with those mutations that interfere directly with the binding of Bcr-Abl with IM, for example, T315I.[20-22] Notably, in an early clinical trial, AMN107 has shown significant clinical activity against IM-resistant CML.[23]

Recent studies from our laboratory have also demonstrated that treatment with hydroxamic acid analog (HA) histone deacetylase inhibitors (HDIs) leads to increased levels of p21 and p27, as well

From the Department of Interdisciplinary Oncology, H. Lee Moffitt Cancer Center, Tampa, FL; the MD Anderson Cancer Center, Houston, TX; and Novartis Pharmaceutical Inc, Cambridge, MA

Reprints: Kapil Bhalla, Interdisciplinary Oncology Program, Moffitt Cancer Center and Research Institute, University of South Florida, 12902 Magnolia Dr, MRC 3 East, Rm 3056, Tampa, FL 33612; e-mail: bhallakn@moffitt.usf.edu.

Submitted November 23, 2005; accepted February 28, 2006. Prepublished online as *Blood* First Edition Paper, March 14, 2006; DOI 10.1182/blood-2005-11-4639.

The publication costs of this article were defrayed in part by page charge payment. Therefore, and solely to indicate this fact, this article is hereby marked "advertisement" in accordance with 18 U.S.C. section 1734.

Two of the authors (P.A. and P.W.M.) are employed by Novartis Pharmaceutical Inc, whose products, LBH589 and AMN107, were studied in the present work.

as induces the levels of prodeath proteins (eg, Bax, Bak, and Bim) and down-regulates antiapoptotic proteins, (eg, Bcl-x_L, XIAP, survivin, and AKT) in human leukemia cells.[24-26] Collectively, this results in inhibition of cell growth and induces apoptosis of leukemia cells.[27-29] Recent studies from our laboratory have also demonstrated that treatment with the HA-HDIs SAHA, LAQ824, and LBH589 alone depleted Bcr-Abl, as well as induced apoptosis and sensitized human leukemia cells to apoptosis induced by IM.[27-29] By inhibiting HDAC6 and inducing acetylation of hsp90, LAQ824 and LBH589 attenuated the ATP-binding and chaperone function of hsp90.[30] This led to polyubiquitylation, proteasomal degradation, and depletion of hsp90 client proteins, including Bcr-Abl, c-Raf, and AKT.[28,29,31] Notably, our studies also showed that treatment with LAQ824 or LBH589 reduced the levels of the highly IM-refractory Bcr-AblT315I and induced apoptosis of primary IM-refractory CML-BC cells.[28,29] Treatment with LAQ824 and LBH589 has also been shown to induce apoptosis of acute myelogenous leukemia (AML) cells, including those that contain FLT-3 mutations, while relatively sparing NBMCs.[26,28,29] On the basis of the strong rationale generated by these observations taken together, we determined the combined effects of AMN107 and LBH589 against cultured and primary human CML cells. Additionally, we also determined the effect of this combination against mouse pro-B BaF3 cells with ectopic expression of the unmutated Bcr-Abl or with mutant Bcr-AblE255K and Bcr-AblT315I, as well as against IM-resistant primary CML cells, including those that harbor the point mutation Bcr-Abl T315I.

Materials and methods

Reagents and antibodies

LBH589 and AMN107 were provided by Novartis Pharmaceuticals (East Hanover, NJ). Polyclonal anti-PARP, anti–caspase-9, anti–caspase-3, and anti–p-ERK1/2 antibodies were purchased from Cell Signaling Technology (Beverly, MA). Polyclonal anti–STAT-5 and goat polyclonal anti–Pim-2 antibody, as well as monoclonal anti–c-Myc and anti-Abl antibodies, were purchased from Santa Cruz Biotechnology (Santa Cruz, CA). Monoclonal anti–p-STAT5 antibody was purchased from Upstate Biotechnology (Lake Placid, NY). Antibodies for the immunoblot analyses of p21, p27, p-CrkL, CrkL, p-AKT, AKT, Bim, Bcl-x_L, and ERK1/2 were obtained as previously described.[26-30]

Cell lines and cell culture

Bcr-Abl–expressing, CML LAMA-84 and K562 cells were obtained from American Tissue Culture Collection (Manassas, VA) and maintained in culture in RPMI medium containing 10% fetal bovine serum and passaged twice a week, as previously described.[27-30] Mouse pro-B BaF3 cells were cultured in complete RPMI-1640 media supplemented with 10% WEHI medium as the source of IL-3.[32] For the studies described herein, logarithmically growing cells were exposed to the designated concentrations of AMN107 and/or LBH589. Following these treatments, cells or cell pellets were washed free of the drug(s) prior to the performance of the studies.

Site-directed mutagenesis and nucleofection

Three p210 Bcr-Abl constructs were used in the current studies. The p210 Bcr-Abl WT and p210 Bcr-Abl (T315I) constructs were generated as previously described.[28,32] The p210 Bcr-Abl (E255K) mutant was created by site-directed mutagenesis of a Bcr-Abl containing pSVneo construct using a QuikChange II XL kit (Stratagene, Cedar Creek, TX) according to the manufacturer's recommendations, and the resulting clones were sequenced to confirm the point mutation.[32,33] For nucleofection of the p210 Bcr-Abl constructs into BaF3 cells, 5 million BaF3 cells in 100 μL Nucleofector solution V (Amaxa, Gaithersburg, MD) were mixed with 5 μg p210 Bcr-Abl WT, p210 Bcr-Abl (T315I), or p210 Bcr-Abl (E255K) in a cuvette and nucleofected using program G-16.[34] Following nucleofection, the cells were incubated at a concentration of 1×10^6 cells/mL in complete RPMI-1640 media supplemented with 10% WEHI medium as the source of IL-3, overnight, to recover. Stable transfectants of BaF3 cells expressing the WT or mutant form of Bcr-Abl (ie, T315I or E255K) were maintained in RPMI 1640 supplemented with 10% serum, 1.0 U/mL penicillin, 1 μg/mL streptomycin, and 0.75 mg/mL G418. Stably expressing cells were then further selected by removal of IL-3. After confirmation of Bcr-Abl expression by immunoblot analysis, cells were used for the studies described herein.

Primary CML-BC cells and NBMCs

Leukemia cells from the peripheral blood and/or bone marrow of 10 patients who had met the clinical criteria of IM-resistant Ph chromosome-positive CML-BC were harvested and purified, as previously described.[27,28,35] Additionally, NBMCs were harvested and purified, as previously described.[28] Informed consents were signed by all patients to allow use of their cells for these experiments, as part of a clinical protocol approved by the University of South Florida Institutional Review Board (IRB).

Sequencing of *bcr-abl* in CML-BC cells

Using the Trizol method (Invitrogen, Carlsbad, CA), total RNA was isolated from 10 to 15 million cells available from 2 patients, who were suspected to have Bcr-Abl T315I mutation as a result of their failure to respond to treatment with IM and AMN107. Total RNA (5 μg) was reverse transcribed with a first-strand cDNA synthesis kit (Invitrogen). Reverse transcribed cDNAs were used in polymerase chain reaction (PCR) amplifications to amplify a fragment of *bcr-abl* that included the *bcr* junction region and the *c-abl* kinase region as previously described.[13,36] The amplified sequences were agarose gel-purified and cloned into pCR4-TOPO plasmid. The resulting plasmids were transformed into *Escherichia coli* Mach1 cells (Invitrogen) overnight at 37°C. Ten colonies for each sample were checked by colony PCR and subcultured for plasmid isolation. Isolated plasmids were sequence verified with T3 and T7 primers for *c-abl* kinase domain mutations.

Suspension culture or colony growth inhibition

Following treatment with the designated concentrations of AMN107 and/or LBH589 for 48 hours, untreated and drug-treated cells were washed in RPMI 1640 medium. Following this, cells were placed in suspension culture at a concentration of 200 000 cells/mL for 4 days. At the end of this incubation period, cell concentrations and percentage increase in cell numbers were determined. Alternatively, following treatment with the drugs, approximately 200 cells treated under each condition were resuspended in 100 μL RPMI 1640 media containing 10% FBS, then plated in duplicate wells in a 12-well plate containing 1.0 mL Methocult media (Stem Cell Technologies, Vancouver, Canada) per well, according to the manufacturer's protocol. The plates were placed in an incubator at 37°C with 5% CO_2 for 10 days. Following this incubation, colonies consisting of 50 or more cells, in each well, were counted by an inverted microscope, and the percentage of colony growth inhibition compared with the untreated control cells was calculated.

Assessment of percentage of nonviable cells

Cells were stained with trypan blue (Sigma, St Louis, MO). The numbers of nonviable cells were determined by counting the cells that showed trypan blue uptake in a hemocytometer and reported as the percentage of untreated control cells.[28,29]

Apoptosis assessment by annexin V staining

Untreated and drug-treated cells were stained with annexin V and PI, and the percentage of apoptotic cells was determined by flow cytometry, as

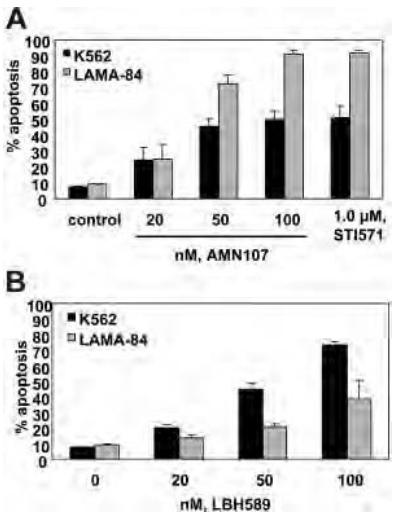

Figure 1. AMN107 and LBH589 induce apoptosis of K562 and LAMA-84 cells. Cells were treated with the indicated concentrations of AMN107 or IM (A) or LBH589 (B) for 48 hours. Following this, the percentage of annexin V–stained apoptotic cells was determined by flow cytometry. Values represented as bar graphs are mean of 3 experiments ± SEM.

described previously.[37,38] Analysis of synergism between AMN107 and LBH589 in inducing apoptosis of K562 and LAMA-84 cells was performed by Median Dose-Effect analysis of Chou and Talalay[39] using the commercially available software (Calcusyn; Biosoft, Ferguson, MO).

Western analyses of proteins

Western analyses were performed using specific antisera or monoclonal antibodies according to previously reported protocols, and the horizontal scanning densitometry was performed on Western blots, as previously described.[37,38]

Immunoprecipitation of Bcr-Abl and immunoblot analyses

Following the designated drug treatments, cells were lysed in lysis buffer (20 mM Tris [pH 8], 150 nM sodium chloride, 1% NP40, 0.1 M sodium fluoride, 1 mM PMSF, 1 mM sodium orthovanadate, 2.5 μg/mL leupeptin, 5 μg/mL aprotinin) for 30 minutes on ice, and the nuclear and cellular debris was cleared by centrifugation.[28,35] Cell lysates (200 μg) were incubated with the Abl-specific monoclonal antibody for 1 hour at 4°C. To this, washed Protein G agarose beads were added and incubated overnight at 4°C. The immunoprecipitates were washed 3 times in the lysis buffer, and proteins were eluted with the SDS sample loading buffer prior to the immunoblot analyses with specific antibodies against anti-Abl or antiphosphotyrosine antibody.[28,35]

Statistical analysis

Significant differences between values obtained in a population of leukemic cells treated with different experimental conditions were determined using the student *t* test. *P* values of less than .05 were assigned significance.

Results

AMN107 and LBH589 induce apoptosis of K562 and LAMA-84 cells

We determined the effects of AMN107 and/or LBH589 in cultured and primary CML-BC cells. We first determined the apoptotic effects of treatment with LBH589 or AMN107 alone on K562 and LAMA-84 cells. Figure 1A and 1B demonstrate that exposure to LBH589 or AMN107 alone induces apoptosis of K562 and LAMA-84 cells in a dose-dependent manner. Consistent with the previous reports, the data also show that AMN107 is approximately 10-fold more potent than IM in inducing apoptosis of K562 and LAMA-84 cells (Figure 1A). Treatment of LAMA-84 cells with AMN107 inhibited the levels of tyrosine phosphorylated Bcr-Abl in a dose-dependent manner, without affecting the levels of Bcr-Abl (Figure 2A). AMN107 treatment also inhibited the levels of p-CrkL (vide infra), suggesting that AMN107 inhibits the TK activity of Bcr-Abl. Treatment with AMN107 attenuated the levels of p-STAT5, as well as lowered the expressions of c-Myc and Bcl-x_L, which are transactivated by STAT5 (Figure 2B). Treatment with AMN107 also inhibited the levels of p-AKT but not AKT, which was associated with induction of p27 levels (Figure 2B). This has also been observed following exposure to IM.[40] Similar effects of AMN107 were also observed in K562 cells (data not shown).

Cotreatment with LBH589 and AMN107 exerts superior anti–Bcr-Abl activity and synergistically induces apoptosis of K562 and LAMA-84 cells

Next, we determined the effects of cotreatment with LBH589 and AMN107 on Bcr-Abl, as well as on the levels of the signaling proteins downstream of Bcr-Abl. Figure 3A demonstrates that, as compared with treatment with either agent alone, relatively low concentrations of LBH589 (20 nM) and AMN107 (50 nM) for 24 hours caused more depletion of Bcr-Abl and induced more p27 levels in K562 cells. In contrast, p21 levels were induced to a similar extent by combined treatment with AMN107 and LBH589, as compared with treatment with LBH589 alone. Combined treatment with LBH589 and AMN107 also caused more attenuation of the levels of p-CrkL, Bcl-xL, and c-Myc but induced more Bim (Figure 3B). Following cotreatment with AMN107 and LBH589, simultaneous induction of Bim and attenuation of Bcl-xL was associated with more PARP cleavage, which is due to increased activity of the effector caspases 3 and 7 during apoptosis.[26,28] Similar effects of LBH589 and AMN107 were also observed against LAMA-84 cells (data not shown). Next, we determined the apoptotic effect of LBH589 and/or AMN107 on suspension culture and colony growth of K562 cells. Figure 4A demonstrates that cotreatment with AMN107 and LBH589 caused

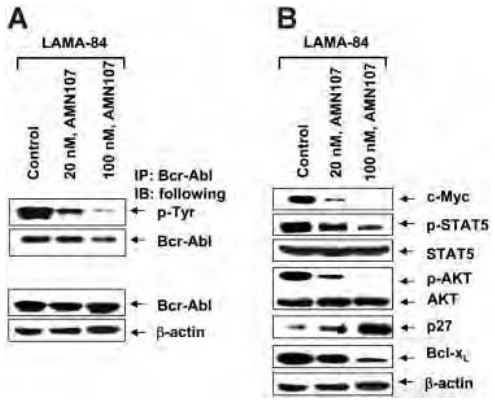

Figure 2. AMN107 inhibits autophosphorylation of Bcr-Abl and attenuates p-STAT5, p-AKT, c-Myc, and Bcl-xL levels. (A) LAMA-84 cells were treated with the indicated concentrations of AMN107 for 24 hours. Following this, immunoprecipitates were obtained with protein G-agarose beads coated with anti-Abl antibody and immunoblotted with antiphosphotyrosine antibody or anti-Abl antibody. (B) Alternatively, cell lysates of LAMA-84 cells were used for Western blot analyses of p-STAT5, STAT5, c-Myc, Bcl-xL, p-AKT, AKT, and p27, using specific antibodies. The levels of β-actin served as the loading control.

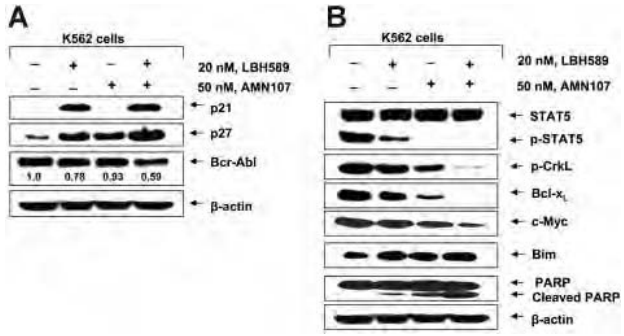

Figure 3. Cotreatment with LBH589 and AMN107 causes greater attenuation of p-AKT, p-STAT5, p-CrkL, Bcl-xL, and c-Myc but induces more p27, Bim, and PARP cleavage in K562 cells. (A) Following treatment of K562 cells with 20 nM LBH589 and/or 50 nM AMN107 for 24 hours, Western blot analyses of Bcr-Abl, p21, and p27 was performed on the cell lysates. The levels of β-actin served as the loading control. (B) Following treatment of K562 or LAMA-84 cells with 20 nM LBH589 and/or 50 nM AMN107 for 24 hours, Western blot analyses of p-STAT5, STAT5, p-CrkL, Bcl-xL, c-Myc, Bim, and PARP was performed on the cell lysates. The levels of β-actin served as the loading control.

significantly more inhibition of colony growth than treatment with either drug alone ($P < .05$). Similar effect of the combination was also observed against suspension culture growth of K562 cells (data not shown). We also determined the apoptotic effect (increase in the percentage of annexin V–positive cells) of the combined treatment with AMN107 and LBH589 in K562 and LAMA-84 cells. Notably, exposure to the combination of AMN107 and LBH589 exerted synergistic apoptotic effect in K562 and LAMA-84 cells, as determined by the median dose-effect isobologram analysis described by Chou and Talalay.[39] For AMN107 and LBH589, the combination index values were less than 1.0 in each cell type (Figure 4A-B). The CI values for K562 were 0.47, 0.36, 0.45, 0.45, and 0.45, respectively, and the CI values for LAMA84 were 0.85, 0.22, 0.21, and 0.16, respectively. The effect of AMN107 and/or LBH589 was also determined against NBMCs. Although AMN107 had no effect (up to 1.0 μM), exposure to 20 and 50 nM LBH589 for 48 hours induced loss of survival of 13.1% and 15.9% of NBMCs (mean of 2 samples with experiments performed in duplicate). Cotreatment with AMN107 did not significantly increase the loss of survival of NBMCs because of exposure to 50 nM LBH589 ($P > .05$).

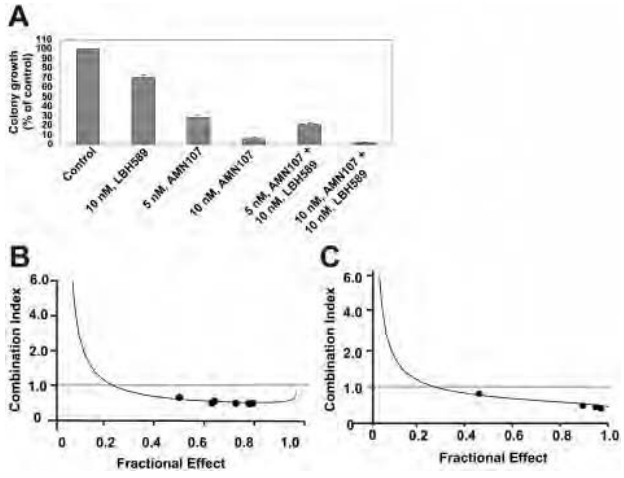

Figure 4. Cotreatment with LBH589 and AMN107 inhibits more colony growth than either agent alone and induces synergistic apoptotic effects. (A) K562 cells were treated with the indicated concentrations of LBH589 and/or AMN107 for 48 hours. Following this, colony growth in semisolid medium was assessed after 7 days. The bar graphs represent the mean percentage values ± SEM of untreated control colony growth. K562 cells (B) and LAMA-84 cells (C) were treated with LBH589 and AMN107 at a fixed ratio of 1 to 2, respectively, with concentrations ranging between 10 and 100 nM, for 48 hours. Following this, the percentage of annexin V–stained apoptotic cells was determined by flow cytometry. Using Calcusyn software (Biosoft), the analysis of the dose-effect relationship for LBH589 and AMN107-induced apoptosis of K562 or LAMA-84 cells was performed according to the median effect method of Chou and Talalay.[39] The combination index (CI) values were calculated for 3 independent experiments. $CI < 1$, $CI = 1$, and $CI > 1$ represent synergism, additivity, and antagonism of the 2 agents, respectively.

LBH589 depletes mutant Bcr-Abl levels and induces apoptosis of IM-resistant BaF3 cells expressing Bcr-AblT315I or Bcr-AblE255K

Next, we determined the effect of treatment with LBH589 and/or AMN107 on BaF3 cells with ectopic expression of either the unmutated Bcr-Abl or of the point mutant Bcr-AblE255K or Bcr-AblT315I. Similar to the effects seen in K562 and LAMA824 cells with endogenous expression of Bcr-Abl, AMN107 induced apoptosis of BaF3/Bcr-Abl cells in a dose-dependent manner (Figure 5A). Additionally, cotreatment with AMN107 and LBH589 induced significantly more apoptosis of BaF3/Bcr-Abl cells than either agent alone (Figure 5A; $P < .05$). Although exposure to IM induced dose-dependent apoptosis of BaF3/Bcr-Abl cells, BaF3/Bcr-AblT315I cells were resistant to IM up to levels as high as 10 μM (data not shown). In contrast, BaF3/Bcr-AblT315I cells were as sensitive as BaF3/Bcr-Abl cells to apoptosis induced by treatment with LBH589 alone (Figure 5A,B). Treatment with 50 nM LBH589 for 48 hours induced apoptosis in approximately 30% of BaF3/Bcr-Abl T315I cells (Figure 5B). Lower levels of LBH589 were less effective (data not shown). In contrast, BaF3/Bcr-AblT315I cells were resistant to AMN107 levels as high as 2000 nM (Figure 5B). Notably, cotreatment with 2000 nM but not 100 nM AMN107 significantly increased LBH589-induced apoptosis of BaF3/Bcr-AblT315I cells ($P < .01$; Figure 5B). Against BaF3/Bcr-AblE255K cells, although 100 nM AMN107 was ineffective, exposure to 200 (not shown) and 500 nM AMN107 induced apoptosis of 26.0% and 43.0% of cells, respectively (Figure 5C). Again, cotreatment with AMN107 (500 nM) and LBH589 (50 nM) induced significantly more apoptosis of BaF3/Bcr-AblE255K cells than treatment with either agent alone ($P < .01$),

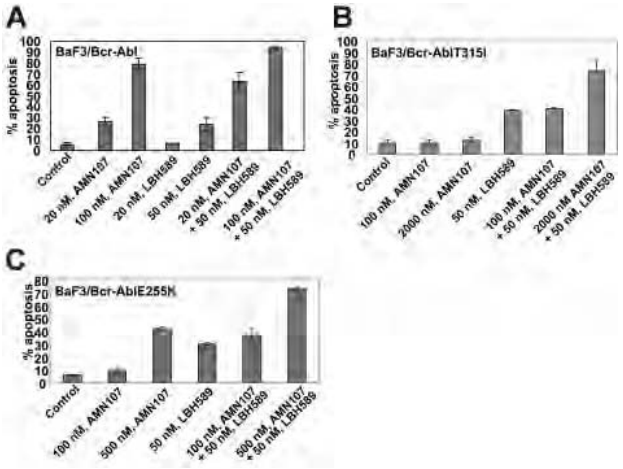

Figure 5. Cotreatment with LBH589 and AMN107 induces more apoptosis of BaF3/Bcr-Abl, BaF3/Bcr-AblT315I, and BaF3/Bcr-AblE255K cells. Cells were treated with the indicated concentrations of LBH589 and/or AMN107 for 48 hours, and the percentage of apoptotic cells was determined by annexin V staining followed by flow cytometry. Values (mean ± SEM of 3 experiments performed in duplicate) are depicted as bars.

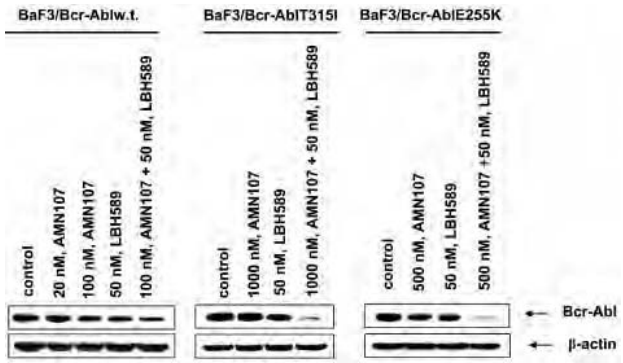

Figure 6. Cotreatment with LBH589 and AMN107 causes more depletion of Bcr-Abl in BaF3/Bcr-Abl, BaF3/Bcr-AblT315I, and BaF3/Bcr-AblE255K cells. Cells were treated with the indicated concentrations of LBH589 and/or AMN107 for 24 hours. Following this, the cell lysates were harvested and immunoblotted with the anti–Bcr-Abl antibody. The levels of β-actin served as the loading control.

although cotreatment with 100 nM AMN107 was less effective (Figure 5C). Cotreatment with higher concentrations of AMN107 (1.0 or 2.0 μM) also enhanced LBH589-induced apoptosis of BaF3/Bcr-AblE255K (data not shown). Next, we also correlated the apoptotic effects of AMN107 and/or LBH589 with their effects on the levels of Bcr-Abl in BaF3/Bcr-Abl, BaF3/Bcr-AblE255K, and BaF3/Bcr-AblT315I cells. Treatment with any of the levels of AMN107 tested alone did not lower the levels of Bcr-Abl in any of the 3 cell types (Figure 6). Exposure to AMN107 also did not affect the levels of p-CrkL or CrkL (data not shown). In contrast, exposure to 50 nM LBH589 for 24 hours lowered Bcr-Abl levels in all 3 BaF3 transfectants. Notably, as compared with treatment with either agent alone, cotreatment with LBH589 and AMN107 induced more depletion of Bcr-Abl in BaF3/Bcr-Abl cells. Notably, combined treatment with LBH589 and AMN107 caused a more pronounced decline in the levels of Bcr-AblT315I and Bcr-Abl E255K levels in BaF3/Bcr-AblT315I and BaF3/Bcr-AblE255K cells, respectively (Figure 6). Similar effect was noted on p-CrkL but not CrkL levels (data not shown).

Cotreatment with AMN107 and LBH589 causes more attenuation of Bcr-Abl and loss of viability of primary, IM-resistant CML cells than either agent alone

We next determined the antileukemia effects of LBH589 and/or AMN107 against primary CML cells isolated from the peripheral blood and/or bone marrow samples from 10 patients who had relapsed with IM-resistant CML-BC. Three of these samples were documented to have the expression of Bcr-AblT315I (samples 8, 9, and 10). In the remaining samples of IM-refractory primary CML cells (samples 1 to 7), the mutational status of Bcr-Abl could not be determined, because of inadequate sample size. Table 1 indicates that in the samples 1 to 7 both AMN107 and LBH589 induced loss of cell viability, which was dose dependent. Additionally, in these samples, cotreatment with LBH589 (20 or 50 nM) and AMN107 induced more loss of cell viability than treatment with either agent alone. Sample 7 was relatively resistant to lower concentrations of AMN107 but sensitive to LBH589 (Table 1). In the 3 samples with Bcr-AblT315I mutation (samples 8, 9, and 10), treatment with AMN107 did not augment loss of cell viability, whereas exposure to LBH589 alone for 48 hours markedly inhibited cell viability in a dose-dependent manner (Table 1). Notably, in these samples (8, 9, and 10), cotreatment with 50 or 100 nM AMN107 did not increase LBH589-induced loss of cell viability (Table 1). In one sample (no. 9), although exposure to even 2.0 μM AMN107 was ineffective, cotreatment of 50 nM LBH589 with 2.0 μM AMN107 induced apoptosis of 63.7% of cells, as compared with apoptosis of 42.0% of cells treated with 50 nM LBH589 alone (Table 1). Western blot analyses of the total cell lysates of sample 5 showed that cotreatment with 50 nM LBH589 and 100 nM AMN107 for 24 hours resulted in more attenuation of Bcr-Abl, p-CrkL, and p-STAT5 than treatment with either agent alone (Figure 7A). In contrast, in sample 9, treatment with even 1000 nM AMN107 alone had little effect on the levels of Bcr-Abl, p-CrkL, and p-STAT5, whereas cotreatment with 50 nM LBH589 and AMN107 markedly depleted the levels of Bcr-AblT315I, as well as of p-CrkL and p-STAT5 (Figure 7B). These findings were similar to those in BaF3 cells with the ectopic expression of Bcr-AblT315I.

Table 1. Effect of LBH589 and/or AMN107 on percentage of nonviable primary CML cells

Patient sample	Control	AMN107, 50 nM	AMN107, 100 nM	LBH589, 20 nM	LBH589, 50 nM	50 nM AMN107 + 50 nM LBH589	100 nM AMN107 + 50 nM LBH589
1	2.3	8.5	16.8	4.8	32.9	46.5	48.6
2	11.2	24.7	32.4	17.2	28.5	47.0	ND
3	7.1	29.0	44.0	39.0	56.0	62.0	63.0
4	9.6	30.7	35.8	16.5	28.6	42.6	49.2
5	2.2	18.6	29.0	22.8	38.6	58.9	67.6
6	5.0	10.8	23.0	34.6	60.1	69.4	68.8
7	8.0	10.6	22.4	24.6	51.0	58.1	62.9
Mean ± SEM	6.5 ± 1.2	19.0 ± 3.3	29.1 ± 3.2	22.8 ± 4.0	42.2 ± 4.7	54.9 ± 3.4*	60.0 ± 3.1*
8†	9.5	12.1	10.5	23.5	37.8	38.1	38.0
9†	16.0	17.5	16.4	28.8	42.0	42.9	43.0
10†	15.0	13.8	14.7	35.9	47.4	47.6	46.2
Mean ± SEM	13.5 ± 1.7	14.5 ± 1.3	13.9 ± 1.4	29.4 ± 2.9	42.2 ± 2.3	42.9 ± 2.2‡	42.4 ± 1.9‡

Samples of primary, IM refractory CML-BC cells, including 3 samples with expression of Bcr-AblT315I mutation (samples 8, 9, and 10), were treated with the indicated concentrations of LBH589 and/or AMN107 for 48 hours, and the percentage of nonviable cells was determined by the trypan blue exclusion method. The values represent mean of 2 experiments performed in duplicate.

ND represents treatment not studied.

*Values significantly greater than those following treatment with either agent alone at the indicated concentrations ($P < .05$).

†Samples with expression of Bcr-AblT315I.

‡Values not significantly different than those following treatment with 50 nM LBH589 alone ($P > .05$).

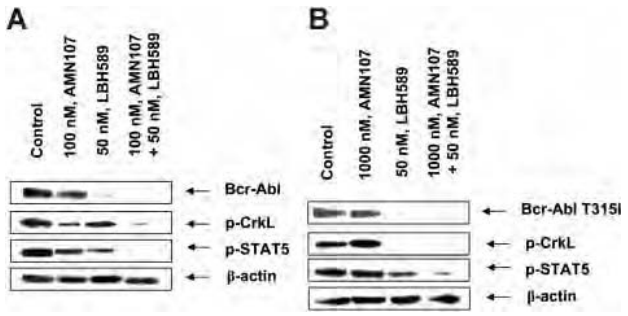

Figure 7. Cotreatment with LBH589 and AMN107 depletes the levels of Bcr-Abl, p-CrkL, and p-STAT5 in IM-resistant primary CML-BC cells. Two purified samples of IM-resistant CML-BC cells, sample 5 without a known mutation in Bcr-Abl (A) and sample 9 with expression Bcr-AblT315I (B), were exposed to LBH589 and/or AMN107 for 24 hours. Following this, the cell lysates were harvested and immunoblotted with the anti–Bcr-Abl, p-CrkL, or p-anti–p-STAT5 antibody. The levels of β-actin served as the loading control.

Discussion

In this report, we demonstrate for the first time that treatment with a combination of the pan-HDAC inhibitor LBH589 and the Bcr-Abl TK inhibitor AMN107 synergistically induced apoptosis of cultured mouse pro-B BaF3 and human CML cells with ectopic and endogenous expression of the unmutated Bcr-Abl, respectively. The combination is also more active than either drug alone against BaF3 cells with ectopic expression of the mutant Bcr-AblE255K or Bcr-AblT315I, as well as against IM-resistant primary CML cells. LBH589 also inhibits HDAC6, leading to the acetylation of hsp90 and inhibition of its ATP-binding and chaperone function.[30] Not only does this deplete Bcr-Abl but also attenuates the levels of other progrowth and prosurvival signaling protein kinases (eg, c-Raf and AKT), which are known to be hsp90 client proteins.[30,31,41,42] Additionally, treatment with an HA-HDI such as LBH589 results in attenuation of the levels of the Bcl-2 and IAP family of proteins. LBH589 also induced Bim, a protein induced by the forkhead family of transcription factors that are repressed by phosphorylation by AKT.[43,44] Phosphorylation by extracellular signal regulated kinases is also known to diminish the association of Bim with Bax, which inhibits apoptosis.[45] Collectively, these effects lower the threshold for apoptosis,[46] which may explain why treatment with LBH589 also sensitized the cultured mouse BaF3/Bcr-Abl and human CML cells to apoptosis induced by AMN107. We have previously reported that the combination of a pan-HDAC inhibitor with a TK inhibitor, in which the TK is a client protein of hsp90 (eg, Her-2 and FLT-3) induces more apoptosis than either the HDI or the TK inhibitor alone.[47,48] Present findings demonstrate a similar superior activity of the combination against Bcr-Abl–transformed cells.

Recent studies have tracked the response to IM by determining its effect on the *bcr-abl* mRNA transcript level through quantitative real-time polymerase chain reaction.[17] These studies have shown that treatment with IM may not deplete CML stem cells, and a significant proportion of patients develop acquired resistance to IM because of mutations in the Bcr-Abl kinase domain.[12-15,17] Amplification and increased expression of Bcr-Abl in CML progenitor cells may also confer IM resistance.[49] A combination incorporating LBH589, which not only induces apoptosis through non–Bcr-Abl–dependent mechanisms but also lowers unmutated or mutant Bcr-Abl levels, and AMN107, which is more potent than IM in inhibiting Bcr-Abl TK activity, has the potential of overriding several of the IM-resistance mechanisms in CML progenitor cells. IM resistance may also be due to the dependence of CML cells for their growth and survival not on Bcr-Abl but on Lyn or the other signaling kinases.[16,34,35,50] Again, on the basis of the multiple mechanisms of activity noted herein, LBH589 could potentially override non–Bcr-Abl and Bcr-Abl–dependent mechanisms of resistance in CML progenitor cells.[30,35] Mutations in the kinase domain of Bcr-Abl conferring IM resistance fall into 2 main groups, that is, those inhibiting contact with IM and those that prevent Bcr-Abl from achieving the inactive conformation required for the binding of IM to Bcr-Abl. The point mutants Bcr-Abl E255K and Bcr-AblT315I have been recognized as the important and common examples of 2 groups of mutations that confer clinical resistance to IM.[12-14] In the E255K mutation, which is located within the ATP-binding region (P loop) of the kinase domain of Bcr-Abl, glycine is replaced by lysine.[12-14] This results in a significant decrease in the sensitivity of Bcr-AblE255K to IM in the kinase assay and in conferring IM resistance on BaF3/Bcr-AblE255K cells.[12-15] In Bcr-Abl the threonine 315 makes a hydrogen bond contact with IM, and a single nucleotide C-to-T change that results in a threonine-to-isoleucine substitution at this residue has been shown to confer a high level of resistance to not only IM but also AMN107 and dasatinib.[13,22,36] Recent preclinical studies have demonstrated that AMN107 and the dual Abl/Src kinase inhibitor dasatinib are not only more potent in inhibiting unmutated Bcr-Abl TK but also active against most of the mutant forms of Bcr-Abl, except Bcr-AblT315I.[19-22,36] Note that treatment with hsp90 inhibitors has been reported to induce depletion of the mutant forms of Bcr-Abl and induce growth arrest and apoptosis of IM-resistant CML cells.[33,35] Indeed, mutant forms of Bcr-Abl appear to be more susceptible than unmutated Bcr-Abl to depletion induced by the hsp90 inhibitors.[29,33] A similar observation has also been reported with respect to the mutant versus unmutated forms of other hsp90 client proteins (eg, FLT-3).[29,48] LBH589-mediated inhibition of the chaperone function of hsp90 may be responsible for the depletion of the Bcr-AblE255K and Bcr-AblT315I levels in LBH589-treated BaF3/Bcr-AblE255K and BaF3/Bcr-AblT315I cells, respectively.

In early clinical trials, both AMN107 and dasatinib have exhibited a promising level of clinical activity in IM-resistant CML.[23,51] However, a substantial proportion of patients fail to achieve cytogenetic complete remission, especially in patients with more advanced phases of CML.[23,51] Cells from these patients may harbor additional chromosomal abnormalities and genetic perturbations that often involve the recruitment of corepressors and HDAC activity. This can potentially repress genes involved in differentiation and apoptosis.[1,24,52,53] Under these scenarios, cotreatment with LBH589 and AMN107 may override these mechanisms and induce growth arrest and apoptosis, as was reported in the K562 and the primary CML blast crisis cells.[29] Additionally, cotreatment with LBH589 and AMN107 not only attenuates Bcr-Abl but also depletes the downstream, progrowth, and prosurvival signaling molecules, including p-AKT, p-ERK1/2, and p-STAT5. Thus, LBH589-mediated "longitudinal" 2-step inhibition of the signaling initiated by Bcr-Abl may be responsible for augmenting the growth inhibitory and apoptotic activity of LBH589 and AMN107 against CML-BC cells. A similar rationale has also been proposed to explain the synergistic effects of the combination of an mTOR inhibitor and IM against CML cells.[54] A more pronounced inhibition of p-STAT5 resulting from cotreatment with LBH589 and AMN107 also correlated with greater attenuation of the STAT-5 target gene products Bcl-x_L and c-Myc.[4-6] Additionally, Bcl-2 family members have been shown to act in a complementary

manner to promote Bcr-Abl–mediated induction of leukemia.[55,56] Collectively, the more dramatic inhibitory effects on several progrowth and prosurvival signaling molecules may contribute to the synergistic apoptotic effects of the combination of LBH589 and AMN107 in the cultured and primary CML cells. However, it should be noted that in the absence of in vivo data documenting similar effects of the combination, the clinical significance of these observations should be cautiously interpreted.

Albeit preliminary, data presented here also indicate that cotreatment with LBH589 sensitizes BaF3/Bcr-AblE255K and BaF3/Bcr-AblT315I cells to higher but clinically achievable levels of AMN107. Because higher concentrations of AMN107 are able to inhibit the Bcr-Abl TK activity of the mutant Bcr-AblE255K, it is likely that cotreatment with LBH589 further enhances this activity of AMN107 by depleting the levels of Bcr-AblE255K and because of other downstream mechanisms cited. However, the structural basis for how cotreatment with LBH589 leads to increased activity of AMN107 ($\geq$ 1.0 μM) against the contact inhibitory mutant Bcr-AblT315I is not entirely clear. It is possible that LBH589 may collaborate with AMN107 in significantly inhibiting the non–TK-dependent prosurvival mechanisms mediated by Bcr-Abl in CML cells. However, further studies are needed to characterize these mechanisms and determine how these would sensitize Bcr-AblT315I to the combination of LBH589 and AMN107. Alternatively, it is conceivable that LBH589-mediated inhibition of hsp90 chaperone function for Bcr-Abl affects its conformation in a manner that allows higher concentrations of AMN107 to interact with and inhibit Bcr-AblT315I.[57] In a recent report, the non-ATP competitive Bcr-Abl kinase inhibitor ON012380 was shown to inhibit the activity of Bcr-AblT315I.[58,59] Therefore, it would be important to determine whether cotreatment with LBH589 would further augment the activity of ON012380 against CML cells expressing Bcr-AblT315I.

References

1. Ren R. Mechanisms of BCR-ABL in the pathogenesis of chronic myelogenous leukaemia. Nat Rev Cancer. 2005;5:172-183.
2. Sawyers CL. Opportunities and challenges in the development of kinase inhibitor therapy for cancer. Genes Dev. 2003;17:2998-3010.
3. Melo JV, Deininger MW. Biology of chronic myelogenous leukemia—signaling pathways of initiation and transformation. Hematol Oncol Clin North Am. 2004;18:545-568.
4. Gesbert F, Griffin JD. BCR-ABL activates transcription of the BCL-X gene through STAT5. Blood. 2000;96:2269-2276.
5. Hoover RR, Gerlach MJ, Koh EY, Daley GQ. Cooperative and redundant effects of STAT5 and Ras signaling in BCR/ABL transformed hematopoietic cells. Oncogene. 2001;20:5826-5835.
6. Rascle A, Johnston JA, Amati B. Deacetylase activity is required for recruitment of the basal transcription machinery and transactivation by STAT5. Mol Cell Biol. 2003;23:4162-4173.
7. Skorski T, Bellacosa A, Nieborowska-Skorska M, et al. Transformation of hematopoietic cells by BCR/ABL requires activation of a PI-3k/Akt-dependent pathway. EMBO J. 1997;16:6151-6161.
8. Reuther J, Reuther GW, Cortez D, Pendergast AM. A requirement for NFκB activation in Bcr-Abl-mediated transformation. Genes Dev. 1998;12:968-981.
9. Jonuleit T, Van der Kuip H, Miething C, et al. Bcr-Abl kinase down-regulates cyclin-dependent kinase inhibitor p27 in human and murine cell lines. Blood. 2000;96:1933-1939.
10. Kuwana T, Bouchier-Hayes L, Chipuk JE, et al. BH3 domains of BH3-only proteins differentially regulate Bax-mediated mitochondrial membrane permeabilization both directly and indirectly. Mol Cell. 2005;17:525-535.
11. Aichberger KJ, Mayerhofer M, Krauth MT, et al. Low-level expression of proapoptotic Bcl-2-interacting mediator in leukemic cells in patients with chronic myeloid leukemia: role of BCR/ABL, characterization of underlying signaling pathways, and reexpression by novel pharmacologic compounds. Cancer Res. 2005;65:9436-9444.
12. Druker BJ. Imatinib as a paradigm of targeted therapies. Adv Cancer Res. 2004;91:1-30.
13. Shah NP, Nicoll JM, Nagar B, et al. Multiple BCR-ABL kinase domain mutations confer polyclonal resistance to the tyrosine kinase inhibitor imatinib (STI571) in chronic phase and blast crisis chronic myeloid leukemia. Cancer Cell. 2002;2:117-125.
14. Shah NP, Sawyers CL. Mechanisms of resistance to STI571 in Philadelphia chromosome-associated leukemias. Oncogene. 2003;22:7389-7395.
15. Hochhaus A, La Rosee P. Imatinib therapy in chronic myelogenous leukemia: strategies to avoid and overcome resistance. Leukemia. 2004;18:1321-1331.
16. Donato NJ, Wu JY, Stapley J, et al. Imatinib mesylate resistance through BCR-ABL independence in chronic myelogenous leukemia. Cancer Res. 2004;64:672-677.
17. Michor F, Hughes TP, Iwasa Y, et al. Dynamics of chronic myeloid leukaemia. Nature. 2005;435:1267-1270.
18. Nagar B, Bornmann WG, Pellicena P, et al. Crystal structures of the kinase domain of c-Abl in complex with the small molecule inhibitors PD173955 and imatinib (STI-571). Cancer Res. 2002;62:4236-4243.
19. O'Hare T, Walters DK, Deininger MW, Druker BJ. AMN107: tightening the grip of imatinib. Cancer Cell. 2005;7:117-119.
20. Golemovic M, Verstovsek S, Giles F, et al. AMN107, a novel aminopyrimidine inhibitor of Bcr-Abl, has in vitro activity against imatinib-resistant chronic myeloid leukemia. Clin Cancer Res. 2005;11:4941-4947.
21. Weisberg E, Manley PW, Breitenstein W, et al. Characterization of AMN107, a selective inhibitor of native and mutant Bcr-Abl. Cancer Cell. 2005;7:129-141.
22. O'Hare T, Walters DK, Stoffregen EP, et al. In vitro activity of Bcr-Abl inhibitors AMN107 and BMS-354825 against clinically relevant imatinib-resistant Abl kinase domain mutants. Cancer Res. 2005;65:4500-4505.
23. Kantarjian H, Ottmann O, Cortes J, et al. AMN107, a novel aminopyrimidine inhibitor of Bcr-Abl, has significant activity in imatinib-resistant bcr-abl positive chronic myeloid leukemia (CML) [abstract]. Proc Am Soc Clin Oncol. 2005;24:3014.
24. Bhalla KN. Epigenetic and chromatin modifiers as targeted therapy of hematologic malignancies. J Clin Oncol. 2005;23:3971-3993.
25. Lindemann RK, Gabrielli B, Johnstone RW. Histone-deacetylase inhibitors for the treatment of cancer. Cell Cycle. 2004;3:779-788.
26. Guo F, Sigua C, Tao J, et al. Cotreatment with histone deacetylase inhibitor LAQ824 enhances Apo-2L/tumor necrosis factor-related apoptosis inducing ligand-induced death inducing signaling complex activity and apoptosis of human acute leukemia cells. Cancer Res. 2004;64:2580-2589.
27. Nimmanapalli R, Fuino L, Stobaugh C, Richon V, Bhalla K. Cotreatment with the histone deacetylase inhibitor suberoylanilide hydroxamic acid (SAHA) enhances imatinib-induced apoptosis of Bcr-Abl-positive human acute leukemia cells. Blood. 2003;101:3236-3239.
28. Nimmanapalli R, Fuino L, Bali P, et al. Histone deacetylase inhibitor LAQ824 both lowers expression and promotes proteasomal degradation of Bcr-Abl and induces apoptosis of Imatinib Mesylate-sensitive or -refractory chronic myelogenous leukemia-blast crisis cells. Cancer Res. 2003;63:5126-5135.
29. George P, Bali P, Annavarapu S, et al. Combination of the histone deacetylase inhibitor LBH589 and the hsp90 inhibitor 17-AAG is highly active against human CML-BC cells and AML cells with activating mutation of FLT-3. Blood. 2005;105:1768-1776.
30. Bali P, Pranpat M, Bradner J, et al. Inhibition of histone deacetylase 6 acetylates and disrupts the chaperone function of heat shock protein 90: a novel basis for antileukemia activity of histone deacetylase inhibitors. J Biol Chem. 2005;280:26729-26734.
31. Bagatell R, Whitesell L. Altered Hsp90 function in cancer: a unique therapeutic opportunity. Mol Cancer Ther. 2004;3:1021-1030.
32. La Rosee P, Corbin AS, Stoffregen EP, Deininger MW, Druker BJ. Activity of the Bcr-Abl kinase inhibitor PD180970 against clinically relevant Bcr-Abl isoforms that cause resistance to imatinib mesylate (Gleevec, STI571). Cancer Res. 2002;62:7149-7153.
33. Gorre ME, Ellwood-Yen K, Chiosis G, Rosen N, Sawyers CL. BCR-ABL point mutants isolated from patients with imatinib mesylate-resistant chronic myeloid leukemia remain sensitive to inhibitors of the BCR-ABL chaperone heat shock protein 90. Blood. 2002;100:3041-3044.
34. Ptasznik A, Nakata Y, Kalota A, Emerson SG, Gewirtz AM. Short interfering RNA (siRNA) targeting the Lyn kinase induces apoptosis in primary, and drug-resistant, BCR-ABL1(+) leukemia cells. Nat Med. 2004;10:1187-1189.
35. Nimmanapalli R, O'Bryan E, Huang M, et al. Molecular characterization and sensitivity of STI-571 (Imatinib Mesylate, Gleevec)-resistant, Bcr-Abl positive, human acute leukemia cells retain sensitivity to SRC kinase inhibitor PD180970 and 17-allylamino-17-demethoxygeldanamycin (17-AAG). Cancer Res. 2002;62:5761-5769.
36. Shah NP, Tran C, Lee FL, Chen P, Norris D, Sawyers CL. Overriding imatinib resistance with a novel ABL kinase inhibitor. Science. 2004;305:399-401.
37. Fang G, Kim C, Perkins C, et al. CGP57148 (STI-571) induces differentiation and apoptosis and sensitizes Bcr-Abl positive human leukemia cells

to apoptosis due to antileukemic drugs. Blood. 2000;96:2246-2256.

38. Perkins C, Kim CN, Fang G, Bhalla KN. Arsenic induces apoptosis of multidrug-resistant human myeloid leukemia cells that express Bcr-Abl or overexpress MDR, MRP, Bcl-2, or Bcl-x(L). Blood. 2000;95:1014-1022.
39. Chou TC, Talalay P. Quantitative analysis of dose-effect relationships: the combined effects of multiple drugs or enzyme inhibitors. Adv Enzyme Regul. 1984;22:27-55.
40. Andreu EJ, Lledo E, Poch E, et al. BCR-ABL induces the expression of Skp2 through the PI3K pathway to promote p27Kip1 degradation and proliferation of chronic myelogenous leukemia cells. Cancer Res. 2005;65:3264-3272.
41. Nimmanapalli R, O'Bryan E, Bhalla K. Geldanamycin and it analogue 17-allylamino-17-demothoxygeldanamycin (17-AAG) lowers Bcr-Abl level and induces apoptosis and differentiation of Bcr-Abl positive human leukemic blasts. Cancer Res. 2001;61:1799-1804.
42. Nimmanapalli R, O'Bryan E, Kuhn D, Yamaguchi H, Wang H-G, Bhalla, K. Regulation of 17-AAG-induced apoptosis: role of Bcl-2, Bcl-xL, and Bax downstream of 17-AAG-mediated down-regulation of Akt, Raf-1, and Src kinases. Blood. 2003; 102:269-275.
43. Moller C, Alfredsson J, Engstrom M, et al. Stem cell factor promotes mast cell survival via inactivation of FOXO3a-mediated transcriptional induction and MEK-regulated phosphorylation of the proapoptotic protein Bim. Blood. 2005;106:1330-1336.
44. Scheijen B, Ngo HT, Kang H, Griffin JD. FLT3 receptors with internal tandem duplications promote cell viability and proliferation by signaling through Foxo proteins. Oncogene. 2004;23:3338-3349.
45. Harada H, Quearry B, Ruiz-Vela A, Korsmeyer SJ. Survival factor-induced extracellular signal-regulated kinase phosphorylates BIM, inhibiting its association with BAX and proapoptotic activity. Proc Natl Acad Sci U S A. 2004;101:15313-15317.
46. Danial NN, Korsmeyer SJ. Cell death: critical control points. Cell. 2004;116:205-219.
47. Fuino L, Bali P, Wittmann S, et al. Histone deacetylase inhibitor LAQ824 down-regulates Her-2 and sensitizes human breast cancer cells to trastuzumab, taxotere, gemcitabine, and epothilone B. Mol Cancer Ther. 2003;2:971-984.
48. Bali P, George P, Cohen P, et al. Superior activity of the combination of histone deacetylase inhibitor LAQ824 and the FLT-3 kinase inhibitor PKC412 against human acute myelogenous leukemia cells with mutant FLT-3. Clin Cancer Res. 2004; 10:4991-4997.
49. Gorre ME, Mohammed M, Ellwood K, et al. Clinical resistance to STI-571 cancer therapy caused by Bcr-Abl gene mutation or amplification. Science. 2001;293:876-880.
50. Dai Y, Rahmani M, Pei XY, Dent P, Grant S. Bortezomib and flavopiridol interact synergistically to induce apoptosis in chronic myeloid leukemia cells resistant to imatinib mesylate through both Bcr/Abl-dependent and -independent mechanisms. Blood. 2004;104:509-518.
51. Sawyers CL, Shah NP, Kantarjian HM, et al. A phase I study of BMS-354825 in patients with imatinib-resistant and intolerant accelerated and blast phase chronic myeloid leukemia (CML): results from CA180002 [abstract]. Proc Amer Soc Clin Oncol. 2005;24:6520.
52. Calabretta B, Perrotti D. The biology of CML blast crisis. Blood. 2004;103:4010-4022.
53. Frohling S, Scholl C, Gilliland DG, Levine RL. Genetics of myeloid malignancies: pathogenetic and clinical implications. J Clin Oncol. 2005;23:6285-6295.
54. Mohi MG, Boulton C, Gu TL, et al. Combination of rapamycin and protein tyrosine kinase (PTK) inhibitors for the treatment of leukemias caused by oncogenic PTKs. Proc Natl Acad Sci U S A. 2004; 101:3130-3135.
55. Jaiswal S, Traver D, Miyamoto T, Akashi K, Lagasse E, Weissman IL. Expression of BCR/ABL and BCL-2 in myeloid progenitors leads to myeloid leukemias. Proc Natl Acad Sci U S A. 2003;100:10002-10007.
56. Nieborowska-Skorska M, Hoser G, Kossev P, Wasik MA, Skorski T. Complementary functions of the antiapoptotic protein A1 and serine/threonine kinase pim-1 in the BCR/ABL-mediated leukemogenesis. Blood. 2002;99:4531-4539.
57. Gambacorti-Passerini C, Gasser M, Ahmed S, Assouline S, Scapozza L. Abl inhibitor BMS354825 binding mode in Abelson kinase revealed by molecular docking studies. Leukemia. 2005;19:1267-1269.
58. Gumireddy K, Baker SJ, Cosenza SC, et al. A non-ATP-competitive inhibitor of BCR-ABL overrides imatinib resistance. Proc Natl Acad Sci U S A. 2005;102:1992-1997.
59. Burgess MR, Skaggs BJ, Shah NP, Lee FY, Sawyers CL. Comparative analysis of two clinically active BCR-ABL kinase inhibitors reveals the role of conformation-specific binding in resistance. Proc Natl Acad Sci U S A. 2005;102:3395-3400.

ORIGINAL ARTICLE

Nilotinib in Imatinib-Resistant CML and Philadelphia Chromosome–Positive ALL

Hagop Kantarjian, M.D., Francis Giles, M.D., Lydia Wunderle, M.D., Kapil Bhalla, M.D., Susan O'Brien, M.D., Barbara Wassmann, M.D., Chiaki Tanaka, M.D., Paul Manley, Ph.D., Patricia Rae, B.Sc., William Mietlowski, Ph.D., Kathy Bochinski, M.B.A., Andreas Hochhaus, M.D., James D. Griffin, M.D., Dieter Hoelzer, M.D., Maher Albitar, M.D., Ph.D., Margaret Dugan, M.D., Jorge Cortes, M.D., Leila Alland, M.D., and Oliver G. Ottmann, M.D.

ABSTRACT

BACKGROUND

Resistance to imatinib mesylate can occur in chronic myelogenous leukemia (CML). Preclinical in vitro studies have shown that nilotinib (AMN107), a new BCR-ABL tyrosine kinase inhibitor, is more potent than imatinib against CML cells by a factor of 20 to 50.

METHODS

In a phase 1 dose-escalation study, we assigned 119 patients with imatinib-resistant CML or acute lymphoblastic leukemia (ALL) to receive nilotinib orally at doses of 50 mg, 100 mg, 200 mg, 400 mg, 600 mg, 800 mg, and 1200 mg once daily and at 400 mg and 600 mg twice daily.

RESULTS

Common adverse events were myelosuppression, transient indirect hyperbilirubinemia, and rashes. Of 33 patients with the blastic phase of disease, 13 had a hematologic response and 9 had a cytogenetic response; of 46 patients with the accelerated phase, 33 had a hematologic response and 22 had a cytogenetic response; 11 of 12 patients with the chronic phase had a complete hematologic remission.

CONCLUSIONS

Nilotinib has a relatively favorable safety profile and is active in imatinib-resistant CML. (ClinicalTrials.gov number, NCT00109707.)

From the Department of Leukemia, University of Texas M.D. Anderson Cancer Center, Houston (H.K., F.G., S.O., J.C.); J.W. Goethe Universität, Frankfurt, Germany (L.W., B.W., D.H., O.G.O.); Moffitt Cancer Center, Tampa, Fla. (K.B.); Novartis Pharmaceuticals, East Hanover, N.J. (C.T., P.M., P.R., W.M., K.B., M.D., L.A.); Quest Diagnostics, San Juan Capistrano, Calif. (M.A.); Fakultät fur Klinische Medizin Mannheim, Universität Heidelberg, Mannheim, Germany (A.H.); and the Department of Medical Oncology, Dana–Farber Cancer Institute, Boston (J.D.G.). Address reprint requests to Dr. Kantarjian at the Department of Leukemia, Unit 428, University of Texas M.D. Anderson Cancer Center, P.O. Box 301402, Houston, TX 77230-1402, or at hkantarj@mdanderson.org.

Drs. Kantarjian and Giles contributed equally to this article.

N Engl J Med 2006;354:2542-51.

The chimeric *BCR-ABL* gene, created by the formation of the Philadelphia chromosome (Ph), encodes a fusion protein, BCR-ABL. The unregulated activity of the ABL tyrosine kinase in BCR-ABL is the cause of chronic myeloid leukemia (CML). Imatinib mesylate, an inhibitor of the BCR-ABL tyrosine kinase, improves the outcome in CML.[1,2] However, the annual progression rate during treatment of chronic-phase CML with imatinib is 4 percent.[3] Imatinib is active alone or in combination in newly diagnosed Ph-positive acute lymphoblastic leukemia (ALL).[4-7]

Nilotinib (AMN107, Novartis) is a new, orally active, aminopyrimidine-derivative tyrosine kinase inhibitor that is more potent against CML cells in vitro than is imatinib.[8-12] Like imatinib, nilotinib functions through competitive inhibition at the ATP-binding site of BCR-ABL, leading to the inhibition of tyrosine phosphorylation of proteins that are involved in the intracellular signal transduction that *BCR-ABL* mediates. Nilotinib has a higher binding affinity and selectivity for the ABL kinase than does imatinib. It also has 20 to 50 times the inhibitory activity of imatinib in imatinib-sensitive CML cell lines and 3 to 7 times the activity in imatinib-resistant cell lines. Nilotinib was also active in 32 of 33 imatinib-resistant cell lines with mutant ABL kinases.[8-12] This report summarizes the results of a phase 1 dose-escalation study of nilotinib in patients with CML and Ph-positive ALL whose disease was resistant to imatinib.

Methods

Patients

Patients with Ph-positive imatinib-resistant CML or ALL were eligible. Accelerated and blastic phases of CML were defined as previously described.[13-16] Patients with a platelet count of 800,000 per cubic millimeter or more or with clonal evolution were also considered to have the accelerated phase of disease. Clonal evolution was defined by the presence of additional chromosomal abnormalities in the Ph-positive cells, excluding variant Ph translocations, a loss of chromosome Y, or constitutional abnormalities.[13,14] Patients with only clonal evolution have a better prognosis and were analyzed separately.[17] Patients with imatinib-resistant chronic-phase CML were enrolled in the study after the first four dose cohorts. Imatinib resistance was defined as a lack of complete hematologic response after 3 months of imatinib treatment, a lack of any cytogenetic response (Ph-positive cells, >95 percent) after 6 months of treatment, a lack of a substantial cytogenetic response (Ph-positive cells, >35 percent) after 12 months of treatment, or a relapse after a hematologic response or a substantial cytogenetic response.

Patients had to be at least 18 years of age and have an adequate performance status and normal hepatic, renal, and cardiac function. Patients who had received imatinib therapy seven days before or hydroxyurea two days before the study began were not eligible to participate. The study was conducted in accordance with the Declaration of Helsinki. Patients gave written informed consent, according to institutional guidelines. The study was approved by the institutional review board at each study center.

Study Design and Therapy

The study was designed to evaluate the safety and tolerability of nilotinib. Patients were successively assigned to one of nine dose cohorts, ranging from 50 to 1200 mg once daily and from 400 to 600 mg twice daily. Patients received nilotinib daily unless unacceptable adverse events or disease progression occurred. Dose escalation (not exceeding two dose levels beyond the level administered to newly enrolled patients) was permitted for patients with an inadequate response and no prohibitive toxic effects. Patients who had been treated at lower doses had the option to receive higher doses, with escalation to a level that was declared safe. During the first cycle of therapy or at times of worsening disease before intrapatient dose escalation, patients were allowed to receive cytoreductive therapy (leukaphereses and hydroxyurea) to control elevated counts of blasts, platelets, or both. Responses in patients requiring leukapheresis or hydroxyurea concurrently with nilotinib could not be evaluated. The selection of the dose and the determination of the maximum dose that was tolerated followed a continuous modified reassessment method,[18] described in the Supplementary Appendix (available with the full text of this article at www.nejm.org).

The academic investigators and representatives of the sponsor, Novartis, designed the study and collected and analyzed the data. Drs. Kantarjian and Alland, who wrote the article with help from all the authors, vouch for the accuracy and completeness of the data and the analysis. All data were available to all investigators.

ASSESSMENT OF TOXIC EFFECTS AND RESPONSE

Complete blood counts and biochemical analysis were obtained weekly for the first eight weeks and then every other week. Bone marrow assessments were done on days 15 and 28 of the first cycle and on day 28 of every even-numbered cycle. Patients were evaluated for cytogenetic response at baseline and in repeated analyses if they had a response. Safety assessments included an evaluation of adverse events, hematologic and cardiac-enzyme assessment, biochemical testing, urinalysis, electrocardiography, and physical examination.

Toxic effects were graded according to the National Cancer Institute's Common Terminology Criteria for Adverse Events (version 3.0). Criteria

Table 1. Characteristics of the Study Group.

Characteristic	Patients (N=119)	Characteristic	Patients (N=119)
Age — yr		Duration of nilotinib administration — mo	
Median	60	Chronic	
Range	15–83	Median	4.9
Female sex — no. (%)	62 (52)	Range	1.4–9.3
Presence of splenomegaly — no. (%)	32 (27)	Accelerated	
Hemoglobin <10 g/dl — no. (%)	40 (34)	Median	5.1
White-cell count >50,000/mm^3 — no. (%)	41 (34)	Range	0.3–12.6
Platelets <100,000/mm^3 — no. (%)	98 (82)	Accelerated, clonal evolution only	
Phase of CML — no. (%)		Median	5.0
Blastic		Range	0.1–9.6
Myeloid	24 (20)	Myeloid blastic	
Lymphoid	9 (8)	Median	2.9
Accelerated blastic		Range	0.4–10.7
Clonal evolution only	10 (8)	Lymphoid blastic	
Other accelerated criteria	46 (39)	Median	1.4
Chronic*		Range	0.9–9.7
Active disease	12 (10)	Highest previous daily dose of imatinib — mg	
Complete hematologic remission	5 (4)	Chronic	
Ph-positive ALL — no. (%)	13 (11)	Median	600
Duration of phase of CML — mo†		Range	400–800
Chronic		Accelerated	
Median	59.7	Median	800
Range	12.9–167.4	Range	400–1000
Accelerated		Accelerated, clonal evolution only	
Median	90.6	Median	600
Range	7.2–226.9	Range	400–800
Accelerated, clonal evolution only		Myeloid blastic	
Median	59.0	Median	600
Range	8.1–126.7	Range	400–800
Myeloid blastic		Lymphoid blastic	
Median	49.9	Median	600
Range	3.8–186.9	Range	400–800
Lymphoid blastic		Ph-positive ALL	
Median	19.4	Median	600
Range	3.2–82.9	Range	400–800
		Presence of baseline mutation in *BCR-ABL* — no./total no. (%)	41/91 (45)

* Patients with chronic-phase CML were enrolled in the study after the first four dose cohorts.
† The duration of disease was calculated from the date of the first diagnosis of CML to the date of the first administration of nilotinib.

with respect to hematologic and cytogenetic responses have been described previously.[1,16,17,19-21] Cytogenetic responses were as follows (percentages refer to the percentage of Ph-positive metaphases): complete response, 0 percent; partial response, 1 to 35 percent; minor response, 36 to 65 percent; and minimal response, 66 to 95 percent.[16] Response criteria among patients with Ph-positive ALL were described previously.[5,20]

OTHER ANALYSES

Patients were evaluated for the inhibition of biomarker phosphorylation, the mutational status of *BCR-ABL*, and Gilbert's syndrome. The methods used in these analyses are detailed in the Supplementary Appendix.

RESULTS

PATIENTS

At three centers, from May 25, 2004, to May 4, 2005, we enrolled 119 patients whose disease was resistant to imatinib. The patients were assigned to receive daily doses of nilotinib according to the following dosing schedule: 50 mg (7 patients), 100 mg (7), 200 mg (10), 400 mg (10), 600 mg (6), 800 mg (19), and 1200 mg (10) or to receive 400 mg twice daily (32) or 600 mg twice daily (18). The characteristics of patients are shown in Table 1. As of June 15, 2005, 66 patients remained in the study, including all 17 patients with chronic-phase CML. Reasons for discontinuation included adverse events (8 patients), death during the study period (5), disease progression (35), and withdrawal of consent (5). Four patients who withdrew their consent underwent hematopoietic stem-cell transplantation.

PHARMACOKINETICS

The median time to peak concentrations of nilotinib was three hours after administration, and the mean peak concentration was 3.6 μM at steady state among patients receiving 400 mg twice daily. The apparent half-life of the drug was 15 hours. The steady-state level was achieved by day 8. The steady-state serum level of the drug was two to three times the level measured after the first dose. With the administration of daily doses at the steady-state level, the peak concentration and the area under the concentration–time curve increased among patients receiving 50 to 400 mg of the drug and reached a plateau among patients receiving more than 400 mg. Considering that saturation may have been caused by gastrointestinal absorption, the dose was reduced to 400 mg twice daily and then was further escalated to 600 mg twice daily. Exposure at the steady-state level was greater with 400 mg twice daily than with a daily dose of 800 mg, and there was a dose-proportional increase in exposure between 400 mg twice daily and 600 mg twice daily (Fig. 1).

The mean serum trough level at the steady-state level was 1.0 μM at 400 mg daily, 1.7 μM at 400 mg twice daily, and 2.3 μM at 600 mg twice daily. All trough levels exceeded the 50 percent inhibitory concentration of cellular phosphorylation of BCR-ABL (20 to 57 nM, depending on cell type) and 32 of 33 BCR-ABL kinase mutants (19 to 709 nM).[12]

SAFETY PROFILE

No dose-limiting toxic effects were seen at doses of up to 600 mg daily. Dose-limiting toxic effects occurred among 18 patients at doses higher than 600 mg. Such effects included an elevation in bilirubin level (predominantly grade 3), mostly indirect bilirubin (nine patients); a grade 3 elevation

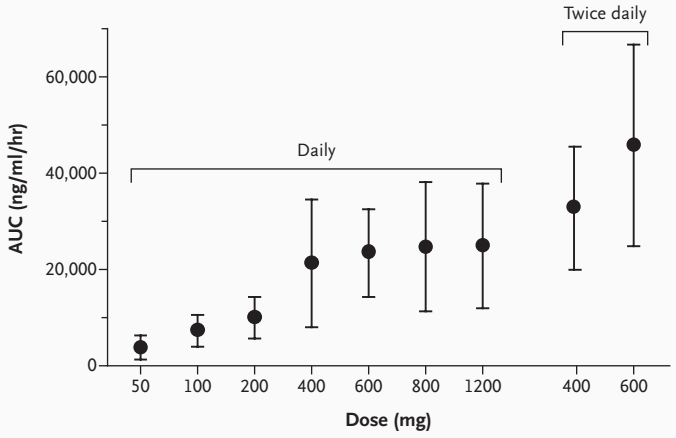

Figure 1. Total Steady-State Serum Levels of Nilotinib, According to the Daily Dose.

The graph shows the area under the concentration–time curve (AUC) during the first 24 hours after the first dose of nilotinib was administered, according to the total amount of drug patients received either once or twice daily. The points represent the mean levels of the drug, and the I bars represent the standard deviations. The total number of patients in whom levels were tested were as follows: 50 mg daily (3 patients), 100 mg daily (4 patients), 200 mg daily (3 patients), 400 mg daily (8 patients), 600 mg daily (4 patients), 800 mg daily (18 patients), and 1200 mg daily (8 patients), as well as 400 mg twice daily (30 patients) and 600 mg twice daily (18 patients).

in the aminotransferase level (three patients); a grade 4 elevation in the lipase level (one patient); a grade 3 or 4 elevation in amylase and lipase levels (two patients, one of whom had grade 2 pancreatitis); grade 4 hematologic toxic effects (two patients); and a grade 3 subdural hematoma (one patient). The method of continuous modified reassessment indicated that 600 mg administered twice daily is the maximum tolerated dose. (The posterior probability of dose-limiting toxicity was 0.30, which is discussed in the Supplementary Appendix.)

Table 2 presents a list of adverse events with an incidence of at least 4 percent that were potentially associated with nilotinib. Thrombocytopenia (21 percent) and neutropenia (14 percent) were mainly grade 3 or 4 and appeared to increase with increasing doses of the drug. Pruritus, rash, and dry skin were almost exclusively grade 1 or 2. When all categories of rash were combined, there appeared to be a dose-related increase in incidence.

Grade 3 elevations in levels of alanine aminotransferase and aspartate aminotransferase were infrequent and observed at daily doses of 600 mg or more. Elevations in total, conjugated, and unconjugated bilirubin levels accounted for 14 percent of adverse events. These increases were primarily in unconjugated bilirubin and were not accompanied by an increase in levels of aminotransferase or evidence of increased hemolysis; the increased levels often occurred during the first week of therapy. The frequency and grade of elevation in bilirubin levels increased with increasing amounts of nilotinib. Elevations frequently resolved spontaneously with continued administration of nilotinib. There was a positive correlation ($P=0.009$) between the presence of the $(TA)_7/(TA)_7$ sequence in the promoter regions of the gene encoding bilirubin uridine diphosphoglucuronate (UDP) glucuronosyltransferase 1A1, a genotype associated with Gilbert's syndrome,[22] and the incidence of grade 3 or 4 elevations of total bilirubin levels, as well as a higher mean level of bilirubin. Among 14 patients with Gilbert's syndrome, 7 had elevations in bilirubin levels, as compared with 10 of 97 patients who did not have the syndrome.

A grade 3 elevation in the amylase level was reported in one patient, and six patients had grade 3 or 4 elevations in lipase levels; of those six patients, three reported having abdominal pain. One of these patients (with a history of pancreatitis) had grade 2 pancreatitis. Among patients with available laboratory data, grade 3 or 4 elevations in lipase levels were seen in 9 of 55 patients (16 percent), and grade 3 elevations in amylase levels were seen in 3 of 57 patients (5 percent). All the increased levels were observed at daily doses of 600 mg or more.

In an exploratory analysis of more than 2200 electrocardiograms from 119 patients, the only abnormality associated with nilotinib was in the corrected QT interval by Fridericia's formula (QTcF), which appeared to increase by 5 to 15 msec in the study group. One patient had two adverse cardiac events associated with nilotinib, which included pericardial effusion (grade 1) and atrial fibrillation (grade 2), with no elevation in cardiac enzymes.

After the data cutoff for our study, two study patients died unexpectedly. One patient was a 30-year-old man with CML in complete remission; an autopsy confirmed an overdose of methadone. The other patient was a 56-year-old man with CML in an accelerated phase; there was no autopsy, and the cause of death was unknown.

RESPONSE

All patients in our study had disease that was resistant to imatinib. Overall, of 33 patients with the blastic phase, 13 had a hematologic response to nilotinib (39 percent) (Table 3) and 9 patients (27 percent) had a cytogenetic response, 6 of whom had a major cytogenetic response (Ph-positive cells in metaphase, ≤35 percent). Of 46 patients with accelerated-phase CML (excluding those with clonal evolution only), 33 had a hematologic response; 22 had a cytogenetic response, and 9 of those responses were major. Among the 10 patients who had clonal evolution as the only feature of the accelerated phase of CML, 5 had active disease and 5 were in complete hematologic remission. All 5 patients with clonal evolution and hematologic disease had a complete hematologic response; 6 of 10 had a major cytogenetic response (Table 3).

Table 4 shows the results in patients who had accelerated or blastic phases of disease who had a dose escalation owing to inadequate response at the initial dose level. Overall, 13 of 23 patients who were initially treated at daily doses of 50 to 400 mg had hematologic responses when they received 600 mg daily or 400 mg twice daily. At

Table 2. Adverse Events Reported by at Least 4 Percent of Patients.*

Adverse Event†	50–200 mg/Day (N=24)		400 mg/Day (N=10)		600–1200 mg/Day (N=35)		400 mg Twice Daily (N=32)		600 mg Twice Daily (N=18)		Any Dose (N=119)	
	Grade 1 or 2	Grade 3 or 4	Grade 1 or 2	Grade 3 or 4	Grade 1 or 2	Grade 3 or 4	Grade 1 or 2	Grade 3 or 4	Grade 1 or 2	Grade 3 or 4	Grade 1 or 2	Grade 3 or 4
	percent of patients											
Nonhematologic event												
Rash (all types)	17	0	10	0	20	3	22	0	28	6	20	2
Pruritus	21	0	10	0	17	0	6	3	22	6	15	2
Dry skin	13	0	10	0	17	0	6	0	11	0	12	0
Constipation	17	0	10	0	3	0	0	0	22	0	8	0
Nausea, vomiting, or both	8	0	0	0	6	0	13	0	6	0	8	0
Increase in both total and conjugated bilirubin levels	4	0	0	0	0	3	6	3	17	11	5	3
Fatigue	0	0	0	0	0	3	16	0	6	0	5	1
Increase in unconjugated bilirubin level	0	0	0	0	0	6	6	3	0	11	2	4
Alopecia	13	0	10	0	6	0	0	0	6	0	6	0
Increase in lipase level	0	0	0	0	0	3	0	9	0	11	0	5
Increase in level of ALT, AST, or both	0	0	0	0	0	9	3	3	0	0	1	3
Hematologic event												
Thrombocytopenia	0	13	0	20	0	17	3	25	0	28	1	20
Neutropenia	0	8	0	10	3	14	0	9	0	22	1	13
Anemia	0	4	0	10	9	6	0	6	0	6	3	6

* Safety data are presented by dividing patients into five groups on the basis of values in the area under the concentration–time curve as follows: group 1 (50, 100, and 200 mg daily), group 2 (400 mg daily), group 3 (600, 800, and 1200 mg daily), group 4 (400 mg twice daily), and group 5 (600 mg twice daily). Many patients received a higher dose of study drug than the dose they received in their initial cohort. The mean number of intrapatient dose escalations (increases by 50 to 400 mg daily), ranged from 4.3 to 1.5. Therefore, in the first three groups of the initial-dose cohort, the patients in each group who reported having adverse events may actually have been receiving a higher dose than the amount indicated.

† Laboratory adverse events were reported only if they required therapy, constituted a serious adverse event, were clinically significant, or prompted withdrawal from the study. Other grade 3 or 4 adverse events reported by no more than 3 percent of patients were abdominal pain (3 percent); bone marrow depression, an increase in blood amylase level, and bone pain (2 percent); and febrile neutropenia, subdural or subarachnoid hemorrhage, musculoskeletal pain, and thrombosis (1 percent). ALT denotes alanine aminotransferase, and AST aspartate aminotransferase.

Table 3. Hematologic and Cytogenetic Responses.*

Variable	Total No. of Patients	Hematologic Response					Cytogenetic Response†					
		Active Disease‡	Complete Hematologic Response	Marrow Response	Return to Chronic Phase	Total	Complete Response	Partial Response	Minor Response	Minimal Response	Major Response	Total
		number of patients/total number (percent)										
Transformed CML												
Accelerated phase												
Hematologic disease	46	46	21	3	9	33/46 (72)	6	3	4	9	9 (20)	22 (48)
Clonal evolution only§	10	5	5	NA	NA	5/5 (100)	2	4	1	2	6 (60)	9 (90)
Total	56	51	26	3	9	38/51 (74)	8	7	5	11	15 (27)	31(55)
Blastic phase												
Myeloid	24	24	2	2	6	10/24 (42)	1	4	2	0	5 (21)	7 (29)
Lymphoid	9	9	0	1	2	3/9 (33)	1	0	0	1	1 (11)	2 (22)
Total	33	33	2	3	8	13/33 (39)	2	4	2	1	6 (18)	9 (27)
Chronic-phase CML	17	12	11	NA	NA	11/12 (92)	6	0	0	3	6 (35)	9 (53)

* NA denotes not applicable.
† The cytogenetic response was categorized as follows: complete response, no Ph-positive cells in the bone marrow; partial response, 1 percent to 35 percent Ph-positive cells; minor response, 36 percent to 65 percent Ph-positive cells; and minimal response, 66 percent to 95 percent Ph-positive cells.
‡ Patients had active disease when they entered the study.
§ The presence of clonal evolution is the only criterion for the accelerated-phase designation.

once-daily doses of 600 mg or more, less than 10 percent of patients required a dose escalation. Response rates at the twice-daily doses of 400 and 600 mg were similar.

Among 17 patients with the chronic phase of disease, the median duration of therapy was 4.9 months (range, 1.4 to 9.3), and all of the patients have continued therapy. At the present time, 11 of 12 patients with active disease have had a complete hematologic remission. There were cytogenetic responses in 9 of 17 patients who could be evaluated, including 6 responses that were complete (Table 3). Complete cytogenetic responses were noted in 3 of 12 patients who had hematologic disease at baseline and in 3 of 5 patients who were in complete hematologic remission at the start of therapy (Table 5).

One of 10 patients with Ph-positive ALL (hematologic relapse) had a partial hematologic response, and 1 of 3 patients with Ph-positive ALL and persistent molecular signs of ALL had a complete molecular remission.

SIGNALING MOLECULES

Phosphorylation of AKT, CRKL, STAT1, and STAT5 in all cells was compared at baseline and on day 15 in patients in blastic and accelerated phases of disease whose leukemic cells had phosphorylation of these proteins at baseline and who received 400 or 600 mg of nilotinib twice daily. In all four signaling molecules, there was significantly decreased phosphorylation on day 15 of nilotinib treatment, as compared with that at baseline after adjustment for multiple testing (overall significance level for all comparisons, 0.05). (See the section entitled "Assessment of Biomarker Inhibition" in the Supplementary Appendix.)

ABL MUTATIONS AND RESPONSE TO NILOTINIB

In about 50 percent of samples, a duplicate baseline sample was available for confirmatory analysis of *ABL* mutations by an academic laboratory; the concordance was 100 percent between the central and academic laboratories. A total of 51 *ABL* mutations were observed in 37 of 91 patients who had a baseline assessment for mutational status. Nilotinib was active in patients with and in those without mutations, but there were no significant differences in the response rates between the two groups. (See the section entitled "Assessment of *BCR-ABL* Mutational Status" in the Supplementary Appendix.) Two patients with a T315I muta-

Table 4. Dose Escalation and Hematologic Response in Patients with Accelerated and Blastic Phases of Disease.

Initial Nilotinib Dose	Phase of Disease	Patients in Dose Cohort	Patients Receiving Dose Escalation*	Best Hematologic Response with Dose Escalation
50–200 mg daily	Accelerated	9	8	400 mg daily: 3 patients with complete hematologic response; 1 patient with return to chronic phase 800 mg daily: 1 patient with return to chronic phase 400 mg twice daily: 1 patient with complete hematologic response
	Blastic	11	9	400 mg daily: 1 patient with return to chronic phase 800 mg daily: 2 patients with return to chronic phase
400 mg daily	Accelerated	4	3	400 mg twice daily: 1 patient with marrow response; 2 patients with complete hematologic response
	Blastic	3	3	600 mg daily: 1 patient with return to chronic phase

* Patients with an inadequate response to treatment received an escalation in the dose of nilotinib. A total of 4 of 45 patients in cohorts that received daily doses of nilotinib of 600 mg or more had an escalation in dose, and no responses were observed as a result of the escalations.

tion (one with chronic-phase CML and one with blastic-phase CML) had no response to nilotinib.

DISCUSSION

This phase 1 study of nilotinib defined the dose-limiting toxic effects and the maximum tolerated dose of the drug. We also report adverse events associated with treatment and an assessment of the activity of nilotinib in imatinib-resistant CML. We found that nilotinib has activity in imatinib-resistant CML, including in cases with mutations in the gene that encodes the ABL kinase that cause imatinib resistance.[8-12]

Imatinib therapy has side effects that can be dose-limiting in 10 percent of patients.[23] In this study, nilotinib was not associated with the common toxic effects seen with imatinib (e.g., fluid retention, edema, and weight gain) or with pleural effusions. Frequently noted side effects of nilotinib were mild-to-moderate rashes; transient, clinically insignificant elevations of indirect bilirubin levels; and myelosuppression, which was dose-related and dose-limiting. The method of continuous modified reassessment selected the twice-daily dose of nilotinib of 600 mg as the maximum tolerated dose, but the value of lower doses should be explored, since the 400-mg twice-daily dose appeared to have a response rate similar to that of the 600-mg twice-daily dose and had a better safety profile. The incidence of grade 3 or 4 neutropenia was 22 percent with 600 mg twice daily and 9 percent with 400 mg twice daily; the incidence of increased indirect bilirubinemia was 11 percent with 600 mg twice daily and 3 percent with 400 mg twice daily. The recommended dose of nilotinib for phase 2 studies is 400 mg twice daily, with possible dose escalation to 600 mg twice daily in patients with an inadequate response.

Nilotinib has a serum half-life of 15 hours and thus was initially given as a single daily dose. However, saturation of serum levels was observed with this schedule at doses ranging from 400 to 1200 mg daily. When the schedule was modified to a twice-daily regimen, there were increases of 50 to 80 percent in peak serum levels and in levels in the area under the concentration–time curve at the same total daily dose of nilotinib (Fig. 1). At a steady-state level of twice-daily doses of 400 mg and 600 mg, there was a significant reduction in phosphorylation of AKT, CRKL, STAT1, and STAT5, as compared with levels at baseline.

The rates of hematologic response in patients with resistance to imatinib were 75 percent for patients with the accelerated phase and 39 percent for those with the blastic phase. Cytogenetic response rates in these two phases were 55 percent and 27 percent, respectively. The rate of

Table 5. Response to Nilotinib among Patients with Chronic-Phase CML, According to the Starting-Dose Cohort.*

Nilotinib Dose	Patients with Active Disease	Patients without Active Disease	Complete Hematologic Response†	Cytogenetic Response‡		
				Complete	Minimal	Total
			number of patients (percent)			
400–1200 mg once daily	3	1	3 (100)	2 (50)	0	2 (50)
400 mg twice daily	5	3	5 (100)	3 (38)	2 (25)	5 (63)
600 mg twice daily	4	1	3 (75)	1 (20)	1 (20)	2 (40)
All doses	12	NA	11 (92)	3 (25)	2 (17)	5 (42)
	NA	5	NA	3 (60)	1 (20)	4 (80)

* NA denotes not applicable.
† The rate of complete hematologic response was determined by dividing the number of patients who had a complete hematologic response by the number of patients with active disease at baseline.
‡ No partial or minor cytogenetic responses were noted. The rate of cytogenetic response was determined by dividing the number of patients who had a cytogenetic response by the total number of patients.

complete hematologic response in patients with chronic-phase CML was 92 percent, and the rate of complete cytogenetic response was 35 percent. The disease of all these patients was resistant to imatinib (median dose, 800 mg).

Mutations in the gene that encodes the ABL kinase, a mechanism of resistance to imatinib, were noted in 45 percent of patients. In this study, response rates were similar in patients with and those without such mutations. Two patients with a mutation of T315I did not have a response to nilotinib, as predicted from preclinical studies.[11,12] These findings suggest that nilotinib may overcome mutation-associated resistance to imatinib.

Our results in patients with Ph-positive ALL who did not have a response to imatinib suggest that nilotinib has limited efficacy in this subgroup, since only 2 of 13 such patients had a response to the drug. Therefore, nilotinib may have a limited role in patients with Ph-positive ALL.

We found that nilotinib prolongs the QTcF interval in some patients. One unexplained sudden death was reported beyond the follow-up time analysis. This finding indicates the need for careful monitoring for cardiac events and arrhythmias in all patients who are receiving nilotinib and a strict avoidance of medications that may prolong the QTcF interval.

In summary, nilotinib has a relatively favorable safety profile, and preliminary results obtained with a relatively short follow-up period indicate that the drug is active in CML. Phase 2 studies of nilotinib and other BCR-ABL inhibitors, such as dasatinib,[24] are ongoing in patients with CML.

Supported by a grant from Novartis Pharmaceuticals.

Dr. Kantarjian reports having received lecture fees from Bristol-Myers Squibb and Novartis Pharmaceuticals and research grants from Bristol-Myers Squibb, Novartis Pharmaceuticals, and MGI Pharma; Dr. Giles, research grants from Bristol-Myers Squibb and Novartis Pharmaceuticals; Dr. Bhalla, consulting fees and research grants from Novartis Pharmaceuticals; Dr. Hochhaus, consulting fees and research grants from Novartis Pharmaceuticals, Bristol-Myers Squibb, and Roche and lecture fees from Novartis Pharmaceuticals and Bristol-Myers Squibb; Dr. Griffin, consulting fees and research grants from Novartis Pharmaceuticals and research grants from the National Institutes of Health; Dr. Cortes, research grants from Bristol-Myers Squibb and Novartis Pharmaceuticals; and Dr. Ottmann, consulting fees from Novartis Pharmaceuticals. Drs. Tanaka, Manley, Mietlowski, Dugan, and Alland and Ms. Rae and Ms. Bochiniski report having an equity interest in Novartis Pharmaceuticals and being employees of the company. No other potential conflict of interest relevant to this article was reported.

REFERENCES

1. O'Brien SG, Guilhot F, Larson RA, et al. Imatinib compared with interferon and low-dose cytarabine for newly diagnosed chronic-phase chronic myeloid leukemia. N Engl J Med 2003;348:994-1004.
2. Kantarjian H, Talpaz M, O'Brien S, et al. High-dose imatinib mesylate therapy in newly diagnosed Philadelphia chromosome-positive chronic phase chronic myeloid leukemia. Blood 2004;103:2873-8.
3. Silver RT, Talpaz M, Sawyers CL, et al. Four years of follow-up of 1027 patients with late chronic phase (L-CP), accelerated phase (AP), or blast crisis (BC) chronic myeloid leukemia (CML) treated with imatinib in three large phase II trials. Blood 2004;104:11a. abstract.
4. Towartari M, Yanada M, Usui N, et al. Combination of intensive chemotherapy with imatinib can rapidly induce high-quality complete remission for a majority of pa-

tients with newly diagnosed BCR-ABL–positive acute lymphoblastic leukemia. Blood 2004;104:3507-12.
5. Ottmann OG, Druker BJ, Sawyers CL, et al. A phase 2 study of imatinib in patients with relapsed or refractory Philadelphia chromosome-positive acute lymphoid leukemias. Blood 2002;100:1965-71.
6. Ottmann OG, Wassmann B, Goekbuget N, et al. A randomized trial of imatinib versus chemotherapy induction followed by concurrent imatinib and chemotherapy as first-line treatment in elderly patients with de novo Philadelphia-positive acute lymphoblastic leukemia. Blood 2003;102:226a. abstract.
7. Thomas DA, Faderl S, Cortes J, et al. Treatment of Philadelphia chromosome-positive acute lymphocytic leukemia with hyper-CVAD and imatinib mesylate. Blood 2004;103:4396-407.
8. Verstovsek S, Golemovic M, Kantarjian H, et al. AMN107, a novel aminopyrimidine inhibitor of p190 BCR-ABL activation and of in vitro proliferation of Philadelphia-positive acute lymphoblastic leukemia cells. Cancer 2005;104:1230-6.
9. Golemovic M, Verstovsek S, Giles F, et al. AMN107, a novel aminopyrimidine inhibitor of Bcr-Abl, has in vitro activity against imatinib-resistant chronic myeloid leukemia. Clin Cancer Res 2005;11:4941-7.
10. Weisberg E, Manley PW, Breitenstein W, et al. Characterization of AMN107, a selective inhibitor of native and mutant Bcr-Abl. Cancer Cell 2005;7:129-4. [Erratum, Cancer Cell 2005;7:399.]
11. O'Hare T, Walters DK, Stoffregen EP, et al. In vitro activity of Bcr-Abl inhibitors AMN107 and BMS-354825 against clinically relevant imatinib-resistant Abl kinase domain mutants. Cancer Res 2005;65:4500-5.
12. Manley P, von Bubnoff N, Duyster J, et al. AMN107: inhibitory profile against wild-type and mutant forms of the BCR-ABL tyrosine kinase. Presented at the 96th annual meeting of the American Association for Cancer Research, Anaheim, Calif., April 16–20, 2005. abstract.
13. Faderl S, Talpaz M, Estrov Z, Kantarjian HM. Chronic myelogenous leukemia: biology and therapy. Ann Intern Med 1999;131:207-19.
14. Kantarjian HM, Dixon D, Keating MJ, et al. Characteristics of accelerated disease in chronic myelogenous leukemia. Cancer 1988;61:1441-6.
15. Kantarjian HM, Keating MJ, Talpaz M, et al. Chronic myelogenous leukemia in blast crisis: analysis of 242 patients. Am J Med 1987;83:445-54.
16. Kantarjian H, Sawyers C, Hochhaus A, et al. Hematologic and cytogenetic responses to imatinib mesylate in chronic myelogenous leukemia. N Engl J Med 2002;346:645-52. [Erratum, N Engl J Med 2002;346:1923.]
17. Cortes JE, Talpaz M, Giles F, et al. Prognostic significance of cytogenetic clonal evolution in patients with chronic myelogenous leukemia on imatinib mesylate therapy. Blood 2003;101:3794-800.
18. O'Quigley J, Shen LZ, Gamst A. Two-sample continual reassessment method. J Biopharm Stat 1999;9:17-44.
19. Kantarjian HM, Cortes J, O'Brien S, et al. Imatinib mesylate (STI571) therapy for Philadelphia chromosome-positive chronic myelogenous leukemia in blast phase. Blood 2002;99:3547-53.
20. Cortes J, Talpaz M, O'Brien S, et al. Molecular responses in patients with chronic myelogenous leukemia in chronic phase treated with imatinib mesylate. Clin Cancer Res 2005;11:3425-32.
21. Cohen MH, Johnson JR, Pazdur R. U.S. Food and Drug Administration Drug Approval Summary: conversion of imatinib mesylate (STI571; Gleevec) tablets from accelerated approval to full approval. Clin Cancer Res 2005;11:12-9.
22. Bosma P, Chowdhury J, Bakker C, et al. The genetic basis of the reduced expression of bilirubin UDP-glucuronosyltransferase 1 in Gilbert's syndrome. N Engl J Med 1995;333:1171-5.
23. Deininger M, O'Brien S, Ford JM, Druker BJ. Practical management of patients with chronic myeloid leukemia receiving imatinib. J Clin Oncol 2003;21:4255-6.
24. Talpaz M, Shah NP, Kantarjian H, et al. Dasatinib in imatinib-resistant Philadelphia chromosome–positive leukemias. N Engl J Med 2006;354:2531-41.

Cotreatment with Vorinostat (Suberoylanilide Hydroxamic Acid) Enhances Activity of Dasatinib (BMS-354825) against Imatinib Mesylate–Sensitive or Imatinib Mesylate–Resistant Chronic Myelogenous Leukemia Cells

Warren Fiskus,[1] Michael Pranpat,[1] Maria Balasis,[1] Purva Bali,[1] Veronica Estrella,[1] Sandhya Kumaraswamy,[1] Rekha Rao,[1] Kathy Rocha,[1] Bryan Herger,[1] Francis Lee,[2] Victoria Richon,[3] and Kapil Bhalla[1]

Abstract

Purpose: We determined the effects of vorinostat [suberoylanilide hydroxamic acid (SAHA)] and/or dasatinib, a dual Abl/Src kinase (tyrosine kinase) inhibitor, on the cultured human (K562 and LAMA-84) or primary chronic myelogenous leukemia (CML) cells, as well as on the murine pro-B BaF3 cells with ectopic expression of the unmutated and kinase domain-mutant forms of Bcr-Abl.

Experimental Design: Following exposure to dasatinib and/or vorinostat, apoptosis, loss of clonogenic survival, as well as the activity and levels of Bcr-Abl and its downstream signaling proteins were determined.

Results: Treatment with dasatinib attenuated the levels of autophosphorylated Bcr-Abl, p-CrkL, phospho-signal transducer and activator of transcription 5 (p-STAT5), p-c-Src, and p-Lyn; inhibited the activity of Lyn and c-Src; and induced apoptosis of the cultured CML cells. Combined treatment of cultured human CML and BaF3 cells with vorinostat and dasatinib induced more apoptosis than either agent alone, as well as synergistically induced loss of clonogenic survival, which was associated with greater depletion of Bcr-Abl, p-CrkL, and p-STAT5 levels. Cotreatment with dasatinib and vorinostat also attenuated the levels of Bcr-AblE255K and Bcr-AblT315I and induced apoptosis of BaF3 cells with ectopic expression of the mutant forms of Bcr-Abl. Finally, cotreatment of the primary CML cells with vorinostat and dasatinib induced more loss of cell viability and depleted Bcr-Abl or Bcr-AblT315I, p-STAT5, and p-CrkL levels than either agent alone.

Conclusions: As shown here, the preclinical *in vitro* activity of vorinostat and dasatinib against cultured and primary CML cells supports the *in vivo* testing of the combination in imatinib mesylate–sensitive and imatinib mesylate–resistant CML cells.

The fusion oncogene *bcr-abl* encoded Bcr-Abl tyrosine kinase activates many pro-growth and cell survival mechanisms, which confer resistance to apoptosis (1, 2). These include increased phosphorylation and transactivation by signal transducer and activator of transcription-5 (STAT5), which leads to increased expression of the antiapoptotic Bcl-x_L and Pim-2 protein (3–5), as well as increased Ras/Raf/mitogen-activated protein kinase/extracellular signal–regulated kinase (ERK) kinase/ERK1/2, AKT, and nuclear factor-κB activity (1, 2, 6, 7). Through deregulated AKT activity, Bcr-Abl inhibits the forkhead transcription regulator FOXO3a, which leads to depletion of the cyclin-dependent kinase-2 inhibitor p27 and the BH3 domain-only–containing proapoptotic Bim protein (8–10). Collectively, these molecular perturbations promote cell proliferation and survival and contribute to Bcr-Abl-mediated leukemia transformation of bone marrow progenitor cells. Clinical studies have shown that Bcr-Abl tyrosine kinase remains a therapeutic target in all phases of chronic myelogenous leukemia (CML; ref. 11). Although highly active in inducing clinical and cytogenetic complete remissions in many CML patients, resistance to imatinib mesylate (IM; Gleevec) is an increasing clinical problem in CML, especially in the accelerated phase and blast crisis phase where only short-term responses are observed (11). The major mechanisms of resistance to IM include mutations in the kinase domain of *bcr-abl*, amplification of the *bcr-abl* gene, as well as Bcr-Abl-independent mechanisms of resistance (12–16). Within the Bcr-Abl kinase domain, close to 40 known point mutations have been described. These have been linked to IM resistance in CML (17). The mutations are of two broad categories: those that directly interfere with the ability of IM to bind to the kinase

Authors' Affiliations: [1]Department of Interdisciplinary Oncology, H. Lee Moffitt Cancer Center, Tampa, Florida; [2]Bristol-Myers Squibb Co., Princeton, New Jersey; and [3]Merck & Co., Inc., Boston, Massachusetts

Received 4/21/06; revised 7/3/06; accepted 7/25/06.

The costs of publication of this article were defrayed in part by the payment of page charges. This article must therefore be hereby marked *advertisement* in accordance with 18 U.S.C. Section 1734 solely to indicate this fact.

Requests for reprints: Kapil Bhalla, Interdisciplinary Oncology Program, H. Lee Moffitt Cancer Center and Research Institute, University of South Florida, 12902 Magnolia Drive, MRC 3 East, Room 3056, Tampa, FL 33612. Phone: 813-745-6861; Fax: 813-745-6817; E-mail: bhallakn@moffitt.usf.edu.

doi:10.1158/1078-0432.CCR-06-0980

domain (e.g., T315I) and those that impair the ability of Bcr-Abl to achieve inactive conformation required for binding to IM (e.g., E255K, P-loop mutation; ref. 18). Bcr-Abl mutations impart varying degrees of resistance to IM. Some remain susceptible to higher concentrations of IM whereas others that interfere directly with the binding of Bcr-Abl to IM (e.g., T315I, involving the gatekeeper threonine residue) confer the highest form of resistance to IM (19). These findings highlight the need to develop and test novel anti-Bcr-Abl agents that are more potent than IM and/or are able to override the resistance to IM due to either mutations or amplifications of Bcr-Abl.

BMS-354825 (dasatinib) is a synthetic, small-molecule, thiazole-based, orally bioavailable, ATP-competitive, dual Abl/Src kinase inhibitor (20). Dasatinib has been shown to inhibit the activity of the Src kinase family members c-Src and Lyn (21, 22). Dasatinib is able to bind the active and inactive conformations of Abl and inhibits the tyrosine kinase activity of Bcr-Abl (23, 24). Dasatinib is ~325-fold more potent than IM in inhibiting the activity of Bcr-Abl (25, 26). CrkL is a 39-kDa, tyrosine-phosphorylated adaptor protein, which is involved in hematopoietic and leukemia cell signaling and is an important substrate of Bcr-Abl (27). Inhibition of Bcr-Abl activity in CML cells has been gauged by the decline in the levels of phosphorylated CrkL (13). Importantly, *in vitro* studies have shown that dasatinib is also able to inhibit most clinically significant IM-resistant mutant isoforms of Bcr-Abl, but is ineffective against Bcr-AblT315I due to steric hindrance caused by the side chain of the isoleucine (23, 26). Dasatinib prolongs the survival of mice with IM-resistant, Bcr-Abl-dependent leukemia, but the drug was ineffective against tumors expressing the mutant Bcr-AblT315I (23). In phase I and early phase II studies, dasatinib has been reported to induce complete hematologic and cytogenetic responses in patients with IM-resistant or IM-intolerant chronic phase of CML (28, 29). However, the responses are significantly lower in patients with more advanced phases of CML. Taken together, these findings suggest that to override primary or acquired mechanisms of resistance in advanced phases of CML, dasatinib would have to be combined with novel agents that are not only active against IM-resistant mutant forms of Bcr-Abl but would also be effective in overriding non-Bcr-Abl-dependent mechanisms of IM resistance (30).

Vorinostat [suberoylanilide hydroxamic acid (SAHA)] is a hydroxamic acid–based polar histone deacetylase inhibitor (31). Treatment with hydroxamic acid analogue histone deacetylase inhibitors leads to increased levels of genes involved in cell cycle regulation such as p21 and p27, generation of reactive oxygen species, induction of TNF-related apoptosis-inducing ligand and its death receptors, as well as up-regulation of the levels of the pro-death proteins (e.g., Bax, Bak and Bim; refs. 32–38). These agents are also known to deplete the levels of antiapoptotic proteins (e.g., Bcl-2, Bcl-x_L, X-linked inhibitor of apoptosis, survivin, AKT, and Pim-2) in human leukemia cells (32–38). Collectively, these effects inhibit cell cycle growth, lower the threshold to apoptotic stimuli, and induce apoptosis of CML cells. Recent studies from our laboratory have shown that treatment with the hydroxamic acid analogue histone deacetylase inhibitors alone (e.g., vorinostat, LAQ824, and LBH589) also depleted Bcr-Abl, as well as induced apoptosis and sensitized Bcr-Abl-expressing leukemia cells to apoptosis induced by IM (35–37). By inducing acetylation of heat shock protein 90 (hsp90) through inhibition of histone deacetylase 6, treatment with hydroxamic acid analogue histone deacetylase inhibitors was shown to inhibit the ATP-binding and chaperone function of hsp90 (39). This led to polyubiquitylation, proteasomal degradation, and depletion of hsp90 client proteins, including Bcr-Abl, c-Raf, and AKT (36, 37, 39). Significantly, our studies also showed that treatment with hydroxamic acid analogue histone deacetylase inhibitors reduced the levels of the highly IM-refractory Bcr-AblT315I and induced apoptosis of primary IM-refractory CML blast crisis cells (36, 37). Based on the strong rationale generated by these observations, we determined the combined effects of dasatinib and vorinostat against cultured and primary, IM-sensitive or IM-resistant, human CML cells, including those that expressed Bcr-AblT315I. We also determined the effects of the combination against mouse pro-B BaF3 cells with ectopic expression of the unmutated Bcr-Abl or Bcr-AblE255K and Bcr-AblT315I.

Materials and Methods

Reagents and antibodies. Dasatinib (BMS-354825) was kindly provided by Bristol-Myers Squibb (Princeton, NJ). Vorinostat (SAHA) was kindly provided by Merck (Boston, MA). Monoclonal c-Abl antibody, polyclonal anti-STAT5A/B, polyclonal anti-Lyn, polyclonal anti-c-Src, monoclonal c-Myc, and goat polyclonal anti-Pim-2 were purchased from Santa Cruz Biotechnology (Santa Cruz, CA). Monoclonal anti-p-STAT5, monoclonal anti-p27, monoclonal anti-Bcl-x_L, and monoclonal anti-phosphotyrosine were purchased from BD Biosciences (San Diego, CA). Polyclonal p-AKT was purchased from Biosource, Inc. (Camarillo, CA). Anti–phospho-c-Src and anti–phospho-Lyn were purchased from Cell Signaling Technology (Beverly, MA). Antibodies for the immunoblot analyses of p21, p-CrkL, CrkL, AKT, Bim, Bcl-x_L, and ERK1/2 were obtained as previously described (35–40).

Creation of BaF3/Bcr-Abl, BaF3/Bcr-AblE255K, and BaF3/Bcr-AblT315I cell lines. Mutant Bcr-Abl-containing plasmids were generated by site-directed mutagenesis of pSTARp210Bcr-Abl or pSVNeoBcr-Abl, as previously described (36). Briefly, the p210Bcr-AblE255K and p210Bcr-AblT315I constructs were created by site-directed mutagenesis of a Bcr-Abl-containing pSVNeo construct using a QuikChange II XL kit (Stratagene, Cedar Creek, TX) according to the recommendations of the manufacturer, and the resulting clones were sequenced to confirm the point mutation (41, 42). For nucleofection of the p210 Bcr-Abl constructs into BaF3 cells, 5×10^6 BaF3 cells in 100 μL of Nucleofector solution V (Amaxa, Gaithersburg, MD) were mixed with 5 μg of either p210 Bcr-Abl wild type, p210 Bcr-Abl (T315I), or p210 Bcr-Abl (E255K) in a cuvette and nucleofected using program G-16. Following nucleofection, the cells were incubated at a concentration of 1×10^6/mL in complete RPMI 1640 supplemented with 10% WEHI medium as the source of IL-3, overnight, to recover. Stable transfectants of BaF3 cells expressing the wild-type or mutant form of Bcr-Abl (i.e., T315I or E255K) were maintained in RPMI 1640 supplemented with 10% serum, 1.0 unit/mL penicillin, 1 μg/mL streptomycin, and 0.75 mg/mL G418. Stably expressing cells were then further selected by removal of IL-3. After confirmation of Bcr-Abl expression by immunoblot analysis, cells were used for the studies described below.

Cell lines and cell culture. Bcr-Abl-expressing CML LAMA-84 and K562 cells were obtained and maintained in culture as previously described (35–37). Logarithmically growing cells were exposed to the designated concentrations of dasatinib and/or vorinostat. Following these treatments, cells or cell pellets were washed free of the drug(s) before the conduction of the studies.

Primary CML cells. CML cells from the peripheral blood and/or bone marrow of 11 patients who had met the clinical criteria of

IM-resistant advanced phase of CML were harvested and purified as previously described (35–37). Informed consents were signed by all patients to allow use of their cells for these experiments, as part of a clinical protocol approved by the University of South Florida Institutional Review Board.

Colony growth inhibition. Following treatment with the designated concentrations of dasatinib and/or vorinostat for 48 hours, untreated and drug-treated cells were washed in RPMI 1640. Then, 200 cells treated under each condition were plated in duplicated wells in a 12-well plate containing 1.0 mL of Methocult medium (Stem Cell Technologies, Inc., Vancouver, Canada) per well according to the protocol of the manufacturer. The plates were placed in an incubator at 37°C with 5% CO_2 for 7 days. Following this incubation, colonies consisting of ≥50 cells in each well were counted with an inverted microscope and the percent colony growth inhibition compared with the untreated control cells was calculated.

Cell lysis and protein quantitation. Untreated or drug-treated cells were centrifuged and the cell pellets were resuspended in 200 μL of lysis buffer [1% Triton X-100, 1 mmol/L phenylmethylsulfonyl fluoride, 10 μg/mL leupeptin, 1 μg/mL pepstatin A, 2 μg/mL aprotinin, 20 mmol/L *p*-nitrophenyl phosphate, 0.5 mmol/L sodium orthovanadate, and 1 mmol/L 4-(2-aminoethyl) benzenesulfonylfluoride hydrochloride] and incubated on ice for 30 minutes. The cell lysates were centrifuged and an aliquot of each cell lysate was diluted 1:10 and protein quantitated with a bicinchoninic acid protein quantitation kit (Pierce, Rockford, IL) according to the protocol of the manufacturer.

Western blot analysis. Western blot analyses of Bcr-Abl, p-STAT5, p-CrkL, p-Lyn, p-Src, STAT5, CrkL, c-Src, Lyn, p21, p27, Bcl-x_L, α-tubulin, and β-actin were done on total cell lysates using specific antisera or monoclonal antibodies, as previously described (35–40). The expression level of either β-actin or α-tubulin was used as the loading control for the Western blots.

Immunoprecipitation of Src and Bcr-Abl and immunoblot analysis. Following designated treatments, cells were lysed with the lysis buffer as described above. Bcr-Abl was immunoprecipitated from total cell lysates of untreated and drug-treated cells with a monoclonal anti-c-Abl antibody from Santa Cruz Biotechnology and incubated at 4°C for 1 to 2 hours on a rotator. Prewashed protein-G beads were added to the lysate mixture and incubated overnight at 4°C on a rotator. The immunoprecipitates were washed four times with lysis buffer and eluted from the agarose beads by boiling with 6× SDS sample buffer before immunoblot analysis. Total c-Src was immunoprecipitated from treated or untreated total cell lysates with a rabbit polyclonal antibody from Santa Cruz Biotechnology and incubated at 4°C for 1 to 2 hours on a rotator. Prewashed protein-A beads were added to the lysate mixture and incubated overnight at 4°C on a rotator. The immunoprecipitates were washed and eluted for SDS-PAGE as described above.

Src kinase assay. K562 or LAMA-84 cells (10^7) were treated with dasatinib for 24 hours. One milligram of total cell lysate was used for immunoprecipitation of either Src or Lyn. For immunoprecipitation, 3 μg of anti-v-Src monoclonal antibody (Calbiochem, San Diego, CA) or 5 μg of anti-Lyn (Santa Cruz Biotechnology) were incubated for 3 hours with the total cell lysate on a rotator at 4°C (22, 43). Protein-G beads were added to the lysate-antibody mixture and incubated on a rotator overnight at 4°C. The following day, the agarose beads were washed six times with 500 μL of lysis buffer and once with 500 μL of 1× kinase buffer [100 mmol/L Tris-HCl (pH 7.2), 125 mmol/L $MgCl_2$, 5 mmol/L $MnCl_2$, 2 mmol/L EGTA, 2 mmol/L DTT, and 250 μmol/L Na_3VO_4]. For the kinase reaction, the beads were resuspended in 30 μL of 1× kinase buffer. Ten micrograms of glutathione *S*-transferase–purified Gab1CT and 10 μCi of [γ-^{32}P]ATP (Perkin-Elmer, Boston, MA) were added and the reaction was incubated at 30°C for 15 minutes (43). The kinase reactions were terminated by adding 5 μL of 6× SDS sample buffer and boiling the samples for 5 minutes. The boiled samples were centrifuged briefly to pellet the agarose beads. The proteins were separated by SDS-PAGE, transferred to nitrocellulose, and visualized by autoradiography.

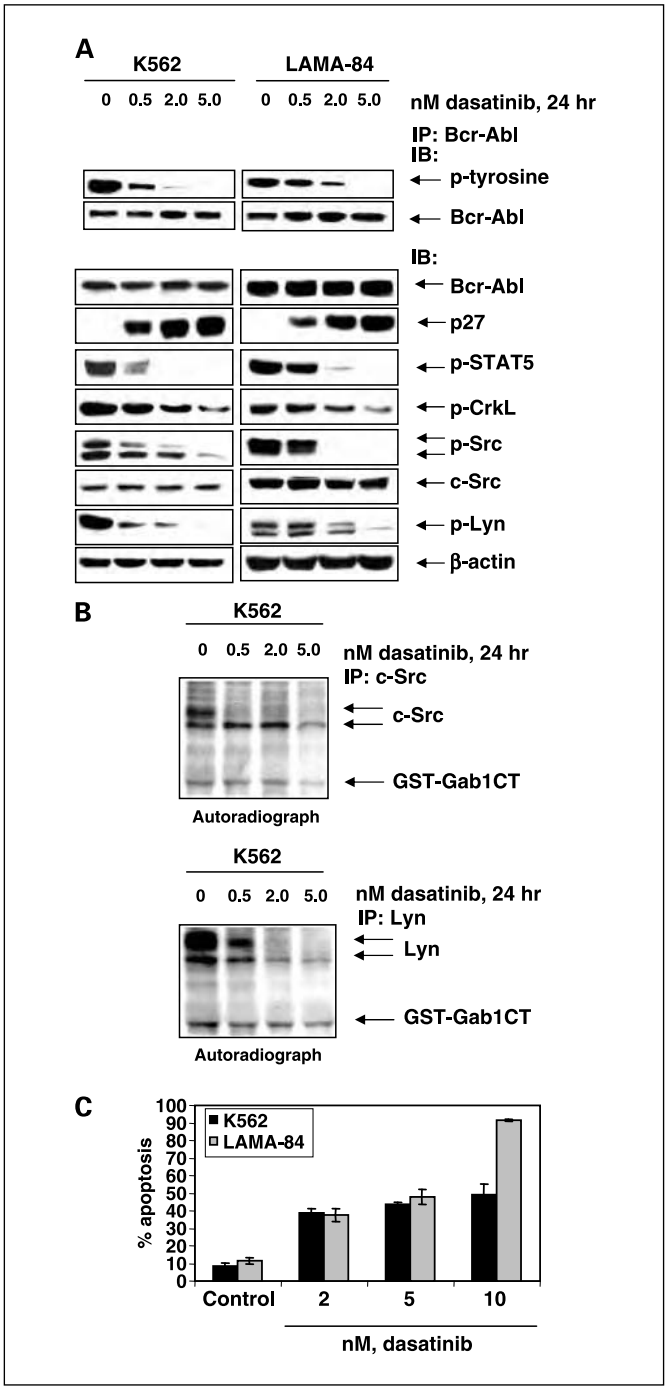

Fig. 1. Treatment with dasatinib diminishes activity of Bcr-Abl and Src family proteins, attenuates the levels of downstream Bcr-Abl targets, and induces apoptosis in cultured CML blast crisis cells K562 and LAMA-84. *A,* K562 and LAMA84 cells were treated with the indicated concentrations of dasatinib for 24 hours. Then, Bcr-Abl was immunoprecipitated from total cell lysates and Western blot analysis was done for tyrosine-phosphorylated Bcr-Abl. The blot was stripped and probed for total Bcr-Abl levels. Immunoblot analysis was done for Bcr-Abl, p-STAT5, p-CrkL, p27, Bcl-x_L, p-Src (Tyr^{416}), p-Lyn, and c-Src from the same lysates. The level of β-actin served as the loading control. *B,* K562 cells were treated with the indicated concentrations of dasatinib for 24 hours. Then, c-Src and Lyn were immunoprecipitated separately from the same cell lysates. Src and Lyn kinase assays were done in the presence of [γ-^{32}P]ATP. After the kinase reactions, proteins were resolved by SDS-PAGE and transferred to nitrocellulose membranes. Autophosphorylation of Src or Lyn and phosphorylation of an exogenous substrate (Gab1CT) were visualized by autoradiography. *C,* K562 and LAMA-84 cells were treated with the indicated concentrations of dasatinib for 48 hours. Following treatment, the percentages of Annexin V–stained apoptotic cells were measured by flow cytometry. Columns, mean of three experiments; bars, SE.

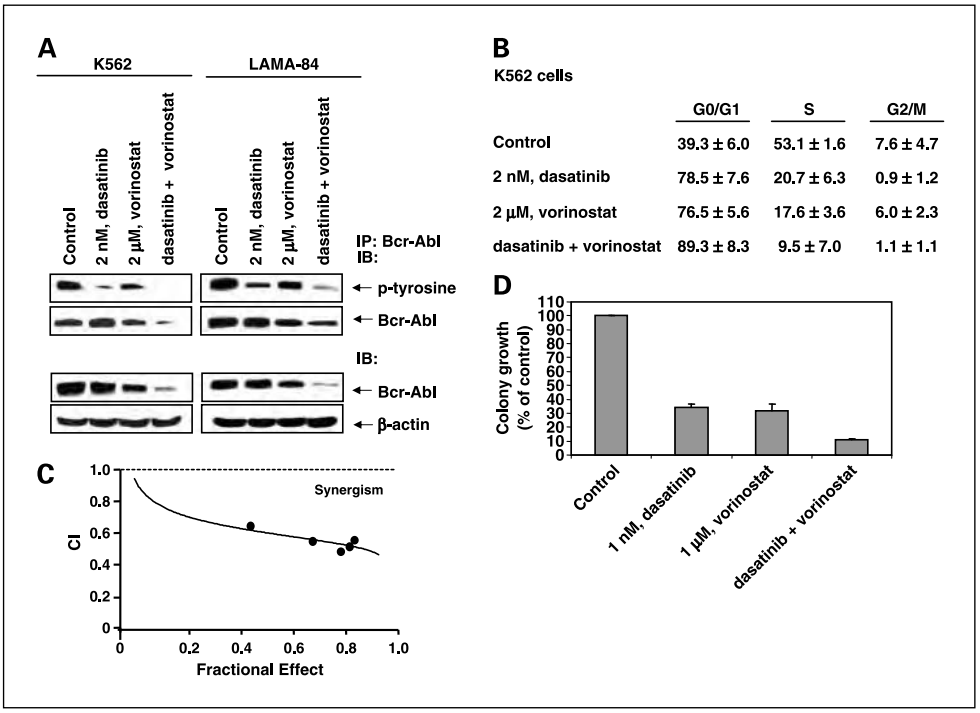

Fig. 2. Cotreatment with dasatinib and vorinostat causes more depletion of Bcr-Abl activity, induces greater cell cycle arrest, inhibits more colony growth than either agent alone, and induces synergistic apoptotic effects. *A,* K562 and LAMA-84 cells were treated with the indicated concentrations of dasatinib and/or vorinostat for 24 hours. Bcr-Abl was immunoprecipitated from the total cell lysates and Western blot analysis was done for tyrosine-phosphorylated Bcr-Abl. The blot was stripped and probed for total Bcr-Abl levels. Immunoblots were done for Bcr-Abl levels on the same cell lysates. The levels of β-actin served as the loading control. *B,* K562 cells were treated with dasatinib and/or vorinostat for 24 hours. Cells were fixed and stained for cell cycle analysis by flow cytometry. *C,* analysis of dose-effect relationship for dasatinib (1-5 nmol/L) and vorinostat (1-5 μmol/L) for the apoptotic effects after 48 hours of exposure was done according to the median effect of Chou and Talalay. Then, the combination index values were calculated. Combination index (*CI*) <1, combination index = 1, and combination index >1 represent synergism, additivity, and antagonism of the two agents, respectively. *D,* K562 cells were treated with the indicated concentrations of dasatinib and/or vorinostat for 48 hours. Then, colony growth in semisolid medium was assessed after 7 days. Columns, mean percent values of untreated control colony growth.

Analysis of cell cycle status. K562 or LAMA-84 cells were treated with dasatinib and/or vorinostat for 24 hours. Cells were washed and fixed in 70% ethanol overnight. Fixed cells were stained with propidium iodide and subjected to flow cytometry and analyses with ModFit 3.0 (35–37).

Assessment of apoptosis by Annexin V staining. Untreated or drug-treated cells were stained with Annexin V (PharMingen, San Diego, CA) and propidium iodide and the percentage of apoptotic cells was determined by flow cytometry (35–37). To analyze synergism between dasatinib and vorinostat in inducing apoptosis, K562 cells were treated with dasatinib (1-5 nmol/L) and vorinostat (1-5 μmol/L) at a constant ratio of 1:1,000 for 48 hours. The percentage of apoptotic cells was determined by flow cytometry. The combination index for each drug combination was obtained by median dose effect of Chou and Talalay using the combination index equation within the commercially available software Calcusyn (Biosoft, Ferguson, MO; ref. 44). Combination index values of <1.0 represent synergism of the two drugs in the combination.

Assessment of percentage of nonviable cells. Cells were stained with trypan blue (Sigma, St. Louis, MO). The numbers of nonviable cells were determined by counting the cells that showed trypan blue uptake in a hemocytometer and reported as percentage of untreated control cells (36, 37).

Results

Dasatinib inhibits Bcr-Abl, c-Src, and Lyn tyrosine kinase activities and induces apoptosis of K562 and LAMA84 cells. As a dual Abl/Src kinase inhibitor, dasatinib is a significantly more potent inhibitor of unmutated Bcr-Abl than Imatinib (IM) and is able to inhibit the activity of nearly all of the mutant forms of Bcr-Abl (23, 25, 26). Although dasatinib has been shown to inhibit ectopically expressed unmutated and mutated Bcr-Abl, the kinase inhibitory effects of dasatinib have not been documented against endogenous Bcr-Abl and c-Src in human CML cells. Therefore, we first determined the kinase inhibitory, cell cycle, and apoptotic effects of dasatinib in the cultured CML K562 and LAMA-84 cells. Figure 1A and B clearly shows that exposure to low nanomolar concentrations of dasatinib inhibits the autophosphorylation of Bcr-Abl and c-Src, as well as depletes the kinase activity of the immunoprecipitated c-Src and Lyn, as measured by the decrease in the phosphorylation of the Gab1CT substrate in the *in vitro* kinase assay (22). Concomitantly, dasatinib attenuated the intracellular levels of p-STAT5, p-CrkL, p-Src, and p-Lyn in a dose-dependent manner. This was accompanied by a striking increase in p27 but a decline in the levels of c-Myc and Bcl-x_L, which are transactivated by STAT5. No significant change occurred in the levels of Bcr-Abl and c-Src or of Lyn, STAT5, and CrkL. Exposure to 2.0 to 10 nmol/L dasatinib also induced apoptosis of K562 and LAMA-84 in a dose-dependent manner, with ~90% apoptosis of LAMA-84 and 50% apoptosis of K562 cells at the 10 nmol/L concentration of dasatinib (Fig. 1C).

Cotreatment with vorinostat and dasatinib exerts synergistic effects in K562 and LAMA-84 cells. In a previous report, we showed that treatment with vorinostat attenuates Bcr-Abl, AKT, and c-Raf levels and induces cell cycle growth arrest and apoptosis of CML cells. Additionally, vorinostat was shown to sensitize CML cells to apoptosis induced by IM (35). Next, we determined the effects of the combined treatment with

vorinostat and dasatinib on cell cycle status, apoptosis, and clonogenic survival of K562 and LAMA-84 cells. As compared with the treatment with vorinostat or dasatinib alone, cotreatment with vorinostat and dasatinib caused more depletion of the levels of autophosphorylated Bcr-Abl (Fig. 2A). Treatment with vorinostat and dasatinib also attenuated Bcr-Abl levels more than treatment with vorinostat alone (Fig. 2A). This was accompanied by marked accumulation of the cells in the G_1 phase and concomitant decline in the percent of cells in the S phase of the cell cycle (Fig. 2B), again more with the combination than with either agent alone. Combined treatment with vorinostat and dasatinib also induced synergistic apoptotic effects against K562 cells, as determined by the median dose-effect isobologram analysis described by Chou and Talalay (Fig. 2C). For dasatinib and vorinostat, the combination index values were <1.0 in all cases. The combination index values were 0.65, 0.55, 0.48, 0.51, and 0.56, respectively. A similar effect was noted against LAMA-84 cells (data not shown). The effects of dasatinib and vorinostat were also determined against normal bone marrow progenitor cells. Whereas dasatinib (up to 20 nmol/L) had no effect, exposure to 2.0 μmol/L vorinostat induced loss of survival of 15.9% of normal bone marrow progenitor cells (mean of two samples with experiments done in duplicate). This loss of survival was not augmented by cotreatment with 20 nmol/L dasatinib (data not shown). We next determined the effects of dasatinib and/or vorinostat on the colony growth of K562 cells. Figure 2D shows that cotreatment with dasatinib and vorinostat caused significantly more inhibition of colony growth than treatment with either drug alone ($P < 0.01$). We also determined whether cotreatment with vorinostat enhances the effects of dasatinib on Bcr-Abl activity and on the downstream pro-growth and pro-survival signaling in K562 and LAMA-84 cells. As shown in Fig. 3, compared with treatment with either agent alone, cotreatment with vorinostat and dasatinib produced a greater decline in the levels of p-CrkL in K562 and LAMA-84 cells. Combined treatment was also highly effective in lowering the levels of Bcl-x_L, p-Src, and p-Lyn. Whereas vorinostat alone induced p21, cotreatment with dasatinib abrogated vorinostat-induced p21 levels.

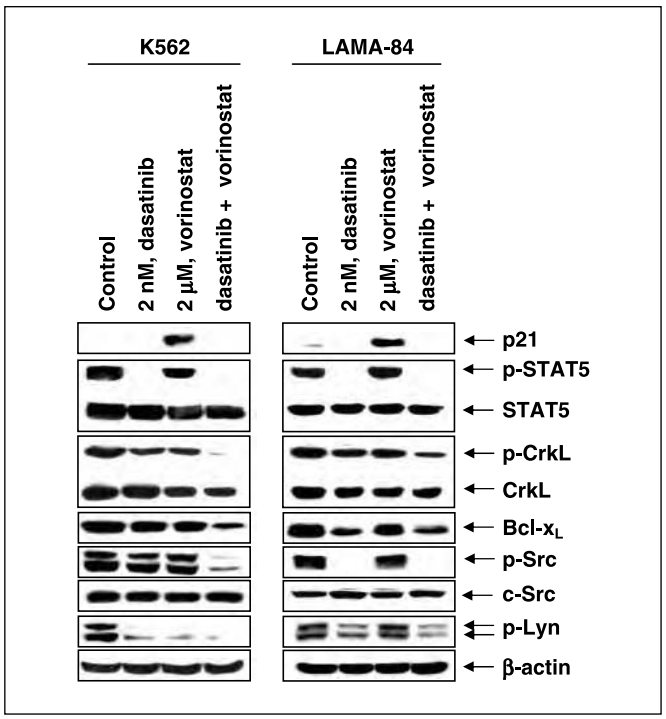

Fig. 3. Cotreatment with dasatinib and vorinostat enhances anti-Bcr-Abl activity and attenuates levels of Bcr-Abl and p-CrkL greater than either agent alone in K562 than in LAMA-84 cells. Following treatment with 2 nmol/L dasatinib and/or 2 μmol/L vorinostat for 24 hours, Western blot analysis of p-STAT5, STAT5, p-CrkL, CrkL, p21, Bcl-x_L, p-Src, p-Lyn, and c-Src was done on total cell lysates from K562 and LAMA-84. The levels of β-actin served as the loading control.

Dasatinib and vorinostat induce apoptosis in BaF3 cells expressing unmutated or mutant Bcr-Abl. Next, we determined the effects of dasatinib and/or vorinostat in BaF3 cells with ectopic expression of either the unmutated Bcr-Abl or the point mutants Bcr-AblE255K or Bcr-AblT315I. Similar to the effects seen in K562 and LAMA-84 with endogenous expression of Bcr-Abl, treatment with 5.0 to 20 nmol/L dasatinib induced apoptosis in BaF3/Bcr-Abl cells in a dose-dependent manner (Fig. 4A). Following treatment with 20 nmol/L dasatinib, >70% of cells showed apoptosis. In contrast, BaF3/Bcr-AblE255K cells were relatively less sensitive to dasatinib-induced apoptosis, showing a dose-dependent increase in apoptosis at higher concentrations of dasatinib (20-2,000 nmol/L; Fig. 4A). BaF3/Bcr-AblT315I cells were resistant to IM up to levels as high as 10 μmol/L (data not shown). BaF3/Bcr-AblT315I-expressing cells were also resistant to apoptosis induced by high levels of dasatinib (2.0 μmol/L). Treatment with dasatinib alone did not lower the levels of Bcr-Abl in BaF3 cells with ectopic expression of either the unmutated Bcr-Abl or the point mutants Bcr-AblE255K or Bcr-AblT315I (Fig. 4B and C). Whereas exposure to 5.0 nmol/L dasatinib markedly inhibited autophosphorylation of the unmutated Bcr-Abl, higher concentration of dasatinib (20 nmol/L) achieved a similar effect against Bcr-AblE255K (Fig. 4B). Similarly, the higher dasatinib levels were required to attenuate p-STAT5 and p-CrkL levels in BaF3/Bcr-AblE255K versus BaF3/Bcr-Abl cells (Fig. 4B). Dasatinib did not appreciably inhibit autophosphorylation of Bcr-Abl (data not shown) or lower p-STAT5 and p-CrkL levels in BaF3/Bcr-AblT315I cells (Fig. 4C). On the other hand, in a dose-dependent manner, vorinostat induced apoptosis not only of BaF3/Bcr-Abl and BaF3/Bcr-AblE255K but also of BaF3/Bcr-AblT315I cells (Fig. 4D). Exposure to 2.0 μmol/L vorinostat resulted in apoptosis of ~40% of BaF3/Bcr-AblE255K cells (Fig. 4D). Notably, treatment with ≥1.0 μmol/L vorinostat induced more apoptosis of BaF3/Bcr-AblT315I than of BaF3/Bcr-Abl cells. This is consistent with previous reports showing that cells expressing the IM-resistant T315I point mutant are more sensitive to hydroxamic acid analogue histone deacetylase inhibitors than unmutated Bcr-Abl-expressing cells (36, 37).

Cotreatment with vorinostat enhances dasatinib-induced apoptosis of IM-resistant BaF3 cells including those expressing Bcr-AblT315I. We also determined the effects of treatment with vorinostat on the levels of Bcr-Abl and downstream signaling targets in BaF3/Bcr-Abl, BaF3/Bcr-AblE255K, and BaF3/Bcr-AblT315I cells. Treatment of the BaF3 transfectants with vorinostat depleted Bcr-AblT315I > Bcr-AblE255K > unmutated Bcr-Abl levels (Fig. 5A). In contrast, exposure to up to 2.0 μmol/L dasatinib had no effect on the unmutated or mutant forms of Bcr-Abl (Fig. 5A, and data not shown). Next, we determined the effects of cotreatment with vorinostat and

dasatinib on the levels of Bcr-Abl in BaF3/Bcr-Abl, BaF3/Bcr-AblE255K, and BaF3/Bcr-AblT315I cells. As compared with treatment with either agent alone, combined treatment with vorinostat and dasatinib markedly depleted the levels of both of the mutant forms of Bcr-Abl in BaF3 cells. Based on the sensitivity to apoptosis with dasatinib noted in Fig. 4A, we used higher concentrations of dasatinib in the combination against BaF3/Bcr-AblE255K and BaF3/Bcr-AblT315I cells (Fig. 5A). Cotreatment with vorinostat and dasatinib, more than either agent alone, also depleted the levels of p-STAT5 and p-CrkL in BaF3 cells with ectopic expression of unmutated Bcr-Abl or of Bcr-AblE255K or Bcr-AblT315I (Fig. 5A). The mechanism underlying the striking decrease in p-STAT5 levels without any change in STAT5 levels is not obvious. However, it may be that cotreatment with the high levels of dasatinib employed in this experiment might render the upstream tyrosine kinase (responsible for phosphorylation of STAT5) more susceptible to depletion due to vorinostat-mediated disruption of the chaperone function of hsp90 for the tyrosine kinase. Additionally, similar to the effects seen in K562 and LAMA-84 cells with endogenous expression of Bcr-Abl, cotreatment with vorinostat and dasatinib versus treatment with either agent alone induced significantly more apoptosis of BaF3/Bcr-Abl cells (Fig. 5B; $P < 0.05$). Notably, combined treatment with vorinostat and dasatinib was also more effective than either agent alone in inducing apoptosis of BaF3/Bcr-AblT315I and BaF3/Bcr-AblE255K cells (Fig. 5C and D). The combination induced apoptosis of ~90% of BaF3/Bcr-AblE255K and 60% of BaF3/Bcr-AblT315I cells (Fig. 5C and D).

Cotreatment with dasatinib and vorinostat exerts superior antileukemia activity against primary IM-resistant CML cells. We next determined the antileukemia effects of dasatinib and/or vorinostat against primary IM-resistant CML cells isolated from the peripheral blood and/or bone marrow from 11 patients who had relapsed with IM-resistant CML blast crisis cells. Two of these samples were documented to express Bcr-AblT315I (samples 10 and 11). In the remaining samples of IM-resistant primary CML cells (samples 1-9), due to inadequate sample size, the mutational status of Bcr-Abl could not be determined. Table 1 indicates that in the samples 1 to 9, dasatinib induced loss of cell viability in a dose-dependent manner. Exposure to 2.0 μmol/L vorinostat alone also induced loss of cell viability in all of the samples, including samples 10 and 11. Notably, whereas in samples 1 to 9, cotreatment with dasatinib and vorinostat induced more loss of cell viability, in samples 10 and 11, addition of dasatinib did not augment the loss of cell viability due to treatment with vorinostat alone. One sample (CML #4) yielded sufficient cells for immunoprecipitation of Bcr-Abl to evaluate the effect of dasatinib and/or vorinostat on autophosphorylation and levels of Bcr-Abl, as well as on levels of p-STAT5 and p-CrkL. As was observed in K562 cells, dasatinib inhibited autophosphorylation of Bcr-Abl without affecting Bcr-Abl levels (Fig. 6A). Treatment with dasatinib also attenuated the levels of p-STAT5 and p-CrkL, with little effect on STAT5 and CrkL levels (Fig. 6A). Whereas exposure of sample no. 4 cells to 2.0 μmol/L vorinostat alone depleted the levels of Bcr-Abl, p-STAT5, and p-CrkL, cotreatment with

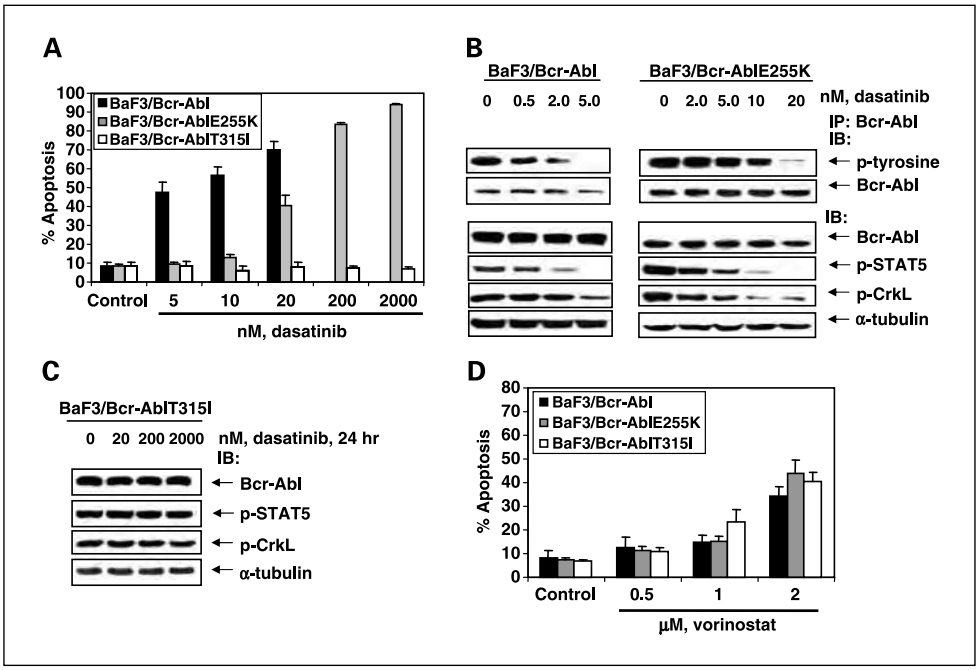

Fig. 4. Treatment with dasatinib depletes Bcr-Abl activity and induces apoptosis of pro-B BaF3 cells with ectopic expression of unmutated or mutant Bcr-AblE255K but not of Bcr-AblT315I. *A,* BaF3 cells with ectopic expression of either unmutated or mutant Bcr-AblE255K or Bcr-AblT315I were treated with the indicated concentrations of dasatinib for 48 hours. After treatment, the percentage of Annexin V – stained apoptotic cells was determined by flow cytometry. Columns, mean of three experiments; bars, SE. *B,* BaF3/Bcr-Abl and BaF3/Bcr-AblE255K cells were treated with the indicated concentrations of dasatinib for 24 hours. Then, Bcr-Abl was immunoprecipitated from total cell lysates and immunoblotted for tyrosine-phosphorylated Bcr-Abl. The blot was stripped and probed for total Bcr-Abl levels. Immunoblot analysis was done for Bcr-Abl, p-STAT5, and p-CrkL in the total cell lysates from the same cells. The level of α-tubulin served as the loading control. *C,* BaF3/Bcr-AblT315I cells were treated with the indicated concentrations of dasatinib for 24 hours. Then, Western blot analysis of Bcr-Abl, p-STAT5, and p-CrkL was done on the total cell lysates. Levels of α-tubulin served as the loading control. *D,* BaF3/Bcr-Abl, BaF3/Bcr-AblE255K, and BaF3/Bcr-AblT315I cells were treated with the indicated concentrations of vorinostat for 48 hours. After treatment, the percentage of Annexin V – stained apoptotic cells was determined by flow cytometry. Columns, mean of three experiments; bars, SE.

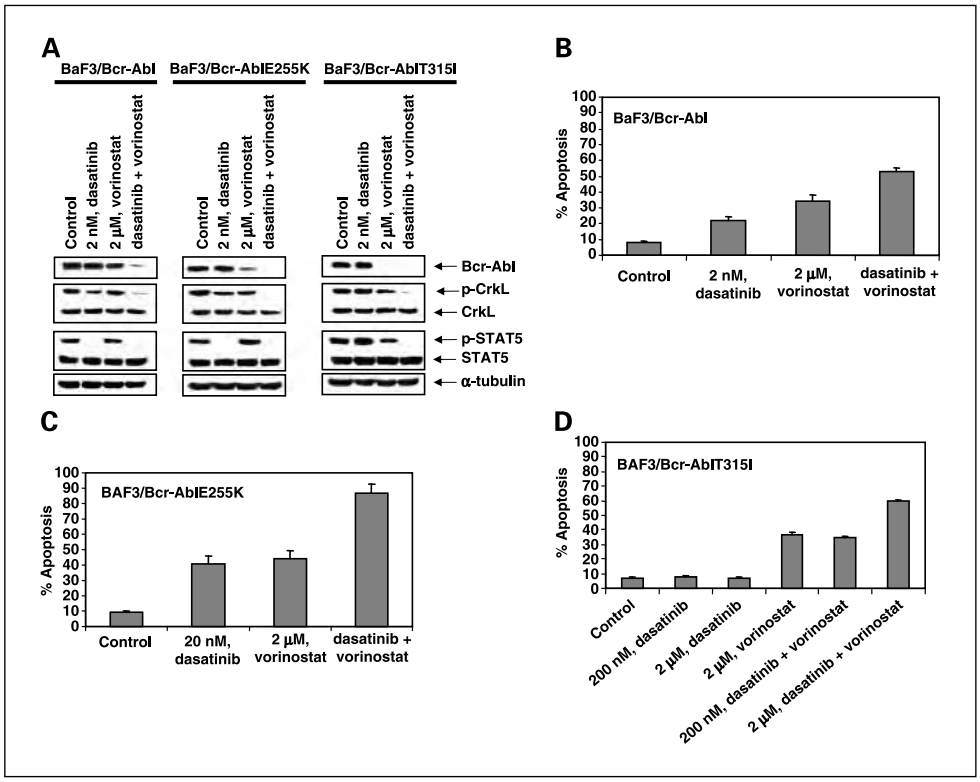

Fig. 5. Cotreatment with dasatinib and vorinostat attenuates Bcr-Abl and p-CrkL levels greater than either agent alone and induces more apoptosis in BaF3/Bcr-Abl BaF3/Bcr-AblE255K and BaF3/Bcr-AblT315I cells. *A,* cells were treated with the indicated concentrations of dasatinib and/or vorinostat for 24 hours. Western blot analysis was done for Bcr-Abl, p-CrkL, CrkL, p-STAT5, and STAT5 on the total cell lysates from each cell line. The levels of α-tubulin served as the loading control. *B* to *D,* BaF3/Bcr-Abl, BaF3/Bcr-AblE255K, and BaF3/Bcr-AblT315I cells were treated with the indicated concentrations of dasatinib and/or vorinostat for 48 hours. Following treatment, the percentage of Annexin V – stained apoptotic cells was determined by flow cytometry. Columns, mean of three experiments done in duplicate; bars, SE.

dasatinib (2 nmol/L) and vorinostat (2.0 μmol/L) was even more effective than treatment with either agent alone in attenuating Bcr-Abl, p-STAT5, and p-CrkL (Fig. 6B). These findings are consistent with the increased lethality exerted against sample no. 4 cells by the combination of dasatinib (2 nmol/L) and vorinostat (2.0 μmol/L; Fig. 6B). Treatment with dasatinib was clearly less effective in depleting the levels of p-STAT5 in the primary versus cultured CML cells. Although the mechanisms underlying this disparity have not been elucidated, it is possible that in primary cells, STAT5 phosphorylation may be mediated by the activity of Src as well as another tyrosine kinase(s), which is not inhibited by dasatinib.

Discussion

Previous reports have separately described the activity of the pan-histone deacetylase inhibitor vorinostat and the dual Abl/Src tyrosine kinase inhibitor dasatinib against Bcr-Abl-expressing human CML cells (25, 26, 35). Here we show for the first

Table 1. Dasatinib and/or vorinostat induces loss of viability of primary CML blast crisis cells

Sample no.	Untreated	% Nonviable cells						
		2 nmol/L, dasatinib	5 nmol/L, dasatinib	10 nmol/L, dasatinib	2 μmol/L, vorinostat	2 nmol/L, dasatinib + vorinostat	5 nmol/L, dasatinib + vorinostat	10 nmol/L, dasatinib + vorinostat
1	2.2	12.4	23.9	33.0	41.6	46.7	56.4	63.5
2	5.0	20.8	24.1	27.5	57.9	64.6	64.4	77.8
3	14.6	24.6	28.0	ND	30.4	44.0	55.7	ND
4	12.8	44.5	49.7	55.8	66.2	80.1	82.6	86.0
5	15.0	32.6	42.7	46.3	43.5	48.3	53.6	56.8
6	10.6	12.0	16.9	25.8	28.0	35.2	38.0	44.7
7	4.2	10.2	16.6	22.4	17.8	24.3	23.4	34.4
8	8.8	11.3	18.0	25.0	26.9	30.0	32.7	35.0
9	6.1	8.9	12.8	16.7	17.3	19.6	24.4	37.3
10*	13.7	13.4	14.0	15.5	35.1	35.4	36.6	37.5
11*	14.7	15.9	14.8	15.8	38.1	47.0	47.2	45.7

NOTE: Peripheral blood or bone marrow from nine IM-resistant or refractory patients and two samples with mutant Bcr-AblT315I (*) were treated with the indicated doses of dasatinib and/or vorinostat for 48 hours. Then, the percentages of nonviable cells for each drug alone or drug combination were determined by trypan blue uptake in a hemocytometer. Values represent the percentage of nonviable cells from each condition as compared with untreated cells.

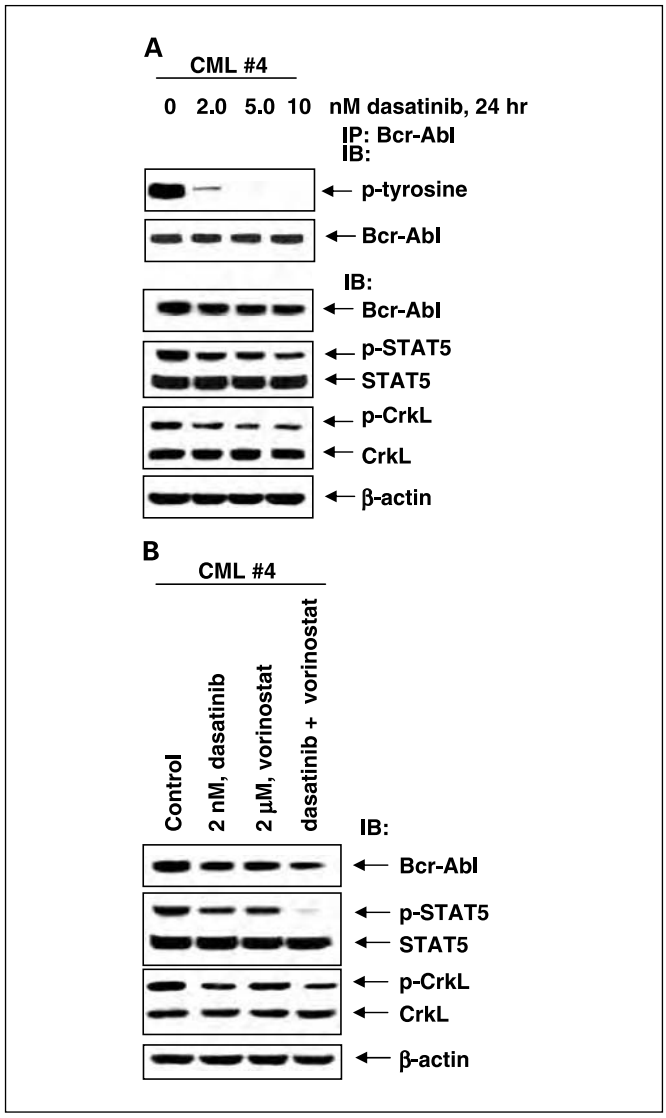

Fig. 6. The effect of dasatinib and/or vorinostat on primary CML blast crisis cells. *A,* primary CML cells were treated with the indicated concentrations of dasatinib for 24 hours. Bcr-Abl was immunoprecipitated from the total cell lysates and immunoblotted for tyrosine-phosphorylated Bcr-Abl. Blots were stripped and probed for total Bcr-Abl levels. Western blot analysis was done for Bcr-Abl, p-STAT5, STAT5, p-CrkL, and CrkL on total cell lysates from the same cells. The levels of β-actin served as the loading control. *B,* CML blast crisis cells were treated with dasatinib and/or vorinostat for 24 hours. After this, Western blot analysis was done for Bcr-Abl, p-STAT5, STAT5, p-CrkL, and CrkL on the total cell lysates. The level of β-actin served as the loading control.

time that combined treatment with vorinostat and dasatinib is significantly more active than either agent alone against human CML cells with endogenous expression of the unmutated Bcr-Abl. Notably, the combination is also more active against BaF3 cells with ectopic expression of Bcr-Abl or its mutant isoforms Bcr-AblE255K or Bcr-AblT315I, as well as against IM-resistant human primary CML cells. Treatment with pan-histone deacetylase inhibitors, including vorinostat, has been shown to inhibit the activity of histone deacetylase 6, which induces the acetylation of hsp90 (39, 40, 45). This inhibits the ATP binding and chaperone function of hsp90, thereby disrupting the association of hsp90 with its client proteins, including Bcr-Abl, c-Raf, and AKT (37, 39). In turn, this promotes polyubiquitylation and proteasomal degradation of the client proteins (46). Vorinostat has also been shown to down-modulate the levels of the Bcl-2 and the inhibitor of apoptosis family member proteins (35, 40). Additionally, treatment with vorinostat up-regulates the levels of Bim, a protein induced by the forkhead family of transcription factors that are repressed by phosphorylation by AKT (8, 10). By attenuating c-Raf and in turn inhibiting the activity of the ERK, which is known to phosphorylate Bim and diminish its association with Bcl-2 and Bcl-x_L, vorinostat also promotes the proapoptotic effects of Bim (47, 48). Collectively, these effects lower the threshold and promote vorinostat-induced apoptosis (49). The reported findings also explain why cotreatment with vorinostat sensitizes BaF3/Bcr-Abl and human CML cells to dasatinib-induced apoptosis. That the combination of vorinostat and dasatinib induces more apoptosis of Bcr-Abl transformed cells is also consistent with several previous reports where cotreatment with a hydroxamic acid analogue histone deacetylase inhibitor and a tyrosine kinase inhibitor, targeting a tyrosine kinase that is a bona fide hsp90 client protein (e.g., Bcr-Abl, Her-2, and FLT-3), was shown to induce more apoptosis than treatment with either agent alone (35, 50, 51). Our findings show that, as compared with treatment with vorinostat alone, cotreatment with dasatinib mediates more depletion of unmutated or mutant Bcr-Abl. Although we do not have any experimental evidence to clarify the mechanism underlying this effect, it is possible that inhibition of Bcr-Abl activity and autophosphorylation may make it more susceptible to polyubiquitylation and proteasomal degradation due to vorinostat-mediated disruption of the chaperone function of hsp90.

Recent studies have suggested that treatment with IM may be ineffective against CML stem cells (17), and acquired resistance to IM due to mutations in the Bcr-Abl kinase domain is a common occurrence (12–15, 17). Amplification and increased expression of Bcr-Abl in CML progenitors may also confer IM resistance (12–14, 30). Dasatinib is clearly a more potent inhibitor than IM of the unmutated Bcr-Abl tyrosine kinase activity, and dasatinib is also able to inhibit most of the mutant forms of Bcr-Abl (23, 26–30). Vorinostat is shown here to not only deplete the levels of the unmutated and mutant forms of Bcr-Abl but also induces apoptosis of CML cells through Bcr-Abl-independent mechanisms. This is important because IM resistance may also be due to the dependence of CML cells for their growth and survival on signaling kinases other than Bcr-Abl (e.g., Lyn or mitogen-activated protein kinase; refs. 16, 52, 53). Therefore, the combination of vorinostat with dasatinib has the potential of overriding many, if not all, of the IM resistance mechanisms in CML progenitor cells. Additionally, based on the multiple mechanism of activity noted above, the combination may also be able to override Bcr-Abl-independent and Bcr-Abl-dependent resistance mechanisms prevalent in the CML stem cells (31, 36, 54). Mutations in the kinase domain of Bcr-Abl conferring IM resistance fall into two main groups: those that inhibit contact with IM and those that prevent Bcr-Abl from achieving the inactive conformation required for the binding of IM to Bcr-Abl. The point mutants Bcr-AblE255K and Bcr-AblT315I have been recognized as the important and common examples of two groups of mutations that confer clinical resistance to IM (12–15). In the E255K mutation, which is located within the ATP-binding region (P-loop) of

the kinase domain of Bcr-Abl, glycine is replaced by lysine (12–14). This results in a significant decrease in the sensitivity of Bcr-AblE255K to IM in the kinase assay and in conferring IM resistance on BaF3/Bcr-AblE255K cells (12–15). In Bcr-Abl, Thr^{315} makes a hydrogen bond contact with IM, and a single-nucleotide change (C to T) that results in a threonine to isoleucine substitution at this residue has been shown to confer high level of resistance not only to IM but also to dasatinib (13, 18, 19). Recent preclinical studies have shown that dasatinib is not only more potent in inhibiting unmutated Bcr-Abl tyrosine kinase but is also active against most of the mutant forms of Bcr-Abl, except Bcr-AblT315I (23–26). It is noteworthy that treatment with hsp90 inhibitors has been reported to induce depletion of the mutant forms of Bcr-Abl and induce growth arrest and apoptosis of IM-resistant CML cells (42, 46). Indeed, mutant forms of Bcr-Abl seem to be more susceptible than unmutated Bcr-Abl to depletion induced by the hsp90 inhibitors (42). A similar observation has also been reported with respect to the mutant versus unmutated forms of other hsp90 client proteins (e.g., FLT-3; ref. 37). Vorinostat-mediated inhibition of the chaperone function of hsp90 may be responsible for the depletion of the Bcr-AblE255K and Bcr-AblT315I levels in dasatinib-treated BaF3/Bcr-AblE255K and BaF3/Bcr-AblT315I cells, respectively.

In early clinical trials, dasatinib has exhibited promising level of clinical activity in IM-resistant CML (28, 30). However, a substantial proportion of patients fail to achieve cytogenetic complete remission, especially in patients with more advanced phases of CML (28, 30, 55). Cells from these patients may harbor additional chromosomal abnormalities and genetic perturbations that often involve the recruitment of corepressors and histone deacetylase activity. This can potentially repress genes involved in differentiation and apoptosis (1, 31, 56, 57). Cotreatment with vorinostat may override these mechanisms and sensitize leukemia cells to dasatinib-induced growth arrest and apoptosis, as was reported in the primary CML blast crisis cells (35). Additionally, cotreatment with vorinostat and dasatinib not only attenuates Bcr-Abl but also depletes the downstream pro-growth and pro-survival signaling molecules, including p-AKT, p-ERK1/2, and p-STAT5. Accordingly, vorinostat may be exerting a "longitudinal" two-step inhibition of the signaling initiated by Bcr-Abl, thus augmenting the growth inhibitory and apoptotic activity of dasatinib against CML blast crisis cells. A similar effect may explain the superior activity of the combination of a mammalian target of rapamycin inhibitor and IM against CML cells (58). Cotreatment with vorinostat and dasatinib also caused more inhibition of p-STAT5, which was associated with more attenuation of the STAT5 target gene products Bcl-x_L and c-Myc (3–5). Bcl-2 family members have been shown to act in a complementary manner to promote Bcr-Abl-mediated induction of leukemia (59, 60). Additionally, our findings show that vorinostat-mediated induction of p21 was blocked by cotreatment with dasatinib. This is consistent with previous reports, which have indicated that p21 induction decreases apoptosis induced by histone deacetylase inhibitor, and interruption of histone deacetylase inhibitor–induced p21 potentiates apoptosis due to treatment with histone deacetylase inhibitor (61). Collectively, more dramatic inhibitory effects on several pro-growth and pro-survival signaling molecules may also contribute to the synergistic apoptotic effects of the combination of vorinostat and dasatinib in the cultured and primary CML cells. Because these findings have not been verified *in vivo*, the clinical significance of these observations remains uncertain.

In the present studies, vorinostat is shown to sensitize BaF3/Bcr-AblE255K and BaF3/Bcr-AblT315I cells to clinically achievable levels of dasatinib. Because, at these levels, dasatinib is able to inhibit the Bcr-Abl tyrosine kinase activity of the mutant Bcr-AblE255K, it is likely that cotreatment with vorinostat enhances this activity of dasatinib not only by depleting the levels of Bcr-AblE255K but also through other downstream mechanisms described above. However, the structural basis for how cotreatment with vorinostat leads to increased activity of relatively high levels of dasatinib (2.0 μmol/L) against the contact inhibitory mutant Bcr-AblT315I is not entirely clear. It is also possible that vorinostat augments Bcr-Abl-independent growth inhibitory and cytotoxic mechanisms of dasatinib against Bcr-AblT315I-expressing cells. However, further studies are needed to characterize these mechanisms. Alternatively, it is conceivable that vorinostat-mediated acetylation and inhibition of hsp90 chaperone function for Bcr-Abl affects its conformation in a manner that allows higher concentrations of dasatinib to interact with and inhibit Bcr-AblT315I (24, 25). In a recent report, the non-ATP-competitive Bcr-Abl kinase inhibitor ON012380 was shown to inhibit the activity of Bcr-AblT315I (62). It would also be important to determine whether cotreatment with vorinostat would further augment the activity of ON012380 against CML cells expressing Bcr-AblT315I.

References

1. Ren R. Mechanisms of BCR-ABL in the pathogenesis of chronic myelogenous leukaemia. Nat Rev Cancer 2005;5:172–83.
2. Melo JV, Deininger MW. Biology of chronic myelogenous leukemia-signaling pathways of initiation and transformation. Hematol Oncol Clin North Am 2004; 18:545–68.
3. Gesbert F, Griffin JD. BCR-ABL activates transcription of the BCL-X gene through STAT5. Blood 2000; 96:2269–76.
4. Hoover RR, Gerlach MJ, Koh EY, Daley GQ. Cooperative and redundant effects of STAT5 and Ras signaling in BCR/ABL transformed hematopoietic cells. Oncogene 2001;20:5826–35.
5. Rascle A, Johnston JA, Amati B. Deacetylase activity is required for recruitment of the basal transcription machinery and transactivation by STAT5. Mol Cell Biol 2003;23:4162–73.
6. Skorski T, Bellacosa A, Nieborowska-Skorska M, et al. Transformation of hematopoietic cells by BCR/ABL requires activation of a PI-3k/Akt-dependent pathway. EMBO J 1997;16:6151–61.
7. Reuther J, Reuther GW, Cortez D, Pendergast AM. A requirement for NFκB activation in Bcr-Abl-mediated transformation. Genes Dev 1998;12:968–81.
8. Essafi A, Fernandez de Mattos S, Hassen YA, et al. Direct transcriptional regulation of Bim by FoxO3a mediates STI571-induced apoptosis in Bcr-Abl-expressing cells. Oncogene 2005;24: 2317–29.
9. Jonuleit T, Van der Kuip H, Miething C, et al. Bcr-Abl kinase down-regulates cyclin-dependent kinase inhibitor p27 in human and murine cell lines. Blood 2000; 96:1933–9.
10. Aichberger KJ, Mayerhofer M, Krauth MT, et al. Low-level expression of proapoptotic Bcl-2-interacting mediator in leukemic cells in patients with chronic myeloid leukemia: role of BCR/ABL, characterization of underlying signaling pathways, and reexpression by novel pharmacologic compounds. Cancer Res 2005;65:9436–44.
11. Druker BJ. Imatinib as a paradigm of targeted therapies. Adv Cancer Res 2004;91:1–30.
12. Gorre ME, Mohammed M, Ellwood K, et al. Clinical resistance to STI-571 cancer therapy caused by Bcr-Abl gene mutation or amplification. Science 2001; 293:876–80.
13. Shah NP, Nicoll JM, Nagar B, et al. Multiple BCR-ABL

kinase domain mutations confer polyclonal resistance to the tyrosine kinase inhibitor imatinib (STI571) in chronic phase and blast crisis chronic myeloid leukemia. Cancer Cell 2002;2:117–25.

14. Shah NP, Sawyers CL. Mechanisms of resistance to STI571 in Philadelphia chromosome-associated leukemias. Oncogene 2003;22:7389–95.

15. Hochhaus A, La Rosee P. Imatinib therapy in chronic myelogenous leukemia: strategies to avoid and overcome resistance. Leukemia 2004;18:1321–31.

16. Donato NJ, Wu JY, Stapley J, et al. Imatinib mesylate resistance through BCR-ABL independence in chronic myelogenous leukemia. Cancer Res 2004;64:672–7.

17. Michor F, Hughes TP, Iwasa Y, et al. Dynamics of chronic myeloid leukaemia. Nature 2005;435:1267–70.

18. Nagar B, Bornmann WG, Pellicena P, et al. Crystal structures of the kinase domain of c-Abl in complex with the small molecule inhibitors PD173955 and imatinib (STI-571). Cancer Res 2002;62:4236–43.

19. Carter TA, Wodicka LM, Shah NP, et al. Inhibition of drug resistant mutants of ABL, KIT, and EGF receptor kinases. Proc Natl Acad Sci U S A 2005;102:11011–6.

20. Lombardo LJ, Lee FY, Chen P, et al. Discovery of *N*-(2-chloro-6-methyl-phenyl)-2-(6-(4-(2-hydroxyethyl)-piperazin-1-yl)-2-methylpyrimidin-4-ylamino)thiazole-5-carboxamide (BMS-354825), a dual Src/Abl kinase inhibitor with potent antitumor activity in preclinical assays. J Med Chem 2004;47:6658–61.

21. Nam S, Kim D, Cheng JQ, et al. Action of the Src family kinase inhibitor, dasatinib (BMS-354825) on human prostate cancer cells. Cancer Res 2005;65:9185–9.

22. Chen Z, Lee FY, Bhalla KN, Wu J. Potent inhibition of platelet-derived growth factor-induced responses in vascular smooth muscle cells by BMS-354825. Mol Pharmacol 2006;69:1527–33.

23. Shah NP, Tran C, Lee FY, Chen P, Norris D, Sawyers CL. Overriding imatinib resistance with a novel ABL kinase inhibitor. Science 2004;305:399–401.

24. Gambacorti-Passerini C, Gasser M, Ahmed S, Assouline S, Scapozza L. Abl inhibitor BMS354825 binding mode in Abelson kinase revealed by molecular docking studies. Leukemia 2005;19:1267–9.

25. Burgess MR, Skaggs BJ, Shah NP, Lee FY, Sawyers CL. Comparative analysis of two clinically active Bcr-Abl kinase inhibitors reveals the role of conformation-specific binding in resistance. Proc Natl Acad Sci U S A 2005;102:3395–400.

26. O'Hare T, Walters DK, Stoffregen EP, et al. *In vitro* activity of Bcr-Abl inhibitors AMN107 and BMS-354825 against clinically relevant imatinib-resistant Abl kinase domain mutants. Cancer Res 2005;65:4500–5.

27. Sattler M, Salgia R. Role of the adapter protein CRKL in signal transduction of normal hematopoietic and BCR/ABL-transformed cells. Leukemia 1998;12:637–44.

28. Sawyers CL, Kantarjian H, Shah N, et al. Dasatinib (BMS-354825) in patients with chronic myeloid leukemia (CML) and philadelphia-chromosome positive acute lymphoblastic leukemia (Ph+ ALL) who are resistant or intolerant to imatinib: update of a phase I study [abstract]. Blood 2005;106:38.

29. Hochhaus A, Baccarani M, Sawyers C, et al. Efficacy of dasatinib in patients with chronic phase philadelphia chromosome-positive CML resistant or intolerant to imatinib: first results of the CA180013 "START-C" phase II study [abstract]. Blood 2005;106:41.

30. Shah NP. Loss of response to imatinib: mechanisms and management. Hematology Am Soc Hematol Educ Program 2005;1:183–7.

31. Kelly WK, Marks PA. Drug insight: histone deacetylase inhibitors—development of the new targeted anticancer agent suberoylanilide hydroxamic acid. Nat Clin Pract Oncol 2005;2:150–7.

32. Bhalla KN. Epigenetic and chromatin modulations for targeted therapy of hematologic malignancies. J Clin Oncol 2005;23:3971–93.

33. Minucci S, Pelicci PG. Histone deacetylase inhibitors and the promise of epigenetic (and more) treatments for cancer. Nat Rev Cancer 2006;6:38–51.

34. Dai Y, Rahmani M, Dent P, Grant S. Blockade of histone deacetylase inhibitor-induced RelA/p65 acetylation and NF-κB activation potentiates apoptosis in leukemia cells through a process mediated by oxidative damage, XIAP down-regulation, and c-Jun N-terminal kinase 1 activation. Mol Cell Biol 2005;25:5429–44.

35. Nimmanapalli R, Fuino L, Stobaugh C, Richon V, Bhalla K. Co-treatment with the histone deacetylase inhibitor suberoylanilide hydroxamic acid (SAHA) enhances imatinib induced apoptosis of Bcr-Abl positive human acute leukemia cells. Blood 2003;101:3236–9.

36. Nimmanapali R, Fuino L, Bali P, et al. Histone deacetylase inhibitor LAQ824 both lowers expression and promotes proteosomal degradation of Bcr-Abl and induces apoptosis of imatinib mesylate-sensitive or -refractory chronic myelogenous leukemia blast crisis cells. Cancer Res 2003;63:5126–35.

37. George P, Bali P, Annavarapu S, et al. Combination of the histone deacetylase inhibitor LBH589 and the hsp90 inhibitor 17-AAG is highly active against human CML-BC cells and AML cells with the activating mutation of FLT-3. Blood 2005;105:1768–76.

38. Guo F, Rocha K, Bali P, et al. Abrogation of heat shock protein 70 induction as a strategy to increase antileukemia activity of heat shock protein 90 inhibitor 17-allylamino-demethoxy geldanamycin. Cancer Res 2005;65:10536–44.

39. Bali P, Pranpat M, Bradner J, et al. Inhibition of histone deacetylase 6 acetylates and disrupts the chaperone function of heat shock protein 90: a novel basis for antileukemia activity of histone deacetylase inhibitors. J Biol Chem 2005;280:26729–34.

40. Bali P, Pranpat M, Swaby R, et al. Activity of suberoylanilide hydroxamic acid against human breast cancer cells with amplification of Her-2. Clin Cancer Res 2005;11:6382–9.

41. La Rosee P, Corbin AS, Stoffregen EP, Deininger MW, Druker BJ. Activity of the Bcr-Abl kinase inhibitor PD180970 against clinically relevant Bcr-Abl isoforms that cause resistance to imatinib mesylate (Gleevec, STI571). Cancer Res 2002;62:7149–53.

42. Gorre ME, Ellwood-Yen K, Chiosis G, Rosen N, Sawyers CL. BCR-ABL point mutants isolated from patients with imatinib mesylate-resistant chronic myeloid leukemia remain sensitive to inhibitors of the BCR-ABL chaperone heat shock protein 90. Blood 2002;100:3041–4.

43. Ren Y, Meng S, Mei L, Zhao ZJ, Jove R, Wu J. Roles of Gab1 and SHP2 in paxillin tyrosine phosphorylation and Src activation in response to epidermal growth factor. J Biol Chem 2004;279:8497–505.

44. Chou TC, Talalay P. Quantitative analysis of dose-effect relationships: the combined effects of multiple drugs or enzyme inhibitors. Adv Enzyme Regul 1984;22:27–55.

45. Kovacs JJ, Murphy PJ, Gaillard S, et al. HDAC6 regulates Hsp90 acetylation and chaperone-dependent activation of glucocorticoid receptor. Mol Cell 2005;18:601–7.

46. Whitesell L, Lindquist SL. HSP90 and the chaperoning of cancer. Nat Rev Cancer 2005;5:761–72.

47. Moller C, Alfredsson J, Engstrom M, et al. Stem cell factor promotes mast cell survival via inactivation of FOXO3a-mediated transcriptional induction and MEK-regulated phosphorylation of the proapoptotic protein Bim. Blood 2005;106:1330–6.

48. Harada H, Quearry B, Ruiz-Vela A, Korsmeyer SJ. Survival factor-induced extracellular signal-regulated kinase phosphorylates BIM, inhibiting its association with BAX and proapoptotic activity. Proc Natl Acad Sci U S A 2004;101:15313–7.

49. Danial NN, Korsmeyer SJ. Cell death: critical control points. Cell 2004;116:205–19.

50. Fuino L, Bali P, Wittmann S, et al. Histone deacetylase inhibitor LAQ824 down-regulates Her-2 and sensitizes human breast cancer cells to trastuzumab, taxotere, gemcitabine, and epothilone B. Mol Cancer Ther 2003;2:971–84.

51. Bali P, George P, Cohen P, et al. Superior activity of the combination of histone deacetylase inhibitor LAQ824 and the FLT-3 kinase inhibitor PKC412 against human acute myelogenous leukemia cells with mutant FLT-3. Clin Cancer Res 2004;10:4991–7.

52. Dai Y, Rahmani M, Pei XY, Dent P, Grant S. Bortezomib and flavopiridol interact synergistically to induce apoptosis in chronic myeloid leukemia cells resistant to imatinib mesylate through both Bcr/Abl-dependent and -independent mechanisms. Blood 2004;104:509–18.

53. Ptasznik A, Nakata Y, Kalota A, Emerson SG, Gewirtz AM. Short interfering RNA (siRNA) targeting the Lyn kinase induces apoptosis in primary, and drug-resistant, BCR-ABL1(+) leukemia cells. Nat Med 2004;10:1187–9.

54. Li S, Hu Y, Swerdlow S, Duffy TM, Weinmann R, Lee FY. Targeting BCR-ABL kinase activity-independent signaling pathways and leukemia stem cells is essential for curative therapy of philadelphia chromosome positive (Ph+) leukemia [abstract]. Blood 2005;106:1990.

55. Talpaz M, Rousselot P, Kim DW, et al. A phase II study of dasatinib in patients with chronic myeloid leukemia (CML) in myeloid blast crisis who are resistant or intolerant to imatinib: first results of the CA180006 "START-B" study [abstract]. Blood 2005;106:40.

56. Calabretta B, Perrotti D. The biology of CML blast crisis. Blood 2004;103:4010–22.

57. Frohling S, Scholl C, Gilliland DG, Levine RL. Genetics of myeloid malignancies: pathogenetic and clinical implications. J Clin Oncol 2005;23:6285–95.

58. Mohi MG, Boulton C, Gu TL, et al. Combination of rapamycin and protein tyrosine kinase (PTK) inhibitors for the treatment of leukemias caused by oncogenic PTKs. Proc Natl Acad Sci U S A 2004;101:3130–5.

59. Jaiswal S, Traver D, Miyamoto T, Akashi K, Lagasse E, Weissman IL. Expression of BCR/ABL and BCL-2 in myeloid progenitors leads to myeloid leukemias. Proc Natl Acad Sci U S A 2003;100:10002–7.

60. Nieborowska-Skorska M, Hoser G, Kossev P, Wasik MA, Skorski T. Complementary functions of the antiapoptotic protein A1 and serine/threonine kinase pim-1 in the BCR/ABL-mediated leukemogenesis. Blood 2002;99:4531–9.

61. Rosato RR, Almenara JA, Yu C, Grant S. Evidence of a functional role for p21WAF1/CIP1 down-regulation in synergistic antileukemic interactions between the histone deacetylase inhibitor sodium butyrate and flavopiridol. Mol Pharmacol 2004;65:571–81.

62. Gumireddy K, Baker SJ, Cosenza SC, et al. A non-ATP-competitive inhibitor of BCR-ABL overrides imatinib resistance. Proc Natl Acad Sci U S A 2005;102:1992–7.

Histone deacetylase inhibitors deplete enhancer of zeste 2 and associated polycomb repressive complex 2 proteins in human acute leukemia cells

Warren Fiskus,[1] Michael Pranpat,[1] Maria Balasis,[1] Bryan Herger,[1] Rekha Rao,[1] Arul Chinnaiyan,[2] Peter Atadja,[3] and Kapil Bhalla[1]

[1]Medical College of Georgia Cancer Center, Augusta, Georgia; [2]Department of Pathology, University of Michigan Medical School, Ann Arbor, Michigan; and [3]Novartis Pharmaceuticals, Inc., Cambridge, Massachusetts

Abstract

Human enhancer of zeste 2 (EZH2) protein belongs to the multiprotein polycomb repressive complex 2, which also includes suppressor of zeste 12 (SUZ12) and embryonic ectoderm development (EED). The polycomb repressive complex 2 complex possesses histone methyltransferase activity mediated by the Su(var)3-9, enhancer of zeste, and trithorax domain of EZH2, which methylates histone H3 on lysine (K)-27 (H3K27). In the present studies, we determined that treatment with the hydroxamate histone deacetylase inhibitor LBH589 or LAQ824 depleted the protein levels of EZH2, SUZ12, and EED in the cultured (K562, U937, and HL-60) and primary human acute leukemia cells. This was associated with decreased levels of trimethylated and dimethylated H3K27, with concomitant depletion of the homeobox domain containing HOXA9 and of MEIS1 transcription factors. Knockdown of EZH2 by EZH2 small interfering RNA also depleted SUZ12 and EED, inhibited histone methyltransferase activity, and reduced trimethylated and dimethylated H3K27 levels, with a concomitant loss of clonogenic survival of the cultured acute myelogenous leukemia (AML) cells. EZH2 small interfering RNA sensitized the AML cells to LBH589-mediated depletion of EZH2, SUZ12, and EED; loss of clonogenic survival; and LBH589-induced differentiation of the AML cells. These findings support the rationale to test anti-EZH2 treatment combined with hydroxamate histone deacetylase inhibitors as an antileukemia epigenetic therapy, especially against AML with coexpression of *EZH2, HOXA9*, and *MEIS1* genes. [Mol Cancer Ther 2006;5(12):3096–104]

Received 7/18/06; revised 9/12/06; accepted 10/30/06.

The costs of publication of this article were defrayed in part by the payment of page charges. This article must therefore be hereby marked advertisement in accordance with 18 U.S.C. Section 1734 solely to indicate this fact.

Requests for reprints: Kapil Bhalla, Medical College of Georgia Cancer Center, 1120 15th Street, CN2101A, Augusta, GA 30912. Phone: 706-721-0463; Fax: 706-721-0469. E-mail: kbhalla@mcg.edu

doi:10.1158/1535-7163.MCT-06-0418

Introduction

During development, the polycomb group (PcG), together with trithorax group of proteins, play an important role in the regulation of expression of homeotic (*HOX*) genes (1, 2). Additionally, deregulated expression and function of PcG proteins has been linked to altered cellular proliferation and cancer (3, 4). PcG proteins function in multimeric protein complexes and repress *HOX* genes (2–4). Two of the best-characterized PcG complexes are the polycomb repressive complex (PRC) PRC1 and PRC2 (2, 3). These complexes localize at specific sites called polycomb repressive elements and organize the chromatin into a repressive structure that is unresponsive to chromatin remodeling factors and basal- and gene-specific transcription factors (2–4). Of the two complexes, PRC2 is smaller and contains the PcG proteins enhancer of zeste 2 (EZH2), embryonic ectoderm development (EED) that serves to recruit to the chromatin the PRC1 complex, suppressor of zeste 12 (SUZ12), Yin Yang 1, and the histone-binding protein RbAp46 (2–5). Recently, within the PRC2, EZH2 was shown to interact with and modulate the DNA methyltransferases DNMT1, DNMT3a, and DNMT3b, which affect their binding to the EZH2 target gene promoters (6, 7). Thus, EZH2 is required for DNA methylation of EZH2-targeted promoters. EZH2 may serve as a recruitment platform for DNA methyltransferases, thereby mechanistically linking the two epigenetic silencing systems (6, 7). EZH2 is crucial during embryonic development, as depletion of EZH2 from developing mouse embryos resulted in severe growth retardation and early embryonic lethality (8, 9). EZH2 contains an evolutionarily conserved, COOH-terminal Su(var)3-9, enhancer of zeste, and trithorax domain, which mediates the histone methyltransferase (HMTase) activity specific for lysine (K)-27 of histone H3 (H3K27) that is associated with gene repression (10–12). Besides its catalytic HMTase domain, EZH2 contains highly conserved NH_2-terminal protein interaction domains responsible for binding to EED and a nuclear localization domain (11). EED recruits HDAC activity to the PRC2 complex (12).

There is accumulating evidence that deregulated expression of PcG proteins is involved in cellular transformation and promotes aggressiveness and high proliferation rates in cancers (13, 14). EZH2 overexpression has been especially linked to aggressive tumor formation and poor prognosis in both prostate and breast cancers (15–18). In a subset of cancers, EZH2 locus is amplified resulting in EZH2 overexpression (16–18). This can promote cellular transformation and confer invasiveness in immortalized breast epithelial cells (16). With SUZ12 and EED, EZH2 has been established as the minimum functional PRC2 core

complex exerting gene silencing through methylation of H3K27 and is transcriptionally regulated by the pRB/E2F pathway (3, 13, 19). Activated p53 has also been shown to suppress EZH2 expression (20). Recently, AKT was shown to phosphorylate EZH2 at Ser^{21} and suppresses its methyltransferase activity by impeding EZH2 binding to histone H3 (21). This results in decreased levels of trimethylated H3K27 and derepression of the silenced genes. EZH2 has also been reported to be up-regulated in mantle cell lymphoma as well as coexpressed with BMI-1 (a polycomb protein in the PRC1 complex) in Reed-Sternberg cells in Hodgkin's disease and non-Hodgkin's lymphoma (22–24). Whereas normal bone marrow plasma cells do not express EZH2, during disease progression in primary multiple myeloma, EZH2 expression is induced and correlates with the tumor burden (25). Additionally, a recent report showed that growth factor independence in multiple myeloma cells with N- or K-Ras mutation requires the activity of EZH2. It was also shown that the *in vivo* oncogenic activity of EZH2 depends on the function of its Su(var)3-9, enhancer of zeste, and trithorax domain (25).

Although overexpression of EZH2 has been reported to increase aggressiveness in the various types of cancers, EZH2 expression has not been evaluated previously in acute leukemia. The PRC2 complex has been shown to bind to the promoter and regulate the expression of *homeobox A9 (HOXA9)*, a gene linked to poor prognosis in acute myelogenous leukemia (AML; ref. 3). HOXA9 is the most frequent partner in a fusion oncoprotein with Nup98 (Nup98-HOXA9), resulting from the chromosomal translocation t(7;11)(p15;p15) observed in human leukemia (26–28). HOXA9 is also known to interact with myeloid ecotropic viral integration site 1 homologue (MEIS1), a member of the three–amino acid loop extension subclass of homeodomain-containing proteins (29). The MEIS1-HOXA9 interaction has been reported to rapidly accelerate leukemogenesis in mice (30–32), making these proteins and their interaction a potential therapeutic target for further evaluation. Additionally, in the PRC2 complex, EZH2 is known to interact with histone deacetylases (HDAC) 1 and 2 through the EED protein (13, 33, 34). This suggests that based on the cellular context, the transcriptional repression by the PRC2 complex may be mediated through the activity of the HDACs (18). Therefore, in the present studies, we determined the effect of the hydroxamate HDAC inhibitors (HA-HDI) LBH589 and LAQ824 on EZH2 and PRC2 complex proteins and their HMTase activity in cultured leukemia cell lines K562, U937, and HL-60 as well as in primary human chronic myelogenous leukemia (CML) and AML cells. We also determined the effects of small interfering RNA (siRNA)–mediated knockdown of EZH2 and/or HA-HDI on EZH2 mRNA and protein levels as well as on the clonogenic survival and differentiation of human AML cells.

Materials and Methods

Reagents

LAQ824 and LBH589 were kindly provided by Novartis Pharmaceuticals, Inc. (East Hanover, NJ). Anti-EZH2 monoclonal antibody was purchased from BD Transduction Laboratories (San Jose, CA). Polyclonal anti-SUZ12, anti-EED, anti-HOXA9, Anti-MEIS1/MEIS2/MEIS3, monoclonal anti–trimethylated H3K27, polyclonal anti–dimethylated H3K27, polyclonal anti–acetylated H3K27, polyclonal anti–acetyl histone H3, and polyclonal anti–acetyl histone H4 antibodies were purchased from Upstate (Lake Placid, NY). Anti-p21 antibody was purchased from NeoMarkers (Fremont, CA). Anti–β-actin was purchased from Sigma-Aldrich (St. Louis, MO). Anti-pRb antibody was purchased from Cell Signaling (Beverly, MA).

Cell Culture

K562, HL-60, and U937 cells were cultured in complete RPMI 1640 and incubated at 37°C with 5% CO_2 as described previously (35). Medium was changed every 2 to 3 days, and cells were passaged at a density of 0.25×10^6/mL. Logarithmically growing cell cultures were used for all experiments described below.

Leukemia Blast Cells

Primary AML and CML cells were obtained with informed consent as part of a clinical protocol approved by the Institutional Review Board of the University of South Florida. As described previously (36, 37), peripheral blood samples were collected in heparinized tubes or obtained from leukophoresis units, and mononuclear cells were separated using Lymphoprep (Axis-Shield, Oslo, Norway), washed once with complete RPMI 1640, resuspended in complete RPMI 1640, and counted to determine the number of cells isolated before their use in the various experiments. The purity of the blast population was confirmed to be 80% or better by morphologic evaluation of cytospun cell preparations stained with Wright stain.

Cell Lysis and Protein Quantitation

Untreated and siRNA or drug treated for 48 h, cells were harvested by centrifugation at 1,000 rpm in a swinging bucket rotor for 5 min. Cell pellets were washed with 1× PBS, gently resuspended in 200 μL lysis buffer [1% Triton X-100, 1 mmol/L phenylmethylsulfonyl fluoride, 10 μg/mL leupeptin, 1 μg/mL pepstatin-A, 2 μg/mL aprotinin, 20 mmol/L *p*-nitrophenyl phosphate, 0.5 mmol/L sodium orthovanadate, 1 mmol/L 4-(2-aminoethyl) benzenesulfonylfluoride hydrochloride], and incubated on ice for 30 min as described previously (38). Cell lysates were centrifuged at 12,000 rpm in a tabletop centrifuge for 15 min to remove the nuclear and cellular debris. An aliquot of each cell lysate was diluted 1:10 and quantitated using a bicinchoninic acid protein quantitation kit according to the manufacturer's protocol. Known concentrations of bovine serum albumin were used to establish a standard concentration curve. Proteins were loaded into a 96-well plate and the plate was incubated at 37°C for 20 to 30 min. Protein concentrations were read on a Bio-Rad (Hercules, CA) plate reader using microplate manager version 5.5.

SDS-PAGE and Western Blotting

One hundred micrograms of total cell lysate were used for SDS-PAGE. Western blot analyses of EZH2; SUZ12; EED; HOXA9; MEIS1; trimethylated, dimethylated, or acetylated H3K27; p21; α-tubulin; and β-actin were done

on total cell lysates using specific antisera or monoclonal antibodies as described previously (35–38). The expression level of either β-actin or α-tubulin was used as the loading control for the Western blots. Blots were developed with a chemiluminescent substrate enhanced chemiluminescence (Amersham Biosciences, Piscataway, NJ).

RNA Interference and Nucleofection

For siRNA-mediated down-regulation of EZH2, an EZH2-specific SMARTPool was purchased from Dharmacon (Lafayette, CO). Nonspecific control siRNA was purchased from Ambion (Austin, TX). All siRNA experiments were done at a final concentration of 100 nmol/L duplex siRNA. For nucleofection into K562, U937, or HL-60 cells, Nucleofector Kit V was used (Amaxa, Gaithersburg, MD). For nucleofection, 5 million low-passage cells were mixed with duplex siRNA, and cell-specific nucleofection program (Amaxa) was used to deliver the siRNA duplex into the nucleus of the cells. Following nucleofection, the cells were incubated overnight for recovery. Following this, cells were treated with HDIs for Western blot analyses or cell cycle effects.

Isolation of Histones

Histones were isolated by a modification of a previously described method (39). After the designated treatments, cells were harvested by centrifugation at 700 × *g* and incubated on ice-cold histone isolation buffer [10 mmol/L Tris-HCl, 50 mmol/L sodium bisulfite, 1% Triton X-100, 10 mmol/L $MgCl_2$, 8.6% sucrose (pH6.5)] on ice for 30 min. Cells were Dounce homogenized using a type B pestle. Released nuclei were pelleted, supernatant was removed, and the nuclei were washed briefly with the histone lysis buffer. The nuclei were resuspended in 100 μL ice-cold H_2O, 1.2 μL of concentrated H_2SO_4 were added, and the tubes were incubated on ice for 1 h. The acid-treated nuclei were centrifuged for 5 min at 15,000 rpm. The supernatants were removed to a clean microcentrifuge tube, and 1 mL acetone was added. Histones were precipitated from the acid extracts overnight at −20°C. The extracted histones were centrifuged briefly at 10,000 rpm, air dried, and resuspended in 50 μL water. Protein concentrations were quantitated as described above. For Western blot, 3 to 5 μg of purified histones were used per condition.

RNA Isolation and Reverse Transcription-PCR

RNA was extracted from the cultured and primary cells using the Trizol method (Invitrogen, Carlsbad, CA). Purified RNA was quantitated and reverse transcribed using SuperScript II according to the manufacturer's protocol (Invitrogen). Resulting cDNAs were used in subsequent PCRs for EZH2, SUZ12, and EED (primer sequences available on request). PCRs for β-actin were used as an internal loading control for the PCRs. PCRs were carried out in a gradient Mastercycler (Eppendorf, Westbury, NY) and consisted of a 3-min denaturation at 95°C followed by 30 cycles of 95°C (30 sec), 52°C (30 sec), and 72°C (30 sec) with a final extension at 72°C (10 min). Amplified products were resolved on a 2% agarose gel and recorded with a UV/VIS gel box. Horizontal scanning densitometry was done with ImageQuant 5.2, and band intensity was compared with β-actin.

Cell Cycle Analysis

Following the designated treatments, cells were harvested and washed twice with 1× PBS and fixed in ethanol overnight. Fixed cells were washed twice with 1× PBS and stained with propidium iodide for 15 min at 37°C. Cell cycle data were collected on a flow cytometer with a 488 nmol/L laser and analyzed with ModFit 3.0 as described previously (35–38).

Colony Culture Assay

Following the designated treatments, cells were harvested and washed twice with 1× PBS and ~500 cells were plated in complete Methocult (Stemcell Technologies, Vancouver, British Columbia, Canada) and cultured for 7 to 10 days at 37°C in a 5% CO_2 environment. Colony growth was measured as a percentage of the control cell colony growth as described previously (38).

Leukemia Cell Differentiation

U937 cells were transfected with siRNA over 48 h as described above. Cells were washed with RPMI 1640 and treated with 5 nmol/L LBH589 for 5 days. Following this, cells were centrifuged at 1,000 rpm for 5 min and resuspended in 100 μL of 5% bovine serum albumin/PBS for 15 min. Following this, 5 μL Alexa 488–conjugated anti-CD11b antibody (BD PharMingen, San Diego, CA) and 10 μL propidium iodide (1:100 dilution) were added, and the cells were incubated on ice for 20 min. The percentage of CD11b-expressing cells was determined by flow cytometry. In addition, the percentage of morphologically differentiated cells was estimated using light microscopy of at least 200 Wright-stained cytospun cells. Morphologic criteria for differentiation included the presence of all of the following features: condensation of chromatin, indentation and lobation of the nucleus, as well as decreased basophilia and increased amount and eosinophilic granulation of the cytoplasm.

Nuclear Extract Preparation and HMTase Activity Assay

K562 cells were transfected with either control or EZH2 siRNA for 48 h. Following this, cells were first washed once with 1× PBS and subsequently washed in 1× PBS containing 10 μmol/L Na_3VO_4 and 50 μmol/L NaF. Cells were lysed in 1× hypotonic buffer, and nuclear extracts were prepared as described previously (40). To determine the HMTase activity, a previously described method was used (41). Five microgram of the nuclear extracts were combined with 2 μL of 5× HMTase buffer [250 mmol/L Tris (pH 9.0), 2.5 mmol/L DTT, 5 mmol/L phenylmethylsulfonyl fluoride; Upstate], 0.55 μCi S-adenosyl-L-methionine, 1 μg recombinant histone H3, and diH_2O up to 10 μL. This mixture was gently mixed and incubated at 30°C for 30 min. Following this, 5 μL of each reaction were transferred to p81 phosphocellulose squares and air dried. The assay squares were washed thrice for 15 min with 10% trichloroacetic acid followed by one wash with 95% ethanol for 5 min. The assay squares were air dried and mixed with scintillation fluid, and the activity was measured with a

scintillations counter. The HMTase activity of the samples was subtracted from the activity of a control sample without the nuclear extract.

Results

LBH589 and LAQ824 Deplete the PRC2 Complex Members EZH2, EED, and SUZ12 in a Dose- and Time-Dependent Manner

We first determined the effects of the pan-HDIs LBH589 and LAQ824 on the levels of the core PRC2 complex components (i.e., EZH2, SUZ12, and EED) in the cultured CML K562 and LAMA-84 cells. Exposure to increasing concentrations of LBH589 or LAQ824 in a dose-dependent manner decreased the levels of EZH2, SUZ12, and EED in K562 cells (Fig. 1A). Whereas the depletion of SUZ12 was pronounced, EED was only modestly depleted (Fig. 1A). These effects were noted even after a 4-h exposure to 100 nmol/L LBH589 (Fig. 1B). Similar effects were observed in the cultured AML U937 cells (Fig. 1C). We next determined the effects of LBH589 and LAQ824 on the PRC2 complex components in primary CML and AML cells. Treatment with LBH589 again depleted EZH2 and SUZ12 more than EED in a sample each of primary CML-BC and AML cells (Fig. 1D and E). Similar effects were observed after exposure to LAQ824 (data not shown).

LBH589 Down-regulates PRC2 Complex–Mediated Histone Modifications and Causes Hyperacetylation of H3K27 and of Histone H4

We next determined whether LBH589-mediated depletion of the components of the PRC2 complex is associated with the loss of H3K27 methyltransferase activity and decreased levels of trimethylated and dimethylated bulk H3K27. K562 cells were treated with LBH589 for 24 h and histones were extracted. As shown in Fig. 2A, exposure to LBH589 depleted the levels of trimethylated and dimethylated H3K27, with concomitant increase in the level of acetylated H3K27, suggesting a possible reciprocal relationship between acetylation and methylation status of H3K27; however, it is possible that these events may be unrelated. As was reported previously, LBH589 also induced the overall lysine acetylation of histone H3 and H4 (36). Similar effects on H3K27 methylation and acetylation were also observed in U937 cells (data not shown). PRC2 complex–mediated methylation of H3K27 is known to regulate the expression of HOXA9. Therefore, we

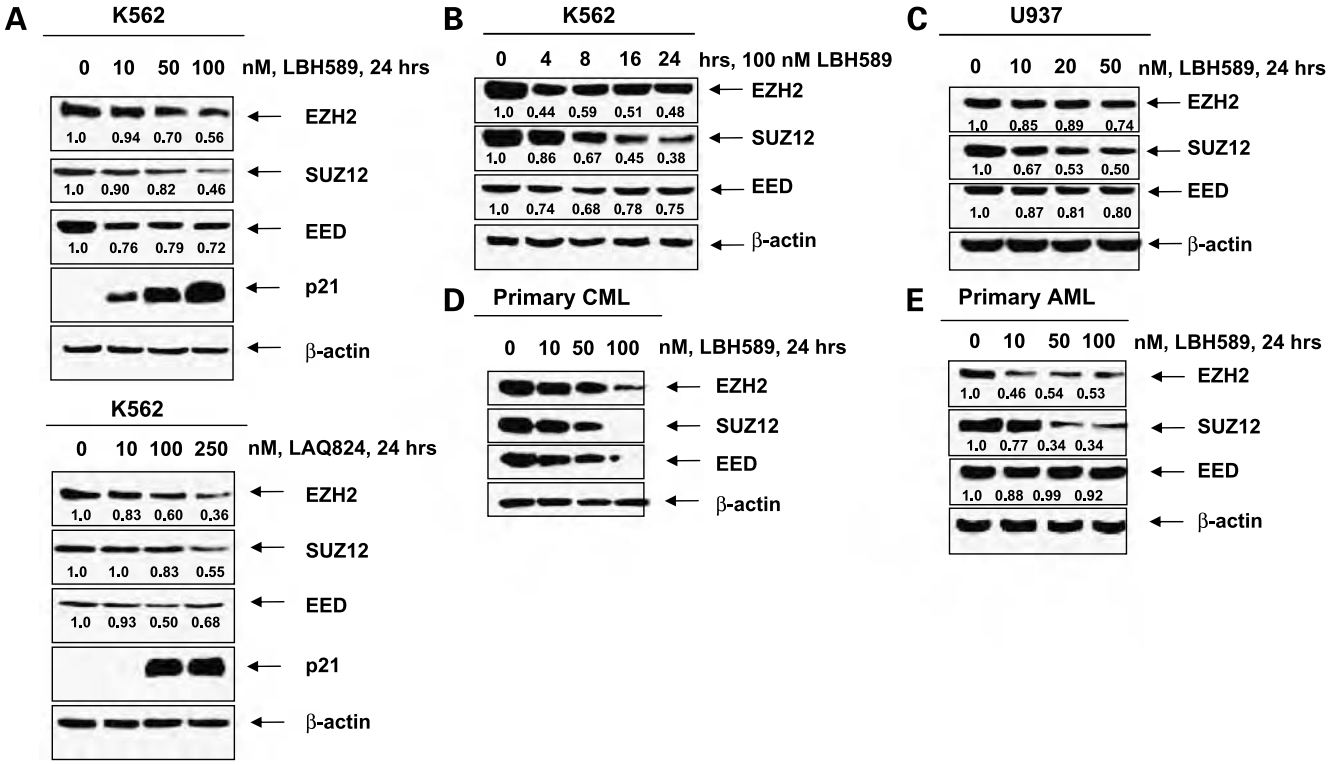

Figure 1. LBH589 and LAQ824 down-regulate members of the PRC2 in a time- and dose-dependent manner in cultured and primary leukemia cells. **A,** Western blot analysis of EZH2, SUZ12, EED, and p21 were done from total cell lysates of K562 cells following a 24-h treatment with the indicated doses of LBH589 or LAQ824. β-Actin levels served as a loading control. **B,** K562 cells were treated with 100 nmol/L of LBH589 for the indicated times and Western blots were done for EZH2, SUZ12, and EED on whole-cell lysates as before. β-Actin levels served as a loading control. **C,** U937 cells were treated with the indicated doses of LBH589 for 24 h. Following this, Western blot analysis was done for EZH2, SUZ12, and EED. The levels of β-actin served as the loading control. **D,** primary CML cells were treated with the indicated doses of LBH589 for 24 h. Immunoblot analysis was done for EZH2, SUZ12, and EED on the total cell lysates. The levels of β-actin served as the loading control. **E,** primary AML cells were treated with the indicated doses of LBH589 for 24 h. Immunoblot analysis was done for EZH2, SUZ12, and EED on cell lysates. The levels of β-actin served as the loading control.

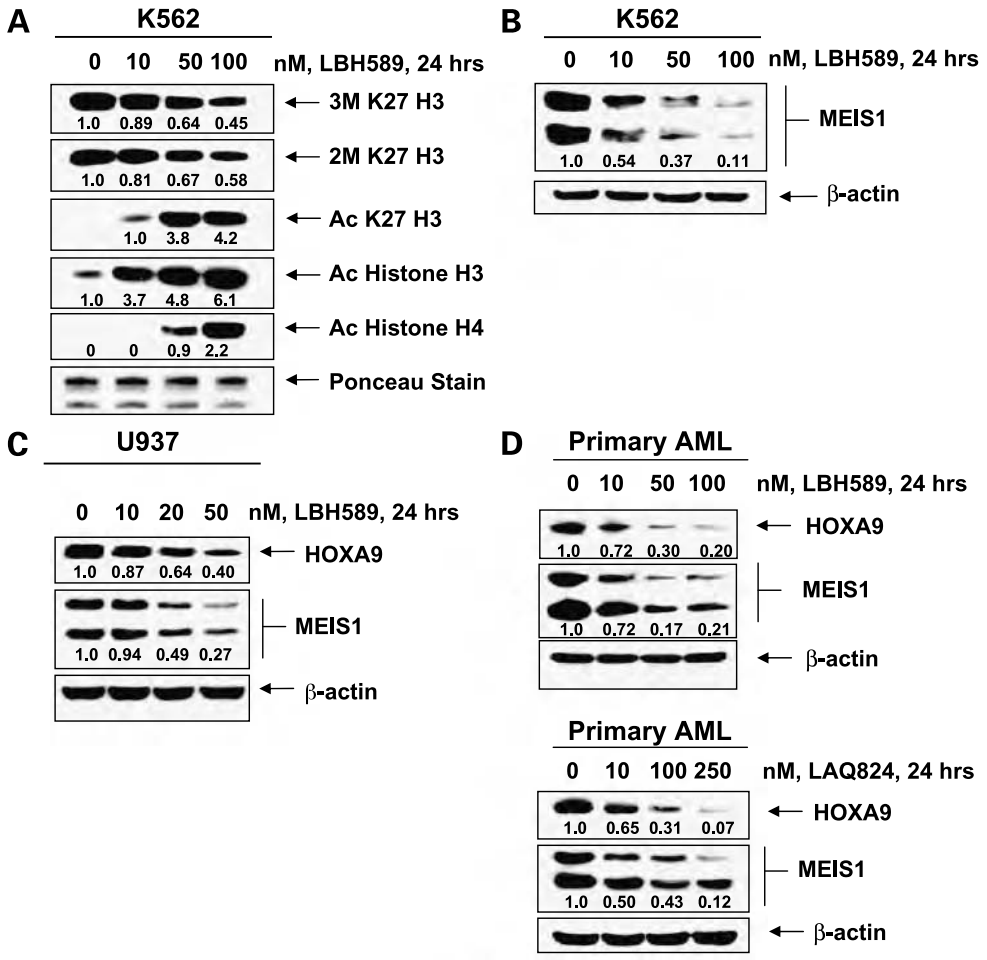

Figure 2. HDIs inhibit H3K27 trimethylation and dimethylation and attenuate levels of HOXA9 and MEIS1 in cultured and primary leukemia cells. **A,** K562 cells were treated with the indicated doses of LBH589 for 24 h. Following this, Western blot analysis for trimethylated H3K27 (*3M K27 H3*), dimethylated H3K27 (*2M K27 H3*), acetylated lysine H3K27 (*Ac K27 H3*), acetyl histone H3 (*Ac histone H3*), and acetyl histone H4 (*Ac Histone H4*) were done on acid-extracted histones. Ponceau-stained histones served as a loading control. **B,** K562 cells were treated with the indicated doses of LBH589 for 24 h. Following treatment, immunoblot analysis was done for MEIS1 and β-actin on the total cell lysates. **C,** U937 cells were treated with the indicated doses of LBH589 for 24 h. Following this, immunoblot analysis was done for HOXA9 and MEIS1 on the total cell lysates. **D,** primary AML cells were treated with the indicated doses of LBH589 or LAQ824 for 24 h. Immunoblot analysis was done for HOXA9 and MEIS1 on the total cell lysates. The levels of β-actin served as the loading control.

determined the effects of LBH589 on HOXA9 as well as on MEIS1 because these two proteins collaborate in the pathogenesis of AML (30, 31). In K562 and U937 cells, exposure to LBH589 in a dose-dependent manner down-regulated HOXA9 and MEIS1 expressions (Figs. 2B and C). LAQ824 exerted a similar effect in U937 cells (data not shown). Both drugs also depleted HOXA9 and MEIS1 levels in two primary AML samples (Fig. 2D).

Treatment with EZH2 siRNA Depletes the Levels of PRC2 Components

We next determined the effects of EZH2 siRNA on PRC2 complex and its activity in K562 cells. Transfection of EZH2 siRNA into the K562 cells resulted in down-regulation of the EZH2 mRNA levels in 24 h by ~60%, without a similar effect on the mRNA levels of SUZ12 or EED (Fig. 3A). However, treatment with EZH2 siRNA not only decreased the protein levels of EZH2 but also resulted in modest depletion of the levels of SUZ12 and EED (Fig. 3A). To determine the combined effects of EZH2 siRNA and treatment with LBH589, we transfected K562 cells with the control or EZH2 siRNA over 48 h with or without the concurrent treatment with 100 nmol/L LBH589 during 24 to 48 h. Exposure to LBH589, along with the control siRNA, again depleted the levels of SUZ12, with less reduction in the levels of EED (Fig. 3B). However, under these conditions of culture, LBH589 was less effective in depleting the levels of SUZ12 and EED. In contrast, cotreatment with LBH589 enhanced EZH2 siRNA–mediated depletion of SUZ12 and EED levels. Concomitantly, siRNA to EZH2 also sensitized the cells to LBH589-mediated induction of p21. Treatment with LAQ824 (250 nmol/L) produced similar effects on the components of the PRC2 complex (data not shown). This suggests that EZH2 siRNA treatment renders K562 cells more sensitive to LBH589- or LAQ824-mediated decline in the levels of EED and SUZ12. We next determined the effects of EZH2 siRNA on HMTase activity in the nuclear extracts of K562 cells. Figure 3C shows that unlike the control siRNA, transfection of EZH2 siRNA produced marked reduction in the H3K27 methyltransferase activity in K562 cells. As was observed following exposure to LBH589, treatment of K562 cells with EZH2 siRNA was also associated with depletion of the levels of trimethylated and dimethylated H3K27, with concomitant increase in the level of acetylated H3K27 (Fig. 3D). We also determined the apoptotic effects of combined treatment of control siRNA or EZH2 siRNA and LBH589. The combination of EZH2 siRNA and LBH589 did not result in greater apoptotic effects than control

siRNA-transfected cells treated with LBH589 (data not shown).

Combined Effects of siRNA to EZH2 and pan-HDIs on PRC2 Complex Components, Differentiation, and Clonogenic Survival of AML Cells

We next determined the effects of treatment with EZH2 siRNA and/or the pan-HDI LBH589 on the levels of the components of the PRC2 complex and clonogenic survival of AML cells. HL-60 and U937 cells were nucleofected with 100 nmol/L control or EZH2 siRNA for 48 h with or without the concurrent treatment with LBH589 during 24 to 48 h. EZH2 siRNA treatment alone depleted the protein levels of EZH2, SUZ12, and EED in AML cells (Fig. 4A and B). As was seen for the CML K562 cells (Fig. 3B), cotreatment with LBH589 enhanced EZH2 siRNA–mediated decline in the levels of EZH2, SUZ12, and EED in U937 (Fig. 4A) and HL-60 cells (Fig. 4B). As compared with treatment with either agent alone, cotreatment with LBH589 and EZH2 siRNA also induced more p21 (Fig. 4A). Whereas treatment with EZH2 siRNA alone induced the expression of HOXA9, combined treatment with LBH589 (25 nmol/L) and EZH2 siRNA depleted HOXA9 and MEIS1 levels in U937 cells (data not shown). Notably, compared with treatment with either agent alone, cotreatment with LBH589 and EZH2 siRNA increased the loss of clonogenic survival of HL-60 and U937 cells (Fig. 4C). We next determined the effect of treatment with EZH2 siRNA and/or LBH589 on the differentiation of U937 cells. Differentiation was assessed by morphologic evaluation of Wright-stained cells and induction of CD11b expression by flow cytometry. Figure 5A and B shows that, compared with treatment of U937 cells with EZH2 siRNA alone, cotreatment with LBH589 and EZH2 siRNA resulted in significantly more CD11b expression and more morphologically differentiated cells ($P < 0.05$). Notably, in the clonogenic survival and differentiation studies, lower concentrations of LBH589 (2.5–5 nmol/L) were used (Figs. 4C and 5).

Discussion

Findings presented here show that treatment with the HA-HDIs LBH589 and LAQ824 or EZH2 siRNA down-regulates EZH2 and the other core components SUZ12 and EED of the PRC2 complex in human acute leukemia cells. This correlated with decreased HMTase activity of EZH2 and reduced trimethylation and dimethylation of H3K27. The protein levels of PRC2 members are in part dependent on the presence of the other partners in the complex and are unstable outside of a functional PRC2

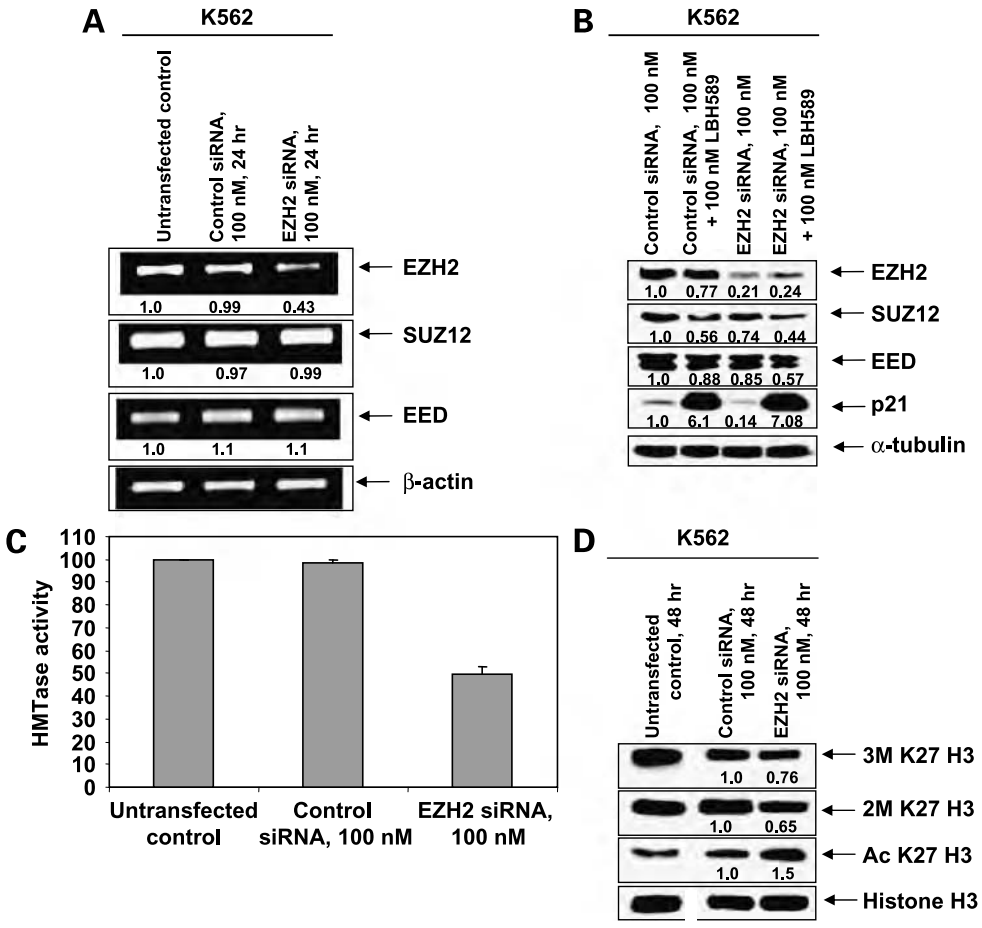

Figure 3. EZH2 siRNA enhances HA-HDI–mediated down-regulation of other PRC2 components, depletes HMTase activity of EZH2, and inhibits trimethylation and dimethylation of histone H3K27 in cultured leukemia cells. **A,** K562 cells were nucleofected with 100 nmol/L of either control siRNA or EZH2 siRNA and incubated for 24 h at 37°C. Total RNA was used for reverse transcription-PCRs of EZH2, SUZ12, and EED. β-Actin–specific reaction served as the loading control for each reaction. **B,** K562 cells were nucleofected with 100 nmol/L of either control siRNA or EZH2 siRNA and incubated for 24 h at 37°C. Twenty-four hours after nucleofection, cells were treated with 100 nmol/L LBH589 and incubated for an additional 24 h. Following this, total cell lysates were used for Western blot analysis of EZH2, SUZ12, EED, MEIS1, and p21. The levels of β-actin were used as the loading control. **C,** K562 cells were nucleofected with 100 nmol/L of either control siRNA or EZH2 siRNA and incubated for 48 h at 37°C. Following this, nuclear extracts were prepared and used for the HMTase activity as described in the text. **D,** K562 cells were left untransfected or nucleofected with 100 nmol/L of either control siRNA or EZH2 siRNA and incubated for 48 h at 37°C. Following this, Western blot analysis was done for trimethylated H3K27, dimethylated H3K27, and acetylated H3K27 on the acid extracted histones. Total histone H3 levels were used as a loading control.

complex (12, 41). Previous studies have also shown that, although it contains the Su(var)3-9, enhancer of zeste, and trithorax domain for HMTase activity for H3K27, to gain catalytic activity EZH2 requires association with SUZ12 and EED (41). Therefore, the depletion of the PRC2 complex components due to treatment with HA-HDI or EZH2 siRNA results in the attenuation of HMTase activity of EZH2 and decreased trimethylation and dimethylation of H3K27 in the leukemia cells. Because EZH2 recruits class I HDACs through their interaction with EED to PRC2 and H3K27 (33), depletion of the PRC2 complex components by EZH2 siRNA and/or HA-HDI also concomitantly promotes the acetylation of H3K27. Whether the mechanism by which the HA-HDIs, such as LBH589, deplete EZH2 levels is transcriptional, post-transcriptional, or increased protein degradation is not described here but is currently under investigation in our laboratory.

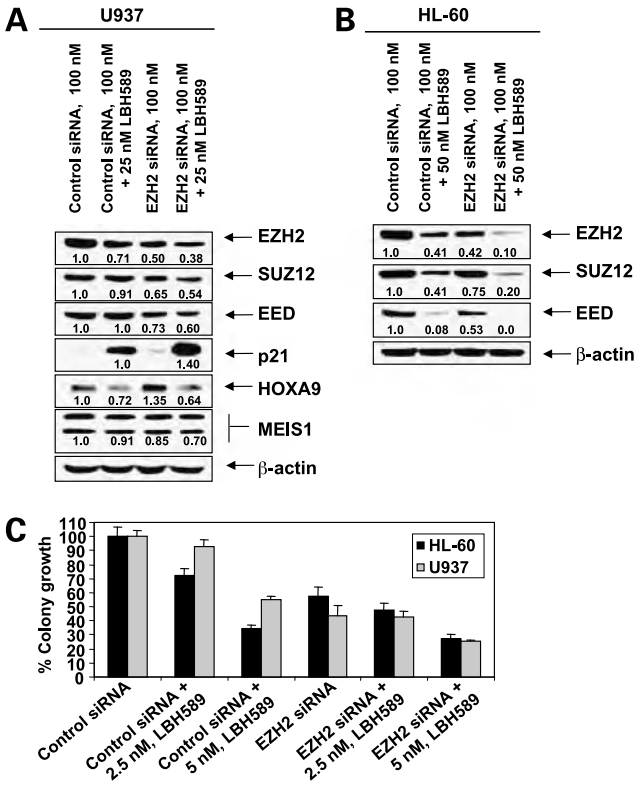

Figure 4. EZH2 siRNA enhances HA-HDI–mediated depletion of the PRC2 complex components and loss of clonogenic survival of AML cells. **A,** U937 cells were transfected with control siRNA or EZH2 siRNA for 24 h followed by a 24-h treatment with 25 nmol/L LBH589. Following this, immunoblot analysis of EZH2, SUZ12, EED, and p21 was done. The levels of β-actin served as the loading control. **B,** HL-60 cells were transfected with control siRNA or EZH2 siRNA for 24 h followed by a 24-h treatment with 50 nmol/L LBH589. Following this, immunoblot analysis of EZH2, SUZ12, and EED was done. The levels of β-actin served as the loading control. **C,** U937 and HL-60 cells were transfected with control or EZH2 siRNA for 24 h. The cells were treated for an additional 24 h with 2.5 or 5.0 nmol/L of LBH589. Cells were washed free of the drug and plated in methylcellulose for 8 d. Following this, the colony growth was determined and expressed as percentage of control colony growth in the bar graphs.

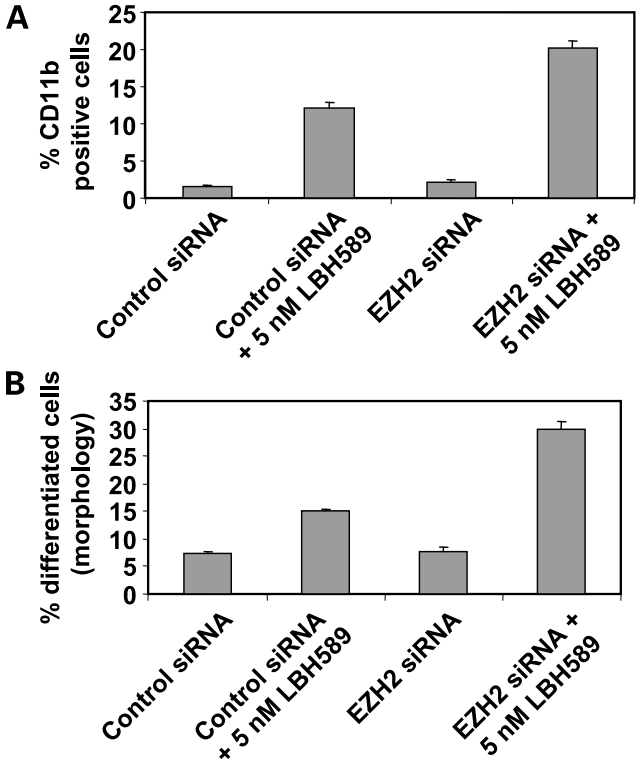

Figure 5. EZH2 siRNA enhances sensitivity to LBH589-mediated differentiation of AML cells. **A,** U937 cells were nucleofected with control or EZH2 siRNA and incubated with 5 nmol/L LBH589 for 5 d. The percentages of differentiated, CD11b-positive cells were determined by flow cytometry. *Columns,* mean of three experiments; *bars,* SE. **B,** alternatively, the percentage of morphologically differentiated cells was determined following Wright staining of cytospun cells. *Columns,* mean of three experiments; *bars,* SE.

EZH2 is often deregulated in many cancer cell types, including prostate, breast, bladder, cutaneous melanoma, and non-Hodgkin's lymphoma (3, 4, 13–18). Although *EZH2* locus is amplified in some cancers (19), EZH2 is also induced by E2F transcription factors (19). Both pRB and p16 repress EZH2 (14, 19). Transcriptionally active p53 has also been shown to suppress EZH2 expression (20). Taken together, these observations explain why EZH2 expression is deregulated in a variety of cancers (14–18). Our preliminary findings show that both cultured and primary AML cells express significant levels of EZH2 protein. This has to be confirmed in a larger sample size of acute leukemia cells. In previous reports, EZH2 overexpression has been shown to increase proliferation, promote invasive potential, and inhibit differentiation (13–17, 34). Notably, EZH2 has oncogenic activity in breast cancer and multiple myeloma cells, where cell transformation and tumor formation requires HMTase activity of EZH2 (16, 25). Conversely, EZH2 down-regulation results in growth arrest and differentiation but not apoptosis (18, 33). In the present studies, we also observed an inhibition of colony growth but not apoptosis of the cultured AML cells following depletion of EZH2 as well as of SUZ12 and EED, by EZH2

siRNA. Treatment with levels of LBH589 and LAQ824 that results in growth arrest, differentiation, and apoptosis was also noted to deplete EZH2, SUZ12, and EED in the CML and AML cells (36, 38). However, the precise mechanistic link between the depletion of the PRC2 complex components and LBH589- or LAQ824-induced growth arrest, differentiation, and loss of clonogenic survival was not established. As noted above, previous reports have shown that EZH2 interacts with and recruits class I HDACs to PRC2 through EED (33). Importantly, EZH2-mediated gene silencing and invasive potential of breast cancers was also noted to be dependent on HDAC activity (16, 18). Our findings are consistent with this in showing that cotreatment with the HA-HDI LBH589 augments EZH2 siRNA–mediated depletion of the PRC2 complex components as well as induction of differentiation. Furthermore, cotreatment LBH589 also enhanced EZH2 siRNA–mediated loss of clonogenic survival of the AML cells.

Although not studied here, the binding to chromatin and gene silencing by PRC1 complex, which consists of >10 subunits, including BMI-1 and the HPC proteins, requires PRC2 complex–mediated trimethylation of H3K27 (6, 42, 43). Notably, PRC1, PRC2, and trimethylated H3K27 cooccupy >1,000 silenced genes, but 40 genes are derepressed in human embryonic fibroblasts depleted of PRC2 components and BMI-1 (44). Of these, HOXA9 is repressed by PRC2 complex–mediated trimethylation of H3K27 and induced by the knockdown of SUZ12 (5). Recently, PRC1 complex has been shown to induce H2AK119 ubiquitin E3 ligase activity, which is associated with the repression of *HOX* genes (45). Therefore, our findings that treatment with EZH2 siRNA, which depletes the levels of PRC2 components and trimethylation of H3K27, increases the levels of HOXA9 is consistent with these reports. In addition, our additional findings that treatment with HA-HDIs depletes HOXA9 levels are also consistent with the previous report that HDAC activity is essential for the expression of HOXA9 and for the endothelial commitment of progenitor cells (46). We further show that treatment with HA-HDIs alone or cotreatment with EZH2 siRNA depleted HOXA9 and MEIS1 levels but induced p21 in the AML cells. This was associated with significantly diminished clonogenic survival but increased differentiation of the AML cells. Transplantation of murine bone marrow cells retrovirally transduced with HOXA9 or the nucleoporin (NUP98)-HOXA9 fusion leads to AML, which is greatly accelerated by the coexpression of *MEIS1* gene (30–32). Therefore, by depleting HOXA9 and MEIS1 levels, cotreatment with EZH2 siRNA and LBH589 may disrupt the biological synergy between the two genes in inducing myeloid leukemia. This suggests that combined treatment with antagonists of PRC2 complex and HA-HDIs may be an attractive targeted therapy against AML with coexpression of HOXA9 and MEIS1.

Whereas BMI-1 is necessary for the self-renewal of hematopoietic stem cells, EZH2 has also been shown to prevent stem cell exhaustion in hematopoietic tissue (47, 48). By down-regulating EZH2 and PRC2, and thereby impairing BMI activity, cotreatment with LBH589 and EZH2 siRNA may also target and deplete leukemia stem cell. However, this has to be directly probed and established. In addition, as noted above, EZH2 can interact with and recruit DNA methyltransferases and thereby promote DNA methylation of EZH2-targeted promoters and their repression (6, 7). Taken together with the findings presented here, these observations create a strong rationale to develop and test the *in vivo* efficacy of a combination of anti-EZH2 and a HA-HDI against AML because this would abrogate three separate mechanisms of epigenetic silencing that promote growth and suppress differentiation. Our preclinical findings support the development of a targeted therapy against EZH2 for AML. This could potentially be of two kinds. One that inhibits the binding of EZH2 with EED, a critical interaction required for EZH2 HMTase activity. The second could be an inhibitor of the COOH-terminal Su(var)3-9, enhancer of zeste, and trithorax domain of EZH2, which mediates the histone lysine methyltransferase activity of the PRC2 complex. This therapeutic strategy has become more attractive, given the recent approval of the DNMT1 inhibitors decitabine and azacytidine for the treatment of advanced stages of myelodysplastic syndromes that often culminate in AML (49).

References

1. Mahmoudi T, Verrijzer CP. Chromatin silencing and activation by polycomb and trithorax group proteins. Oncogene 2001;20:3055–66.
2. Otte A, Kwaks THJ. Gene repression by polycomb group protein complexes: a distinct complex for every occasion? Curr Opin Genet Dev 2003;13:448–54.
3. Jacobs JJ, van Lohuizen M. Polycomb repression: from cellular memory to cellular proliferation and cancer. Biochim Biophys Acta 2002; 1602:151–61.
4. Valk-Lingbeek ME, Bruggerman SWM, van Lohuizen M. Stem cells and Cancer: the polycomb connection. Cell 2004;118:409–18.
5. Cao R, Zhang Y. SUZ12 is required for both the histone methyltransferase activity and silencing function of the Eed/EZH2 complex. Mol Cell 2004;15:57–67.
6. Hernandez-Munoz I, Taghavi P, Kuijl C, Neefjes J, van Lohuizen M. Association of BMI1 with polycomb bodies is dynamic and requires PRC2/EZH2 and the maintenance DNA methyltransferase DNMT1. Mol Cell Biol 2005;25:11047–58.
7. Vire E, Brenner C, Deplus R, et al. The polycomb group protein EZH2 directly controls DNA methylation. Nature 2006;439:871–4.
8. O'Carroll D, Erhardt S, Pagani M, Barton SC, Surani MA, Jenuwein T. The *polycomb*-group gene EZH2 is required for early mouse development. Mol Cell Biol 2001;21:4330–6.
9. Erhardt S, Su IH, Schneider R, et al. Consequences of the depletion of zygotic and embryonic enhancer of zeste 2 during preimplantation mouse development. Development 2003;130:4235–48.
10. Su I, Basavaraj A, Krutchinsky AN, et al. EZH2 controls B cell development through histone H3 methylation and Igh rearrangement. Nat Immunol 2003;4:124–31.
11. Kirmizis A, Bartley SM, Kuzmichev A, et al. Silencing of human polycomb target genes is associated with methylation of histone H3 Lys^{27}. Genes Dev 2004;18:1592–605.
12. Montgomery ND, Yee D, Chen A, et al. The murine polycomb group protein Eed is required for global histone H3 lysine-27 methylation. Curr Biol 2005;15:942–7.
13. Tonini T, Bagella L, D'Andrilli G, Claudio PP, Giordano A. EZH2 reduces the ability of HDAC1-dependent pRb2/p130 transcriptional repression of cyclin A. Oncogene 2004;23:4930–7.
14. Pasini D, Bracken AP, Helin K. Polycomb group proteins in cell cycle progression and cancer. Cell Cycle 2004;3:396–400.

15. Bachmann IM, Halvorsen OJ, Collett K, et al. EZH2 expression is associated with high proliferation rate and aggressive tumor subgroups in cutaneous melanoma and cancers of the endometrium, prostate, and breast. J Clin Oncol 2006;24:268 – 73.

16. Kleer CG, Cao Q, Varambally S, et al. EZH2 is a marker of aggressive breast cancer and promotes neoplastic transformation of breast epithelial cells. Proc Natl Acad Sci U S A 2003;100:11606 – 11.

17. Collett K, Eide GE, Arnes J, et al. Expression of enhancer of zeste homologue 2 is significantly associated with increased tumor cell proliferation and is a marker of aggressive breast cancer. Clin Cancer Res 2006;12:1168 – 74.

18. Varambally S, Dhanasekaran SM, Zhou M, et al. The polycomb group protein EZH2 is involved in progression of prostate cancer. Nature 2002; 419:624 – 9.

19. Bracken AP, Pasini D, Capra M, Prosperini E, Colli E, Helin K. EZH2 is downstream of the pRB-E2F pathway, essential for proliferation, and amplified in cancer. EMBO J 2003;22:5323 – 35.

20. Tang X, Milyavsky M, Shats I, Erez N, Goldfinger N, Rotter V. Activated p53 suppresses the histone methyltransferase EZH2 gene. Oncogene 2004;23:5759 – 69.

21. Cha TL, Zhou BP, Xia W, et al. Akt-mediated phosphorylation of EZH2 suppresses methylation of lysine 27 in histone H3. Science 2005;310: 306 – 10.

22. Visser HPJ, Gunster MJ, Kluin-Nelemans HC, et al. The polycomb group protein EZH2 is upregulated in proliferating, cultured human mantle cell lymphoma. Br J Haematol 2001;112:950 – 8.

23. Raaphorst FM, van Kemenade FJ, Blokzijl T, et al. Coexpression of Bmi-1 and EZH2 polycomb group genes in Reed-Sternberg cells of Hodgkin's disease. Am J Pathol 2000;157:709 – 15.

24. van Kemenade FJ, Raaphorst FM, Blokzijl T, et al. Coexpression of BMI-1 and EZH2 polycomb-group proteins associated with cycling cells and degree of malignancy in B-cell non-Hodgkin lymphoma. Blood 2001; 97:3896 – 901.

25. Croonquist PA, Van Ness B. The polycomb group protein enhancer of zeste homolog 2 (EZH2) is an oncogene that influences myeloma cell growth and the mutant ras phenotype. Oncogene 2005;24: 6269 – 80.

26. Dash AB, Williams IR, Kutok JL, et al. A murine model of CML blast crisis induced by cooperation between BCR/ABL and NUP98/HOXA9. Proc Natl Acad Sci U S A 2002;99:7622 – 7.

27. Iwasaki M, Kuwata T, Yamazaki Y, et al. Identification of cooperative genes for NUP98-9 in myeloid leukemogenesis using a mouse model. Blood 2005;105:784 – 93.

28. Kroon E, Thorsteinsdottir U, Mayotte N, Nakamura T, Sauvageau G. NUP98 – 9 expression in hemopoietic stem cells induces chronic and acute myeloid leukemias in mice. EMBO J 2001;20:350 – 61.

29. Lawrence HJ, Rozenfeld S, Cruz C, et al. Frequent co-expression of the HOXA9 and MEIS1 homeobox genes in human myeloid leukemias. Leukemia 1999;13:1993 – 9.

30. Thorsteinsdottir U, Kroon E, Jerome L, Blasi F, Sauvageau G. Defining roles for HOX and MEIS1 genes in induction of acute myeloid leukemia. Mol Cell Biol 2001;21:224 – 34.

31. Wermuth PJ, Buchberg AM. Meis1-mediated apoptosis is caspase dependent and can be suppressed by co-expression of HoxA9 in murine and human cell lines. Blood 2005;105:1222 – 30.

32. Lawrence HJ, Fischbach NA, Largman C. HOX genes: not just myeloid oncogenes any more. Leukemia 2005;19:1328 – 30.

33. van der Vlag J, Otte AP. Transcriptional repression mediated by the human polycomb-group protein EED involves histone deacetylation. Nat Genet 1999;23:474 – 8.

34. Caretti G, Di Padova M, Micales B, Lyons GE, Sartorelli V. The Polycomb EZH2 methyltransferase regulates muscle gene expression and skeletal muscle differentiation. Genes Dev 2004;18:2627 – 38.

35. Nimmanapalli R, O'Bryan E, Huang M, et al. Molecular characterization and sensitivity of STI-571 (imatinib mesylate, Gleevec)-resistant, Bcr-Abl positive, human acute leukemia cells retain sensitivity to SRC kinase inhibitor PD180970, and 17-allylamino-17-demethoxygeldanomycin (17AAG). Cancer Res 2002;62:5761 – 9.

36. George P, Bali P, Annavarapu S, et al. Combination of the histone deacetylase inhibitor LBH589 and the hsp90 inhibitor 17-AAG is highly active against human CML-BC cells and AML cells with activating mutation of FLT-3. Blood 2005;105:1768 – 76.

37. Nimmanapali R, Fuino L, Bali P, et al. Histone deacetylase inhibitor LAQ824 both lowers expression and promotes proteosomal degradation of Bcr-Abl and induces apoptosis of imatinib mesylate-sensitive or -refractory chronic myelogenous leukemia blast crisis cells. Cancer Res 2003;63:5126 – 35.

38. Fiskus W, Pranpat M, Bali P, et al. Combined effects of novel tyrosine kinase inhibitor AMN107 and histone deacetylase inhibitor LBH589 against Bcr-Abl expressing human leukemia cells. Blood 2006;108: 645 – 52. Epub 2006 Mar 14.

39. Yoshida M, Kijma M, Akita M, Beppu T. Potent and specific inhibition of mammalian histone deacetylase both *in vivo* and *in vitro* by trichostatin A. J Biol Chem 1990;265:17174 – 9.

40. Guo F, Rocha K, Bali P, et al. Abrogation of heat shock protein 70 induction as a strategy to increase antileukemia activity of heat shock protein 90 inhibitor 17-allylamino-demethoxy geldanamycin. Cancer Res 2005;65:10536 – 44.

41. Pasini D, Bracken AP, Jensen MR, Lazzerini Denchi E, Helin K. Suz12 is essential for mouse development and for EZH2 histone methyltransferase activity. EMBO J 2004;23:4061 – 71.

42. Cao R, Wang L, Wang H, et al. Role of histone H3 lysine 27 methylation in polycomb-group silencing. Science 2002;298:1039 – 43.

43. Cao R, Zhang Y. The functions of E(Z)/EZH2-mediated methylation of lysine 27 in histone H3. Curr Opin Genet Dev 2004;14:155 – 64.

44. Bracken AP, Dietrich N, Pasini D, Hansen KH, Helin K. Genome-wide mapping of polycomb target genes unravels their roles in cell fate transitions. Genes Dev 2006;20:1123 – 36.

45. Cao R, Tsukada Y, Zhang Y. Role of Bmi-1 and Ring1A in H2A ubiquitylation and Hox gene silencing. Mol Cell 2005;20:845 – 54.

46. Rossig L, Urbich C, Bruhl T, et al. Histone deacetylase activity is essential for the expression of HoxA9 and for endothelial commitment of progenitor cells. J Exp Med 2005;201:1825 – 35.

47. Lessard J, Sauvageau G. Bmi-1 determines the proliferative capacity of normal and leukaemic stem cells. Nature 2003;423:255 – 60.

48. Kamminga LM, Bystrykh LV, de Boer A, et al. The polycomb group gene Ezh2 prevents hematopoietic stem cell exhaustion. Blood 2006;107: 2170 – 9.

49. Bhalla KN. Epigenetic and chromatin modifiers as targeted therapy of hematologic malignancies. J Clin Oncol 2005;23:3971 – 93.

Leukemia (2006) 20, 1989–1991

www.nature.com/leu

ORIGINAL ARTICLE

Heterogeneity in detecting Abl kinase mutations and better sensitivity using circulating plasma RNA

W Ma[1], H Kantarjian[2], I Jilani[1], M Gorre[1], K Bhalla[3], O Ottmann[4], F Giles[2] and M Albitar[1]

[1]Department of Hematology, Nichols Institute, Quest Diagnostics, San Juan Capistrano, CA, USA; [2]Department of Leukemia, MD Anderson Cancer Center, University of Texas, Houston, TX, USA; [3]Department of Leukemia, H L Moffitt Cancer Center, Tampa, FL, USA and [4]Department of Leukemia, JW Goethe Universitat, Frankfurt, Germany

Most studies test for mutations in the kinase domain of the *abl* gene in chronic myeloid leukemia (CML) using peripheral blood (PB) cells. Frequently, progression of the disease manifests with increased blasts in bone marrow (BM) and not in PB. Simultaneous analysis of plasma, PB cells and BM cells from 41 imatinib-resistent CML patients showed mutations in 63% of PB cells and 68% of plasma or BM cells ($P=0.04$). In discordant patients, 13 mutations were detected in plasma, 11 in BM cells and 9 in PB cells. The T315I mutation was detected in plasma and BM but not PB cells in one patient. We detected no mutations in the plasma of 45 previously untreated CML patients, but two of these patients showed mutations in plasma and not cells by 9 months on therapy. Circulating plasma mRNA is a reliable alternative to BM mRNA for detecting ABL mutations.

Leukemia (2006) **20,** 1989–1991. doi:10.1038/sj.leu.2404355; published online 24 August 2006
Keywords: CML; Abl; kinase; imatinib; mutation; bone marrow

Introduction

Chronic myelogenous leukemia (CML) is caused by chromosomal translocations resulting in a fusion protein, BCR-ABL, with constitutive tyrosine kinase activity. Monotherapy with imatinib, a specific inhibitor of BCR-ABL tyrosine kinase activity, is effective for all stages of CML.[1–3] However, a minority of chronic-phase CML patients and many with advanced disease are initially refractory to imatinib, or develop resistance to it during treatment.[4,5] The most common resistance mechanism is the appearance and clonal selection for point mutations in the ABL kinase domain that partially reduce or completely abrogate the binding affinity of imatinib for its target.[4–7]

It is important to identify what mutations, if any, are present in the BCR-ABL kinase domain of imatinib-resistant patients because the choice of subsequent therapy may depend upon the properties of the mutations present. For example, resistance caused by some mutations that only partially compromise drug binding may be overcome by escalation of the imatinib dose, whereas resistance caused by mutations that completely preclude drug binding, such as T315I, cannot be and will require alternative therapy.[5,8,9] Mutations in the ABL kinase domain are identified by sequencing reverse transcriptase-polymerase chain reaction (RT-PCR) products amplified from BCR-ABL mRNA, which is usually prepared from peripheral blood (PB). This approach assumes that the leukemic cells in PB contain ABL domain mutations that are representative of the total population. However, disease progression in CML patients frequently manifests with increased blasts in bone marrow (BM) rather than in PB. Our previous work has shown that plasma prepared from PB contains tumor-specific DNA, RNA and proteins.[10–13] Therefore, we analyzed whether BCR-ABL kinase-domain mutations detected in plasma correlated with mutations detected in PB and BM cell samples from imatinib-resistant CML patients. Plasma samples from imatinib-sensitive CML patients were also analyzed to assess the reliability of plasma for the detection of mutations during the course of treatment.

Correspondence: Dr M Albitar, Department of Hematopathology, Nichols Institute, Quest Diagnostics, 33608 ortega Highway, Rm#108B, San Juan Capistrano, CA 92690-6130, USA.
E-mail: maher.x.albitar@questdiagnostics.com
Received 15 June 2006; accepted 3 July 2006; published online 24 August 2006

Methods

Parallel BM, PB and plasma samples were obtained from imatinib-resistant CML patients according to IRB-approved protocol. Resistance was defined as failure to achieve or loss of a complete hematologic response after 3 months of therapy or failure or loss of at least a minimal cytogenetic response after 6 months of therapy. Samples were prepared for RT-PCR as described.[7] An 863 bp RT-PCR product encompassing the kinase domain of BCR-ABL was amplified using a forward primer that annealed in BCR exon b2 and a reverse primer that annealed at the junction of ABL exons 9 and 10.[7] The products were sequenced in forward and reverse directions using dye terminator chemistry and an ABI sequencer (Applied Biosystems, Foster City, CA, USA).

Results and discussion

Parallel samples from BM cells, PB cells and plasma from 41 imatinib-resistent CML patients were tested for the presence of mutations in the ABL kinase domain. Mutations in the ABL kinase domain of BCR-ABL were determined by bi-directional sequencing of RT-PCR products. For 33 of 41 (80%) patients, sequencing results were consistent among the three types of samples (Table 1). Only 63% of cases had mutation when PB cells were used, whereas 68% of samples had mutations when plasma or BM cells were used ($P=0.04$). Thirteen of 41 (32%) patients had a wild-type BCR-ABL kinase domain with no amino-acid changes, using the three sample types. Thirteen different amino-acid changes were detected in all three sample types from 20 patients (Table 1). Two of these patients had more than one mutation. Mixed populations of wild-type and mutant kinase domains were detected in all three sample types in six of these 13 cases (46%) (Table 1).

In eight of 41 (20%) imatinib-resistant patients, discordance in detecting ABL kinase mutations was noted between BM cells,

Table 1 Results of BCR-ABL mutation in BM cells, PB cells and plasma samples from imatinib-resistant CML patients

No. of patients	*BM*	*Plasma*	*PB*
Concordant results			
13	None	None	None
2	M244V	M244V	M244V
3	G250E	G250E	G250E
1	G250E, F359I	G250E, F359I	G250E, F359I
1	G250E, F359V	G250E, F359V	G250E, F359V
1	Y253F	Y253F	Y253F
1	F311I	F311I	F311I
1	F311L	F311L	F311L
2	T315I	T315I	T315I
1	F317L	F317L	F317L
1	L324Q	L324Q	L324Q
1	M351T	M351T	M351T
3	F359V	F359V	F359V
1	L387M	L387M	L387M
1	K459Q	K459Q	K459Q
Discordant results			
1	Y253F	Y253F	None
1	E255K	E255K	None
1	D276G, Y456C	D276G	D276G, F486S
1	V299L, T315I, E355G	T315I, E355G	V299L, E355G
1	M351T	M351T, S481silent[a]	M351T
1	M351T	M351T, E279E	M351T, F359V
1	L387M	L387M, K271R	L387M
1	E453K	E453K, F311L	E453K

Abbreviations: BM, bone marrow; CML, chronic myeloid leukemia; PB, peripheral blood.
[a]Silent, nucleotide change did not cause an amino-acid substitution.

plasma and PB cells (Table 1). Among the eight patients with discordant results, 13 different mutations were detected in plasma, 11 in BM cells and 9 in PB cells. Representative sequences from patients with discordance are shown in Figure 1. Interestingly, in all cases, the detection of the mutant peak is more obvious in the plasma samples than in the cells samples. The plasma RNA appeared more enriched by the mutant BCR-ABL mRNA (Figure 1). We speculate that the cells that carry the mutation have higher proliferation and apoptosis and turnover, which leads to higher relative ratio of mutant mRNA. In one patient, the highly resistant T315I mutation was also detected in plasma and BM, but not in PB cells (Table 1). A silent mutation, a nucleotide substitution that did not result in an amino-acid change, was detected in plasma, but not in BM or PB from one patient (Table 1).

PB, BM and plasma samples from 45 imatinib-sensitive CML patients were analyzed. None showed a mutation in the BCR-ABL kinase domain before imatinib treatment. However, in follow-up samples from PB cells and plasma during treatment with imatinib, two of these patients showed the appearance of mutations in plasma, but not in PB cells. One had F311L mutation at 6 months on therapy and the second patient had a silent mutation at G303 at 3 months. Both mutations disappeared at subsequent sampling. One additional patient from this group showed transient F486L mutations at 9 months on therapy in both plasma and PB cell samples. This mutation disappeared by 12 months. A fourth patient showed the E255V mutation in both plasma and PB cells at 6 months with evidence of resistance.

This study not only shows that PB cells are the best source for testing for ABL kinase mutations, but also confirms the value of plasma as a source of RNA for monitoring patients with CML. Our study shows that when plasma is used, the chance of detecting mutation in the ABL kinase domain is better than when PB and BM cells are used. This is consistent with previous

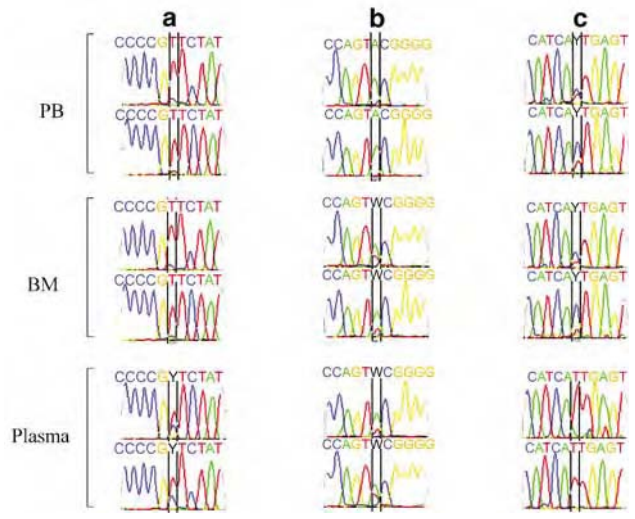

Figure 1 Examples of forward and reverse sequencing of BCR-ABL mRNA from PB cells, BM cells and plasma in patients with discordant results. Panel **a** shows the detection of 931T>C (F311L) mutation in plasma, but not in PB or BM cells, although a minor, not diagnostic peak is seen in BM cells. In panel **b**, both plasma and BM cells show the detection of 758A>T (Y253F), but not in PB cells. In panel **c**, the three sample types show the detection of 944C>T (T315I) mutation, but the plasma shows that almost all the analyzed RNA is of the mutant clone, whereas the PB and BM cells show significant RNA generated from the unmutated clone.

results showing that DNA, RNA and proteins from leukemic cells are found in plasma and plasma is enriched by RNA from aggressive subclone.[12,13] Our data show that free RNA from K562 cells is immediately degraded when added to normal plasma, but when K562 cell lysate is added, the BCR-ABL RNA

can easily be detected (data not shown). This suggests that the RNA detected in the plasma of these patients is most likely not free and perhaps complexed with other proteins. This RNA is most likely resulting from the turnover of cells in various tissues.

The data presented here also support the concept that imatinib-resistant patients have multiple clones of leukemic cells, some containing the wild-type BCR-ABL kinase domain and some a mutated BCR-ABL. This not only indicates that sensitive means must be used to detect subclones, but also suggests that factors other than mutations may play a significant role in the imatinib resistance.

In summary, plasma is a reliable source for mRNA for the detection of BCR-ABL mutations and can be used as an alternative to BM, but PB cells may not be adequate to rule out the presence of mutations in the BCR-ABL kinase domain.

References

1 Kantarjian H, Sawyers C, Hochhaus A, Guilhot F, Schiffer C, Gambacorti-Passerini C *et al.* Hematologic and cytogenetic responses to imatinib mesylate in chronic myelogenous leukemia. *N Engl J Med* 2002; **346**: 645–652.
2 Muller MC, Gattermann N, Lahaye T, Deininger MW, Berndt A, Fruehauf S *et al.* Dynamics of BCR-ABL mRNA expression in first-line therapy of chronic myelogenous leukemia patients with imatinib or interferon alpha/ara-C. *Leukemia* 2003; **17**: 2392–2400.
3 O'Brien SG, Guilhot F, Larson RA, Gathmann I, Baccarani M, Cervantes F *et al.* Imatinib compared with interferon and low-dose cytarabine for newly diagnosed chronic-phase chronic myeloid leukemia. *N Engl J Med* 2003; **348**: 994–1004.
4 Hochhaus A, La Rosee P. Imatinib therapy in chronic myelogenous leukemia: strategies to avoid and overcome resistance. *Leukemia* 2004; **18**: 1321–1331.
5 Deininger M, Buchdunger E, Druker BJ. The development of imatinib as a therapeutic agent for chronic myeloid leukemia. *Blood* 2005; **105**: 2640–2653.
6 Gorre ME, Mohammed M, Ellwood K, Hsu N, Paquette R, Rao PN *et al.* Clinical resistance to STI-571 cancer therapy caused by BCR-ABL gene mutation or amplification. *Science* 2001; **293**: 876–880.
7 Branford S, Rudzki Z, Walsh S, Parkinson I, Grigg A, Szer J *et al.* Detection of BCR-ABL mutations in patients with CML treated with imatinib is virtually always accompanied by clinical resistance, and mutations in the ATP phosphate-binding loop (P-loop) are associated with a poor prognosis. *Blood* 2003; **102**: 276–283.
8 O'Hare T, Walters DK, Deininger MW, Druker BJ. AMN107: tightening the grip of imatinib. *Cancer Cell* 2005; **7**: 117–119.
9 Weisberg E, Manley PW, Breitenstein W, Bruggen J, Cowan-Jacob SW, Ray A *et al.* Characterization of AMN107, a selective inhibitor of native and mutant Bcr-Abl. *Cancer Cell* 2005; **7**: 129–141.
10 Albitar M, Do KA, Johnson MM, Giles FJ, Jilani I, O'Brien S *et al.* Free circulating soluble CD52 as a tumor marker in chronic lymphocytic leukemia and its implication in therapy with anti-CD52 antibodies. *Cancer* 2004; **101**: 999–1008.
11 Manshouri T, Do KA, Wang X, Giles FJ, O'Brien S, Safer H *et al.* Circulating CD20 is detectable in the plasma of patients with chronic lymphocytic leukemia and is of prognostic significance. *Blood* 2003; **101**: 2507–2513.
12 Ahmed M, Giles F, Joe Y, Weber DM, Jilani I, Manshouri T *et al.* Use of plasma DNA in detection of loss of heterozygosity in patients with multiple myeloma. *Eur J Haematol* 2003; **71**: 174–178.
13 Rogers A, Joe Y, Manshouri T, Dey A, Jilani I, Giles F *et al.* Relative increase in leukemia-specific DNA in peripheral blood plasma from patients with acute myeloid leukemia and myelodysplasia. *Blood* 2004; **103**: 2799–2801.

Dasatinib (BMS-354825) inhibits Stat5 signaling associated with apoptosis in chronic myelogenous leukemia cells

Sangkil Nam,[1] Ann Williams,[3] Adina Vultur,[1] Alan List,[3] Kapil Bhalla,[4] David Smith,[2] Francis Y. Lee,[5] and Richard Jove[1]

[1]Molecular Medicine and [2]Information Sciences, Beckman Research Institute, City of Hope National Medical Center, Duarte, California; [3]Interdisciplinary Oncology, Moffitt Cancer Center and Research Institute, Tampa, Florida; [4]Medical College of Georgia Cancer Center, Augusta, Georgia; and [5]Bristol-Myers Squibb Pharmaceutical Research Institute, Princeton, New Jersey

Abstract

Dasatinib (BMS-354825) is a novel, oral, potent, multitargeted kinase inhibitor of Bcr-Abl and Src family kinases (SFK) and is a promising cancer therapeutic agent. Preclinical data indicate that dasatinib is 325-fold more potent than imatinib against cells expressing wild-type Bcr-Abl, and that dasatinib is active against 18 of 19 Bcr-Abl mutations known to cause imatinib resistance. Phase I clinical data show that dasatinib is well tolerated and highly effective for the treatment of imatinib-resistant/imatinib-intolerant chronic myelogenous leukemia (CML) and Philadelphia chromosome–positive acute lymphoblastic leukemia. However, the molecular mechanism of action of dasatinib is not fully understood. In this study, we confirm that dasatinib inhibits tyrosine phosphorylation of SFKs, including Src, Hck, and Lyn, in K562 human CML cells. Significantly, downstream signal transducer and activator of transcription 5 (Stat5) signaling is also blocked by dasatinib as shown by decreases in levels of phosphorylated Stat5 and Stat5 DNA-binding activities. In addition, dasatinib down-regulates expression of Stat5 target genes, including *Bcl-x, Mcl-1*, and *cyclin D1*. Consistent with these results, blockade of Stat5 signaling by dasatinib is accompanied by inhibition of cell proliferation and induction of apoptosis. Surprisingly, Stat5 DNA-binding activities are enhanced with increasing cell density, which is associated with resistance to apoptosis by dasatinib. Our findings indicate that inhibition of Stat5 signaling downstream of Bcr-Abl/SFKs contributes to the action of dasatinib, and, conversely, that increasing cell density up-regulates Stat5 activation and confers resistance to dasatinib. Moreover, the level of phosphorylated Stat5 in CML cells represents a mechanistically relevant biomarker for monitoring inhibition of Bcr-Abl signaling by dasatinib in CML patients using convenient immunocytochemical assays. [Mol Cancer Ther 2007;6(4):1400–5]

Introduction

Signal transducer and activator of transcription (STAT) proteins have been shown to have a major role in survival, proliferation, angiogenesis, and immune evasion of tumors (1–7). One STAT family member (Stat5) is often persistently activated in blood malignancies by non–receptor tyrosine kinases such as Bcr-Abl, Src, and other Src family kinases (SFK; refs. 1, 8–11). Furthermore, constitutive activation of Stat5 up-regulates the expression of genes, including *Bcl-x, Mcl-1*, and *cyclin D1/2*, which are associated with survival and proliferation in chronic myelogenous leukemia (CML) cells (11–14). Taken together, increasing evidence indicates that persistent activation of Stat5 and consequent deregulation of downstream gene expression contribute to malignant progression in CML (1, 7, 15).

Dasatinib is a potent tyrosine kinase inhibitor that targets Bcr-Abl and SFKs (16, 17). Preclinical data indicate that dasatinib is ~2 orders of magnitude more potent than imatinib against cells expressing wild-type Bcr-Abl (18). Furthermore, phase I clinical trials indicate that dasatinib is a promising therapeutic agent for imatinib-resistant/imatinib-intolerant CML patients. Recently, dasatinib has been approved by the Food and Drug Administration and the European Union in all stages of CML and Philadelphia chromosome–positive acute lymphoblastic leukemia resistant or intolerant to prior therapy. However, the molecular mechanism by which dasatinib induces growth arrest and apoptosis of CML cells downstream of Bcr-Abl is not fully understood. In the present study, we report that dasatinib blocks SFK and Stat5 signaling and down-regulates Bcl-x, Mcl-1, and cyclin D1 expression associated with inhibition of proliferation and induction of apoptosis in CML cells. In addition, increasing cell density up-regulates Stat5 activity and confers resistance to dasatinib. Taken together, our data indicate that inhibition of Stat5 signaling downstream of Bcr-Abl/SFKs contributes to the mechanism of action of dasatinib in CML.

Received 7/31/06; revised 12/6/06; accepted 2/16/07.

Grant support: NIH grants CA55652 and CA82533 (R. Jove).

The costs of publication of this article were defrayed in part by the payment of page charges. This article must therefore be hereby marked *advertisement* in accordance with 18 U.S.C. Section 1734 solely to indicate this fact.

Note: A. Vultur is the recipient of a Natural Sciences and Engineering Research Council of Canada postdoctoral fellowship.

Requests for reprints: Richard Jove, Molecular Medicine, Beckman Research Institute, City of Hope National Medical Center, 1500 East Duarte Road, Duarte, CA 91010. Phone: 626-301-8179; Fax: 626-256-8708. E-mail: rjove@coh.org

doi:10.1158/1535-7163.MCT-06-0446

Materials and Methods

Cell Lines and Reagents

K562 human CML and HL-60 human promyelocytic leukemia cells were obtained from the American Type Culture Collection (Manassas, VA). HL-60/Bcr-Abl (expressing ectopic Bcr-Abl protein) and Re-HL-60/Bcr-Abl (imatinib-resistant cells expressing Bcr-Abl protein) were described previously (19). All cells were cultured in RPMI 1640 containing 10% fetal bovine serum. Monoclonal antibodies to Abl, phosphorylated tyrosine, and cyclin D1 were obtained from BD Biosciences (San Diego, CA). Polyclonal antibodies to phosphorylated Stat5 (p-Stat5; Tyr^{694}) and phosphorylated Src ($Tyr^{416/419}$) were obtained from Cell Signaling Technologies (Cambridge, MA). Polyclonal antibodies to Stat5, Bcl-x, Mcl-1, phosphorylated Hck, Hck, and β-actin were from Santa Cruz Biotechnology (Santa Cruz, CA). Monoclonal antibody to c-Src was obtained from Upstate Biotechnology (Lake Placid, NY).

Immunoprecipitation and Western Blot Analyses

Immunoprecipitations and Western blots were done as described previously, with minor modifications (4, 11). Briefly, cell lysates (500 μg) were incubated with Abl antibody at 4°C followed by protein A/G-agarose beads (Pierce, Rockford, IL). Immunoprecipitates or whole-cell lysates were resolved by SDS-PAGE and immunoblotted with specific antibodies. Primary phospho-specific antibodies were incubated in TBS (pH 7.5) with 0.1% Tween 20 and 5% bovine serum albumin with gentle agitation overnight at 4°C. Horseradish peroxidase–conjugated secondary antibodies were incubated in TBS (pH 7.5) with 5% nonfat milk and 0.1% Tween 20 at a 1:2,000 dilution for 1 h at room temperature. Positive immunoreactive proteins were detected using the ECL system (Pierce).

Electrophoretic Mobility Shift Assay

Electrophoretic mobility shift assays were done as described in detail previously (11). To assess Stat5 DNA-binding activity, 8 μg of nuclear protein extract was incubated with ^{32}P-radiolabeled oligonucleotide probe containing the mammary gland factor element, derived from the bovine *β-casein* gene promoter (5-AGATTTCTAG-GAATTCAA-3′; ref. 11). For supershifts, 1 μL of antibody to Stat5 was preincubated with nuclear extract for 30 min before addition of the ^{32}P-labeled mammary gland factor element probe. Resolution of protein-DNA complexes was done by 5% nondenaturing PAGE and detected by autoradiography.

Viability and Apoptosis Assays

3-(4,5-Dimethylthiazol-2-yl)-5-(3-carboxymethoxyphenyl) -2-(4-sulfophenyl)-2*H*-tetrazolium assays were done for cell viability as described by the supplier (Promega, Madison, WI). Cells were seeded in 96-well plates (10,000 per well), incubated overnight at 37°C in 5% CO_2, and exposed to dasatinib for the indicated times. DMSO was used as the vehicle control. Viable cell numbers were determined by tetrazolium conversion to its formazan dye, and absorbance was measured at 490 nm using an automated ELISA plate reader. Apoptosis assays based on loss of membrane integrity were carried out using Annexin V-FITC as described by the supplier (BD Biosciences PharMingen, San Diego, CA). Cells were analyzed using a FACScan flow cytometer to quantify fluorescence.

Statistical Analysis

We compared the means of our two-sample assays by using Dunnett's two-sided *t* tests for controlling the type I error rate under multiple comparisons. For all analyses, $P < 0.01$ was considered statistically significant.

Results and Discussion

Dasatinib Inhibits Tyrosyl Phosphorylation of SFKs in CML Cells

Previous studies showed that dasatinib reduced the levels of phosphorylated Abl in imatinib-resistant mouse Ba/F3 cells expressing recombinant Bcr-Abl (17, 18). To confirm that dasatinib inhibits tyrosyl phosphorylation of endogenous Bcr-Abl in human CML cells, immunoprecipitates were prepared from lysates of K562 cells treated with dasatinib for 4 h. Dasatinib substantially reduced the levels of phosphorylated Bcr-Abl at 1 nmol/L after 4 h treatment (Fig. 1A), in agreement with a prior study showing that dasatinib inhibits Abl kinase activity at 1 to 10 nmol/L in Ba/F3 mouse cells expressing Bcr-Abl (17).

Originally, dasatinib was selected as a small molecule inhibitor of SFKs (16). We also showed that dasatinib directly inhibits the kinase activities of Src and other SFKs in human prostate cancer cells both *in vitro* and *in vivo* (20).

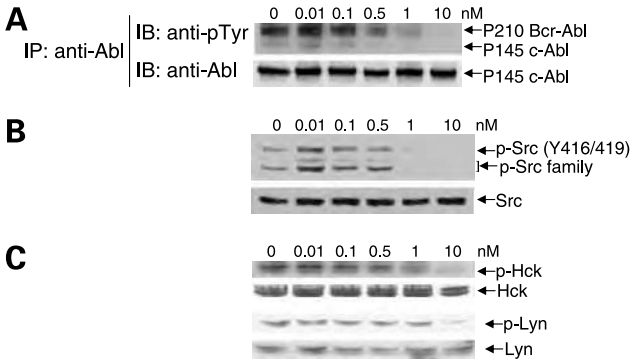

Figure 1. Dasatinib blocks Bcr-Abl and SFK activities. **A,** inhibition of Bcr-Abl phosphorylation in intact cells. K562 human CML cells were treated with dasatinib in a dose-dependent manner for 4 h. Cell lysates (500 μg) were immunoprecipitated with specific antibody to Abl (anti-Abl) at 4°C and then incubated with protein A/G-agarose beads. After bead complexes were washed with immunoprecipitation (*IP*) buffer, samples were boiled, resolved by SDS-PAGE, and immunoblotted with antibodies to phosphorylated tyrosine (*anti-pTyr*) or c-Abl protein. **B,** dasatinib reduces phosphorylation levels of c-Src (Y416/419) and other SFKs in intact cells. CML cells were treated with dasatinib in a dose-dependent manner for 4 h. Western blot analysis was done with specific antibodies to phosphorylated Src (*p-Src*) family and total Src protein. **C,** dasatinib reduces levels of phosphorylated Hck (*p-Hck*) and phosphorylated Lyn (*p-Lyn*). Cell lysates used in (**B**) were immunoblotted with antibodies to phosphorylated Hck and total Hck protein. Lysates were immunoprecipitated with antibody to Lyn and then blotted with antibody to phosphorylated Src family (Y416/419), which cross-reacts with tyrosyl autophosphorylated p-Lyn (Y396).

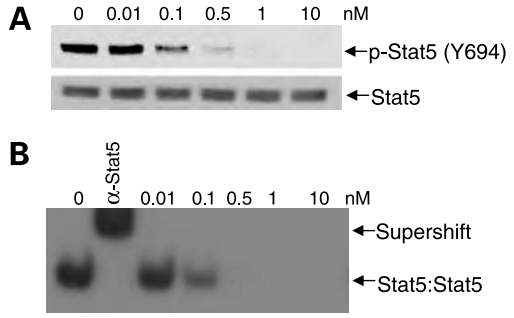

Figure 2. Dasatinib inhibits Stat5 signaling in K562 CML cells. **A,** whole-cell lysates were immunoblotted with specific antibodies to p-Stat5 (Y694) and total Stat5. **B,** dasatinib inhibits Stat5 dimer (Stat5:Stat5) DNA-binding activity. EMSA was done to assess Stat5 DNA-binding activity in nuclear extracts. Supershift with anti-Stat5 antibodies (α-Stat5) confirms that the DNA-binding activity corresponds to Stat5.

To examine the effects of dasatinib on autophosphorylation levels of Src and other SFKs in CML cells, Western blot analyses were done. A dose-dependence study using whole-cell lysates prepared 4 h after treatment with dasatinib revealed significant decreases in autophosphorylation levels of Src and other SFKs (Fig. 1B, *top*) at 1 nmol/L, whereas dasatinib did not affect total Src protein levels (Fig. 1B, *bottom*). Previous studies showed that the Src family members Hck and Lyn bind to Bcr-Abl in CML cells and have an important role in cell growth and survival of hematopoietic cells (9, 10). To identify the SFKs in K562 cells inhibited by dasatinib, we did immunoprecipitation and Western blot analyses with cell lysates used in Fig. 1B. A dose-response study showed a decrease in levels of phosphorylated Hck at 1 nmol/L of dasatinib (Fig. 1C, *top*), whereas dasatinib reduced levels of phosphorylated Lyn at 10 nmol/L (Fig. 1C, *bottom*). These results indicate that dasatinib is a potent inhibitor of Src and Hck kinases and, to a lesser extent, Lyn kinase in CML cells.

Dasatinib Inhibits Stat5 Signaling

Constitutive activation of Bcr-Abl and SFKs results in persistent tyrosyl phosphorylation of Stat5, which translocates to the nucleus and binds to the promoters of genes (1, 15). Western blot analysis using a specific antibody to tyrosyl p-Stat5 revealed that levels of p-Stat5 at Tyr^{694} were substantially reduced by 1 nmol/L dasatinib, whereas levels of total Stat5 protein remained unchanged (Fig. 2A). Consistent with these results, nuclear Stat5:Stat5 dimer DNA-binding activity, as measured by electrophoretic mobility shift assay, was also inhibited in a dose-dependent manner (Fig. 2B). SFKs are associated with Bcr-Abl and cooperate with Bcr-Abl in activation of Stat5 signaling during hematopoietic cell transformation (9, 10, 21). Thus, it is likely that dasatinib blocks Stat5 signaling by inhibiting both Bcr-Abl and SFKs.

It was important to assess if inhibition of the Stat5 signaling pathway by dasatinib is associated with reduced cell viability in CML and Bcr-Abl/Stat5–positive leukemia cells. Human promyelocytic leukemia cells HL-60 (lacking Bcr-Abl), HL-60/Bcr-Abl (expressing ectopic Bcr-Abl), and Re-HL-60/Bcr-Abl (imatinib-resistant cells expressing ectopic Bcr-Abl) were used to investigate if dasatinib activity is dependent on Bcr-Abl/Stat5 signaling in human leukemia cells. Previous studies showed that HL-60 cells lack detectable levels of p-Stat5, consistent with low expression of total endogenous Stat5 proteins in these cells (22, 23). In this study, we show that K562, HL-60/Bcr-Abl, and Re-HL-60/Bcr-Abl cells contain high levels of constitutively active Stat5 protein, whereas HL-60 cells lack activated Stat5 protein (Fig. 3A and B). Dasatinib reduced levels of p-Stat5 and inhibited Stat5 DNA-binding activity in Bcr-Abl/Stat5–positive leukemia cells (Fig. 3A and B). Consistent with inhibition of Stat5 activation, dasatinib significantly inhibited cell viability in Bcr-Abl/Stat5–positive leukemia cells, but not in HL-60 cells lacking Stat5 expression and activity (Fig. 3C). These findings indicate that blockade of the Stat5 signaling pathway by dasatinib

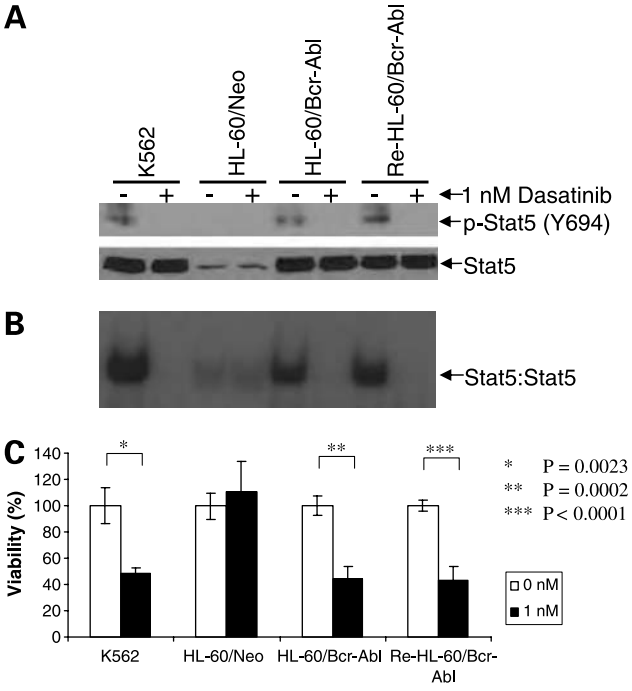

Figure 3. Dasatinib inhibits Stat5 signaling and reduces cell viability in Bcr-Abl–positive cells. K562 CML, HL-60/Neo (lacking Bcr-Abl), HL-60/Bcr-Abl (expressing ectopic Bcr-Abl), and Re-HL-60/Bcr-Abl (imatinib-resistant cells expressing Bcr-Abl) cells were treated with 1 nmol/L dasatinib for 4 h. **A,** Bcr-Abl induces Stat5 activation and dasatinib reduces levels of p-Stat5 in Bcr-Abl–positive cells. Whole-cell lysates were immunoblotted with specific antibodies to p-Stat5 (Y694) and total Stat5. **B,** dasatinib inhibits Stat5 dimer (Stat5:Stat5) DNA-binding activity in Bcr-Abl–positive cells. EMSA was done with nuclear extracts. **C,** 3-(4,5-dimethylthiazol-2-yl)-5-(3-carboxymethoxyphenyl)-2-(4-sulfophenyl)-2*H*-tetrazolium assays were done to determine effects of dasatinib on cell viability. Cells were treated with 1 nmol/L dasatinib for 48 h. 3-(4,5-dimethylthiazol-2-yl)-5-(3-carboxymethoxyphenyl)-2-(4-sulfophenyl)-2*H*-tetrazolium was added to each well for 1 h, and absorbance was measured at 490 nm. Cell viability was normalized to DMSO vehicle. *Columns,* mean for five independent experiments; *bars,* SD. *P* values (DMSO vehicle versus 1 nmol/L dasatinib in each cell line) are shown.

is associated with loss of cell viability. In addition, these observations suggest that inhibition of Bcr-Abl/Stat5 signaling is a relevant biomarker for assessing dasatinib activity in CML patients.

Dasatinib Down-regulates Bcl-x, Mcl-1, and Cyclin D1

Stat5 signaling was shown to be directly involved in cell proliferation and survival in CML by up-regulating the expression of antiapoptotic and proliferation-specific genes such as *Bcl-x, Mcl-1*, and *cyclin D1/2* (1, 11–14). As shown in Fig. 4, inhibition of Stat5 signaling was accompanied by down-regulation of expression of Stat5 target gene products, including *Bcl-x, Mcl-1*, and *cyclin D1*, following treatment with 1 nmol/L dasatinib. The concentration range of dasatinib for down-regulation of these proteins correlates with that for inhibition of Bcr-Abl kinase activity and Stat5 activation in CML cells.

Dasatinib Induces Apoptosis of CML Cells

To assess the biological consequences of dasatinib treatment on CML cells, we did 3-(4,5-dimethylthiazol-2-yl)-5-(3-carboxymethoxyphenyl)-2-(4-sulfophenyl)-2*H*-tetrazolium viability assays and Annexin V apoptosis assays. As shown in Fig. 5A, dasatinib significantly reduced cell viability at 0.5 nmol/L concentration and above in a dose-dependent manner. These results are similar to an earlier study showing that dasatinib inhibits cell growth at <1 nmol/L concentration in CML cells (16). Moreover, dasatinib has antiproliferative activity against all imatinib-resistant mutant Bcr-Abl proteins tested except for the T315I Bcr-Abl mutant (17, 18).

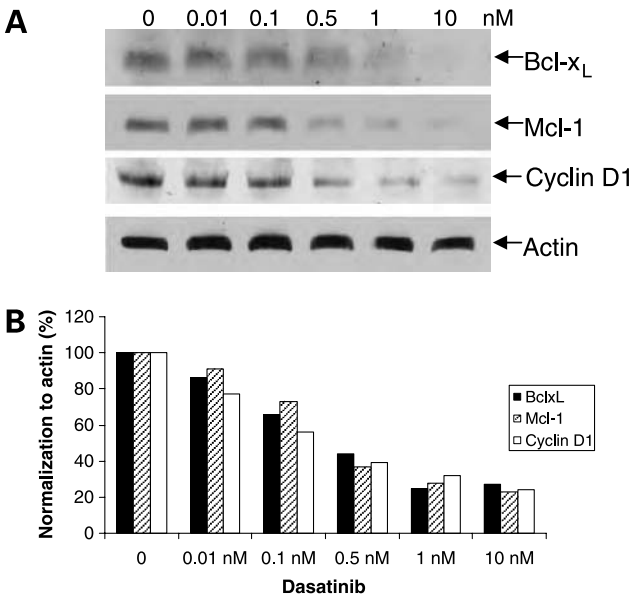

Figure 4. Effects of dasatinib on expression of downstream target genes of Stat5. CML cells were treated with dasatinib in a dose-dependent manner for 24 h. **A,** Western blot analysis was done with specific antibodies to Bcl-x_L, Mcl-1, and cyclin D1 using whole-cell lysates. **B,** normalized protein loading was confirmed by probing with antibodies to actin. Absorbance was analyzed using Quantity One software (Bio-Rad, Hercules, CA), and protein levels were normalized to actin.

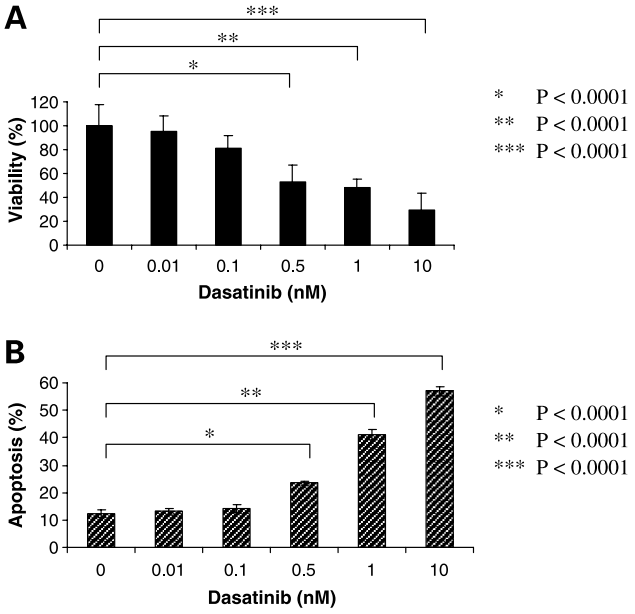

Figure 5. Dasatinib induces apoptosis of K562 human CML cells. **A,** reduction of cell viability. A 3-(4,5-dimethylthiazol-2-yl)-5-(3-carboxymethoxyphenyl)-2-(4-sulfophenyl)-2*H*-tetrazolium assay was done following exposure to dasatinib in a dose-dependent manner. After incubation with dasatinib for the indicated times, 3-(4,5-dimethylthiazol-2-yl)-5-(3-carboxymethoxyphenyl)-2-(4-sulfophenyl)-2*H*-tetrazolium was added to each well for 1 h, and absorbance was measured at 490 nm. Cell viability was compared with DMSO vehicle controls. *Columns,* mean for five independent experiments; *bars,* SD. *P* values (DMSO vehicle versus dasatinib dose). **B,** induction of apoptosis. K562 cells (0.1×10^6/mL) were treated with dasatinib in a dose-dependent manner for 48 h. Annexin V-FITC staining was used as an early marker of apoptosis. Cells were analyzed using a FACScan flow cytometer. *Columns,* mean for four independent experiments; *bars,* SD. *P* values (DMSO vehicle versus dasatinib dose).

Dasatinib also significantly induced apoptosis at 0.5 nmol/L concentration and above in a dose-dependent manner (Fig. 5B) at a cell density of 0.1×10^6/mL. These findings are consistent with down-regulation of the products of the Stat5 downstream target genes *Bcl-x, Mcl-1*, and *cyclin D1* (Fig. 4). The extent of apoptosis is over 50% following 10 nmol/L dasatinib treatment for 48 h (Fig. 5B).

Increasing Cell Density Up-regulates Stat5 DNA-Binding Activity and Confers Resistance to Dasatinib

Recently, Stat3 activity was found to be enhanced with increasing cell-to-cell contact in solid tumor cells (24). To determine whether increasing cell density up-regulates Stat5 activity in K562 CML suspension cultures, Stat5 activity was measured at different cell densities. Time course studies revealed that Stat5 DNA-binding activity increased greatly over time with increasing cell density (Fig. 6A). Levels of p-Stat5 and Stat5 DNA-binding activity were also found to increase as cell density increased at 24 h after cells were seeded (Fig. 6B). To evaluate the ability of dasatinib to inhibit levels of p-Stat5 with increasing cell density, cells were seeded at various cell densities for 24 h

and then exposed to 1 nmol/L dasatinib for 4 h (Fig. 6B, *bottom*). Results show that increasing cell density decreased the activity of dasatinib against Stat5 signaling (Fig. 6B, *bottom*).

To determine whether this increase in Stat5 activity with cell density could result in resistance to dasatinib, cells were seeded for 24 h as in Fig. 6B. Following treatment with dasatinib for 48 h, flow cytometry with Annexin V-FITC staining was done. Coincident with up-regulation of Stat5 activity over increasing cell density as shown in Fig. 6B, induction of apoptosis by dasatinib was significantly reduced in a cell density–dependent manner (Fig. 6C). Stat5 up-regulates the expression of survival genes in hematopoietic cells, including *Bcl-x* (9, 25) and *Mcl-1* (26). Associated with the decreased ability of dasatinib to inhibit levels of p-Stat5 at high cell density, dasatinib was less effective in down-regulating the expression of Bcl-x with increasing cell densities (data not shown). Although dasatinib down-regulates levels of Mcl-1 as shown in Fig. 4, inhibition of Mcl-1 by 1 nmol/L dasatinib was not influenced by cell density (data not shown). Thus, up-regulation of Bcl-x by Stat5 signaling may contribute to CML cell resistance to dasatinib at high cell densities.

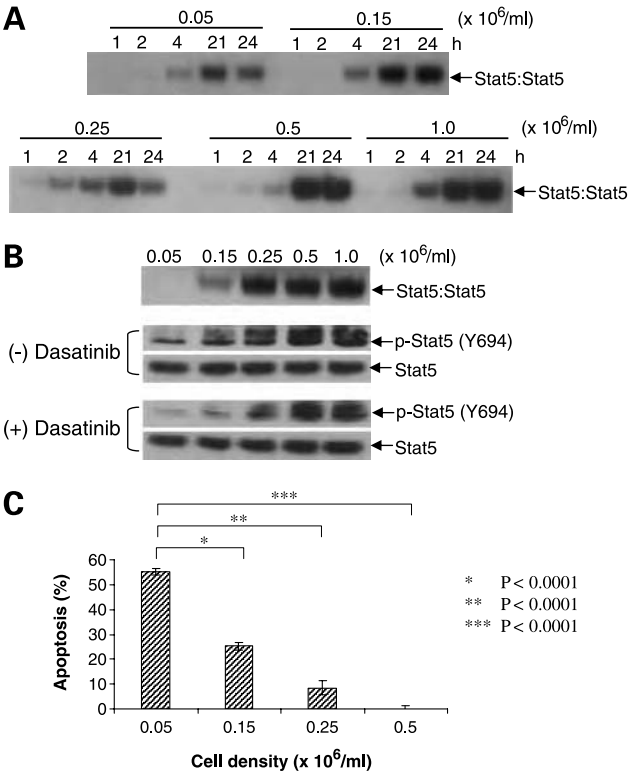

Figure 6. Increasing cell density up-regulates Stat5 DNA-binding activity and confers resistance to dasatinib. **A,** cell densities were increased from 0.05 × 10^6/mL to 1.0 × 10^6/mL at seeding, and cells were incubated for various time intervals. EMSA was done to assess Stat5 DNA-binding activity in nuclear extracts. **B,** cells were incubated at different cell densities for 24 h. EMSA was done with nuclear extracts (*top*). Cells were treated with DMSO or 1 nmol/L dasatinib for 4 h, and Western blot analysis was done with specific antibody to p-Stat5 (*bottom*). After 24 h of incubation, cells were treated with 1 nmol/L dasatinib for 48 h. **C**, annexin V-FITC staining was used as an early marker of apoptosis. **C**, cells were analyzed using a FACScan flow cytometer. *Columns,* mean for three independent experiments; *bars,* SD. *P* values (0.05 × 10^6/mL versus each cell density).

The experiment shown in Fig. 5B was done using a cell density of 0.1 × 10^6/mL. In addition, treatment with 1 nmol/L dasatinib resulted in ~40% apoptosis, whereas the experiment presented in Fig. 6C was done with a range of cell densities (0.05–0.5 × 10^6 cells/mL); hence, treatment with 1 nmol/L dasatinib resulted in a range of apoptosis depending on the cell density. These findings raise the possibility that cell-to-cell interactions increase Stat5 activity and confer resistance to dasatinib in CML cells. Alternatively, higher cell density might reduce the availability of dasatinib to cells, resulting in less dasatinib exposure per individual cell, and therefore contribute to dasatinib resistance. Finally, Stat5 signaling can be activated by cytokine and growth factor stimulation (1, 2, 27), which may be elevated in cell cultures at higher density. Any one or a combination of the above factors may contribute to dasatinib resistance at high cell density.

Therapeutic Implications for CML

In the present study, we provide evidence for a molecular mechanism whereby dasatinib exerts at least part of its therapeutic effects in CML. Our results indicate that dasatinib inhibits Bcr-Abl and SFK activities, thereby blocking Stat5 signaling that is dependent on both Bcr-Abl and SFK activities. This blockade of Stat5 signaling activity is associated with inhibition of downstream survival gene expression, including *Bcl-x* and *Mcl-1*, and induction of apoptosis. Moreover, increasing cell density up-regulates Stat5 activation and results in striking resistance to dasatinib. Although the clinical significance of this latter finding remains to be determined, the condition of high cell density may mimic the tumor microenvironment *in vivo*, resulting in resistance to Bcr-Abl inhibitors. Our findings further suggest that p-Stat5 levels are a mechanistically relevant biomarker for assessing the extent to which dasatinib inhibits Bcr-Abl signal transduction in CML patients.

Acknowledgments

We thank members of our laboratories for stimulating discussions.

References

1. Yu H, Jove R. The STATs of cancer: new molecular targets come of age. Nat Rev Cancer 2004;4:97–105.

2. Bromberg JF, Wrzeszczynska MH, Devgan G, et al. Stat3 as an oncogene. Cell 1999;98:295–303.

3. Kortylewski M, Kujawski M, Wang T, et al. Inhibiting Stat3 signaling in the hematopoietic system elicits multicomponent antitumor immunity. Nat Med 2005;11:1314–21.

4. Nam S, Buettner R, Turkson J, et al. Indirubin derivatives inhibit Stat3 signaling and induce apoptosis in human cancer cells. Proc Natl Acad Sci U S A 2005;102:5998–6003.

5. Schlessinger K, Levy DE. Malignant transformation but not normal cell growth depends on signal transducer and activator of transcription 3. Cancer Res 2005;65:5828–34.

6. Chiarle R, Simmons WJ, Cai H, et al. Stat3 is required for ALK-mediated lymphomagenesis and provides a possible therapeutic target. Nat Med 2005;11:623 – 9.

7. Moriggl R, Sexl V, Kenner L, et al. Stat5 tetramer formation is associated with leukemogenesis. Cancer Cell 2005;7:87 – 99.

8. Nieborowska-Skorska M, Wasik MA, Slupianek A, et al. Signal transducer and activator of transcription (STAT)5 activation by BCR/ABL is dependent on intact Src homology (SH)3 and SH2 domains of BCR/ABL and is required for leukemogenesis. J Exp Med 1999;189:1229 – 42.

9. Wilson MB, Schreiner SJ, Choi HJ, Kamens J, Smithgall TE. Selective pyrrolo-pyrimidine inhibitors reveal a necessary role for Src family kinases in Bcr-Abl signal transduction and oncogenesis. Oncogene 2002;21: 8075 – 88.

10. Klejman A, Schreiner SJ, Nieborowska-Skorska M, et al. The Src family kinase Hck couples BCR/ABL to STAT5 activation in myeloid leukemia cells. EMBO J 2002;21:5766 – 74.

11. Huang M, Dorsey JF, Epling-Burnette PK, et al. Inhibition of Bcr-Abl kinase activity by PD180970 blocks constitutive activation of Stat5 and growth of CML cells. Oncogene 2002;21:8804 – 16.

12. Gesbert F, Griffin JD. Bcr/Abl activates transcription of the Bcl-X gene through STAT5. Blood 2000;96:2269 – 76.

13. Epling-Burnette PK, Liu JH, Catlett-Falcone R, et al. Inhibition of STAT3 signaling leads to apoptosis of leukemic large granular lymphocytes and decreased Mcl-1 expression. J Clin Invest 2001;107:351 – 62.

14. Magne S, Caron S, Charon M, Rouyez MC, Dusanter-Fourt I. STAT5 and Oct-1 form a stable complex that modulates cyclin D1 expression. Mol Cell Biol 2003;23:8934 – 45.

15. Battle TE, Frank DA. The role of STATs in apoptosis. Curr Mol Med 2002;2:381 – 92.

16. Lombardo LJ, Lee FY, Chen P, et al. Discovery of *N*-(2-chloro-6-methyl- phenyl)-2-(6-(4-(2-hydroxyethyl)- piperazin-1-yl)-2-methylpyrimidin-4- ylamino)thiazole-5-carboxamide (BMS-354825), a dual Src/Abl kinase inhibitor with potent antitumor activity in preclinical assays. J Med Chem 2004;47:6658 – 61.

17. Shah NP, Tran C, Lee FY, et al. CL Overriding imatinib resistance with a novel ABL kinase inhibitor. Science 2004;305:399 – 401.

18. O'Hare T, Walters DK, Stoffregen EP, et al. *In vitro* activity of Bcr-Abl inhibitors AMN107 and BMS-354825 against clinically relevant imatinib-resistant Abl kinase domain mutants. Cancer Res 2005;65: 4500 – 5.

19. Nimmanapalli R, O'Bryan E, Huang M, et al. Molecular characterization and sensitivity of STI-571 (imatinib mesylate, Gleevec)-resistant, Bcr-Abl-positive, human acute leukemia cells to SRC kinase inhibitor PD180970 and 17-allylamino-17-demethoxygeldanamycin. Cancer Res 2002;62:5761 – 9.

20. Nam S, Kim D, Cheng JQ, et al. Action of the Src family kinase inhibitor, dasatinib (BMS-354825), on human prostate cancer cells. Cancer Res 2005;65:9185 – 9.

21. Lionberger JM, Wilson MB, Smithgall TE. Transformation of myeloid leukemia cells to cytokine independence by Bcr-Abl is suppressed by kinase-defective Hck. J Biol Chem 2000;275:18581 – 5.

22. Carlesso N, Frank DA, Griffin JD. Tyrosyl phosphorylation and DNA binding activity of signal transducers and activators of transcription (STAT) proteins in hematopoietic cell lines transformed by Bcr/Abl. J Exp Med 1996;183:811 – 20.

23. Spiekermann K, Biethahn S, Wilde S, Hiddemann W, Alves F. Constitutive activation of STAT transcription factors in acute myelogenous leukemia. Eur J Haematol 2001;67:63 – 71.

24. Vultur A, Cao J, Arulanandam R, et al. Cell-to-cell adhesion modulates Stat3 activity in normal and breast carcinoma cells. Oncogene 2004;23: 2600 – 16.

25. Horita M, Andreu EJ, Benito A, et al. Blockade of the Bcr-Abl kinase activity induces apoptosis of chronic myelogenous leukemia cells by suppressing signal transducer and activator of transcription 5-dependent expression of Bcl-xL. J Exp Med 2000;191:977 – 84.

26. Aichberger KJ, Mayerhofer M, Krauth MT, et al. Identification of mcl-1 as a BCR/ABL-dependent target in chronic myeloid leukemia (CML): evidence for cooperative antileukemic effects of imatinib and mcl-1 antisense oligonucleotides. Blood 2005;105:3303 – 11.

27. Buettner R, Mora LB, Jove R. Activated STAT signaling in human tumors provides novel molecular targets for therapeutic intervention. Clin Cancer Res 2002;8:945 – 54.

National Comprehensive Cancer Network®

JNCCN

Volume 5 Number 5 Journal of the National Comprehensive Cancer Network

NCCN Clinical Practice Guidelines in Oncology™

474 **Chronic Myelogenous Leukemia Guidelines**

Chronic myelogenous leukemia (CML) accounts for 15% of adult leukemias. In 2007, an estimated 4500 cases will be diagnosed and 900 patients will die of the disease. The goal of CML therapy is complete remission, which typically progresses from hematologic to cytogenetic remission. These updated 2007 guidelines include changes to several treatment recommendations, including considerations for imatinib dosing, the use of interferon, and management of dasatinib toxicity. Recommendations for hematopoetic stem cell transplantation have also been updated.

Featured Articles

About the Cover

Vanderbilt-Ingram Cancer Center

Vanderbilt-Ingram Cancer Center (VICC; vicc.org) is one of a select few NCI-designated centers in the Southeast and the only NCI-designated Comprehensive Cancer Center in Tennessee. Established under the leadership of Dr. Harold Moses in 1993, VICC brings together the cancer-related research, clinical care, education, prevention, and outreach activities at Vanderbilt University and Medical Center.

VICC's 250 faculty members in 7 research programs generate more than $135 million in research support from public and private sources. VICC focuses its efforts on high-impact basic and translational research and high quality multidisciplinary care, with particularly strong programs in phase I clinical trials, and lung, gastrointestinal, breast, head and neck, melanoma, pediatric, and hematologic malignancies. Its collaborative research initiatives include 3 Specialized Programs of Research Excellence, the Southern Community Cohort Study, and a U54 minority partnership with Meharry Medical College.

The center is led by interim director Jennifer A. Pietenpol, PhD (second photo on cover), Ingram Professor of Cancer Research, a biochemist with a research focus on tumor suppressor and cell cycle checkpoint signaling pathways. For more information about clinical trials, services, or second opinion consultation at VICC, call (800) 811-8480.

blood

2007 110: 3540-3546
Prepublished online Aug 22, 2007;
doi:10.1182/blood-2007-03-080689

Nilotinib (formerly AMN107), a highly selective BCR-ABL tyrosine kinase inhibitor, is effective in patients with Philadelphia chromosome positive chronic myelogenous leukemia in chronic phase following imatinib resistance and intolerance

Hagop M. Kantarjian, Francis Giles, Norbert Gattermann, Kapil Bhalla, Giuliana Alimena, Francesca Palandri, Gert J. Ossenkoppele, Franck-Emmanuel Nicolini, Stephen G. O'Brien, Mark Litzow, Ravi Bhatia, Francisco Cervantes, Ariful Haque, Yaping Shou, Debra J. Resta, Aaron Weitzman, Andreas Hochhaus and Philipp le Coutre

Blood (print ISSN 0006-4971, online ISSN 1528-0020), is published semimonthly by the American Society of Hematology, 1900 M St, NW, Suite 200, Washington DC 20036.

Nilotinib (formerly AMN107), a highly selective BCR-ABL tyrosine kinase inhibitor, is effective in patients with Philadelphia chromosome–positive chronic myelogenous leukemia in chronic phase following imatinib resistance and intolerance

Hagop M. Kantarjian,[1] Francis Giles,[1] Norbert Gattermann,[2] Kapil Bhalla,[3] Giuliana Alimena,[4] Francesca Palandri,[5] Gert J. Ossenkoppele,[6] Franck-Emmanuel Nicolini,[7] Stephen G. O'Brien,[8] Mark Litzow,[9] Ravi Bhatia,[10] Francisco Cervantes,[11] Ariful Haque,[12] Yaping Shou,[12] Debra J. Resta,[12] Aaron Weitzman,[12] Andreas Hochhaus,[13] and Philipp le Coutre[14]

[1]M. D. Anderson Cancer Center, Houston, TX; [2]Universitaetsklinikum Duesseldorf, Duesseldorf, Germany; [3]H. Lee Moffitt Cancer Center, Tampa, FL; [4]Azienda Policlinico Umberto I–Universita La Sapienza, Rome, Italy; [5]S. Orsola–Malpighi University Hospital, University of Bologna, Bologna, Italy; [6]Vrije University (VU) Medisch Centrum, Amsterdam, the Netherlands; [7]Hópital Edouard Herriot, Lyon, France; [8]Royal Victoria Infirmary, Newcastle upon Tyne, United Kingdom; [9]Mayo Clinic, College of Medicine, Rochester, MN; [10]City of Hope National Medical Center, Duarte, CA; [11]Hospital Clinic, Barcelona, Spain; [12]Novartis Pharmaceuticals, Florham Park, NJ; [13]III Medizinische Klinik, Medizinische Fakultät Mannheim, Universität Heidelberg, Mannheim, Germany; and [14]Campus Virchow Klinikum, Charité, Humboldt-Universität, Berlin, Germany

Nilotinib, an orally bioavailable, selective Bcr-Abl tyrosine kinase inhibitor, is 30-fold more potent than imatinib in preclinical models, and overcomes most imatinib resistant *BCR-ABL* mutations. In this phase 2 open-label study, 400 mg nilotinib was administered orally twice daily to 280 patients with Philadelphia chromosome–positive (Ph^+) chronic myeloid leukemia in chronic phase (CML-CP) after imatinib failure or intolerance. Patients had at least 6 months of follow-up and were evaluated for hematologic and cytogenetic responses, as well as for safety and overall survival. At 6 months, the rate of major cytogenetic response (Ph ≤ 35%) was 48%: complete (Ph = 0%) in 31%, and partial (Ph = 1%-35%) in 16%. The estimated survival at 12 months was 95%. Nilotinib was effective in patients harboring *BCR-ABL* mutations associated with imatinib resistance (except T315I), and also in patients with a resistance mechanism independent of *BCR-ABL* mutations. Adverse events were mostly mild to moderate, and there was minimal cross-intolerance with imatinib. Grades 3 to 4 neutropenia and thrombocytopenia were observed in 29% of patients; pleural or pericardial effusions were observed in 1% (none were severe). In summary, nilotinib is highly active and safe in patients with CML-CP after imatinib failure or intolerance. This clinical trial is registered at http://clinicaltrials.gov as ID no. NCT00109707. (Blood. 2007;110: 3540-3546)

Introduction

Chronic myeloid leukemia (CML) is a clonal myeloproliferative disorder characterized by the expansion of hematopoietic cells carrying the Philadelphia chromosome (Ph), resulting from a reciprocal translocation of the long arms of chromosomes 9 and 22. A novel fusion gene is formed, *BCR-ABL*, which encodes a constitutively active protein tyrosine kinase.[1,2]

Imatinib (Gleevec, Glivec; Novartis Pharmaceuticals, Florham Park, NJ), a Bcr-Abl tyrosine kinase inhibitor, has dramatically improved outcome in CML.[3-6] In newly diagnosed patients with CML, imatinib is associated with a complete cytogenetic response rate of 87%, a progression rate to accelerated or blastic phase of 7%, and an estimated 5-year survival rate of 89%.[3,6]

Resistance to imatinib occurs annually in 3% to 4% of patients with CML in chronic phase (CML-CP), and is defined as failure to achieve complete hematologic response (CHR) within 3 months of therapy, any cytogenetic response within 6 months, or major cytogenetic response ($Ph^+ \leq 35\%$) within 12 months, or the development of cytogenetic or hematologic relapse.[7] Resistance can be mediated through *BCR-ABL*–dependent mechanisms, often through mutations in the *ABL* kinase domain (40%–50%), or by mechanisms independent of *BCR-ABL*.[8] In patients with CML and resistance or intolerance to imatinib, alternative treatments are needed.[8-10] Dasatinib, which inhibits Bcr-Abl as well as the Src-family kinases, has produced major cytogenetic responses in 52% of patients with CML-CP following resistance or intolerance to imatinib.[11,12]

Nilotinib (Tasigna; N-[3-[3-(1H-imidazolyl)propoxy] phenyl]-4-methyl-3-[[4-(3-pyridinyl)-2-pyrimidinyl]amino] benzamide; Novartis Pharmaceuticals), a novel orally bioavailable derivative of imatinib, is a tyrosine kinase inhibitor with improved target specificity.[13,14] Based on an understanding of the molecular mechanism of imatinib activity, structural modifications led to the development of nilotinib.[15] Like imatinib, nilotinib inhibits Bcr-Abl by binding to an inactive, DFG-out conformation of the *ABL* kinase domain, thus preventing the enzyme from adopting the catalytically active conformation and blocking the tyrosine phos-

Submitted March 19, 2007; accepted July 27, 2007. Prepublished online as *Blood* First Edition paper, August 22, 2007; DOI 10.1182/blood-2007-03-080689.

The online version of this article contains a data supplement.

The publication costs of this article were defrayed in part by page charge payment. Therefore, and solely to indicate this fact, this article is hereby marked "advertisement" in accordance with 18 USC section 1734.

phorylation of proteins involved in Bcr-Abl signal transduction.[16] The improved binding of nilotinib results in greater potency and selectivity over the KIT and PDGF receptor kinases and has no activity against targets such as the Src-family of tyrosine kinases.[17] In preclinical models, nilotinib was 30 times more potent than imatinib in imatinib-sensitive CML cell lines, and maintained activity in 32 of 33 imatinib-resistant *BCR-ABL* mutant cell lines, encouraging its development in CML.[18] Results from a phase 1 dose escalation study performed in patients with imatinib-resistant CML and Ph$^+$ acute lymphoblastic leukemia (ALL) indicated that nilotinib produced significant hematologic and cytogenetic responses in all phases of CML.[19] Side effects potentially related to nilotinib included grade 3 or 4 hematologic toxicity, with cytopenias in 6% to 20% of patients, as well as transient indirect hyperbilirubinemia and skin rash.

The primary objective of this phase 2 study was to determine the rate of major cytogenetic response in patients with CML-CP following resistance or intolerance to imatinib. The results presented are from an interim analysis conducted on the first 280 consecutively enrolled patients with at least 6 months of follow-up.

Patients, materials, and methods

Patients and study design

Patients with Ph$^+$ CML-CP who were at least 18 years of age were eligible if they had imatinib resistance or intolerance, adequate performance status (World Health Organization Performance Score ≤ 2), and normal hepatic, renal, and cardiac functions. Patients with imatinib resistance had to have been treated with a dose of at least 600 mg daily for 3 months. Patients in accelerated or blastic phases,[20,21] or patients who received treatment with imatinib for 7 days and with hydroxyurea for 2 days prior to nilotinib, were excluded. Potassium and magnesium levels had to be greater than or equal to the lower limit of normal or corrected to within normal range. For safety, patients receiving concomitant medications known to prolong the QT interval or inhibit CYP3A4 were excluded if alternative treatments were not possible. Imatinib resistance was defined as failure to achieve CHR after 3 months, cytogenetic response after 6 months, major cytogenetic response after 12 months, or loss of a hematologic or cytogenetic response at any time during treatment with imatinib. Entry criteria for imatinib intolerance included patients with intolerant symptoms, but who also had never achieved a major cytogenetic response with imatinib. Intolerant symptoms were defined as any nonhematologic toxicity of grade 3 or higher severity, or of grade 2 or higher severity lasting more than 1 month or recurring more than 3 times despite dose reduction and maximal supportive care. The definition of intolerance also included hematologic toxicity of grade 4 severity persisting for more than 7 days. Imatinib-intolerant patients who had previously demonstrated sensitivity to imatinib, as evidenced by a prior major cytogenetic response, were to be excluded from participation in the study.

Nilotinib at a dose of 400 mg twice daily (800 mg/day) was administered to all patients based on safety, tolerability, and pharmacokinetic data from the phase 1 study.[19] Patients were instructed to fast for at least 2 hours prior to and 1 hour after taking nilotinib. In the absence of safety concerns, nilotinib could be escalated to 600 mg twice daily (1200 mg/day) if patients had not obtained a hematologic response at 3 months, a cytogenetic response at 6 months, a major cytogenetic response at 12 months, or if they showed loss of hematologic or cytogenetic response or disease progression at any time. Hematologic and cytogenetic response criteria have been described previously.[22] Cytogenetic responses are as follows: complete, Ph positivity of 0%; partial, Ph positivity of 1% to 35%; minor, Ph positivity of 36% to 65%; and minimal, Ph positivity of 66% to 95%. A major cytogenetic response includes complete and partial cytogenetic responses. Cytogenetic responses were based on the percentage of Ph$^+$ metaphases among 20 or more metaphase cells in each bone marrow sample. Fluorescent in situ hybridization (FISH) studies to document cytogenetic response were accepted if routine cytogenetic studies were not successful or not available at a particular analysis time. Complete blood counts and biochemistries were obtained weekly for the first 8 weeks, and thereafter every 2 weeks. Bone marrow assessments were done on day 28 of cycle 1 and every 3 months. Cytogenetic studies on bone marrow samples were performed at baseline and repeated every 3 months in responding patients. Safety assessments included evaluation of adverse events, hematologic assessment, biochemical testing, urinalysis, cardiac enzyme assessment, serial electrocardiogram evaluation, and physical examination. Adverse events were graded according to the National Cancer Institute Common Terminology Criteria for Adverse Events Version 3.0. Survival was dated from start of nilotinib therapy until death from any cause and censored at last follow-up for patients who were alive. Duration of major cytogenetic response was measured from date of response until the date treatment was discontinued for progression or death. Patients who discontinued for other reasons were censored at date of last treatment and patients still on treatment at data cut-off date.

The study was conducted in accordance with the Declaration of Helsinki. The study protocol was reviewed and approved by the ethics committees or institutional review boards of all participating centers. All patients gave written informed consent according to institutional guidelines.

Assessment of BCR-ABL mutation status

Peripheral blood samples were obtained prior to the first dose of nilotinib. The total blood RNA was reversely transcribed and amplified by nested polymerase chain reaction (PCR) using primers located in the *BCR* and *ABL* regions of the *BCR-ABL* gene. The amplicons that extend over the entire Bcr-Abl tyrosine kinase domain (ranging from amino acid 230-490; GenBank accession no. M14752) and the surrounding regions, were then screened for mutations by direct sequencing technology. This *BCR-ABL* mutation analysis was performed by 5 regional academic laboratories. All 5 laboratories reported reliable detection of mutant clones present at a frequency of 20% or higher.

Statistical considerations

The primary efficacy variable of this study was the overall major cytogenetic response. Secondary efficacy variables included time to major cytogenetic response, duration of major cytogenetic response, CHR, time to and duration of CHR, and overall survival. Response rates were calculated as percentages relative to the respective patient populations. For major cytogenetic response and CHR, 95% confidence intervals (CIs) using Clopper-Pearson limits were determined. Time-to-event variables were summarized and are presented using the Kaplan-Meier method. A Fleming single-stage design was used to test the null hypothesis that the rate of major (complete + partial) cytogenetic response was 10% or less, versus the alternative hypothesis that the true response rate was 20% or more. A minimum of 132 patients were required (assuming a one-sided $P = .025$; power 0.90). A response rate of 21 or more out of 132 would be sufficient to reject the null hypothesis. Because of the activity of the agent, overenrollment on the study was allowed to offer more patients in need of alternative options after imatinib failure access to nilotinib therapy.

Results

A total of 318 patients were enrolled in the study between April 2005 and August 2006, and were treated at 63 centers from 15 countries. Results are presented for the initial cohort of 280 patients with at least 6 months of follow-up or those who prematurely discontinued study treatment. Patient characteristics are shown in Table 1. Their median age was 58 years (range, 21 to 85 years). Patients had received extensive prior therapy: 66% had received interferon-α, 83% had received hydroxyurea, and 25% had received cytarabine. The median duration of CML was

Table 1. Characteristics of the study group

Parameter	Value
No. patients	280
Median age, y (range)	58 (21-85)
Male sex, no. (%)	144 (51)
Median duration of disease, mo (range)	57 (5-275)
Splenomegaly, no. (%)	48 (17)
Median hemoglobin, g/L (range)	120 (77-172)
Median WBC, $\times 10^9$/L (range)	9.9 (0.9-372)
Median platelet count, $\times 10^9$/L (range)	309 (28-2000)
Prior complete hematologic response with imatinib, no. (%)	88 (31)
Prior therapy, no. (%)	
Allogeneic or stem cell transplantation	22 (8)
Hydroxyurea	233 (83)
Cytarabine	71 (25)
Interferon-α, no. (%)	184 (66)
Imatinib resistance, no. (%)	194 (69)
Maximum previous imatinib dose, no. (%)	
Less than 600 mg/day	77 (28)
600 to 800 mg/day	91 (33)
More than 800 mg/day	111 (40)
Chromosomal abnormalities at baseline other than Ph, no. (%)	72 (26)
ABL kinase domain mutations, no. (%)	77* (42)

* indicates n = 182.

57 months; the median duration of prior imatinib therapy was 32 months. A total of 194 (69%) patients had imatinib resistance, and 86 (31%) patients had imatinib intolerance.

The median cumulative duration of nilotinib dose interruptions was low (18 days; range, 1-185 days) relative to the median duration of therapy (261 days; range, 1-502 days). The median duration of exposure for the 318 patients enrolled was 245 days. The median dose intensity of nilotinib was 797 mg/day (range, 151-1112 mg/day), very close to the intended total daily nilotinib dose of 800 mg per day.

As of September 2006, 183 (65%) patients remain on study. Reasons for discontinuation, regardless of causality, included adverse events in 42 (15%) patients, disease progression in 32 (11%) patients, consent withdrawal in 10 (4%) patients, and other reasons in 4% (including abnormal laboratory test [n = 5], death [n = 2], administrative problems [n = 3], loss of follow-up [n = 1], and protocol violations [n = 3]). A total of 17 (6%) patients required discontinuation from study for cytopenia (neutropenia in 9 patients, thrombocytopenia in 8 patients).

Efficacy

Overall, a major cytogenetic response was achieved in 134 of 280 patients (48%; 95% CI, 41.9%-53.9%). Table 2 details the response rates. Rates of major cytogenetic response were 48% (95% CI, 41.2%-55.7%) in patients with imatinib intolerance and 47% (95% CI, 35.7%-57.6%) in patients with imatinib resistance. Complete cytogenetic response was achieved in 88 patients (31%; 95% CI, 26.0%-37.2%). A total of 30 of the 134 patients with major cytogenetic response were categorized based only on FISH evaluations (12 complete cytogenetic responses, 18 partial cytogenetic responses). While there is excellent concordance between conventional and FISH analyses in patients achieving complete cytogenetic response, the concordance rate for partial cytogenetic response is good. If the 18 partial cytogenetic responses are not considered, 116 (41%) of 280 patients would be considered to have achieved a major cytogenetic response with nilotinib therapy. In addition, 5 patients entered the study with a complete cytogenetic response and maintained their response in the study; another 3 patients entered the study in partial cytogenetic response and also maintained their response in the study; and 3 patients had missing baseline assessment but achieved complete cytogenetic response during the study. Therefore, another 11 (4%) patients had documentation of major cytogenetic response during the study. The median time to major cytogenetic response was 2.8 months. Among patients achieving major cytogenetic response, 96% continued on nilotinib without progression or death for at least 6 months from the date of achieving their response (Figure 1). Only 5 (4%) patients in major cytogenetic response discontinued nilotinib due to progression or death (Figure 1). A further 16 (12%) patients in major cytogenetic response lost their major cytogenetic response but were still on treatment at data cut-off. The estimated 12-month overall survival rate was 95% (Figure 2). A CHR, assessable in 185 patients without CHR at baseline, occurred in 74% (95% CI, 67.1%-80.2%) of patients. Complete hematologic responses occurred early (median time to CHR, 1 month). Only 11 (8%) of the 137 patients who had achieved CHR discontinued due to progression or death.

Baseline assessment for the *BCR-ABL* mutation status was available in 182 patients at the time of analysis. A total of 28 different *BCR-ABL* mutations involving 23 amino acids were detected in 42% of the patients (77 of 182 patients), 8% of whom (6 of 77 patients) showed more than 1 mutation. After 6 months of therapy, major cytogenetic response was achieved in 42% of patients and complete cytogenetic response was achieved in 23% of patients with baseline mutations, versus in 51% and 35% of patients without baseline mutations (Table 3). Among patients who did not have CHR at baseline, the rate of CHR at 6 months was 61% and 83% in patients with or without baseline mutations, respectively. Major cytogenetic response and CHR were observed across all *BCR-ABL* genotypes, with the exception of the T315I

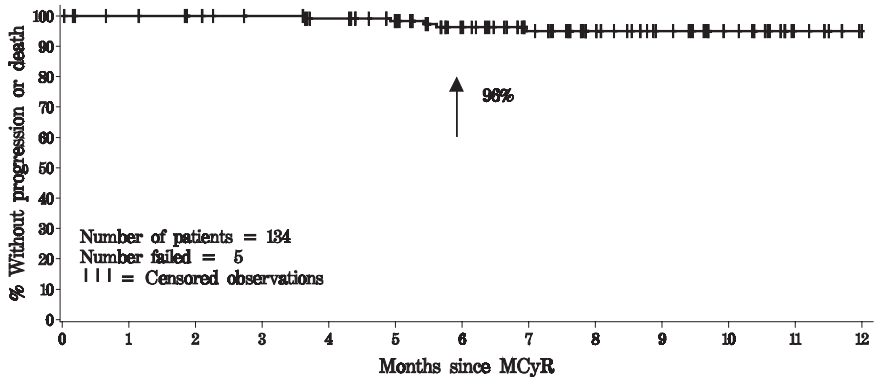

Figure 1. Duration of major cytogenetic response with nilotinib. Only 5 (4%) of the 134 patients who had achieved major cytogenetic response discontinued due to progression or death.

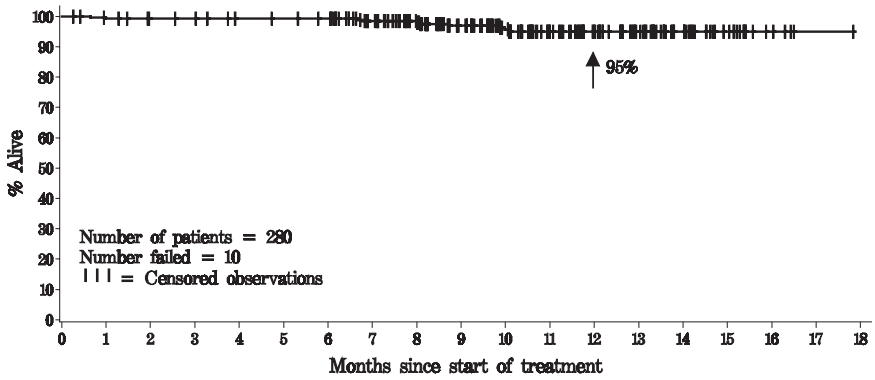

Figure 2. Overall survival in the 280 patients treated with nilotinib. A total of 10 (4%) patients died; 2 during treatment, 8 during long-term follow-up.

mutation identified in 4 (2.2%) of 182 patients, and the E255V and E274K mutation each identified in 1 (0.6%) of 182 patients (Table 3). However, both the E255V and E274K mutations coexisted with a T315I mutation at baseline in these 2 patients. There were 2 patients with a L248V mutation who were not assessable for hematologic and cytogenetic responses.

Although responses were observed broadly across the mutation spectrum, the rate of responses appeared to be affected by the types of mutations identified in patients and their sensitivity to nilotinib as assessed in vitro. Major cytogenetic response and CHR were achieved in 53% (16 of 30) and 77% (17 of 22) of patients with mutations associated with preclinical IC_{50} to nilotinib of less than 100 nM[18] (Table 3; mutation group 1), in 43% (6 of 14) and 50% (6 of 12) of patients with IC_{50} of 101 to 200 nM (Table 3; mutation group 2), and in 15% (2 of 13) and 18% (2 of 11) of patients with IC_{50} of 201 to 800 nM (Table 3; mutation group 3), respectively. Mutation group 4 ($IC_{50} > 800$ nM), which only includes T315I in 4 patients, showed no hematologic and cytogenetic responses.

Safety profile

Adverse events with a suspected relationship to nilotinib are summarized in Table 4. These were generally mild to moderate in severity. The most commonly reported nonhematologic events considered possibly related to nilotinib, and of any grade severity, were rash (28%), nausea and pruritus (24% each), and headache and fatigue (19% each). Grade 3 or 4 toxicities were noted in 3% or less of patients (Table 4). Clinically notable adverse events reported with other Bcr-Abl inhibitors, such as pleural effusions, pericardial effusions, pulmonary edema, and left ventricular dysfunction,[23] were rarely observed with nilotinib (3 [1.1%] patients, all grades 1–2).

The most commonly reported grade 3 or 4 hematologic abnormalities were neutropenia (29%) and thrombocytopenia (29%), with median durations of 15 and 22 days, respectively. Neutropenia and thrombocytopenia were generally manageable with dose interruptions and reductions, which were necessitated in 10% and 19% of patients, respectively. Patients only occasionally required support with hematopoietic growth factors (5%) or platelet transfusions (10%).

The majority of serum biochemistry abnormalities observed with nilotinib were mild to moderate in severity. Grade 3 or 4 elevations in AST and ALT occurred in 1% and 4% of patients, respectively. Grade 3 or 4 bilirubin and lipase elevations occurred in 9% and 14% of patients, respectively. These were self-limited and resolved spontaneously, with continuation of nilotinib at the same dose, within 1 to 2 weeks. Pancreatitis was reported in 3 (1%) patients.

The nonhematologic reasons for imatinib intolerance are presented in Table 5. Cross-intolerance, defined as the occurrence of any grade 3 or higher nilotinib-induced toxicity previously reported in the same patient receiving imatinib, was infrequent, occurring in only 2 (2%) of 86 patients. Almost all imatinib-intolerant patients were able to tolerate therapy with nilotinib. Because of a preclinical signal indicating that nilotinib could potentially prolong the QT interval, frequent electrocardiograms were obtained during this study and analyzed centrally. The effect of nilotinib at steady-state (day 8) on the QTcF interval, measured as a time-averaged mean change from baseline in QTcF (Fridericia[15] correction), was

Table 2. Clinical responses (N=280)

Response	Patients with response, no. (%)		
	Imatinib-resistant, n = 194	Imatinib-intolerant, n = 86	All patients, n = 280
Complete hematologic response*	92 (68)‡	45 (90)§	137 (74)
Cytogenetic response†			
Major	94 (48)	40 (47)	134 (48)
Complete	58 (30)	30 (35)	88 (31)¶
Partial	36 (19)	10 (12)	46 (16)‖
Minor	16 (8)	6 (7)	22 (8)
Minimal	25 (13)	14 (16)	39 (14)

*Evaluation of CHR in patients without CHR at baseline.

†Evaluation of cytogenetic response by FISH or cytogenetics (12 complete cytogenetic responders and 18 partial cytogenetic responders were assigned based on FISH). Patients were only considered a complete (partial) cytogenetic responder if they were more than 0% Ph^+ (> 35% Ph^+) at baseline.

‡(n=135)

§(n=50)

¶In addition, 5 (2%) patients entered the study with a complete cytogenetic response and maintained their response in the study, and 3 (1%) patients had missing baseline assessment but complete cytogenetic response during the study.

‖In addition, 3 (1%) patients entered the study with a partial cytogenetic response and also maintained their response in the study.

Table 3. Baseline BCR-ABL mutation status and response to nilotinib

Baseline mutation (mutation group no.)	Number of patients	Patients achieving response, no. (%)		Number of patients*	Patients achieving CHR, no. (%)
		Major cytogenetic response	Complete cytogenetic response		
Any mutation	77†	32 (42)	18 (23)	62	38 (61)
No mutation	105	54 (51)	37 (35)	58	48 (82)
M244V (1)‡	10	7 (70)	6 (60)	8	7 (87)
L248V (2)	2	0 (0)	0 (0)	1	0 (0)
G250E (2)	4	3 (75)	1 (25)	4	3 (75)
Y253F	1	0 (0)	0 (0)	1	1 (100)
Y253H (3)	7	1 (14)	0 (0)	5	0 (0)
E255K (3)	5	1 (20)	0 (0)	5	2 (40)
E255V (3)	1	0 (0)	0 (0)	1	0 (0)
E274K	1	0 (0)	0 (0)	1	0 (0)
E275K (1)	1	0 (0)	0 (0)	1	1 (100)
D276G (1)	2	1 (50)	1 (50)	1	1 (100)
E279K	2	1 (50)	1 (50)	2	2 (100)
F311L	1	0 (0)	0 (0)	1	1 (100)
T315I4	4	0 (0)	0 (0)	4	0 (0)
F317L (1)	2	0 (0)	0 (0)	2	1 (50)
M351T (1)	11	6 (54)	3 (27)	9	6 (66)
E355A (1)	1	1 (100)	1 (100)	0	NA
E355G (1)	3	2 (67)	1 (33)	1	1 (100)
F359I	2	0 (0)	0 (0)	2	1 (50)
F359V (2)	8	3 (38)	1 (13)	7	3 (43)
L370P	1	1 (100)	1 (100)	0	NA
L387M (1)	1	0 (0)	0 (0)	1	1 (100)
M388I	1	1 (100)	0 (0)	1	1 (100)
H396R	5	3 (60)	1 (20)	4	3 (75)
E450K	1	1 (100)	1 (100)	1	NA
S438C	2	0 (0)	0 (0)	2	2 (100)
E459G	1	1 (100)	1 (100)	1	1 (100)
E459K	2	0 (0)	0 (0)	1	1 (100)
F486S	2	0 (0)	0 (0)	2	1 (50)
Mutation group 1, IC_{50} less than 100 nM§	30	16 (53)	11 (37)	22	17 (77)
Mutation group 2, IC_{50} 101-200 nM	14	6 (43)	2 (14)	12	6 (50)
Mutation group 3, IC_{50} 201-800 nM	13	2 (15)	0 (0)	11	2 (18)
Mutation Group 4, IC_{50} more than 10 000 nM	4	0 (0)	0 (0)	4	0 (0)

NA indicates not applicable.

*Number of patients who did not have CHR at baseline and were assessable for hematologic response.

†A total of 6 (8%) of 77 patients had more than 1 mutation detected at baseline with the following genotypes: H396R/M351T, D276G/M351T, E459K/M351T, E274K/T315I, E255V/M244V/T315I, and H396R/T315I.

‡Number in parentheses refers to the IC_{50}-based grouping.

§Mutations were grouped based on available nilotinib IC_{50} data established in in vitro Ba/F3 proliferation assay:[18] mutation group 1 ($IC_{50} < 100$ nM), mutation group 2 ($IC_{50} = 101$-200 nM), mutation group 3 ($IC_{50} = 201$-800 nM), and mutation group 4 ($IC_{50} > 10\,000$ nM). Individual mutations in each group were notated with the group number. Mutations without group number notation do not have IC_{50} data described in Weisberg et al.[18]

5 milliseconds. Categoric, or outlier analysis of serial electrocardiograms, measuring the number of absolute QTcF intervals exceeding 500 milliseconds, showed an incidence of 1% (3 of 280 patients).

A total of 4 deaths occurred in the study, or within 28 days of discontinuing nilotinib; 1 patient had a myocardial infarction, another died of coronary artery disease, and 2 patients died of sepsis.

Overall, nilotinib was well tolerated as demonstrated by the high dose intensity achieved.

Discussion

Nilotinib, a highly selective and potent Bcr-Abl inhibitor, was very active and safe in this phase 2 study of patients with CML-CP post-imatinib resistance and intolerance. Major cytogenetic response, which correlated with long-term survival and clinical benefit,[5,6] was observed in 48% of patients. Complete cytogenetic responses were noted in 31% of patients. Dasatinib given to patients with CML-CP post-imatinib failure produced a major cytogenetic response rate of 45% at 6 months, and a complete cytogenetic response rate of 33%.[11] With nilotinib, the estimated 1-year overall survival rate was 95% (Figure 1). The estimated percent of patients who achieved a major cytogenetic response and who did not discontinue nilotinib due to progression or death for at least 6 months after achievement of response was 96% (Figure 2). Similar rates of major cytogenetic response were observed in imatinib-resistant and -intolerant patients. This is likely due to the rigorous definition of imatinib intolerance, which excluded imatinib-intolerant patients who had achieved a prior major cytogenetic response (thus, the imatinib-intolerant patients had also relatively less sensitive disease). Among the 134 of 280 patients who achieved a major cytogenetic response, the response was documented only by FISH analysis in 30 patients (12 complete cytogenetic responses, 18 partial cytogenetic responses). Excluding the 18 partial cytogenetic responses documented by FISH, the major cytogenetic response rate with nilotinib would be 41%.

Table 4. Most frequent (5% or more) nonhematologic adverse events associated with nilotinib

Adverse event	Patients, no. (%)	
	All grades	Grade 3/4
Rash	79 (28)	9 (3)
Nausea	66 (24)	3 (1)
Pruritus	67 (24)	3 (1)
Fatigue	52 (19)	3 (1)
Headache	52 (19)	5 (2)
Constipation	34 (12)	0
Diarrhea	32 (11)	6 (2)
Vomiting	30 (11)	2 (< 1)
Myalgia	23 (8)	3 (1)
Extremity pain	13 (5)	2 (< 1)

Mutations in *BCR-ABL* are a known mechanism of resistance to imatinib. In this study, 28 different *BCR-ABL* mutations affecting 23 amino acids were noted in 42% of patients prior to nilotinib therapy. CHR and/or cytogenetic response (major, complete) were observed in patients harboring a variety of *BCR-ABL* mutations associated with imatinib resistance as well as in imatinib-resistant patients without *BCR-ABL* mutation. The rates of major cytogenetic response at 6 months were 42% and 51% in patients with and without baseline mutations, respectively. As predicted by preclinical data,[18] none of the 4 patients with baseline T315I mutation had either CHR or major cytogenetic response during the nilotinib therapy. Thus, nilotinib was effective in patients with *BCR-ABL* mutations, except T315I, as well as in patients with other mechanisms of resistance independent of *BCR-ABL* mutations, demonstrating its clear therapeutic role in patients with imatinib resistance.

Although responses were observed in all genotypes except T315I, patients with *BCR-ABL* mutations that showed higher in vitro sensitivity against nilotinib (cellular $IC_{50} \leq 200$ nM)[18] appeared to have better rates of response than patients with less sensitive mutations (cellular IC_{50} of 201–800 nM; Table 3). These less sensitive mutant clones (described by Weisberg et al[18] as having IC_{50} values of ≥ 200 nM) showed complete in vitro suppression with increased exposure of nilotinib. With nilotinib plasma peak-trough levels of 3600 to 1700 nM at a 400-mg twice-daily dose, it is possible that longer treatment duration may result in further improvement in clinical responses in patients with less sensitive mutations.

In this study, nilotinib was rarely associated with the common toxicities seen with imatinib (eg, fluid retention, edema, cramps, periorbital edema, and weight gain). Commonly noted side effects included mild skin rash, headache, and nausea. Serious grades 3 to 4 nonhematologic side effects were uncommon. Pleural effusions, observed in 10% to 35% of patients on dasatinib[11,23] were observed in only 1% of patients with nilotinib therapy. Peripheral edema, reported in 20% to 30% of patients on imatinib[3,6] and in 18% of patients on dasatinib,[11] was rarely observed in patients on nilotinib. Although nilotinib and imatinib are chemically similar, the minimal occurrence of cross-intolerance between the 2 agents represents also an interesting and important therapeutic advantage (Table 5).

Table 5. Comparison of nonhematologic adverse events observed in imatinib-intolerant patients treated with nilotinib

Grade 3/4 adverse events	Patients with toxicity on imatinib, no.	Patients with toxicity on nilotinib, no.
Rash/skin	25	0
Liver toxicity	10	1
Fluid retention	17	0
Gastrointestinal intolerance	15	1
Musculoskeletal	9	0
Other	10	0
Total	86	2

With nilotinib therapy, neutropenia and thrombocytopenia were modest in severity and infrequently required growth factor support or platelet transfusions. Grades 3 to 4 neutropenia and thrombocytopenia were each reported in 29% of patients. Myelosuppression was the most common adverse event (4%) leading to permanent nilotinib discontinuation. With dasatinib, the rates of grades 3 to 4 neutropenia (49%) and thrombocytopenia (47%) patients with CML-CP after imatinib intolerance and resistance were higher.[11] It has been postulated that a more potent inhibitor of Bcr-Abl may contribute to increased myelosuppression from rapid clearance of *BCR-ABL* expressing malignant hematopoietic cells. Interestingly, despite the greater potency of nilotinib relative to imatinib, the rates of grades 3 to 4 neutropenia and thrombocytopenia in this heavily pretreated population were comparable with those reported in imatinib-treated patients with late CML-CP who were previously treated with interferon-α. Thus, the selectivity of nilotinib against Bcr-Abl (relative to other targets, such as Src-family or c-Kit kinases) may account for the high level of efficacy unaccompanied by higher rates of severe myelosuppression. Nilotinib was well tolerated in this study as demonstrated by the high dose intensity achieved. In contrast, the median dose delivered in the dasatinib studies was about two-thirds of the intended dose (median daily dose delivered was 101 mg; the intended daily dose was 140 mg).[11]

Drug-induced effects on the QT interval are often difficult to accurately assess in patients given the inherent variability around this parameter and the lack of available age- and disease-matched controls providing information on the background incidence of these findings in similar populations. The QT interval results observed in this study were consistent with those observed in similar imatinib-resistant and -intolerant patients with CML treated with dasatinib (pooled analysis of 5 CML studies showed a mean change from baseline in QTcF of 3 to 6 milliseconds; QTcF interval of more than 500 milliseconds observed in 0.7% of patients).

Clinically significant abnormalities in nonhematologic laboratory parameters were infrequent. The most commonly observed biochemical abnormality was hyperbilirubinemia, followed by transient elevations in ALT, AST, and serum lipase. Indirect hyperbilirubinemia, mostly grade 2 or lower severity, was self-limited and reversed spontaneously with continued nilotinib therapy at the same dose. The etiology of hyperbilirubinemia was explored by examining polymorphisms in the uridine diphosphate glucuronosyltransferase 1A1 (*UGT1A1*) gene in 62 patients in the study. Results suggested that the TA repeat polymorphism in *UGT1A1*, which predisposes to Gilbert syndrome, predicted for the susceptibility to nilotinib-induced hyperbilirubinemia. Therefore, it appears that the administration of nilotinib unmasked a clinically benign form of indirect hyperbilirubinemia, which was self-limited, resolving with continued therapy.

In summary, nilotinib is highly active and safe, and provides an alternative effective treatment for patients whose disease becomes resistant or intolerant to imatinib. Nilotinib is also being studied in newly diagnosed CML, where the goal is to prevent the emergence of mutant clones, which may confer clinical benefit over that of the current standard of care, imatinib.

Acknowledgment

This work was supported by research funding from Novartis Pharmaceuticals.

Authorship

Contribution: H.K. designed research, performed research, analyzed data, and wrote the paper. F.G., N.G., K.B., G.A., F.P., G.J.O, F.-E.N., S.G.O'B., M.L., R.B., F.C., and P.le.C. performed research. A. Hochhaus performed research and conducted mutation analysis. A. Haque analyzed data. Y.S. conducted mutation data analysis. D.J.R. wrote paper. A.W. analyzed data and wrote the paper.

Conflict-of-interest disclosure: P.le.C., received a research grant and honoraria from Novartis. F.-E.N. received lecture fees from Novartis; F.G. received research support from Novartis and Bristol-Meyers-Squibb (BMS); H.K. received research support from Novartis and BMS; F.C. received research support from Novartis and the Novartis Advisory Board; A. Hochhaus received research support from Novartis and BMS; N.G. received research support from Novartis; K.B. received research support and a research grant from Novartis; S.G.O'B. received research funding from Novartis, BMS, and Roche; R.B. received research support from Novartis; A. Haque, Y.S., D.J.R., and A.W. are employed by Novartis.

Correspondence: Hagop Kantarjian, Department of Leukemia, Unit 428, The University of Texas M. D. Anderson Cancer Center, P. O. Box 301402, Houston, TX 77230-1402; e-mail: hkantarj@mdanderson.org.

References

1. Faderl S, Talpaz M, Estrov Z, et al. The biology of chronic myeloid leukemia. N Engl J Med. 1999; 341:164-172.
2. Sawyers CL. Chronic myeloid leukemia. N Engl J Med. 1999;340:1330-1340.
3. O'Brien SG, Guilhot F, Larson RA, et al. Imatinib compared with interferon and low-dose cytarabine for newly diagnosed chronic-phase chronic myeloid leukemia. N Engl J Med. 2003;348:994-1004.
4. Kantarjian H, Talpaz M, O'Brien S, et al. High-dose imatinib mesylate therapy in newly diagnosed Philadelphia chromosome–positive chronic phase chronic myeloid leukemia. Blood. 2004;103:2873-2878.
5. Silver RT, Talpaz M, Sawyers CL, et al. Four years of follow-up of 1027 patients with late chronic phase (L-CP), accelerated phase (AP), or blast crisis (BC) chronic myeloid leukemia (CML) treated with imatinib in three large phase II trials [abstract]. Blood. 2004;104:11a.
6. Druker B, Guilhot F, O'Brien SG, et al. Five-year follow-up of patients receiving imatinib for chronic myeloid leukemia. N Engl J Med. 2006;355:2408-2417.
7. Hochhaus A, La Rosée P. Imatinib therapy in chronic myelogenous leukemia: strategies to avoid and overcome resistance. Leukemia. 2004; 18:1321-1331.
8. Gorre ME, Mohammed M, Ellwood K, et al. Clinical resistance to STI-571 cancer therapy caused by *BCR-ABL* gene mutation or amplification. Science. 2001;293:876-880.
9. Shah NP, Tran C, Lee FY, et al. Overriding imatinib resistance with a novel ABL kinase inhibitor. Science. 2004;305:399-401.
10. O'Hare T, Walters DK, Stoffregen EP, et al. In vitro activity of BCR-ABL inhibitors AMN107 and BMS-354825 against clinically relevant imatinib-resistant Abl kinase domain mutants. Cancer Res. 2005;65:4500-4505.
11. Hochhaus A, Kantarjian H, Baccarani M, et al. Dasatinib induces notable hematologic and cytogenetic responses in chronic phase chronic myeloid leukemia after failure of imatinib therapy. Blood. 2007;109:2303-2309.
12. Talpaz M, Shah N, Kantarjian H, et al. Dasatinib in imatinib-resistant Philadelphia chromosome-positive leukemias. N Engl J Med. 2006;354: 2531-2541.
13. Weisberg E, Manley PW, Breitenstein W, et al. Characterization of AMN107, a selective inhibitor of native and mutant Bcr-Abl. Cancer Cell. 2005; 7:129-141.
14. Golemovic M, Verstovsek S, Giles F, et al. AMN107, a novel aminopyrimidine inhibitor of BCR-ABL, has in vitro activity against imatinib-resistant chronic myeloid leukemia. Clin Cancer Res. 2005;11:4941–4947.
15. Cowan-Jacob SW, Fendrich G, Floersheimer A, et al. Structural biology contributions to the discovery of drugs to treat chronic myelogenous leukaemia. Acta Crystallogr D Biol Crystallogr. 2007; 63:80-93.
16. Manley PW, Cowan-Jacob SW, Fendrich G, et al. Bcr-Abl binding modes of dasatinib, imatinib and nilotinib: an NMR study [abstract]. Blood. 2006; 108:224a.
17. Manley PW, Brüggen J, Fabbro D, et al. Extended kinase profiling of the Bcr-Abl inhibitor nilotinib [abstract]. Proc Am Assoc Cancer Res. 2007;48:abstract no. 3249.
18. Weisberg E, Manley P, Mestan J, et al. AMN107 (nilotinib): a novel and selective inhibitor of BCR-ABL. Br J Cancer. 2006;94:1765-1769.
19. Kantarjian H, Giles F, Wunderle L, et al. Nilotinib in imatinib-resistant CML and Philadelphia chromosome-positive ALL. N Engl J Med. 2006;354: 2542-2551.
20. Kantarjian H, Dixon D, Keating MJ, et al. Characteristics of accelerated disease in chronic myelogenous leukemia. Cancer. 1988;61:1441-1446.
21. Kantarjian HM, Keating MJ, Talpaz M, et al. Chronic myelogenous leukemia in blast crisis: an analysis of 242 patients. Am J Med. 1987;83:445-54.
22. Kantarjian H, Sawyers C, Hochhaus A, et al. Hematologic and cytogenetic responses to imatinib mesylate in chronic myelogenous leukemia. N Engl J Med. 2002;346:645-52.
23. Quintas-Cardama A, Kantarjian H, Munden R, et al. Pleural effusion in patients (pts) with chronic myelogenous leukemia (CML) treated with dasatinib after imatinib failure [abstract]. Blood. 2006; 108:abstract no. 2164.

Available online at www.sciencedirect.com
ScienceDirect
Leukemia Research 32 (2008) 643–649
Leukemia Research
www.elsevier.com/locate/leukres

Phosphorylation levels of BCR-ABL, CrkL, AKT and STAT5 in imatinib-resistant chronic myeloid leukemia cells implicate alternative pathway usage as a survival strategy

Iman Jilani [a], Hagop Kantarjian [b], Mercedes Gorre [a], Jorge Cortes [b], Oliver Ottmann [c], Kapil Bhalla [d], Francis J. Giles [b], Maher Albitar [a,*]

[a] *Department of Hematopathology, Quest Diagnostics Nichols Institute, San Juan Capistrano, CA, USA*
[b] *Department of Leukemia, M.D. Anderson Cancer Center, University of Texas, Houston, TX, USA*
[c] *Department of Leukemia, JW Goethe Universität, Frankfurt, Germany*
[d] *Department of Leukemia, H. Lee Moffitt Cancer Center, Tampa, FL, USA*

Received 18 April 2007; received in revised form 17 July 2007; accepted 7 August 2007
Available online 27 September 2007

Abstract

Ex-vivo studies have suggested that imatinib-resistance in chronic myeloid leukemia (CML) patients occurs despite adequate suppression of BCR-ABL activity. Whether BCR-ABL phosphorylation levels differ between imatinib-sensitive and -resistant patients is not known. We compared the phosphorylation of BCR-ABL in 54 previously untreated CML patients and 62 imatinib-resistant CML patients with progressive disease. Resistant patients had significantly lower levels of BCR-ABL, CrkL and AKT phosphorylation than previously untreated patients, but STAT5 phosphorylation showed no difference. These observations suggest that imatinib- resistance is not necessarily dependent on higher activity in BCR-ABL-dependent pathways, but is likely due to the activation of other pathways.

Keywords: Chronic myeloid leukemia; BCR-ABL; CrkL; AKT; STAT5; Imatinib; Resistance; Survival pathways; Tyrosine kinase

1. Introduction

The BCR-ABL oncoprotein is the causative agent in some cases of acute lymphoblastic leukemia (ALL), and most chronic myeloid leukemias (CML). The fused *ABL* and *BCR* genes found in CML are transcribed as a single gene, and like wildtype ABL, the BCR-ABL fusion protein is a protein tyrosine kinase. However, the fusion process results in constitutive activation and the loss of regulatory control [1]. BCR-ABL phosphorylates both itself [2] and downstream signaling proteins, driving the oncogenic transformation of hematopoietic stem cells resulting in CML. Imatinib mesylate (Gleevec, STI-571), a small-molecule inhibitor, is a first-line therapy for CML patients. The drug specifically inhibits BCR-ABL tyrosine kinase activity with high specificity and low toxicity, while causing apoptosis of CML cells [3–5]. The majority of CML patients respond favorably to imatinib, but resistance often develops, especially in blast phase disease. Reportedly, resistance to imatinib treatment is most commonly the result of point mutations that interfere with the binding of the drug to BCR-ABL (reviewed in [6]). Other mechanisms have also been reported, however, and some resistant CML cell lines show resistance even in the presence of imatinib binding and suppression of BCR-ABL fusion protein kinase activity [7–9].

Downstream effectors of the BCR-ABL fusion protein that may contribute to transformation or to sustained proliferation of leukemic cells include the survival kinase AKT, the transcription factor STAT5 [10–13] and the adaptor pro-

* Corresponding author at: Quest Diagnostics Nichols Institute, 33608 Ortega Highway, San Juan Capistrano, CA 92675, USA.
Tel.: +1 949 728 4784; fax: +1 949 728 4990.
E-mail address: maher.x.albitar@questdiagnostics.com (M. Albitar).

0145-2126/$ – see front matter © 2007 Elsevier Ltd. All rights reserved.
doi:10.1016/j.leukres.2007.08.009

tein CrkL [14–17]. AKT, an oncoprotein in its own right, is a serine/threonine kinase involved in the activation of pro-survival pathways downstream of multiple receptors, and has many substrates that regulate metabolism, growth, and the cell cycle (reviewed in [18,19]). AKT is recruited to the plasma membrane by binding to the phospholipid products of phosphoinositide 3-kinase (PI3K), and is activated by phosphorylation at Thr308 by PDK-1, followed by phosphorylation at Ser473 by a controversial kinase often referred to as "PDK-2". PI3K activation and the subsequent activation of AKT are required for BCR-ABL transformation of both myeloid and lymphoid lineage cells (reviewed in [20]), and this activation may be mediated in part by the adaptor protein CrkL. Both CrkL and the adaptor protein c-cbl are highly phosphorylated in an ABL-dependent manner, which facilitates their interaction and creates a putative binding site on c-cbl for the regulatory subunit of PI3K [14]. Phosphorylation of CrkL at Tyr207, and the activation of AKT as measured by phosphorylation at Ser473, can therefore be used as indicators of BCR-ABL kinase activity.

The signal transducer and activator of transcription (STAT) family of transcription factors is involved in signal transduction downstream of multiple cytokines, hormones, and growth factors, and is involved in the regulation of cell survival, proliferation, and differentiation (reviewed in [13]). The pathway leading to activation of family member STAT5 is constitutively active in BCR-ABL cells, and STAT5 activity appears to play a major role in the antiapoptotic and proliferative abilities of BCR-ABL transformed cells, possibly through STAT5-mediated expression of the pro-survival protein Bcl-x_L [21–23]. Inhibition of BCR-ABL kinase activity by imatinib led to suppression of STAT5 binding to the *Bcl-x* promoter, and rendered BCR-ABL-positive cells vulnerable to apoptosis [23]. Previous studies have established phosphorylation of STAT5 at Tyr694 as an indicator of BCR-ABL activity [24], and we have developed a quantitative assay to measure phosphorylation of STAT5 at this site.

To investigate the mechanisms of resistance in our own patient populations, we collected whole blood and/or bone marrow from imatinib-resistant and -naïve patients and compared their BCR-ABL kinase activity, on a per-cell basis, as indicated by the phosphorylation status of downstream proteins CrkL, Akt, and STAT5. Phosphorylation levels of AKT, CrkL, and BCR-ABL itself were reduced in imatinib-resistant cells or plasma as compared to previously untreated cells, while STAT5 phosporylation did not differ between the two groups. These data suggest that resistance to imatinib treatment in CML cells is not necessarily due to greater levels of activity in BCR-ABL target pathways, but may instead be due to the activation of alternative pathways. Imatinib represents the first successful targeted cancer therapy, and identification of the mechanism(s) of resistance to imatinib should lead to greater understanding of the survival pathways active in transformed cells, and ultimately, to new therapeutic targets.

2. Materials and methods

2.1. Patients and samples

We collected EDTA peripheral blood or bone marrow aspirates from 54 imatinib-naïve CML patients and 62 patients with progressive disease at the point of imatinib-resistance. We defined imatinib resistance as failure to achieve or loss of (a) a complete hematological response after 3 months, (b) at least a minimal cytogenetic response after 6 months, or (c) a major cytogenetic response after 12 months. We collected samples according to institutional review board-approved protocols, and all patients provided written informed consent.

2.2. BCR-ABL phosphorylation

Measuring BCR-ABL phosphorylation via flow cytometry has been previously described [25]. Briefly, we coated carboxylated polystyrene beads (Bangs Laboratories, Fishers, IN) with anti-BCR antibody (Santa Cruz Biotechnology, Santa Cruz, CA). We diluted patient plasma samples in assay solution (phosphate-buffered saline (PBS) with 5% bovine serum albumin), denatured with 2% sodium dodecyl sulfate (SDS) at 96 °C, incubated them with conjugated beads, and washed and resuspended them in assay solution. We divided each sample into thirds and incubated each aliquot with the appropriate detection antibody (total ABL, p-ABL (Thr735), or p-ABL (Tyr245)). Total ABL antibody was obtained from Santa Cruz Biotechnology, and p-ABL (Tyr245) and p-Abl (Thr735) were purchased from Cell Signaling Technologies (Beverly, MA). We then washed the beads, incubated them with 1:1 phycoerythrin (PE)-conjugated goat anti-rabbit antibody (mouse and human adsorbed; Jackson ImmunoResearch, West Grove, PA), and washed, resuspended, and analyzed the samples on a FACSCanto flow cytometer (Becton Dickinson, San Jose, CA).

2.3. Quantitative flow cytometry of downstream intracellular proteins

Washed whole blood samples were fixed with formaldehyde, permeabilized with a PBS-buffered saponin-based permeabilizing solution (IntraPrep Permeabilization kit, Beckman Coulter, Fullerton, CA), and incubated with primary antibodies against intracellular proteins. Cells were washed with PBS, and incubated with a PE-conjugated goat anti-rabbit IgG secondary detection antibody (Santa Cruz Biotechnology). We then washed the cells a final time, resuspended them in PBS, and acquired them with a FACSCalibur flow cytometer (Becton Dickinson). Antibodies directed against p-CrkL (Tyr207), p-Akt (Ser473), and p-STAT5 (Tyr694) were obtained from Cell Signaling Technologies (Beverly, MA).

2.4. ABL kinase mutation analysis

RNA was extracted from cells as previously described [26]. An 863 bp RT-PCR product encompassing the kinase domain of BCR-ABL was amplified as using a forward primer that annealed in BCR exon b2 and a reverse primer that annealed at the junction of ABL exons 9 and 10 [26]. The products were sequenced in forward and reverse directions using dye terminator chemistry and an ABI sequencer (Applied Biosystems, Foster City, CA).

2.5. Data analysis

We quantified PE intensities with QuantiBRITE PE beads, a set of pre-calibrated beads in which each of four bead populations has a different calibrated mean number of bound PE molecules/bead (Becton Dickinson). These beads allowed us to generate standard curves for each assay, and convert the mean fluorescence intensity (MFI) of antibody bound to intracellular protein into molecular equivalents, or antibodies bound per cell (ABC). Similarly, these standard curves allowed us to calculate the amount of antibody bound to beads in the BCR-ABL assay. QuantiBRITE beads were acquired with each set of samples assayed. We used FlowJo software (Tree Star, Ashland, OR) to convert flow cytometry output (MFI) into percentage of cells (or beads) positively stained with detection antibodies, and/or antibodies bound per cell (or bead) (ABC).

3. Results

3.1. Levels of BCR-ABL phosphorylation

Activated c-ABL, and therefore also BCR-ABL, are phosphorylated at multiple sites, including Tyr412, Tyr245, and Thr735. In order to study BCR-ABL activation in CML patients, we measured phosphorylation of Tyr245 and Thr735 via a bead-based quantitative flow cytometry assay as previously described [25]. Plasma from 62 imatinib-resistant patients had significantly lower levels of both p-BCR-ABL (Thr735) and p-BCR-ABL (Tyr245) than plasma from 54 imatinib-naïve patients (Fig. 1). To determine what proportion of the total BCR-ABL was phosphorylated in each sample, we calculated the ratio of phosphorylated to total BCR-ABL protein. The mean ratio of p-BCR-ABL (Thr735) to total BCR-ABL was 0.69 (median, 0.64; range, 0.03–1.63) in resistant patients and 0.84 (median, 0.80; range, 0.40–1.67)

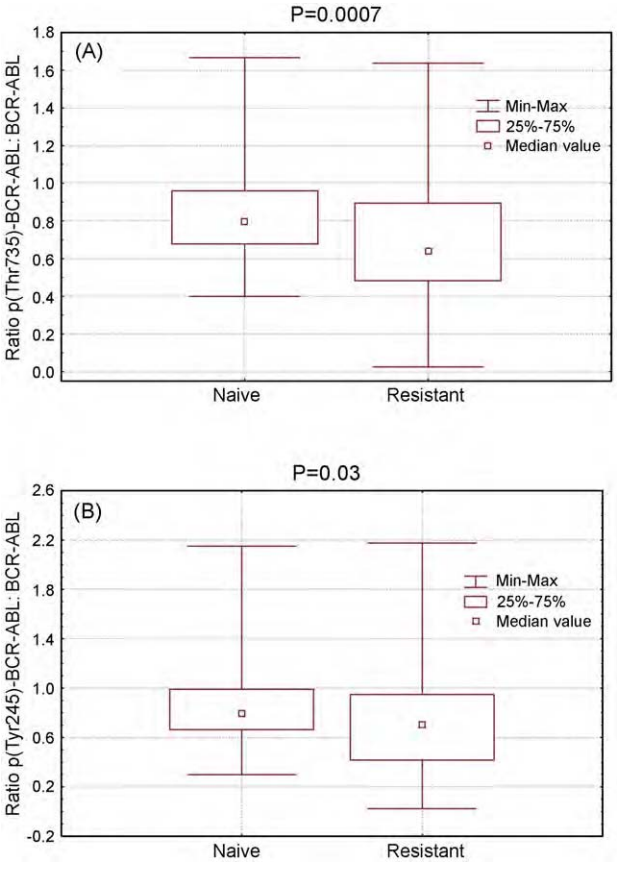

Fig. 1. BCR-ABL phosphorylation levels are lower in imatinib-resistant CML patients than in imatinib-naïve patients. Plasma samples from 62 imatinib-resistant and 54 imatinib-naïve CML patients were sequentially incubated with anti-BCR-coated beads, anti-pABL antibodies (Thr735 or Tyr245) or total ABL antibody, and PE-conjugated secondary antibodies, to specifically detect phosphorylated BCR-ABL and total BCR-ABL protein via flow cytometry. Standard curves for each assay were calculated using QuantiBRITE beads, allowing conversion of MFI values for patient samples to antibodies bound/bead. Ratios of (A) p-BCR-ABL (Thr735) and (B) p-BCR-ABL (Tyr245) to total BCR-ABL protein are shown. *P*-values were calculated using a standard Student's *t*-test.

Table 1
Levels of phosphorylated BCR-ABL, CrkL, AKT, and STAT5 in imatinib-resistant and imatinib-naïve CML samples

	Imatinib-resistant (62 patients)		Imatinib-naïve (54 patients)		*P*-value
	Median[a]	Range	Median	Range	
Ratio: p-BCR-ABL (Thr735): BCR-ABL[b]	0.64	0.03–1.63	0.80	0.40–1.67	0.0007
Ratio: p-BCR-ABL (Tyr245): BCR-ABL	0.71	0.02–2.18	0.80	0.30–2.15	0.03
p-CrkL (Tyr207)[c]	4204	2368–14,772	5982	2368–14,779	0.01
p-AKT (Ser473)	4131	0–62,926	5949	2394–15,904	0.008
p-STAT5 (Tyr694)	3598	0–35,620	4468	1075–10,227	0.53

[a] Median and range values represent the calculation of antibodies bound per bead or cell, as described in Section 2.
[b] BCR-ABL phosphorylation assays performed on plasma.
[c] CrkL, AKT and STAT5 phosphorylation assays performed on cells obtained from whole blood or bone marrow.

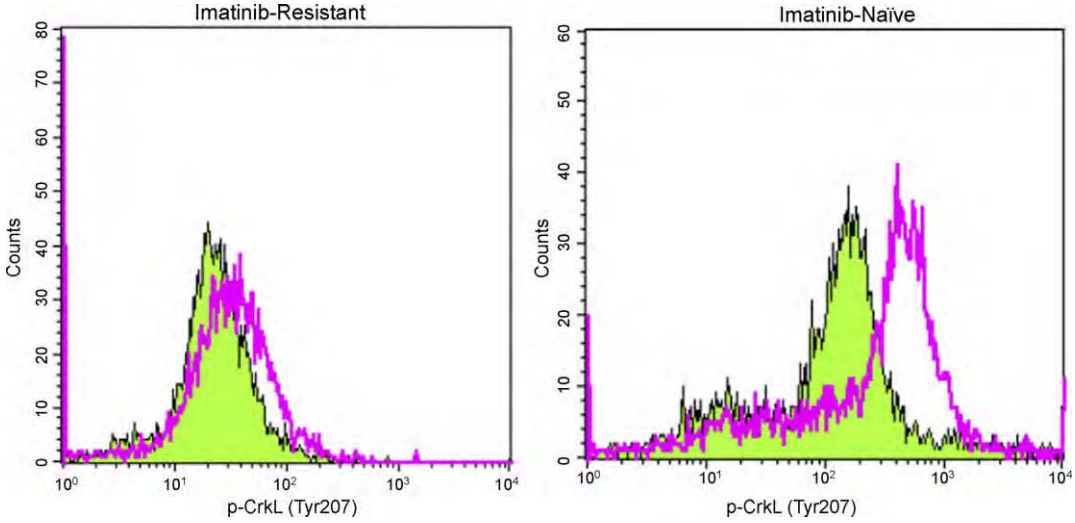

Fig. 2. CrkL phosphorylation is lower in cells from imatinib-resistant CML patients than in imatinib-naïve patients. Peripheral blood cells were fixed, permeabilized, and incubated with anti-p-CrkL (Tyr207) antibody, followed by a PE-conjugated secondary antibody for detection via flow cytometry. Representative flow cytometry histograms of p-CrkL from an imatinib-resistant CML patient and an imatinib-naïve patient are shown (filled, isotype control; line, p-CrkL (Tyr207)).

in imatinib-naïve patients (Fig. 1A and Table 1), while the mean ratio of p-BCR-ABL (Tyr245) to total BCR-ABL was 0.71 (median, 0.71; range, 0.02–2.18) in resistant patients and 0.84 (median, 0.80; range, 0.30–2.15) in imatinib-naive patients (Fig. 1B and Table 1). Phosphorylation of BCR-ABL at Thr735 and Tyr245 was significantly lower in plasma from imatinib-treated CML patients than in imatinib-naïve plasma ($P = 0.0007$ and $P = 0.03$, respectively). These data demonstrate that BCR-ABL phosphorylation is inhibited in imatinib-resistant cells. To test whether the plasma phosphorylation levels reflected the cell levels, we compared the ratios of p-BCR-ABL (Thr735): total BCR-ABL and p-BCR-ABL (Tyr245): total BCR-ABL in plasma with those in cells from the same patient in eight paired samples and we found no statistical difference ($P = 0.21$).

3.2. Levels of CrkL, AKT, and STAT5 phosphorylation

Phosphorylation of downstream effectors of BCR-ABL is indicative of BCR-ABL kinase activity. We therefore compared the phosphorylation of BCR-ABL-dependent sites in the effectors AKT (Ser473), CrkL (Tyr207), and STAT5 (Tyr694) in imatinib-treated versus imatinib-naïve CML patient peripheral blood or bone marrow cells. Representative histograms of p-CrkL (Tyr207) phosphorylation in imatinib-resistant and -naïve patients are shown in Fig. 2, demonstrating a lower level of CrkL phosphorylation in imatinib-resistant CML cells. Further, when MFI data were converted to antibodies bound per cell, and data from 54 imatinib-naïve patients were compared to that of 62 imatinib-resistant patients, the imatinib-resistant cells had significantly

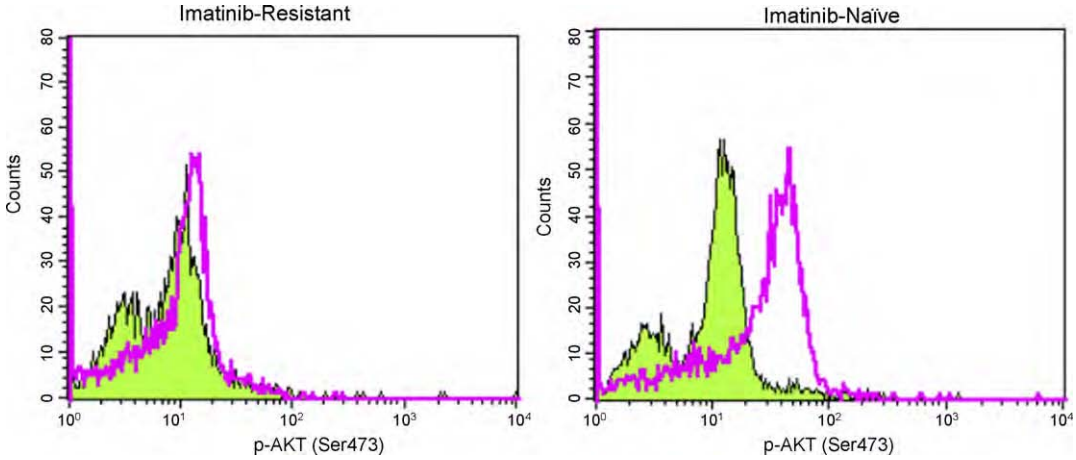

Fig. 3. AKT phosphorylation is lower in imatinib-resistant CML patients than in imatinib-naïve patients. Peripheral blood cells were fixed, permeabilized, and incubated with anti-p-AKT (Ser473) antibody, followed by a PE-conjugated secondary antibody for detection via flow cytometry. Representative flow cytometry histograms of p-AKT from an imatinib-resistant CML patient and an imatinib-naïve patient are shown (filled, isotype control; line, p-AKT (Ser473)).

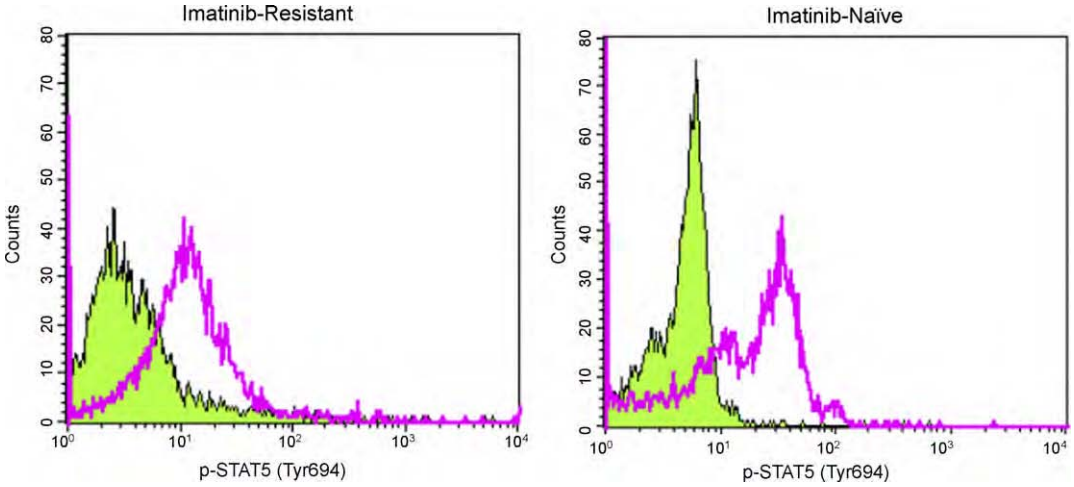

Fig. 4. STAT5 phosphorylation does not differ in imatinib-naïve and –resistant CML patients. Peripheral blood cells were fixed, permeabilized, and incubated with anti-p-STAT5 (Tyr694) antibody, followed by a PE-conjugated secondary antibody for detection via flow cytometry. Representative flow cytometry histograms of p-STAT5 from an imatinib-resistant CML patient and an imatinib-naïve patient are shown (filled, isotype control; line, p-STAT5 (Tyr694)).

lower mean levels of p-CrkL (Table 1). Like CrkL, phosphorylation of AKT (Ser473) was also significantly lower in imatinib-resistant cells as compared to imatinib-naïve cells (Fig. 3 and Table 1). In contrast, phosphorylation of STAT5 did not differ significantly between cells from imatinib-naïve and -resistant patients (Fig. 4 and Table 1). Similar results obtained whether we gated on total cell population or we gated on granulocyte population only.

3.3. BCR-ABL mutated versus unmutated in imatinib-resistant

We investigated whether imatinib-resistant patients who have BCR-ABL mutation differ from those resistant but without BCR-ABL mutation. Direct sequencing of the imatinib-resistant patients showed the presence of BCR-ABL mutation in 27 of the 62 patients (44%). The detected mutations included: G250E, L387M, E45K, M351T, M244V, T315I, Y253F, H396R, F311L, Q252H, F315L, E334G, and D276G. There was no statistical difference in the ratios of p-BCR-ABL: total BCR-ABL (Tyr245 and Thr735) between mutated and unmutated resistant patients. However, patients with mutated BCR-ABL had higher relative p-AKT ($P = 0.04$) as compared with unmutated resistant patients. There was no difference in p-STAT5 or p-CrkL between mutated and unmutated groups. However, we cannot rule out the possibility that a specific mutation might be associated with a specific change in phosphorylation. The number is too small to compare between individual mutations.

4. Discussion

The BCR-ABL kinase-specific inhibitor imatinib is the first targeted small molecule inhibitor to prove effective in the treatment of cancer. However, some CML patients are resistant to the drug, while others develop resistance over time. To date, there has been no direct quantitative comparison of the activity of key signaling pathways known to be involved in BCR-ABL-mediated proliferation and survival. Using quantitative flow cytometry, in this study, we demonstrate that plasma samples from patients exhibiting resistance to imatinib have a lower level of phosphorylation of BCR-ABL itself at two residues indicative of kinase activation (Tyr245 and Thr735). Moreover, the phosphorylation of downstream BCR-ABL targets AKT and CrkL is reduced in imatinib-resistant peripheral blood or bone marrow cells as compared to imatinib-naïve patients, although STAT5 phosphorylation did not differ between the two groups.

Many mechanisms of imatinib-resistance have been observed, and the most common is believed to be the restoration of BCR-ABL tyrosine kinase activity via decreased drug binding, putatively as the result of mutations in BCR-ABL within the drug's binding site or which affect the protein's conformation [6]. The first mutation demonstrated to accomplish this decrease in imatinib-binding was T315I [27], and others have since followed ([28–32]; reviewed in [6]). If the failure of imatinib to bind BCR-ABL is the key component of resistance, future drug design should focus on more effective inhibition of BCR-ABL tyrosine kinase activity. Our findings, however, indicate that the imatinib resistance in our patient population was not the result of reversion to high levels of BCR-ABL signaling due to poor drug binding, as BCR-ABL-dependent phosphorylation was consistently significantly lower in imatinib-resistant patients. Rather, these data suggest that alternative signaling pathways are engaged to maintain survival and proliferation of imatinib-treated CML cells. While binding site mutations undoubtedly confer a survival advantage, especially those mutations that predate imatinib therapy, they are more likely to exist in a subpopulation of leukemic clones that are able to contribute to disease progression [6].

We observed that STAT5 phosphorylation levels in imatinib-resistant and -naïve patients did not differ significantly, despite the demonstrated decreases in activity of known upstream signaling effectors in the resistant cells. These findings support the concept that imatinib resistance may be due to activation of pathways that deviate from the canonical BCR-ABL signaling cascade. Examples include the src-family kinases Lyn and Hck, which are activated by BCR-ABL, and can also be expressed in imatinib-resistant CML cells that exhibit suppressed tyrosine kinase activity [8,33]. Further studies on resistance are needed to examine specific mutations, the potential activation of alternative pathways, the possibility that alternative mechanisms may be associated with one another, and the suitability and efficacy of multi-target therapies in these instances.

Conflicts of interests

None.

Acknowledgements

The authors thank Amber C. Donahue for critical reading and help in preparation of the manuscript.

Contributions. Iman Jilani performed testing and wrote paper. Hagop Kantarjian provided clinical data and analyzed data. Mercedes Gorre performed testing and analyzed data. Jorge Cortes provided clinical data and analyzed data. Oliver Ottmann provided clinical data. Kapil Bhalla provided clinical data. Francis Giles provided clinical data and analyzed data. Maher Albitar wrote paper, provided clinical data, analyzed data and designed study.

References

[1] Lugo TG, Pendergast AM, Muller AJ, Witte ON. Tyrosine kinase activity and transformation potency of bcr-abl oncogene products. Science 1990;247:1079–82.
[2] Brasher BB, Van Etten RA. c-Abl has high intrinsic tyrosine kinase activity that is stimulated by mutation of the Src homology 3 domain and by autophosphorylation at two distinct regulatory tyrosines. J Biol Chem 2000;275:35631–7.
[3] Druker BJ, Talpaz M, Resta DJ, Peng B, Buchdunger E, Ford JM, et al. Efficacy and safety of a specific inhibitor of the BCR-ABL tyrosine kinase in chronic myeloid leukemia. N Engl J Med 2001;344:1031–7.
[4] Druker BJ, Tamura S, Buchdunger E, Ohno S, Segal GM, Fanning S, et al. Effects of a selective inhibitor of the Abl tyrosine kinase on the growth of Bcr-Abl positive cells. Nat Med 1996;2:561–6.
[5] Kantarjian H, Sawyers C, Hochhaus A, Guilhot F, Schiffer C, Gambacorti-Passerini C, et al. Hematologic and cytogenetic responses to imatinib mesylate in chronic myelogenous leukemia. N Engl J Med 2002;346:645–52.
[6] Nardi V, Azam M, Daley GQ. Mechanisms and implications of imatinib resistance mutations in BCR-ABL. Curr Opin Hematol 2004;11:35–43.
[7] Dai Y, Rahmani M, Corey SJ, Dent P, Grant S. A Bcr/Abl-independent, Lyn-dependent form of imatinib mesylate (STI-571) resistance is associated with altered expression of Bcl-2. J Biol Chem 2004;279:34227–39.
[8] Donato NJ, Wu JY, Stapley J, Gallick G, Lin H, Arlinghaus R, et al. BCR-ABL independence and LYN kinase overexpression in chronic myelogenous leukemia cells selected for resistance to STI571. Blood 2003;101:690–8.
[9] Donato NJ, Wu JY, Stapley J, Lin H, Arlinghaus R, Aggarwal BB, et al. Imatinib mesylate resistance through BCR-ABL independence in chronic myelogenous leukemia. Cancer Res 2004;64:672–7.
[10] Nieborowska-Skorska M, Wasik MA, Slupianek A, Salomoni P, Kitamura T, Calabretta B, et al. Signal transducer and activator of transcription (STAT)5 activation by BCR/ABL is dependent on intact Src homology (SH)3 and SH2 domains of BCR/ABL and is required for leukemogenesis. J Exp Med 1999;189:1229–42.
[11] de Groot RP, Raaijmakers JA, Lammers JW, Koenderman L. STAT5-Dependent CyclinD1 and Bcl-xL expression in Bcr-Abl-transformed cells. Mol Cell Biol Res Commun 2000;3:299–305.
[12] Klejman A, Schreiner SJ, Nieborowska-Skorska M, Slupianek A, Wilson M, Smithgall TE, et al. The Src family kinase Hck couples BCR/ABL to STAT5 activation in myeloid leukemia cells. EMBO J 2002;21:5766–74.
[13] Benekli M, Baer MR, Baumann H, Wetzler M. Signal transducer and activator of transcription proteins in leukemias. Blood 2003;101:2940–54.
[14] Hemmeryckx B, van Wijk A, Reichert A, Kaartinen V, de Jong R, Pattengale PK, et al. Crkl enhances leukemogenesis in BCR/ABL P190 transgenic mice. Cancer Res 2001;61:1398–405.
[15] Sattler M, Salgia R, Okuda K, Uemura N, Durstin MA, Pisick E, et al. The proto-oncogene product p120CBL and the adaptor proteins CRKL and c-CRK link c-ABL, p190BCR/ABL and p210BCR/ABL to the phosphatidylinositol-3' kinase pathway. Oncogene 1996;12:839–46.
[16] Skorski T, Bellacosa A, Nieborowska-Skorska M, Majewski M, Martinez R, Choi JK, et al. Transformation of hematopoietic cells by BCR/ABL requires activation of a PI-3k/Akt-dependent pathway. EMBO J 1997;16:6151–61.
[17] Tang X, Downes CP, Whetton AD, Owen-Lynch PJ. Role of phosphatidylinositol 3-kinase and specific protein kinase B isoforms in the suppression of apoptosis mediated by the Abelson protein-tyrosine kinase. J Biol Chem 2000;275:13142–8.
[18] Brazil DP, Yang ZZ, Hemmings BA. Advances in protein kinase B signalling: AKTion on multiple fronts. Trends Biochem Sci 2004;29:233–42.
[19] Downward J. PI 3-kinase, Akt and cell survival. Semin Cell Dev Biol 2004;15:177–82.
[20] Kharas MG, Fruman DA. ABL oncogenes and phosphoinositide 3-kinase: mechanism of activation and downstream effectors. Cancer Res 2005;65:2047–53.
[21] de Groot RP, Raaijmakers JA, Lammers JW, Koenderman L. STAT5-Dependent CyclinD1 and Bcl-xL expression in Bcr-Abl-transformed cells. Mol Cell Biol Res Commun 2000;3:299–305.
[22] Gesbert F, Griffin JD. Bcr/Abl activates transcription of the Bcl-X gene through STAT5. Blood 2000;96:2269–76.
[23] Horita M, Andreu EJ, Benito A, Arbona C, Sanz C, Benet I, et al. Blockade of the Bcr-Abl kinase activity induces apoptosis of chronic myelogenous leukemia cells by suppressing signal transducer and activator of transcription 5-dependent expression of Bcl-xL. J Exp Med 2000;191:977–84.
[24] Jacobberger JW, Sramkoski RM, Frisa PS, Ye PP, Gottlieb MA, Hedley DW, et al. Immunoreactivity of Stat5 phosphorylated on tyrosine as a cell-based measure of Bcr/Abl kinase activity. Cytometry A 2003;54:75–88.
[25] Detection of chromosome translocation by bead-based flow cytometry.Chan HE, Jilani I, Chang R, Albitar M, editors. Monoclonal antibodies: methods and protocols. Methods in molecular biology. Clifton, NJ: Humana Press; 2007. Chapter 12.

[26] Ma W, Kantarjian H, Jilani I, Gorre M, Bhalla K, Ottmann O, et al. Heterogeneity in detecting Abl kinase mutations and better sensitivity using circulating plasma RNA. Leukemia 2006;20:1989–91.
[27] Gorre ME, Mohammed M, Ellwood K, Hsu N, Paquette R, Rao PN, et al. Clinical resistance to STI-571 cancer therapy caused by BCR-ABL gene mutation or amplification. Science 2001;293:876–80.
[28] Barthe C, Gharbi MJ, Lagarde V, Chollet C, Cony-Makhoul P, Reiffers J, et al. Mutation in the ATP-binding site of BCR-ABL in a patient with chronic myeloid leukaemia with increasing resistance to STI571. Br J Haematol 2002;119:109–11.
[29] Ricci C, Scappini B, Divoky V, Gatto S, Onida F, Verstovsek S, et al. Mutation in the ATP-binding pocket of the ABL kinase domain in an STI571-resistant BCR/ABL-positive cell line. Cancer Res 2002;62:5995–8.
[30] Roche-Lestienne C, Soenen-Cornu V, Grardel-Duflos N, Lai JL, Philippe N, Facon T, et al. Several types of mutations of the Abl gene can be found in chronic myeloid leukemia patients resistant to STI571, and they can pre-exist to the onset of treatment. Blood 2002;100:1014–8.
[31] Roumiantsev S, Shah NP, Gorre ME, Nicoll J, Brasher BB, Sawyers CL, et al. Clinical resistance to the kinase inhibitor STI-571 in chronic myeloid leukemia by mutation of Tyr-253 in the Abl kinase domain P-loop. Proc Natl Acad Sci USA 2002;99:10700–5.
[32] Shah NP, Nicoll JM, Nagar B, Gorre ME, Paquette RL, Kuriyan J, et al. Multiple BCR-ABL kinase domain mutations confer polyclonal resistance to the tyrosine kinase inhibitor imatinib (STI571) in chronic phase and blast crisis chronic myeloid leukemia. Cancer Cell 2002;2:117–25.
[33] Donato NJWJ, Kong LY, Meng F, Lee F, Talpaz M. Constitutive activation of SRC-family kinases in chronic myelogenous leukemia patients resistant to imatinib mesylate in the absence of BCR-ABL mutations: a rationale for use of SRC/ABL dual kinase inhibitor-based therapy. Blood (ASH Annual Meeting Abstracts) 2005;106. Abstract 1087.

Available online at www.sciencedirect.com
ScienceDirect
Leukemia Research 32 (2008) 936–943
Leukemia Research
www.elsevier.com/locate/leukres

An immunological method for the detection of BCR-ABL fusion protein and monitoring its activation

Iman Jilani [a], Hagop Kantarjian [b], Homan Faraji [a], Mercedes Gorre [a], Jorge Cortes [b], Oliver Ottmann [c], Kapil Bhalla [d], Susan O'Brien [b], Francis Giles [b], Maher Albitar [a,*]

[a] *Department of Hematology, Quest Diagnostics Nichols Institute, 33608 Ortega Highway, San Juan Capistrano, CA 92690, USA*
[b] *Department of Leukemia, M.D. Anderson Cancer Center, University of Texas, Houston, TX 77030, USA*
[c] *Department of Leukemia, JW Goethe Universitat, Frankfurt, Germany*
[d] *Department of Leukemia, H.L. Moffitt Cancer Center, Tampa, FL 33612, USA*

Received 15 April 2007; received in revised form 13 November 2007; accepted 13 November 2007
Available online 26 December 2007

Abstract

We have developed a simplified sandwich immunoassay to measure free circulating total and phosphorylated fusion BCR-ABL protein in patients with the t(9;22)(q34;q11) chromosomal translocation. The assay is based on immunoprecipitating BCR-ABL protein using beads coated with anti-BCR antibody and detecting the fusion protein with anti-ABL antibody and flow cytometry. We show that this method allows the quantification of this protein in the plasma and may allow the measurement of tumor load. This method also allows the measurement of the level of phosphorylation of the immunoprecipitated BCR-ABL using antibodies against phosphorylated ABL protein, which can be used for monitoring of therapy with kinase inhibitors. The sensitivity of this immunoassay was comparable to the sensitivity of reverse transcription-polymerase chain reaction (RT-PCR) assay. This technique is useful in monitoring patients with chronic myeloid leukemia (CML) or acute lymphoblastic leukemia (ALL), but the same approach can be used in other translocations and has the potential of multiplexing.

Keywords: BCR-ABL; Fusion protein; CML; Beads; Phosphorylation; MDR; Imatinib

1. Introduction

As in most of the chromosomal translocations that result in fusion protein, the BCR-ABL fusion protein is a constitutively active tyrosine kinase. Recently this BCR-ABL fusion protein has been successfully targeted for therapy by a specific tyrosine kinase inhibitor, imatinib (STI571; Gleevec®, Novartis Pharmaceuticals Corporation, East Hanover, NJ) [1–3]. Despite the success of this drug, a significant fraction of patients (10–30%) respond poorly or develop resistance to imatinib therapy [4]. Resistance to imatinib therapy has spurred development of new, more specific kinase inhibitors such as BMS-354825 and AMN107 that target resistant forms of the BCR-ABL protein [4–6]. Monitoring residual disease in CML patients currently depends on RT-PCR assay of BCR-ABL mRNA, however the RT-PCR assay presents inherent difficulties with variability and standardizing quantitation [7,8]. In addition, it has become increasingly important to be able to assay the activity of the BCR-ABL protein in CML patients as a potential diagnostic tool to predict response or prognosis, and as a means of monitoring efficacy and response to therapy.

The BCR-ABL protein, in the absence of inhibition, is phosphorylated on Thr-735 in the conserved 14-3-3 protein binding motif and on Tyr-245 in the linker region between the SH2 and catalytic domains of the ABL portion of the fusion. Autophosphorylation at Tyr-245 is involved in the activation mechanism of the kinase whereas the role of phosphorylation at Thr-735 remains unclear [9–11]. Importantly, the phosphorylation state of these residues serves as an indicator of BCR-ABL kinase activity. Therefore, an accurate, direct, and quantitative measure of BCR-ABL protein levels and its activity is needed.

* Corresponding author. Tel.: +1 949 728 4784; fax: +1 949 728 4990.
E-mail address: maher.x.albitar@questdiagnostics.com (M. Albitar).

0145-2126/$ – see front matter © 2007 Elsevier Ltd. All rights reserved.
doi:10.1016/j.leukres.2007.11.023

We report a simplified immunoassay for measuring levels of BCR-ABL protein and its phosphorylation state that is suitable for routine analysis in clinical laboratories. Since we have demonstrated previously that leukemic cells pour their proteins into circulation, for example, cCD20 and cCD52 [12,13], plasma from peripheral blood samples of CML patients was tested for BCR-ABL protein using this new assay. The immunoassay detected levels of BCR-ABL protein with a sensitivity comparable to the reverse transcriptase-polymerase chain reaction assay used to measure minimal residual disease. More importantly, the immunoassay was able to measure the proportion of BCR-ABL that was phosphorylated on Thr-735 and Tyr-245, providing valuable information on the kinase activity of the BCR-ABL protein in CML patients.

2. Patients, materials, and methods

2.1. Patient samples

All samples were collected and processed according to institutional guidelines and an IRB-approved protocol. Patients were diagnosed with CML based on clinical findings, cytogenetics, FISH studies, and RT-PCR analysis. Plasma was prepared from peripheral blood samples collected from previously untreated CML patients ($n = 54$) who were to be treated with imatinib (Gleevec®, Novartis Pharmaceuticals Corporation). Additional samples from these patients were collected at 3 months ($n = 33$), 6 months ($n = 13$), 9 months ($n = 13$), and 12 months ($n = 6$) after initiation of imatinib treatment. The number of follow-up samples is too smalls, but obtaining additional samples from the same cohort from the same institution was not possible due to the departure of two of the coauthors from the original institution, which created logistic difficulties. However, we also tested 590 samples that were Philadelphia-positive by cytogenetic analysis, including 95 samples from patients with acute lymphoblastic leukemia (ALL), all of which were confirmed by cytogenetics or FISH. These samples were from patients who had been treated by various regimens, including interferon and imatinib, and some patients were known to be resistant. Peripheral blood from 96 healthy individuals and 20 acute myeloid leukemia (AML) patients with translocations other than BCR-ABL was also collected for use as negative controls. All samples were collected in tubes containing EDTA (ethylenediaminetetraacetic acid), centrifuged, and the plasma stored at −70 °C until assayed.

2.2. Bead-based BCR-ABL protein immunoassay

Carboxylated polystyrene beads (Bangs Laboratories, Fishers, IN) were coated with antibodies directed against BCR protein (Santa Cruz Biotechnology, Santa Cruz, CA) according to the manufacturer's protocol. Plasma or cell lysate samples were diluted 1:50 in phosphate-buffered saline (PBS) containing 2% bovine serum albumin (BSA), denatured with 2% sodium dodecyl sulfate (SDS) at 96 °C for 4 min, and centrifuged at 13,000 rpm for 2 min at room temperature. The supernatant was incubated with 30 μl anti-BCR conjugated beads at room temperature for 2 h with constant mixing, followed by three washes with PBS/2% BSA, and resuspension in 600 μl of the same solution. Each sample was then divided into three equal aliquots. Five microliters of antibodies specific for total ABL (Santa Cruz Biotechnology), ABL phosphorylated on Thr-735 (Cell Signaling Technology, Beverly, MA), or ABL phosphorylated on Tyr-245 (Cell Signaling Technology) (using amino acid numbering of the c-ABL protein) was added to the aliquots. The mixtures were then incubated at room temperature for 1 h. The beads were then washed three times with PBS/2% BSA and resuspended in 200 μl of the same solution, followed by addition of 10 μl mouse and human adsorbed, goat anti-rabbit antibody labeled with one molecule of phycoerythrin (PE) per molecule of antibody (Santa Cruz Biotechnology). After room temperature incubation for 30 min, the beads were again washed three times in PBS/2% BSA plus 2% sodium azide, and resuspended in 500 μl PBS/2% BSA. Fluorescence signals were acquired by the FACSCanto flow cytometry platform and were quantitated with the QuantiBrite Bead system (Becton Dickinson Immunocytometry Systems, San Jose, CA). Data were analyzed using Flow-Jo software (Tree Star Inc., Ashland, OR). The use of 1:1 PE labeling allowed the staining intensity on the bead surface to be converted to number of molecules bound per bead using the QuantiBrite Bead system in Flow-Jo. The percentage of positive beads was multiplied by the mean number of molecules per bead, and then converted to the number of molecules per 100 beads per 10 μl of plasma, the arbitrary units used for quantitation of BCR-ABL protein species in this paper.

2.3. In vitro treatment with imatinib and AMN107

Imatinib mesylate and AMN107 (kindly provided by Novartis Pharmaceuticals, Basel, Switzerland) were made as 10 mM stocks in DMSO and stored at −20 °C. K562 cells were maintained in RPMI-1640 supplemented with 10% fetal bovine serum and antibiotics. 1×10^6 K562 cells were plated in 6-well tissue culture plates and treated with DMSO alone, imatinib, or AMN107 at different concentrations. Cell cultures were incubated for 18 h at 37 °C in 5% CO_2. Cells were then washed two times with PBS, lysed, and the lysates analyzed by the bead-based BCR-ABL assay.

2.4. RT-PCR assay for BCR-ABL mRNA

We used a standard real-time quantitative RT-PCR assay for BCR-ABL mRNA. Briefly, extracted sample RNA was subjected to a single tube real-time RT-PCR reaction to measure the quantity of the two types of BCR-ABL fusion transcripts (b2a2/b3a2 and e1a2). An additional amplification for the *abl* gene was performed to control for sample

RNA quality and as a reference for relative quantification. The results are reported as a ratio between the quantities of the BCR-ABL fusion mRNA and the internal control mRNA [14].

2.5. Statistical analysis

Patient characteristics were summarized using standard descriptive statistics for continuous variables and tabulations for categorical variables. Relationships between continuous variables were assessed with Spearman rank correlations. The chi-square test was used to assess relationships between categorical variables. Factors found to be statistically significant at the 5% level.

3. Results

3.1. Characterization of the immunoassay for BCR-ABL

The immunoassay is performed using beads as a solid support with phycoerythrin fluorescence detection. The assay

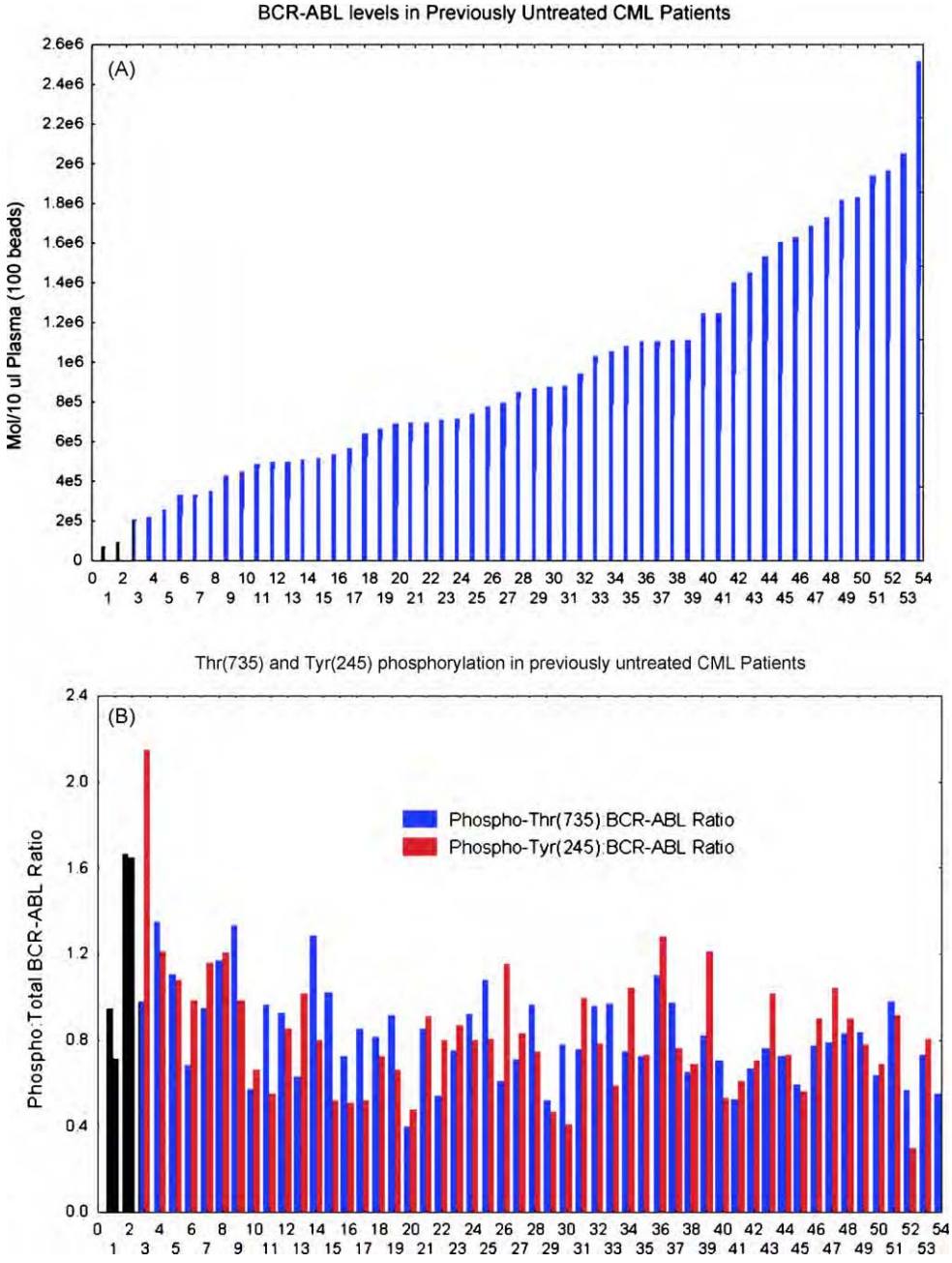

Fig. 1. Detection of BCR-ABL protein and its phosphorylation using bead in patients with CML. (A) Levels of total BCR-ABL in 54 previously untreated CML patients sorted from lower level to highest. Clear variation between patients is seen. (B) There is no significant difference in the relative phosphorylation of BCR-ABL between previously untreated patients. The same patients shown in panel (A) are shown in panel (B) in the same order.

measures the levels of the BCR-ABL fusion protein, as well as its activity, which is indicated by the phosphorylation state of the Thr-735 and Tyr-245 residues in the ABL portion of the protein. Plasma from peripheral blood of normal subjects produced signals similar to those for bovine serum albumin alone, which was similar to isotypic control, indicating that normal plasma could serve as a negative control. Plasma from peripheral blood of CML and Philadelphia-positive ALL patients yielded significant signals above the threshold set by the negative control, demonstrating the ability of the assay to detect BCR-ABL and tyrosine-phosphorylated BCR-ABL protein in these samples. Plasma samples from 96 normal subjects all produced negative results (value of 0 or less) in the immunoassays, and plasma samples from 20 AML patients with various cytogenetic abnormalities other than the Philadelphia chromosome also showed negative results (signal below the threshold for positive results, supporting the specificity of the assay. The AML samples included three patients with acute promyelocytic leukemia, two patients with inversion 16 and three patients with translocations involving the MML gene on chromosome 11 (11q23). By contrast, all 54 samples from previously untreated CML patients and 590 samples from confirmed Philadelphia-positive ALL and CML patients were positive for BCR-ABL.

Significant variation in the levels of BCR-ABL protein was observed among previously untreated patients. As shown in Fig. 1A levels of BCR-ABL protein in previously untreated CML patients varied from 68,835 to 2,512,752 mol/10 μl (37-folds with standard deviation (S.D.) of 566,224) (Fig. 1A). In contrast, phosphorylation levels (ratio of phosphor-BCR-ABL:BCR-ABL) for both Thr-735 and Tyr-245 did not vary significantly (median of 0.8 for both and S.D. of 0.2 and 0.3, respectively) (Fig. 1B). Differences between levels of the BCR-ABL protein among patients are most likely represent differences in tumor load. We found significant ($P < 0.01$) correlation between BCR-ABL protein levels in plasma with LDH ($r = 0.35$), percent of promyelocytes/myelocytes ($r = 0.40$), and white blood cells ($r = 0.49$). Although further confirmation is needed, the demonstration that pre-therapy phosphorylation levels are not significantly different between those with high levels of disease and those with low levels suggests that the difference between these patients is mainly due to early versus late detection. The difference between patients in levels of BCR-ABL protein may have implication for therapy and dosing. Further studies are needed to test if patients with high levels of BCR-ABL protein require higher dosing of imatinib.

The second tested group of patients who were previously treated ($n = 590$) were randomly selected and were at various stages of their disease. BCR-ABL protein was positive in all these patients. When protein results were correlated with RT-PCR, 14 (2%) were negative by RT-PCR and positive by protein. No patient was positive by RT-PCR and negative by protein assay. All tested samples had viable and adequate quantity of RNA as confirmed by the demonstration of adequate (CT < 33) internal control (ABL gene mRNA) [15]. The median level of BCR-ABL protein in these patients was 373,592 mol/10 μl plasma. The phosphorylation levels (ratio of phosphor-BCR-ABL:BCR-ABL) for Thr-735 and Tyr-245 were 0.6 (for both), but with significant variation (S.D. = 0.4 for both) due to the heterogeneity of this group. However, there was no significant correlation between the protein levels and levels of mRNA as detected by RT-PCR. This is not surprising, since the protein levels were measured in plasma, while the RT-PCR was performed on peripheral blood cells. The plasma protein levels reflect the total volume in the body, while the RT-PCR reflects the percent of cells with the Philadelphia chromosome. However, a direct correlation between RT-PCR analysis of cells and plasma BCR-ABL protein measurement in plasma and correlation with clinical

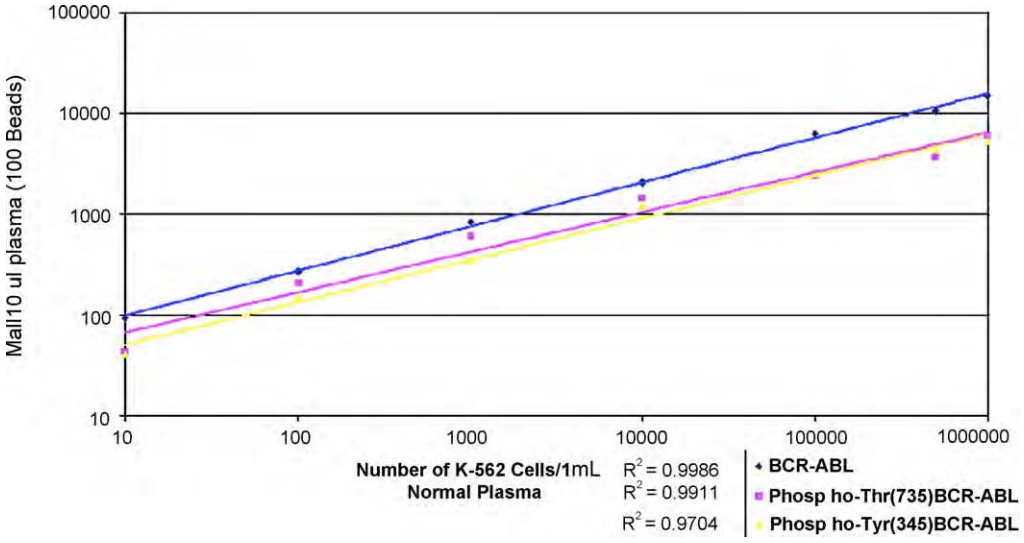

Fig. 2. Sensitivity and linearity of the immunoassay for detecting total and phosphorylated BCR-ABL protein. BCR-ABL-positive K-562 cells were diluted in plasma obtained from normal subjects.

outcome and behavior is important to fully understand the clinical value of this approach.

To determine the sensitivity of the assay, BCR-ABL-positive K562 cells were lysed and diluted in normal plasma. Detection of BCR-ABL protein, phosphorylated Thr-735, and phosphorylated Tyr-245 was linear over 5 orders of magnitude of input cell numbers (Fig. 2). Lysate from as few as 10 cells per 1 ml of plasma could be reliably detected by the immunoassay. However, there is a difference in the magnitude of changes in measured protein versus the input protein. As shown in this figure, the magnitude of increase in the levels of the measurable proteins is significantly lower than the input protein, but remains linear.

When the same sample was analyzed in five independent experiments, coefficients of variation (CV) were 6.09% for BCR-ABL protein, and 8.49–9.62% for phosphorylated BCR-ABL protein, indicating excellent precision for the assay. The stability of the plasma samples at room temperature was assessed over a 96 h period. There was excellent relative stability with CV values below 15% at 96 h. However, whole blood samples when collected in EDTA were stable up to 48 h. The CV of testing was >20% when whole blood samples were tested after 48 h of collection. All patients samples reported in this study were analyzed within 48 h of collection.

In order to assess the ability of the immunoassay to detect changes in the degree of BCR-ABL phosphorylation that might be expected during treatment of CML, cultures of the CML-derived cell line K562 were analyzed after treatment with the kinase inhibitor imatinib, which is currently in wide use as a chemotherapeutic agent, or with AMN107, a newly developed kinase inhibitor that is more specific for the ABL kinase. Treatment with 5 μM imatinib or AMN107, which approximates the peak steady state levels of imatinib in plasma following the standard dose for chronic phase CML (4.6 μM) [16], resulted in four- to nine-fold decreases in the phosphorylation states of Thr-735 and Tyr-245 relative to control treatment with vehicle (Table 1). Treatment with 0.05 μM imatinib or AMN107, a concentration well below the trough concentration of imatinib found in plasma during a standard regimen (2.13 μM) [16], still achieved measurable reductions in the phosphorylation states of Thr-735 and Tyr-245, ranging from 1.33- to 1.43-fold. These results confirm the ability of the phospho-BCR-ABL immunoassay to detect decreases in Thr-735 and Tyr-245 phosphorylation occurring as a result of treatment with a kinase-inhibitory chemotherapeutic agent. In other word, this confirms the specificity of our assay in detecting the phosphorylation levels in BCR-ABL fusion protein (Table 1).

3.2. Use of the BCR-ABL protein immunoassay to monitor CML patients treated with imatinib

The immunoassay was used to monitor BCR-ABL protein levels and phosphorylation state in CML patients before and during treatment with imatinib. Elevated levels of BCR-ABL protein in plasma from peripheral blood were found at baseline prior to treatment (Fig. 3, panel A). BCR-ABL protein levels decreased after 3 and 6 months of treatment. Levels of BCR-ABL protein phosphorylation at Thr-735 and/or Tyr-245 also showed decreases after 3 and 6 months of imatinib treatment, similar to those seen for total BCR-ABL protein (Fig. 3, panels B and C). All changes from pretreatment values were statistically significant ($P < 0.01$).

To determine the potential of this assay in monitoring patients with CML, we collected plasma samples from peripheral blood from patients with CML at different time points after initiation of imatinib treatment and analyzed by both the immunoassay for BCR-ABL protein and the standard cell-based RT-PCR assay for BCR-ABL mRNA. In samples obtained after 6, 9, and 12 months on therapy, BCR-ABL was detected by both methods in 22 of 32 samples. BCR-ABL was detected by the protein assay but not the RT-PCR assay in four samples, by the RT-PCR assay but not the protein assay in one sample, and by neither assay in five samples. These results indicate high sensitivity for the protein assay and with results comparable to the cell-based RT-PCR assay. For samples obtained at 3 months of therapy, the results from the two methods agreed for 23 of 33 samples. Five samples were negative according to the cell-based RT-PCR assay and positive by the plasma protein assay, and conversely, five samples were negative according to the protein assay and positive by the RT-PCR assay. All tested samples by RT-PCR had viable and adequate quantity of RNA as confirmed by the demonstration of adequate internal control (ABL gene mRNA) [15].

As noted above, overall BCR-ABL phosphorylated at Thr-735 and/or Tyr-745 decreased during imatinib treatment in a pattern similar to the decrease of total BCR-ABL protein. To determine whether the reduction in phosphorylated BCR-ABL protein with imatinib therapy correlated with a clinical

Table 1
Effects of kinase inhibitors on phosphorylation of BCR-ABL in K-562 cells

Cell treatment	Phosphorylation on Thr-735		Phosphorylation on Tyr-245	
	Proportion of total BCR-ABL	Fold decrease vs. vehicle	Proportion of total BCR-ABL	Fold decrease vs. vehicle
Vehicle	0.36		0.53	
AMN107, 0.05 μM	0.27	1.33	0.37	1.43
AMN107, 5 μM	0.09	4.00	0.06	8.83
Imatinib, 0.05 μM	0.19	1.91	0.32	1.66
Imatinib, 5 μM	0.08	4.5	0.11	4.81

Phosphorylation of BCR-ABL on Thr-735 and Tyr-245 was not detected in control lysates from a normal, cell line, nor in control assays of PBS.

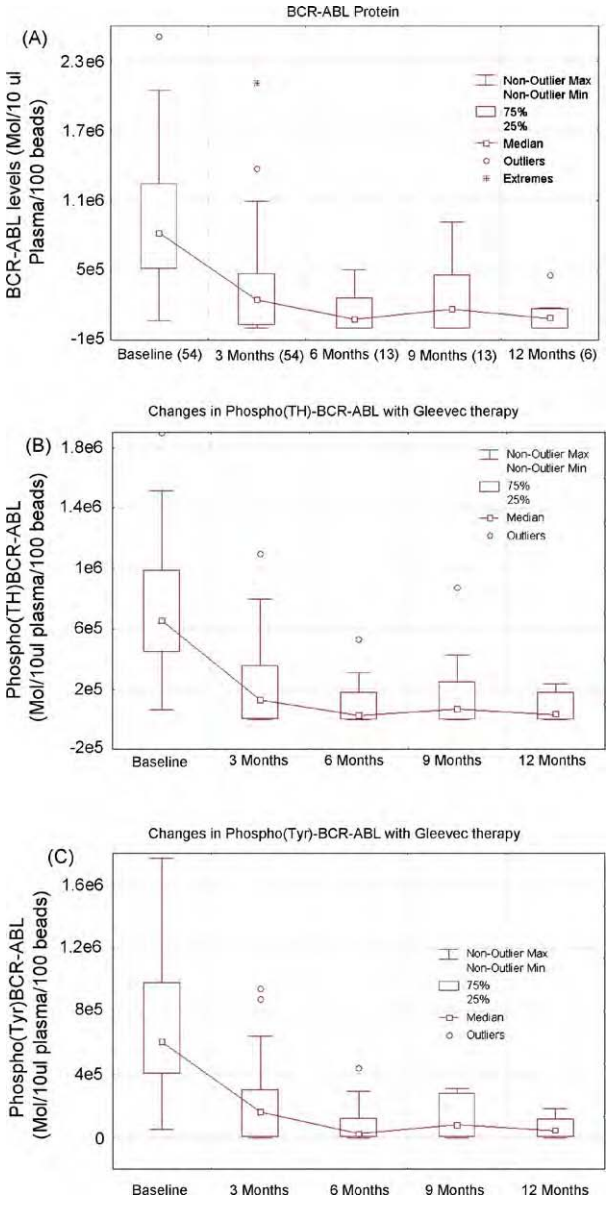

Fig. 3. Levels of total and phosphorylated BCR-ABL protein in CML patients before and during imatinib treatment. Plasma prepared from peripheral blood of CML patients was assayed by the immunoassay method for total BCR-ABL protein (panel A), BCR-ABL protein phosphorylated on Thr-735 (panel B), and BCR-ABL protein phosphorylated on Tyr-245 (panel C).

response, patients were divided into two subgroups by results of RT-PCR assays of BCR-ABL mRNA after 3 months of treatment, those with a higher level of disease and those who demonstrated a molecular response to treatment. There were no significant differences between the two groups of patients at baseline prior to treatment (Fig. 4). In patients with a higher level of disease (defined as a ratio of BCR-ABL mRNA to reference ABL mRNA of >0.05 at 3 months), the proportions of BCR-ABL protein that were phosphorylated at Thr-735 and/or Tyr-245 were not significantly reduced from baseline after 3 months of treatment (Fig. 4, panel A). By contrast, in patients who demonstrated a molecular response to imatinib treatment (BCR-ABL:ABL mRNA ratio <0.05 at 3 months), the proportions of BCR-ABL protein that were phosphorylated at Thr-735 and/or Tyr-245 were significantly reduced ($P = 0.01$; Fig. 4, panel B).

4. Discussion

The abnormal kinase activity of the BCR-ABL protein is the hallmark of CML and is responsible for transformation of hematopoietic cells, leading to proliferation and reduced apoptosis. An inhibitor specific for the ABL kinase, imatinib, has become the most important treatment for CML, and research for more effective inhibitors continues. The best currently available method for routine measurement of residual disease in CML patients employs RT-PCR to detect BCR-ABL mRNA [7,8]. However, an assay of the BCR-ABL protein itself and its kinase activity would provide the most direct measures of disease activity, progression, and response to treatment. Such an assay that could be rapidly and routinely performed in clinical laboratories would be very useful for monitoring treatment of CML patients.

The large size and unstable nature of the BCR-ABL protein have limited its detection and measurement of its activity by standard Western blot analysis. Immunoprecipitation on beads after a minor denaturation step appears to preserve the integrity of this large and complex protein, apparently maintaining its overall structure and phosphorylation state. The bead-based ELISA assay presented in this paper depends on initial immunoprecipitation of proteins with a BCR-specific antibody, followed by detection of the BCR-ABL fusion protein with an ABL-specific antibody. Phosphorylation of BCR-ABL was detected by using antibodies directed against phosphorylated Thr-735 and Tyr-245 in the ABL domain of the fusion protein. The bead-based assay clearly detected BCR-ABL protein specifically and reliably: all normal samples tested were negative. The assay was linear over a 5-log range, showed excellent reproducibility, and could detect BCR-ABL from as few as 10 input K562 cells in 1 ml of plasma.

We have previously demonstrated that leukemic cells pour their proteins, DNA, and RNA into plasma [12,13]. In this paper, we used plasma prepared from peripheral blood samples to detect the BCR/ABL fusion protein and its phosphorylation in CML and Philadelphia-positive ALL patients. The use of plasma prepared from peripheral blood has the obvious advantage of convenient sampling. More importantly, plasma reflects the entire body and is not influenced by sampling as are cell samples from bone marrow or peripheral blood. In addition, using plasma allows for better quantification and standardization because the copy number of the fusion protein can be normalized to a specific amount of plasma. Reliable quantification of BCR-ABL is important because levels of BCR-ABL or its degree of phosphorylation, which vary from one patient to another as demonstrated in Fig. 1, may reflect the tumor mass. Variation in tumor mass

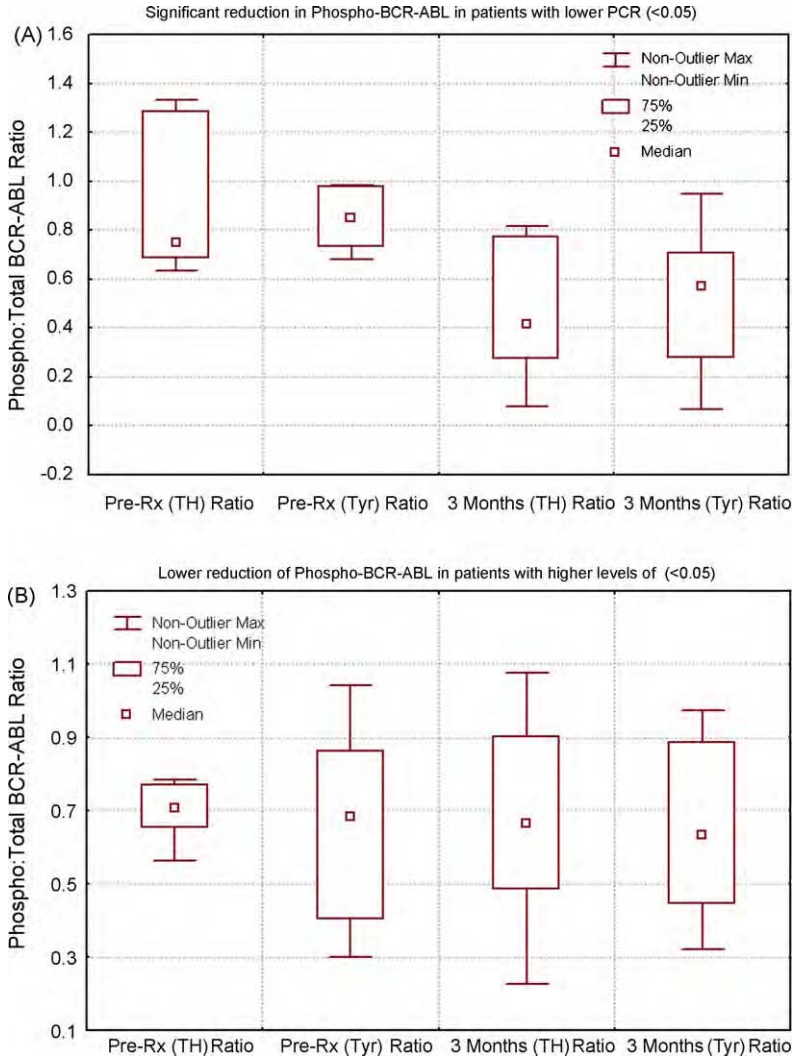

Fig. 4. Decreased levels of BCR-ABL phosphorylation in CML patients with a molecular response to imatinib treatment. Molecular response was defined as a ratio of BCR-ABL to ABL mRNA of <0.05, as determined by RT-PCR after 3 months of treatment. The proportions of total BCR-ABL protein that were phosphorylated on Thr-735 (TH) and Tyr-245 (Tyr) are shown prior to and after 3 months of treatment for CML patients who did not show a molecular response (panel A), and for those with a molecular response (panel B). Significantly lower proportions of phosphorylated BCR-ABL were found in patients showing a molecular response to treatment compared with those who did not ($P = 0.01$).

may be useful for determining the optimal dose of imatinib, although clinical trials are needed to confirm this notion. It is possible that patients with high levels of BCR-ABL in plasma (high tumor bulk) would benefit from a dose of imatinib that is greater than the recommended 400 mg; perhaps this subset of patients should be treated with 600 or 800 mg of imatinib.

BCR/ABL protein levels determined from plasma of CML patients declined after treatment with imatinib from the elevated levels found at diagnosis. Results of the immunoassay for BCR-ABL protein in CML patient samples after 3–12 months of imatinib treatment showed a pattern of reduction that paralleled the results found with cell-based RT-PCR analysis of BCR-ABL mRNA. However, when compared with RT-PCR ratios the changes in protein levels are not to the same order of magnitude. The change in the median from pretherapy is approximately 600,000 at 3 months and 735,000 at 12 months. The two assays measure completely different dimensions of the disease. The BCR-ABL protein assay measures changes in the tumor mass of the disease, whereas the RT-PCR assay measures the ratio of leukemic cells to normal cells and is therefore influenced by the recovery of normal hematopoietic cells. Unlike the cell-based assay of BCR-ABL mRNA, the plasma immunoassay directly monitors BCR-ABL protein, thereby accounting for any effects of post-transcriptional regulatory mechanisms on synthesis of BCR-ABL.

The kinase activity of the BCR-ABL protein is indicated by the phosphorylation state of Thr-735 and Tyr-245 in the ABL domain, which occurs by autophosphorylation in the case of Tyr-245 [9,10]. The proportions of total BCR-ABL protein that were phosphorylated on these residues as determined by the immunoassay correlated well with ex-vivo treatment of CML-derived cultured K562 cells by clinically

relevant concentrations of imatinib and AMN107, similar to the results described for assay by Western blot or immunoprecipitation. Analysis of plasma samples from CML patients showed that BCR-ABL kinase activity, as indicated by levels of phosphorylation on these residues, decreased after imatinib treatment. Thus, imatinib treatment decreased both the amount of BCR-ABL protein, and the activity of that BCR-ABL protein that remained. In the subgroup of CML patients identified by RT-PCR as molecular responders to imatinib therapy, the proportions (ratio) of BCR-ABL protein phosphorylated on Thr-735 and Tyr-245 were significantly decreased, whereas they were not significantly changed in the subgroup that lacked a molecular response. Together, these observations suggest that our immunoassay of BCR-ABL phosphorylation might be useful to monitor the efficacy of therapy and perhaps predict at an early stage of therapy which patients may require a change in dosing or a combination therapeutic regimen. However, further studies with a larger number of patients are needed to validate the clinical value of this approach.

Conflict of interest

None.

Acknowledgement

All work was performed at Quest Diagnostics Nichols Institute.

References

[1] Kantarjian H, Sawyers C, Hochhaus A, Guilhot F, Schiffer C, Gambacorti-Passerini C, et al., International STI571 CML Study Group. Hematologic and cytogenetic responses to imatinib mesylate in chronic myelogenous leukemia. N Engl J Med 2002;346: 645–52.

[2] O'Brien SG, Guilhot F, Larson RA, Gathmann I, Baccarani M, Cervantes F, et al., IRIS Investigators. Imatinib compared with interferon and low-dose cytarabine for newly diagnosed chronic-phase chronic myeloid leukemia. N Engl J Med 2003;348:994–1004.

[3] Deininger M, Buchdunger E, Druker BJ. The development of imatinib as a therapeutic agent for chronic myeloid leukemia. Blood 2005; 105:2640–53.

[4] Hochhaus A, La Rosee P. Imatinib therapy in chronic myelogenous leukemia: strategies to avoid and overcome resistance. Leukemia 2004;18:1321–31.

[5] Martinelli G, Soverini S, Rosti G, Cilloni D, Baccarani M. New tyrosine kinase inhibitors in chronic myeloid leukemia. Haematologica 2005;90:534–41.

[6] O'Hare T, Walters DK, Deininger MW, Druker BJ. AMN107: tightening the grip of imatinib. Cancer Cell 2005;7:117–9.

[7] Kantarjian HM, Talpaz M, Cortes J, O'Brien S, Faderl S, Thomas D, et al. Quantitative polymerase chain reaction monitoring of BCR-ABL during therapy with imatinib mesylate (STI571; gleevec) in chronic-phase chronic myelogenous leukemia. Clin Cancer Res 2003;9: 160–6.

[8] Müller MC, Gattermann N, Lahaye T, Deininger MW, Berndt A, Fruehauf S, et al. Dynamics of BCR-ABL mRNA expression in first-line therapy of chronic myelogenous leukemia patients with imatinib or interferon alpha/ara-C. Leukemia 2003;17:2392–400.

[9] Brasher BB, Van Etten RA. c-Abl has high intrinsic tyrosine kinase activity that is stimulated by mutation of the Src homology 3 domain and by autophosphorylation at two distinct regulatory tyrosines. J Biol Chem 2000;275:35631–7.

[10] Salomon AR, Ficarro SB, Brill LM, Brinker A, Phung QT, Ericson C, et al. Profiling of tyrosine phosphorylation pathways in human cells using mass spectrometry. Proc Natl Acad Sci USA 2003;100:443–8.

[11] Marley SB, Lewis JL, Schneider H, Rudd CE, Gordon MY. Phosphatidylinositol-3 kinase inhibitors reproduce the selective antiproliferative effects of imatinib on chronic myeloid leukaemia progenitor cells. Br J Haematol 2004;125:500–11.

[12] Albitar M, Do KA, Johnson MM, Giles FJ, Jilani I, O'Brien S, et al. Free circulating soluble CD52 as a tumor marker in chronic lymphocytic leukemia and its implication in therapy with anti-CD52 antibodies. Cancer 2004;101:999–1008.

[13] Rogers A, Joe Y, Manshouri T, Dey A, Jilani I, Giles F, et al. Relative increase in leukemia-specific DNA in peripheral blood plasma from patients with acute myeloid leukemia and myelodysplasia. Blood 2004;103:2799–801.

[14] Cortes J, Giles F, O'Brien S, Thomas D, Albitar M, Rios MB, et al. Results of imatinib mesylate therapy in patients with refractory or recurrent acute myeloid leukemia, high-risk myelodysplastic syndrome, and myeloproliferative disorders. Cancer 2003;97:2760–6.

[15] Ma W, Tseng R, Gorre M, Jilani I, Keating M, Kantarjian H, et al. Plasma RNA as an alternative to cells for monitoring molecular response in patients with chronic myeloid leukemia. Haematologica 2007;92:170– 5.

[16] Peng B, Hayes M, Resta D, Racine-Poon A, Druker BJ, Talpaz M, et al. Pharmacokinetics and pharmacodynamics of imatinib in a phase I trial with chronic myeloid leukemia patients. J Clin Oncol 2004;22:935–42.

Cotreatment with Vorinostat Enhances Activity of MK-0457 (VX-680) against Acute and Chronic Myelogenous Leukemia Cells

Warren Fiskus,[1] Yongchao Wang,[1] Rajeshree Joshi,[1] Rekha Rao,[1] Yonghua Yang,[1] Jianguang Chen,[1] Ravindra Kolhe,[1] Ramesh Balusu,[1] Kelly Eaton,[1] Pearl Lee,[1] Celalettin Ustun,[1] Anand Jillella,[1] Carolyn A. Buser,[2] Stephen Peiper,[1] and Kapil Bhalla[1]

Abstract

Purpose: We determined the effects of vorinostat (suberoylanalide hydroxamic acid) and/or MK-0457 (VX-680), an Aurora kinase inhibitor on the cultured human (HL-60, OCI-AML3, and K562) and primary acute myelogenous leukemia (AML) and chronic myelogenous leukemia (CML), as well as on the murine pro-B BaF3 cells with ectopic expression of the unmutated and mutant forms of Bcr-Abl.

Experimental Design: Following exposure to MK-0457 and/or vorinostat, apoptosis, loss of viability, as well as activity and levels of Aurora kinase and Bcr-Abl proteins were determined.

Results: Treatment with MK-0457 decreased the phosphorylation of Aurora kinase substrates including serine (S)10 on histone H3 and survivin, and led to aberrant mitosis, DNA endoreduplication as well as apoptosis of the cultured human acute leukemia HL-60, OCI-AML3, and K562 cells. Combined treatment with vorinostat and MK-0457 resulted in greater attenuation of Aurora and Bcr-Abl (in K562) kinase activity and levels as well as synergistically induced apoptosis of OCI-AML3, HL-60, and K562 cells. MK-0457 plus vorinostat also induced synergistic apoptosis of BaF3 cells with ectopic overexpression of wild-type or mutant Bcr-Abl. Finally, cotreatment with MK-0457 and vorinostat induced more loss of viability of primary AML and imatinib-refractory CML than treatment with either agent alone, but exhibited minimal toxicity to normal CD34+ progenitor cells.

Conclusions: Combined *in vitro* treatment with MK-0457 and vorinostat is highly active against cultured and primary leukemia cells. These findings merit *in vivo* testing of the combination against human AML and CML cells, especially against imatinib mesylate–resistant Bcr-AblT315I–expressing CML Cells.

The Aurora kinases are a family of serine/threonine kinases that play an important role in maintaining the fidelity of mitosis by regulating spindle formation, chromosome segregation, and cytokinesis (1–3). Aurora A localizes to the centrosomes and spindle poles and is involved in centrosome maturation and duplication (1–3). Aurora B, a chromosomal passenger protein, localizes to centromeres, midzone microtubules, and midbodies. Aurora B plays a role in chromosomal alignment, spindle assembly checkpoint, and cytokinesis (1–3). The gene encoding Aurora A is on the long arm of chromosome 20 (20q13.2-13.3), a region that is frequently amplified in epithelial cancers (2, 4–6). Aurora A overexpression is also commonly observed in human acute leukemia cells (2). Aurora B is often co-overexpressed with Aurora A (7, 8). Phosphorylation of Aurora A at threonine 288 is required for the kinase activity of Aurora A and for mitotic entry (9, 10). Ectopic overexpression of Aurora A transforms normal cells and leads to aberrant chromosome segregation, genomic instability, and activation of oncogenic pathways (2, 6, 11). Consistent with this, deregulated Aurora kinase activity in cancer cells leads to defects in centrosome function, aberrant spindle assembly, misalignment of chromosomes, abnormal cytokinesis, and genetic instability (6, 11). Several proteins that have important roles in cell division are known substrates phosphorylated by Aurora kinases. These include serine 10 on histone H3, CENP-A, and survivin (12). Due to the pivotal role that Aurora A and Aurora B plays in mitosis, novel agents that abrogate the activities of Aurora A and/or Aurora B kinase have been developed and are being tested for antitumor efficacy (8, 12). MK-0457 (VX-680) is a small molecule inhibitor that inhibits the activity of Aurora A, Aurora B, and Aurora C kinases with inhibition constants (K_i) of 0.6, 18, and 4.6 nmol/L, respectively (1, 12). However, the phenotypic effects induced by treatment with this agent in cancer cells are consistent with Aurora B–specific inhibition similar to AZD1152 and ZM447439 (e.g., depletion of histone H3 serine 10 phosphorylation, inhibition of cell division, misalignment of the chromosomes, and polyploidy; refs. 12, 13). In transformed cells with mitotic checkpoint errors, MK-0457

Authors' Affiliations: [1]Medical College of Georgia Cancer Center, Augusta, Georgia and [2]Merck & Co., Inc., North Wales, Pennsylvania

Received 3/19/08; revised 5/21/08; accepted 5/26/08.

The costs of publication of this article were defrayed in part by the payment of page charges. This article must therefore be hereby marked *advertisement* in accordance with 18 U.S.C. Section 1734 solely to indicate this fact.

Requests for reprints: Kapil Bhalla, MCG Cancer Center, Medical College of Georgia, 1120 15th Street, CN-2101 Augusta, GA 30912. Phone: 706-721-0566; Fax: 706-721-0469; E-mail: kbhalla@mcg.edu.

doi:10.1158/1078-0432.CCR-08-0721

Translational Relevance

This article describes preclinical *in vitro* findings demonstrating the synergistic antileukemia activity of a novel combination of the pan-histone deacetylase inhibitor vorinostat and the Aurora kinase inhibitor MK-0457 in the treatment of acute myelogenous leukemia (AML) and chronic myelogenous leukemia (CML). Treatment with MK-0457 inhibits the activity of Aurora kinase A and B, as well as induces cell cycle G_2-M phase accumulation, endoreduplication, and apoptosis of AML and CML cells. Vorinostat induces acetylation of heat shock protein 90 (hsp90), disrupts the chaperone association of hsp90 with Aurora kinases, thereby depleting Aurora kinase level and activity in AML and CML cells. Importantly, cotreatment with MK-0457 and vorinostat exerts synergistic depletion of Aurora kinases and induces apoptosis of AML and CML cells, including those with imatinib-resistant, dasatinib-resistant, and nilotinib-resistant mutant Bcr-AblT315I. These studies support the rationale for testing the combination of vorinostat and MK-0457 in patients with relapsed AML or CML.

treatment blocks cell cycle progression, leading to accumulation of cells with greater than 4N DNA content, mitotic slippage, ultimately inducing apoptosis (13, 14). At nanomolar concentrations, MK0457 has also been shown to inhibit Fms-related tyrosine kinase-3 (FLT-3) and Bcr-Abl tyrosine kinases, including the imatinib-resistant, nilotinib-resistant, and dasatinib-resistant mutant Bcr-AblT315I (15, 16). Recently, MK0457 showed antileukemia efficacy in patients with imatinib-refractory chronic myelogenous leukemia (CML) harboring Bcr-AblT315I (17).

Vorinostat (suberoylanilide hydroxamic acid) is a hydroxamic acid analogue pan-histone deacetylase inhibitor (HA-HDI; ref. 18). Vorinostat has been shown to inhibit both class I and II HDACs and alter the expression of up to 10% of genes in transformed cells (19). This is associated with growth arrest, differentiation, and apoptosis of human leukemia more than normal cells (19, 20). Treatment with HDIs lead to increased levels of the cell cycle inhibitor proteins p21 and p27, generation of reactive oxygen species, as well as up-regulation of the proapoptotic proteins, e.g., Bax, Bak, and Bim (19–22). HA-HDIs are also known to deplete the levels of antiapoptotic proteins, e.g., Bcl-2, Bcl-x_L, Mcl-1, XIAP, and survivin in human leukemia cells (19–22). By inhibiting HDAC6, a predominantly cytosolic HDAC that is known to deacetylate hsp90 (20–22), treatment with HA-HDIs induces hsp90 acetylation (20, 23). This inhibits the chaperone function of hsp90, which directs hsp90 client proteins, including c-Raf, AKT, FLT-3, and Bcr-Abl, to polyubiquitylation and degradation by the 26S proteasome (23). Thus, treatment with HA-HDIs may not only epigenetically influence gene expression, but through inhibition of hsp90, may also deplete the levels of progrowth and prosurvival proteins, e.g., Bcr-Abl in human leukemia cells. Additionally, our previous findings have highlighted that depletion of the levels of Bcr-Abl with HA-HDI treatment coupled with inhibition of the Bcr-Abl activity by treatment with Bcr-Abl kinase inhibitor imatinib, nilotinib, or dasatinib exerts synergistic apoptotic effects against leukemia cells with wild-type Bcr-Abl (21, 24, 25). Similar effects were noted when mutant FLT-3 was targeted by the combination of HA-HDI with a FLT-3 kinase inhibitor (26). Recent reports indicate that Aurora kinases may also require chaperone association with hsp90, and inhibition of its chaperone function may lead to depletion of Aurora kinases (27). Inhibition of Aurora kinase activity has also been shown to exert anti–acute myelogenous leukemia (AML) activity (13, 28, 29). Taken together, these findings created a strong rationale to determine the antileukemia effects of the combination of vorinostat and MK-0457 against AML and CML cells with unmutated or mutant Bcr-Abl. Findings presented here show that combined treatment with vorinostat and MK-0457 is highly active and exerts superior antileukemia activity than either agent alone against cultured and primary AML and CML cells, including those expressing the P-loop mutant Bcr-AblE255K or the gatekeeper mutation Bcr-AblT315I (25).

Materials and Methods

Reagents and antibodies. MK-0457 and vorinostat were kindly provided by Merck & Co., Inc. Monoclonal c-Abl antibody, and polyclonal anti-STAT5A/B were purchased from Santa Cruz Biotechnology. Monoclonal anti–p-STAT5 and monoclonal antiphosphotyrosine were purchased from BD Biosciences. Polyclonal anti–phospho-Aurora A, anti–phospho-survivin, and monoclonal anti-survivin were purchased from Abcam. Rabbit monoclonal anti–Aurora A, Aurora B, and phospho-Ser10 histone H3 antibodies were purchased from Epitomics, Inc. Antibodies for the immunoblot analyses of p-CrkL and CrkL were purchased from Cell Signaling Technologies. Other reagents and antibodies used in the studies were procured as previously reported (21–26). Mouse monoclonal anti-hsp90, rat monoclonal anti-hsp90, and polyclonal anti-hsp70 antibodies were purchased from StressGen Biotechnologies, Corp. Affinity-purified polyclonal antibody against Ac-K69-hsp90 was generated by Alpha Diagnostic based on the synthetic 12–amino acid peptide flanking K69 (acetylated and unacetylated) ETLTDPSKLDSGK.

Cell lines and cell culture. CML-BC K562 cells and AML HL-60 cells were obtained and maintained in culture, as previously described (23–26). OCI-AML-3 cells were cultured in α-MEM medium with 1% penicillin/streptomycin and 1% nonessential amino acids. Logarithmically growing cells were exposed to the designated concentrations of MK-0457 and/or vorinostat. Following these treatments, cells or cell pellets were washed free of the drug(s) prior to the performance of the studies.

Creation of BaF3/Bcr-Abl, BaF3/Bcr-AblE255K, and BaF3/Bcr-AblT315I cell lines. Mutant p210Bcr-AblE255K and p210Bcr-AblT315I containing plasmids were generated by site-directed mutagenesis, as previously described (21, 25). The p210 Bcr-Abl constructs were nucleofected into BaF3 cells, as previously described (21, 25). After confirmation of Bcr-Abl expression by immunoblot analysis, cells were used for the studies described below.

Primary AML blasts and CML cells. Primary acute myeloid leukemia (AML) and imatinib-resistant CML cells were obtained with informed consent as part of a clinical protocol approved by the Institutional Review Board of the Medical College of Georgia. Peripheral blood or bone marrow aspirate samples were collected in heparinized tubes, and mononuclear cells were separated using Lymphoprep (Axis-Shield), washed once with complete RPMI 1640 medium, resuspended in complete RPMI 1640 and counted to determine the number of cells isolated prior to their use in the various experiments. The purity of the blast populations were confirmed to be 80% or better by morphologic evaluation of cytospun cell preparations stained with Wright stain (24, 25). Banked, de-linked, and de-identified donor peripheral blood

CD34+ mononuclear cells procured for recipients who had since died were purified by immunomagnetic beads conjugated with anti-CD34 antibody prior to use in the cell viability assay (StemCell Technologies).

Cell cycle analysis. Following the designated treatments, cells were harvested and washed twice with 1× PBS and fixed in ethanol overnight. Fixed cells were washed twice with 1× PBS and stained with propidium iodide for 15 min at 37°C. Cell cycle data were collected on a flow cytometer with a 488 nmol/L laser and analyzed with ModFit 3.0, as previously described (24). Cells with <2N DNA content (sub-G_1) were also determined (24).

Confocal microscopy. HL-60, OCI-AML3, and K562 cells were cultured in the presence or absence of MK-0457 for 24 h. Cells were cytospun onto glass slides and fixed with 4% paraformaldehyde for 10 min. Following this, the slides were blocked with 5% bovine serum albumin for 30 min and incubated with FITC-conjugated α-tubulin and Dy547-conjugated γ-tubulin (Abcam) at a dilution of 1:50 in blocking buffer for 2 h. For MPM-2 staining, cells were stained for 1 h with a FITC-conjugated MPM-2 antibody at a 1:100 dilution. Following three washes with PBS, the cells were mounted using Vectashield with 4′,6-diamidino-2-phenylindole and imaged at 63× using a Zeiss LSM510 confocal microscope.

Assessment of apoptosis by Annexin V staining. Untreated or drug-treated cells were stained with Annexin V (Pharmingen) and propidium iodide and the percentage of apoptotic cells were determined by flow cytometry. To analyze the synergism between MK-0457 and vorinostat in inducing apoptosis, cells were treated with MK-0457 (20-150 nmol/L) and vorinostat (0.2-1.5 μmol/L) at a constant ratio of 1:10 for 48 h. The percentage of apoptotic cells was determined by flow cytometry, as previously described (21, 22). The combination index (CI) for each drug combination was obtained by median dose-effect of Chou and Talalay (30) using the CI equation within the commercially available software Calcusyn (Biosoft). CI < 1.0 represents the synergism of the two drugs in combination.

Assessment of percentage of nonviable cells. Following designated treatments, cells were stained with trypan blue (Sigma). The number of nonviable cells were determined by counting the cells that showed trypan blue uptake in a hemocytometer, and was reported as a percentage of untreated control cells.

Cell lysis and protein quantitation. Untreated or drug-treated cells were centrifuged and the cell pellets were resuspended in 200 μL of lysis buffer [20 mmol/L Tris (pH 8), 150 nmol/L sodium chloride 1% Triton X-100, 1 mmol/L phenylmethylsulfonyl fluoride, 10 μg/mL leupeptin, 1 μg/mL pepstatin-A, 2 μg/mL aprotinin, 20 mmol/L p-nitrophenyl phosphate, 1.0 mmol/L sodium orthovanadate, and 1 mmol/L 4-(2-aminoethyl) benzenesulfonylfluoride hydrochloride] and incubated on ice for 30 min. The cell lysates were centrifuged and an aliquot of each cell lysate was diluted 1:10 and protein quantitated using a bicinchoninic acid protein quantitation kit (Pierce), according to the manufacturer's protocol.

Immunoprecipitation of hsp90 and immunoblot analyses. Following the designated treatments, cells were lysed for 30 min on ice, and the nuclear and cellular debris were cleared by centrifugation. Cell lysates (500 μg) were incubated with a rat monoclonal anti-hsp90 antibody (StressGen), for 1 h at 4°C. Washed Protein G agarose beads were added to this solution and incubated overnight at 4°C. The immunoprecipitates were washed thrice in the lysis buffer and proteins were eluted with the SDS sample loading buffer prior to the immunoblot analyses with specific antibodies against acetyl-K69 hsp90, Aurora A, or total hsp90 levels.

SDS-PAGE and Western blotting. One hundred micrograms of total cell lysate was used for SDS-PAGE. Western blot analyses of Bcr-Abl, p-STAT5, pCrkL, p-Aurora A/B, Aurora A, Aurora B, p-survivin, survivin, p-Ser10 histone H3, histone H3, and Bim were done on total cell lysates using specific antisera or monoclonal antibodies. The expression level of either β-actin or α-tubulin was used as the loading control for the Western blots. Blots were developed with a chemiluminescent substrate ECL (Amersham Biosciences).

Statistical analysis. Significant differences between values obtained in a population of leukemic cells treated with different experimental conditions were determined using Student's t test. $P < 0.05$ values were considered significant.

Results

MK-0457 treatment induces cell cycle arrest, multipolar spindle formation, as well as attenuates Aurora kinase activity and induces apoptosis and endoreduplication in cultured CML-BC and AML cell lines. We first determined the effects of MK-0457 treatment on the cell cycle status of the cultured CML-BC K562 and the AML HL-60 and OCI-AML3 cells. Table 1 shows that exposure to increasing concentrations of MK-0457 caused a dose-dependent accumulation of cells in the G_2-M phase with a concomitant decline in the G_1 and S phases of the cell cycle in all of the three cell lines examined. Following a 24-hour exposure to 50 nmol/L of MK-0457, >80% of cells were in the G_2-M phase of the cell cycle in K562 and HL-60 cells. OCI-AML3 cells were relatively less sensitive to the cell cycle effects of MK-0457. Although the greatest cell cycle–inhibitory effects were observed at 24 hours for all three cell lines, treatment with MK-0457 for 8 hours, but not for shorter exposure intervals, resulted in an increase in the percentage of cells in G_2-M (data not shown). Immunofluorescent staining of α-tubulin and γ-tubulin in HL-60 and OCI-AML3 cells, followed by confocal immunofluorescent microscopy, showed that α-tubulin and γ-tubulin localized to the mitotic spindle and the centrosomes, respectively (Fig. 1A). Exposure to MK-0457 for 24 hours resulted in the development of aberrant mitosis showing multiple spindle poles. In HL-60 cells, this was seen after exposure to MK-0457 levels as low as 20 nmol/L, whereas concentrations of ≥50 nmol/L were required to induce multipolar spindles in OCI-AML3 (Fig. 1A) and K562 (data not shown) cells. Also, exposure to MK-0457 dose-dependently decreased the staining of OCI-AML3 cell with a monoclonal

Table 1. MK-0457 treatment induces G_2-M arrest in leukemia cells

Cells and treatment	Cells (%)		
	G_0-G_1	S	G_2-M
K562			
Untreated	26.8 ± 0.6	58.5 ± 2.9	14.7 ± 2.3
20 nmol/L MK-0457	31.6 ± 1.9	0.5 ± 0.2	67.9 ± 1.8
50 nmol/L MK-0457	12.7 ± 3.3	1.5 ± 0.4	85.8 ± 2.9
100 nmol/L MK-0457	3.4 ± 1.5	1.9 ± 0.9	94.7 ± 2.5
HL-60			
Untreated	41.7 ± 1.2	44.3 ± 0.5	14.0 ± 0.8
20 nmol/L MK-0457	36.3 ± 0.8	23.6 ± 0.4	40.1 ± 0.8
50 nmol/L MK-0457	2.3 ± 0.5	17.2 ± 0.9	80.4 ± 0.5
100 nmol/L MK-0457	2.6 ± 0.3	18.5 ± 1.1	78.8 ± 0.9
OCI-AML3			
Untreated	61.6 ± 0.7	30.6 ± 0.5	7.7 ± 0.3
20 nmol/L MK-0457	61.5 ± 0.7	21.8 ± 0.3	16.7 ± 0.4
50 nmol/L MK-0457	37.5 ± 0.9	17.6 ± 0.8	44.9 ± 0.8
100 nmol/L MK-0457	19.9 ± 0.6	16.3 ± 2.5	63.7 ± 0.3

NOTE: K562, HL-60, and OCI-AML3 cells were treated with the indicated doses of MK-0457 for 24 h. Then, the cells were fixed and stained for cell cycle analysis by flow cytometry. Values represent the mean of three experiments ± SE.

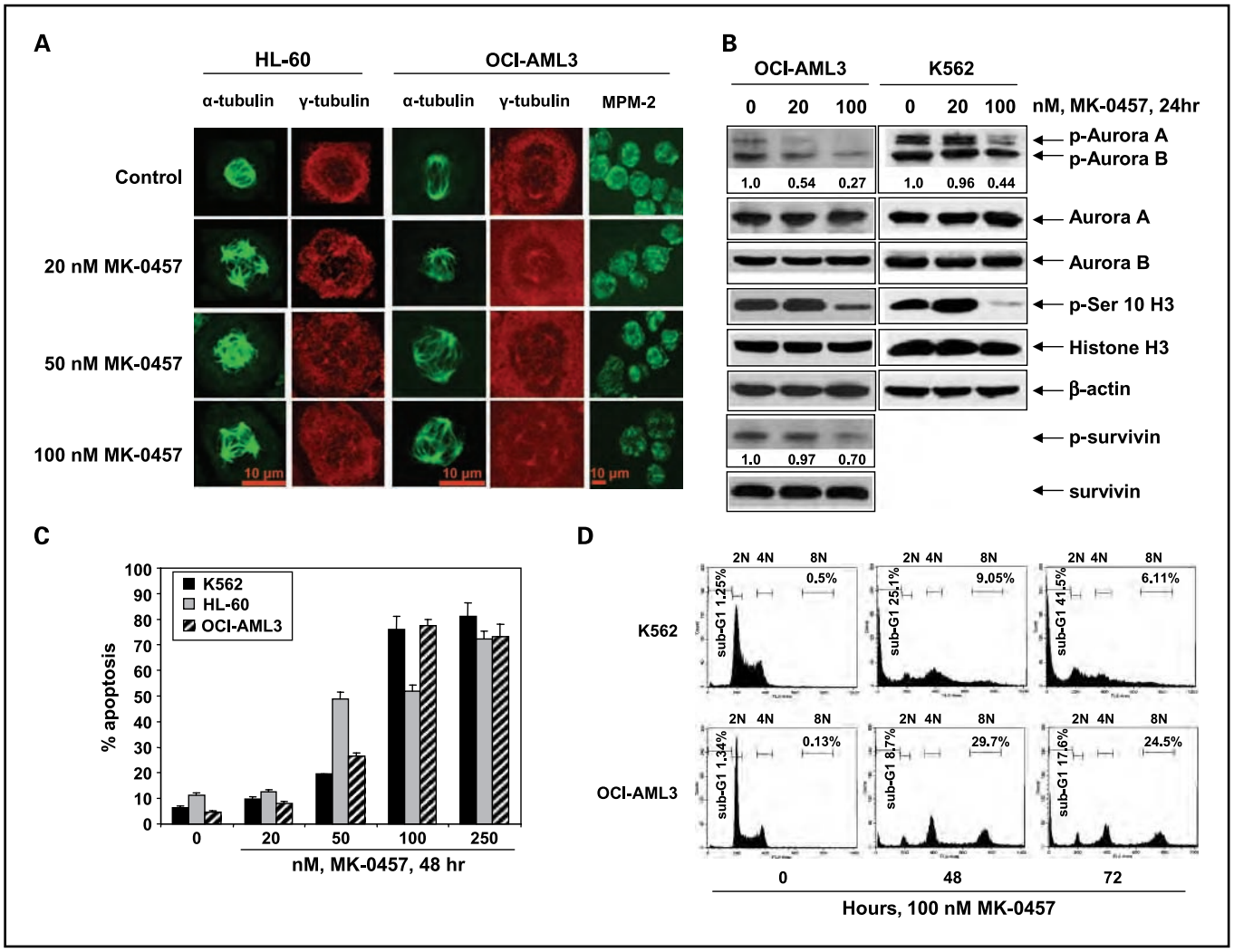

Fig. 1. MK-0457 treatment induces multipolar spindle formation and endoreduplication in acute leukemia cells. *A,* HL-60 and OCI-AML3 cells were treated with the indicated doses of MK-0457 for 24 h. Following this, cells were fixed with paraformaldehyde and stained with anti–α-tubulin, anti–γ-tubulin, or anti–MPM-2 antibodies and imaged at 63× by confocal microscopy. *B,* OCI-AML3 (*left*) and K562 (*right*) cells were treated with the indicated doses of MK-457 for 24 h. Following this, immunoblot analysis was done on total cell lysates or extracted histones for p-Aurora A/B, Aurora A, Aurora B, p-survivin, survivin, and p-Ser10 histone. The levels of β-actin or total histone H3 in the cell lysates served as the loading control. *C,* K562, HL-60, and OCI-AML3 cells were treated with the indicated doses of MK-0457 for 48 h. Following treatment, the percentages of Annexin V–stained apoptotic cells were determined by flow cytometry. Columns, mean of three experiments; bars, SE. *D,* K562 and OCI-AML3 cells were treated with 100 nmol/L of MK-0457 for the indicated times. Then, the cells were fixed and stained with propidium iodide and DNA content was determined by flow cytometry.

MPM-2 antibody (which stains mitotic phosphoproteins), as shown by immunofluorescent microscopy (Fig. 1A). K562 and HL-60 cells do not contain increased copy numbers (gene amplification) of the Aurora A gene, as determined by fluorescence *in situ* hybridization, using a probe containing the entire Aurora A gene and an additional 71-kb of the downstream sequence of the long arm of chromosome 20 (data not shown). We next determined the inhibitory effects of MK-0457 on Aurora kinase and MK-0457–induced apoptosis in the cultured acute leukemia OCI-AML3, HL-60, and K562 cells. Figure 1B shows that exposure of OCI-AML3 cells to MK-0457 (20 or 100 nmol/L) depleted the kinase activity of Aurora A and Aurora B, as measured by the decrease in levels of autophosphorylated Aurora A and Aurora B, without affecting the levels of Aurora A and Aurora B. Exposure to 100 nmol/L of MK-0457 was also accompanied by decreased levels of the phosphorylated serine 10 on histone H3 (Fig. 1B). Treatment with MK-0457 exerted similar effects in K562 cells (Fig. 1B). MK-0457 also depleted the levels of threonine 34–phosphorylated survivin in OCI-AML3 and K562 cells (see below), without affecting survivin levels (Fig. 1B). Exposure to 20 to 250 nmol/L of MK-0457 dose-dependently induced apoptosis of K562, HL-60, and OCI-AML3 cells (Fig. 1C). Following exposure to 100 nmol/L of MK-0457, >75% of K562 and OCI-AML3 cells were apoptotic, whereas apoptosis of 55% of HL-60 cells was observed (Fig. 1C). We next determined whether MK-0457 induced endoreduplication of DNA in the leukemia cells. Treatment of K562 and OCI-AML3 cells with 100 nmol/L of MK-0457 for 48 hours led to an increase in the percentage of cells with 8N DNA content (Fig. 1D). Endoreduplication was most evident in OCI-AML3 cells, with nearly 30% of cells possessing greater than 4N DNA content compared with 9.0%

in K562 cells. After 72 hours of exposure, the percentage of cells with 8N DNA content decreased in both OCI-AML3 and K562 cells (Fig. 1D). This was due to the increase in the percentage of cells with <2N DNA (sub-G_1) content to 17.6% and 41.5%, respectively. Taken together with the observed decrease in MPM-2 staining and increased endoreduplication, this suggested "mitotic slippage" and increased apoptosis.

Vorinostat depletes Aurora A kinase levels and enhances MK-0457–mediated apoptosis in AML and CML-BC cells. In previous reports, we showed that treatment with vorinostat induces the levels of the prodeath proteins and depletes prosurvival proteins, which is associated with growth arrest and apoptosis of acute leukemia cells (23, 25). We have also previously shown that HDAC inhibitors disrupt the chaperone association of hsp90 with its client proteins (23). We next determined the effects of vorinostat treatment on the chaperone association of hsp90 with Aurora A in OCI-AML3 cells. Treatment with vorinostat for 8 hours resulted in an abrogation of the binding of Aurora A with hsp90 in hsp90 immunoprecipitates, as well as an increase in acetylated hsp90 as determined by immunoblot analysis following staining with an acetylated lysine 69-specific hsp90 antibody. We also observed depletion of the levels of Aurora A in total cell lysates as well as induction of hsp70 and total cellular levels of acetylated hsp90 (Fig. 2A). We next determined whether vorinostat-mediated depletion of Aurora A and Aurora B was due to their proteasomal degradation. Figure 2B shows that partial depletion of Aurora A, Aurora B, and c-Raf due to treatment of OCI-AML3 cells by vorinostat was restored by cotreatment with the proteasome inhibitor bortezomib. Here, the levels of c-Raf, which is chaperoned by hsp90, served as the positive control (21). Similar effects were observed in K562 cells following treatment with vorinostat and bortezomib (data not shown). These data suggest that vorinostat-mediated depletion of Aurora A and Aurora B is at least partially due to the disruption of chaperone association of hsp90 with Aurora A and B, leading to their degradation by the 26S proteasome. We next determined the effects of vorinostat and/or MK-0457 on the levels and activity of Aurora kinases in the cultured acute leukemia HL-60, OCI-AML3, and K562 cells. Figure 2C shows that treatment with 1.0 μmol/L of vorinostat alone attenuated the total Aurora A and B levels in OCI-AML3 and K562 cells.

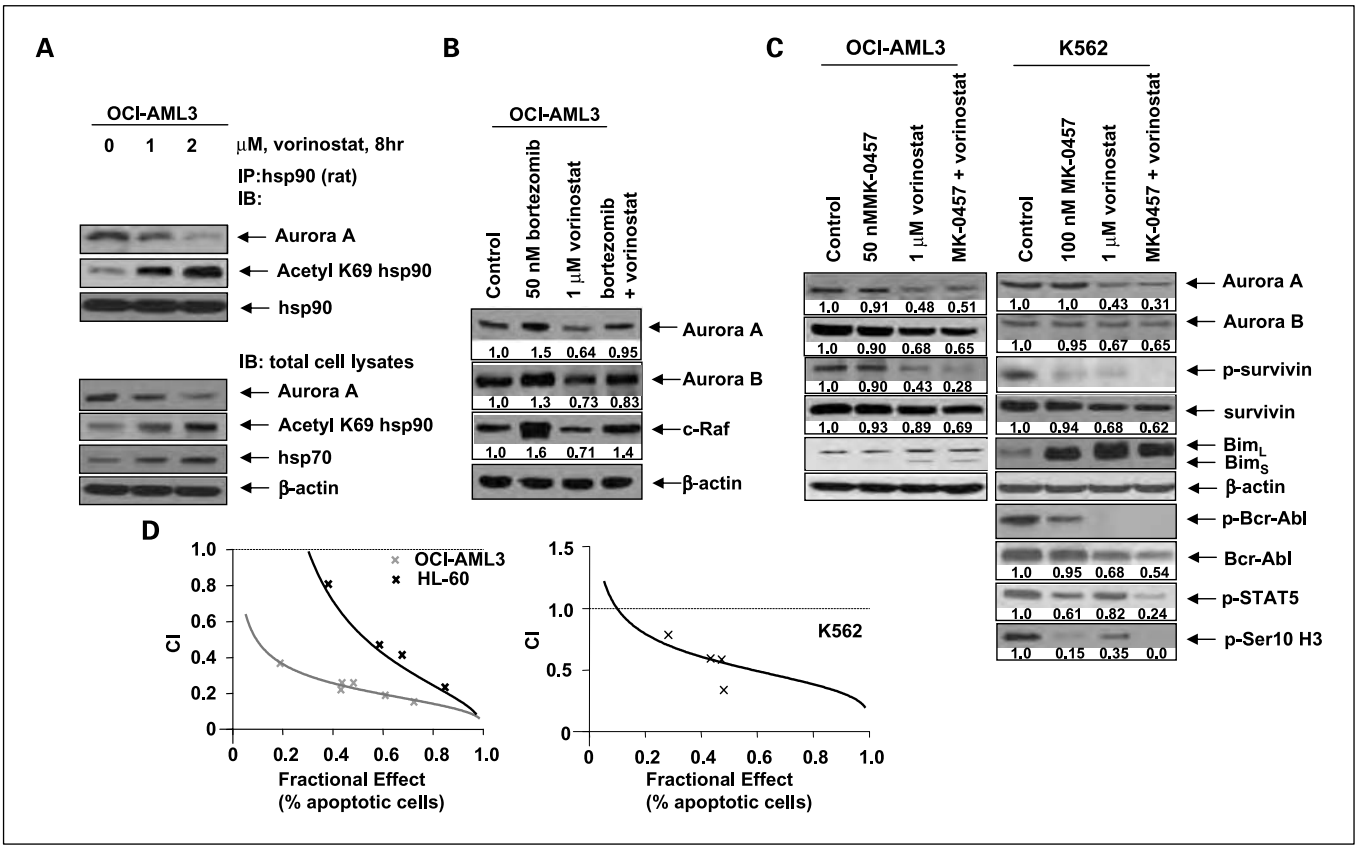

Fig. 2. Vorinostat depletes the levels of Aurora A, inhibits its chaperone association with hsp90, induces Bim expression, and combined treatment with MK-0457 exerts synergistic apoptotic effects in AML cells. *A,* OCI-AML3 cells were treated with vorinostat for 8 h. Following this, hsp90 was immunoprecipitated from the cell lysates and immunoblot analysis was done for Aurora A, acetylated K69 hsp90, and total hsp90 levels. Alternatively, immunoblot analysis was done for Aurora A, hsp70, and acetylated K69 hsp90. The levels of β-actin in the cell lysates served as the loading control. *B,* OCI-AML3 cells were treated with the indicated doses of bortezomib and/or vorinostat for 16 h. Immunoblot analysis was done for Aurora A, Aurora B, and c-Raf on the total cell lysates. The levels of β-actin in the lysates served as the loading control. Densitometry was done with ImageQuant version 5.2. *C,* OCI-AML3 and K562 cells were treated with the indicated doses of MK-0457 and/or vorinostat for 24 h. Western blot analysis was done for p-Aurora A/B, Aurora A, Aurora B, p-survivin, total survivin, and Bim on the total cell lysates. Additionally, immunoblot analysis was done for p-Bcr-Abl, Bcr-Abl, p-STAT5, and p-Ser10 H3 in K562 cells. The levels of β-actin in the cell lysates served as the loading control. *D,* analysis of dose-effect relationship for MK-0457 (20-150 nmol/L) and vorinostat (0.2-2.0 μmol/L) for the apoptotic effects after 48 h of exposure in HL-60, OCI-AML3 (*left*), and K562 (*right*) cells was done according to the median dose-effect method of Chou and Talalay. Following this, the CI values were calculated. CI < 1, CI = 1, and CI > 1 represent synergism, additivity, and antagonism of the two agents, respectively.

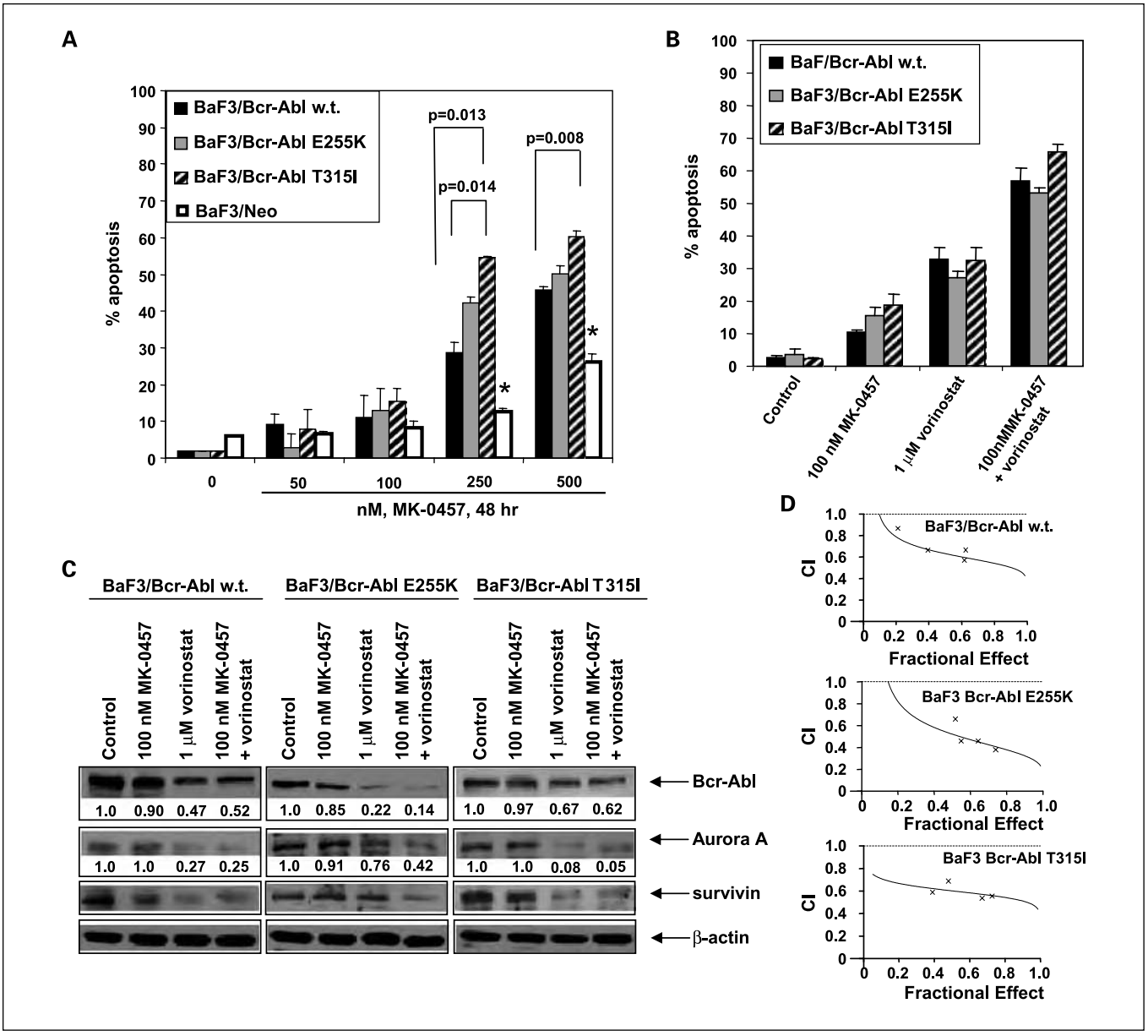

Fig. 3. Effects of MK-457 and/or vorinostat on BaF3 cells expressing unmutated and mutant forms of Bcr-Abl. *A,* BaF3/Bcr-Abl wild-type, BaF3/Bcr-AblE255K, BaF3/Bcr-AblT315I cells, and BaF3/Neo cells were treated with the indicated concentrations of MK-0457 for 48 h. Then the percentages of Annexin V – positive apoptotic cells were assessed by flow cytometry. Columns, mean of three experiments; bars, SE. The *P* values indicate the level of statistical significance of the two values compared; *, significantly less value as compared with similarly treated BaF3/Bcr-Abl wild-type, BaF3/Bcr-AblE255K, and BaF3/Bcr-AblT315I cells. *B,* BaF3/Bcr-Abl wild-type, BaF3/Bcr-AblE255K, and BaF3/Bcr-AblT315I cells were treated with the indicated concentrations of MK-0457 and/or vorinostat for 48 h. Following this, the percentage of Annexin V – positive apoptotic cells was determined by flow cytometry. Columns, mean of three experiments; bars, SE. *C,* BaF3/Bcr-Abl wild-type, BaF3/Bcr-AblE255K, and BaF3/Bcr-AblT315I cells were treated with the indicated concentrations of MK-0457 and/or vorinostat for 24 h. Immunoblot analysis was done for Bcr-Abl, Aurora A, and survivin. The level of β-actin in the lysates served as the loading control. *D,* analysis of dose-effect relationship for MK-0457 (50-150 nmol/L) and vorinostat (0.2-1.5 μmol/L) for the apoptotic effects after 48 h of exposure in BaF3/Bcr-Abl wild-type, BaF3/Bcr-Abl E255K, and BaF3/Bcr-Abl T315I cells was done according to the median dose-effect method of Chou and Talalay. Following this, the CI values were calculated for each cell line.

Although vorinostat only slightly depleted the total survivin levels, it attenuated p-survivin levels. Conversely, treatment with vorinostat alone increased the levels of the long and short isoforms of Bim (Bim_L and Bim_S) in OCI-AML3 cells (Fig. 2C). Notably, cotreatment with vorinostat (1.0 μmol/L) and MK-0457 (50 nmol/L) caused greater depletion of p-survivin in OCI-AML3 cells than treatment with either agent alone (Fig. 2C, *left*). Combined treatment also induced slightly more Bim_L and Bim_S expressions in OCI-AML3 cells. Vorinostat and/or MK-0457 exerted similar effects in HL-60 cells (data not shown). In K562 cells, combined treatment with vorinostat (1.0 μmol/L) and MK-0457 (100 nmol/L) caused more depletion of p-survivin, survivin, and Aurora A levels, whereas Bim induction was slightly less than what was observed following treatment with vorinostat alone (Fig. 2C). However, cotreatment with vorinostat and MK-0457 caused more depletion of p-STAT5, as well as of Bcr-Abl than treatment with either agent alone. This was also associated with a

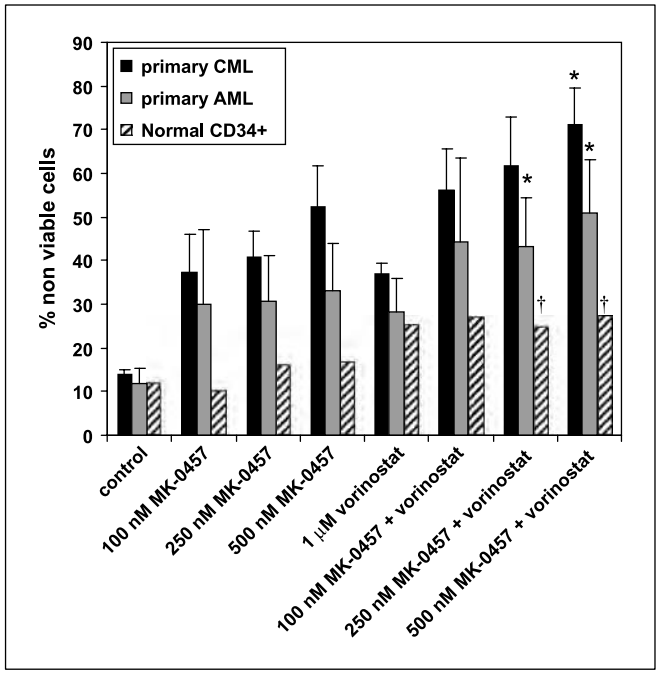

Fig. 4. Vorinostat enhances MK-0457–mediated loss of viability of primary AML and CML cells. Bone marrow samples from four CML, three AML patients, and two normal CD34+ samples were treated with the indicated concentrations of MK-0457 and/or vorinostat for 48 h. Following this, the percentages of nonviable cells for each drug alone or in combination were determined by trypan blue dye uptake in a hemocytometer. Columns, mean; bars, SE. *, $P < 0.05$, significantly greater values than those following treatment with either agent alone at the indicated concentrations in the CML and AML samples. †, $P < 0.05$, significantly lower values in normal CD34+ versus leukemia samples for the drug combinations.

profound attenuation of p-Bcr-Abl and phosphorylated serine 10 on histone H3, p-survivin and Aurora A expression. We next determined the apoptotic effects of cotreatment with MK-0457 and vorinostat. As compared with treatment with either agent alone, cotreatment with vorinostat and MK-0457 synergistically induced apoptosis of OCI-AML3, HL-60, and K562 cells, as determined by the median dose-effect method described by Chou and Talalay (Fig. 2D, *left* and *right*). For MK-0457 and vorinostat, the CI values were <1.0 for all the tested doses of the two drugs.

MK-0457 inhibits activity of Bcr-Abl and induces cell death in BaF3 cells with overexpression of unmutated or mutant Bcr-Abl. We next determined the activity of MK-0457 against murine pro-B BaF3 cells with ectopic overexpression of either wild-type (unmutated) Bcr-Abl or the point mutants Bcr-Abl E255K and Bcr-Abl T315I. Treatment with MK-0457 (100-500 nmol/L) dose-dependently increased the percentage of apoptotic cells in BaF3 with wild-type or mutant forms of Bcr-Abl (Fig. 3A). Higher concentrations of MK-0457 induced significantly more apoptosis of the BaF3/Bcr-AblT315I and BaF3/Bcr-AblE255K versus BaF3/Bcr-Abl cells (Fig. 3A), whereas the control BaF3/Neo cells were the least sensitive to MK-0457 ($P < 0.01$; Fig. 3A). These data also show that MK-0457 is highly active against Bcr-AblT315I–expressing cells, which are otherwise quite resistant to imatinib, dasatinib, and nilotinib (21, 24, 25). Less activity against BaF3/Neo cells also suggests that the ectopic expression of the wild-type or mutant forms of Bcr-Abl makes BaF3 cells more sensitive to MK-0457, and that most of the lethal effects of MK-0457 are dependent on its anti–Bcr-Abl activity in Bcr-Abl–expressing BaF3 cells. Cotreatment with vorinostat (1.0 μmol/L) and MK-0457 (100 nmol/L) also induced significantly more loss of cell viability in BaF3 cells with wild-type or mutant forms of Bcr-Abl, as compared with treatment with either agent alone ($P < 0.01$; Fig. 3B). This was associated with considerable depletion of Bcr-Abl, Aurora A, and survivin levels in BaF3 cells expressing either the wild-type or mutant forms of Bcr-Abl, following cotreatment with vorinostat and MK-0457 (Fig. 3C). Importantly, the median dose-effect method showed that combined treatment with vorinostat (0.5-2 μmol/L) and MK-0457 (50-200 nmol/L) exerted synergistic apoptotic effects against BaF3/Bcr-AblT315I, Bcr-AblE255K, and BaF3/Bcr-Abl cells (Fig. 3D). For MK-0457 and vorinostat, the CI values were <1.0 for all of the tested doses of the two drugs.

Cotreatment with MK-0457 and vorinostat inhibits Aurora kinase activity and exerts superior antileukemia activity against primary CML and AML cells. We next determined the antileukemia effects of MK-0457 and/or vorinostat against four imatinib-refractory primary CML cells, three AML blast samples, as well as against normal human CD34+ progenitor cells. For the CML samples, the mechanism underlying imatinib refractoriness was unknown. Figure 4 shows that treatment with MK-0457 (100-500 nmol/L) or 1.0 μmol/L of vorinostat induced loss of cell viability of the primary CML and AML cells to a variable extent. However, as compared with treatment with either agent alone, cotreatment with MK-0457 and vorinostat induced more loss of cell viability in each of the CML and AML samples tested. When mean values for the loss of cell viability in CML and AML samples were considered, the combination of 500 nmol/L of MK-0457 and vorinostat (1.0 μmol/L) induced more loss of cell viability than either agent alone (Fig. 4). Notably, normal CD34+ progenitor cells were, in general, less susceptible to the toxic effect of MK-0457 than AML or CML cells (Fig. 4). Additionally, cotreatment with MK-0457 (100-500 nmol/L) and vorinostat (1.0 μmol/L) induced more loss of cell viability in CML or AML versus normal CD34+ progenitor cells. One AML and one CML sample yielded a sufficient number of cells to allow for immunoblot analysis of Aurora kinase activity and levels. Similar to the cultured OCI-AML3 and K562 cells, treatment with MK-0457 alone inhibited p-Aurora A, p-Aurora B, and p-survivin levels in the primary AML and CML cells (Fig. 5A). In the primary CML cells, MK-0457 also induced Bim_{EL} levels in a dose-dependent manner. In primary CML and AML cells, cotreatment with MK-0457 (50 nmol/L) and vorinostat (1.0 μmol/L) attenuated p-Aurora A, p-Aurora B, and p-survivin levels, as well as induced Bim_{EL} to a greater extent than treatment with either agent alone (Fig. 5B-C). As was observed in K562 cells, in primary CML cells, cotreatment with MK-0457 (100 nmol/L) and vorinostat (1.0 μmol/L) also caused greater depletion of Bcr-Abl, p-STAT5, and p-CrkL than treatment with either agent alone (Fig. 5D). These findings are consistent with the greater loss of cell viability observed in primary AML and CML cells, following cotreatment with vorinostat and MK-0457 (Fig. 4).

Discussion

Although individually, both vorinostat and MK-0457 have been reported to induce *in vitro* growth arrest and apoptosis of

human AML cells (13, 18), in the present studies, we show for the first time that combined treatment with vorinostat and MK-0457 synergistically induces apoptosis of AML cell lines. Previously, we had also described the synergistic activity of the combinations of HA-HDI with the Bcr-Abl kinase inhibitors imatinib, nilotinib, and dasatinib against cultured CML cell lines with wild-type Bcr-Abl (21, 24, 25). Although nilotinib and dasatinib inhibit the most commonly observed Bcr-Abl mutants, they are ineffective against Bcr-AblT315I, which has been referred to as the "gatekeeper" threonine at residue 315 in the Abl kinase domain (31). Recently, MK-0457 was shown to have clinical activity against CML cells with the Bcr-AblT315I mutation (17). In the present studies, we have confirmed that clinically achievable concentrations of MK-0457 not only inhibit Aurora A and B activities but also attenuate the activity of wild-type and mutant forms of Bcr-Abl, including Bcr-AblT315I. This was associated with the apoptosis of cells expressing wild-type or mutant Bcr-Abl. However, importantly, our present studies show for the first time that cotreatment with MK-0457 and vorinostat synergistically induces apoptosis of CML cell lines or BaF3 cells with wild-type or the mutant Bcr-AblE255K and Bcr-AblT315I.

The expression and activity of Aurora A and B are regulated in a cell cycle–dependent manner, with up-regulation in the G_2-M phase and rapid down-regulation after mitosis (1–3). Although not amplified, expression of Aurora A and B was easily detectable in cultured and primary AML and CML cells. Treatment with MK-0457 inhibited p-Aurora A and p-Aurora B

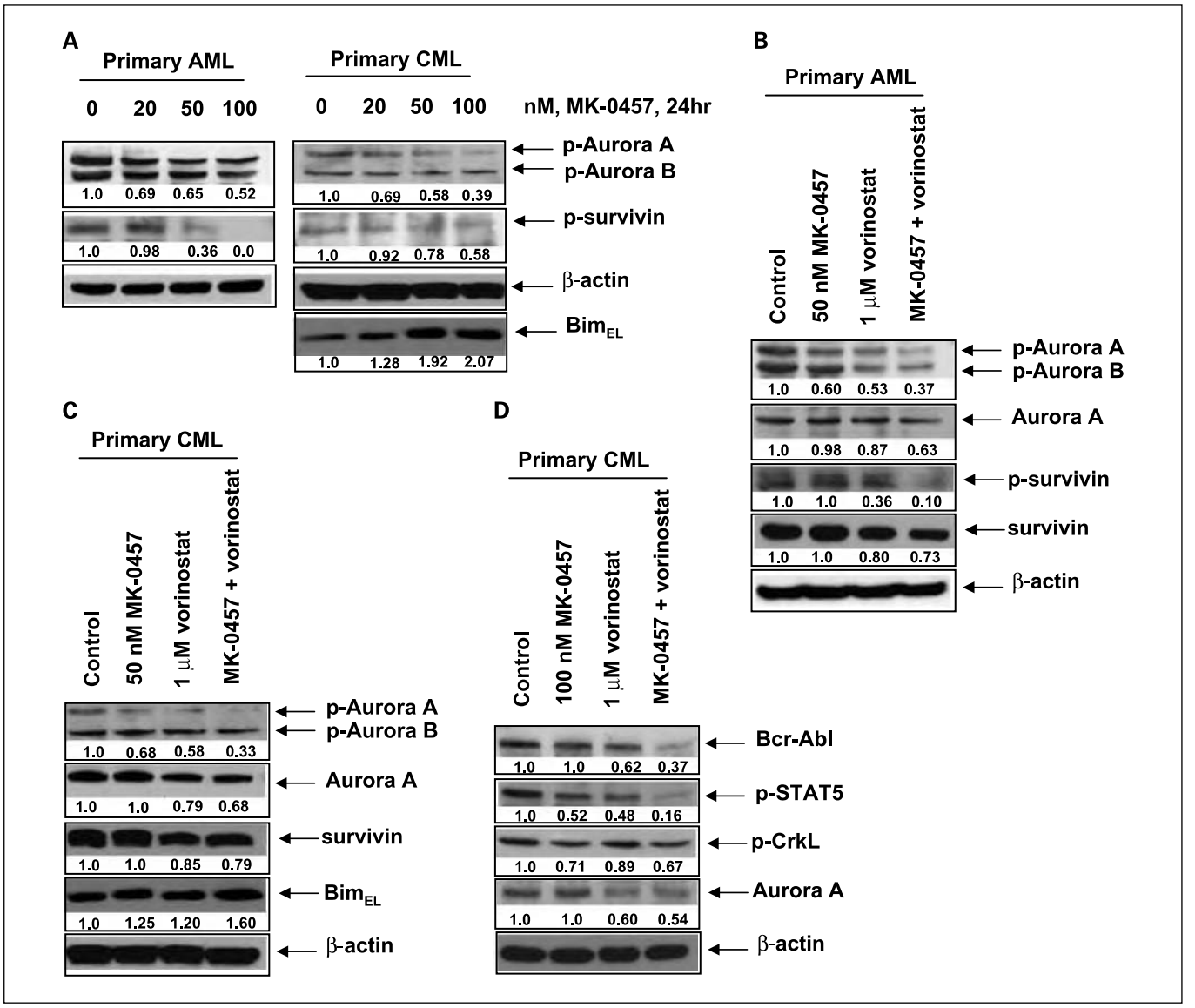

Fig. 5. The effect of MK-0457 and/or vorinostat on primary AML and CML cells. *A,* primary AML and CML cells were treated with the indicated concentrations of MK-0457 for 24 h. After this, Western blot analysis was done for p-Aurora A/B and p-survivin. The levels of β-actin in the total cell lysates served as the loading control. *B* and *C,* primary AML and CML cells were treated with the indicated concentrations of MK-0457 and/or vorinostat for 24 h. Following this, immunoblot analysis was done for p-Aurora A, Aurora A, p-survivin, and survivin. The levels of β-actin in the cell lysates served as the loading control. *D,* primary CML cells were treated with the indicated concentrations of MK-0457 and/or vorinostat for 24 h. Then, immunoblot analysis was done for Bcr-Abl, p-STAT5, p-CrkL, and Aurora A. The levels of β-actin in the cell lysates served as the loading control.

levels in the acute leukemia cells, suggesting that it inhibits the autophosphorylation activities of Aurora A and B (9). This was accompanied by decreased phosphorylation of serine 10 on histone H3 and reduced levels of p-survivin, both substrates of Aurora B (1, 3, 13). Concomitantly, treatment with MK-0457 also caused aberrant centrosome duplication, as well as induced multipolar spindle formation, G_2-M phase accumulation, decreased MPM-2 mitotic phosphoprotein staining, endoreduplication, and apoptosis of AML and CML cells (13). MK-0457 has been reported to induce endoreduplication in cells with a compromised postmitotic checkpoint, thereby allowing cells to proceed through S phase without undergoing cell division and cytokinesis (14). Cells which fail to divide accumulate greater than 8N DNA content and ultimately undergo cell death (13, 14). As previously reported, treatment with vorinostat induced Bim, a proapoptotic protein induced in leukemia cells by the forkhead family of transcription factors, which also lowers the threshold for apoptosis (32). Unlike MK-0457, vorinostat treatment depleted the protein levels of Aurora A and B in AML and CML cells. The underlying mechanism may be manifold. First, by inhibiting HDAC6, vorinostat induced hsp90 acetylation (Fig. 2A). This has been shown to inhibit the ATP-binding and chaperone function of hsp90 (23, 25), which in turn abrogates the chaperone association of hsp90 with its client proteins including Bcr-Abl, FLT-3, and c-Raf, promoting their degradation by the 26S proteasome (23, 26). HDAC inhibitors have recently been reported to deplete the association of Aurora A with hsp90, thereby promoting its degradation by the proteasome (28). This is consistent with our findings demonstrating decreased chaperone association of hsp90 with Aurora A in hsp90 immunoprecipitates and that cotreatment with bortezomib partly restores the depletion of Aurora A caused by vorinostat. Although not shown, HDAC inhibitors such as vorinostat may in part transcriptionally down-regulate Aurora A and B. Taken together, these observations may explain vorinostat-mediated down-regulation of the activity and levels of Aurora A and B.

Although the precise mechanism(s) underlying the synergistic apoptotic effects of the combination of vorinostat and MK-0457 against AML cells is not clear, several intracellular perturbations induced by the combination may explain this synergy. As compared with either agent alone, cotreatment with vorinostat plus MK-0457 induced marked inhibition of p-Aurora A and B, greater depletion of p-survivin and survivin, and more attenuation of phosphorylated serine 10 on histone H3 (data not shown) in OCI-AML3 and HL-60 cells. In contrast, as compared with treatment with vorinostat alone, cotreatment with MK-0457 and vorinostat caused similar depletion of Aurora A and B. However, cotreatment with vorinostat and MK-0457 caused more up-regulation of Bim isoforms, thus further sensitizing AML cells to the cytotoxicity of the combination. Collectively, more potent inhibition of the activities of Aurora kinases and survivin, combined with greater induction of Bim may be responsible for the superior anti-AML activity of vorinostat plus MK-0457. Similar to AML cells, as compared with treatment with vorinostat alone, cotreatment with MK-0457 and vorinostat also caused more depletion of p-survivin and phosphorylated serine 10 on histone H3 in K562 cells, but similar effects on the levels of Aurora A and Aurora B. However, combination of vorinostat and MK-0457 attenuated the activities of both Aurora and Bcr-Abl kinases, which may explain its synergistic apoptotic effects in K562 cells. In phase I/II clinical trials, MK-0457 showed significant clinical activity in patients with imatinib mesylate–resistant CML producing clinical responses in three patients (17). The T315I mutation in Bcr-Abl mediates clinical resistance to the current targeted therapeutic agents, imatinib, nilotinib, and dasatinib (31). The activity of MK-0457 against Bcr-Abl mutants in which other tyrosine kinases fail, particularly against Bcr-AblT315I, may be due to the manner in which MK-0457 binds to the Abl kinase domain. Crystal structures of MK-0457 with the Bcr-Abl kinase domain show that MK-0457 does not bind deeply to the Abl kinase domain and unlike imatinib, nilotinib, and dasatinib, this binding is not disrupted by the steric hindrance of a threonine to isoleucine substitution at residue 315 (15, 31). This attribute of MK-0457 allows it to associate with an active conformation of Bcr-Abl and inhibit the kinase activity of mutant Bcr-Abl in imatinib mesylate–resistant CML cells. In preclinical models, vorinostat has also been shown to deplete the levels of mutant forms of Bcr-Abl and exerts enhanced cytotoxic effects of dasatinib against mutant Bcr-AblE255K and Bcr-Abl T315I–containing cells (25). Therefore, consistent with these findings, our present results show that cotreatment with vorinostat and MK-0457 more effectively depletes Bcr-AblE255K and Bcr-AblT315I levels and exerts synergistic apoptotic effects against imatinib-resistant mutant Bcr-AblE255K and Bcr-Abl T315I–expressing cells.

Our findings also show the superior activity of MK-0457 plus vorinostat, as compared with treatment with either agent alone, against primary AML and imatinib-refractory CML cells. However, the effects were variable and less than additive. However, the antileukemia effects of the combination were associated with more inhibition of the activities of Aurora kinases and greater induction of Bim in AML cells. In CML cells, in addition to its inhibitory effects on Aurora kinases, the combination produced greater depletion of Bcr-Abl and its phosphorylated substrates p-STAT5, as well as more induction of Bim. Taken together, these findings are consistent with more lethal effects of the combination against primary AML and CML cells. Recent studies have highlighted that cytokinetically quiescent CML stem cells may escape the lethal effect of Bcr-Abl kinase inhibitors because they also harbor refractory Bcr-Abl mutations or possess membrane transporters of which the Bcr-Abl kinase inhibitor may be a substrate (33–35). A recent report has highlighted that hsp90 inhibitors may also have activity against Bcr-Abl expressing CML stem cells (36). Because pan-HDAC inhibitors such as vorinostat also inhibit hsp90 function, in combination with MK-0457, they may also exert cytotoxic effects against CML stem cells. Our findings also show that the combination is relatively less toxic against normal CD34+ human bone marrow progenitor cells. Taken together with previous reports, our preclinical findings presented here create a strong rationale for *in vivo* testing of the combined treatment with vorinostat and MK-0457 for AML and for CML resistant to Bcr-Abl kinase inhibitors.

Disclosure of Potential Conflicts of Interest

Coauthor Carolyn Buser is an employee of Merck & Co., Inc., and the corresponding author, Kapil Bhalla, has received a clinical and laboratory research grant from Merck & Co., Inc. All other authors have no competing financial interests.

References

1. Keen N, Taylor S. Aurora-kinase inhibitors as anticancer agents. Nat Rev Cancer 2004;4:927–36.
2. Marumoto T, Zhang D, Saya H. Aurora-A—a guardian of poles. Nat Rev Cancer 2005;5:42–50.
3. Fu J, Bian M, Jiang Q, Zhang C. Roles of Aurora kinases in mitosis and tumorigenesis. Mol Cancer Res 2007;5:1–10.
4. Fukushige S, Waldman FM, Kimura M, et al. Frequent gain of copy number on the long arm of chromosome 20 in human pancreatic adenocarcinoma. Genes Chromosomes Cancer 1997;19:161–9.
5. Nishida N, Nagasaka T, Kashiwagi K, Boland CR, Goel A. High copy amplification of the Aurora-A gene is associated with chromosomal instability phenotype in human colorectal cancers. Cancer Biol Ther 2007;6:525–33.
6. Zhou H, Kuang J, Zhong L, et al. Tumour amplified kinase STK15/BTAK induces centrosome amplification, aneuploidy and transformation. Nat Genet 1998;20:189–93.
7. Bischoff JR, Anderson L, Zhu Y, et al. A homologue of Drosophila aurora kinase is oncogenic and amplified in human colorectal cancers. EMBO J 1998;17:3052–65.
8. Schmit TL, Ahmad N. Regulation of mitosis via mitotic kinases: new opportunities for cancer management. Mol Cancer Ther 2007;6:1920–31.
9. Zhang Y, Ni J, Huang Q, Ren W, Yu L, Zhao S. Identification of the auto-inhibitory domains of Aurora-A kinase. Biochem Biophys Res Commun 2007;357:347–52.
10. Hirota T, Kunitoku N, Sasayama T, et al. Aurora-A and an interacting activator, the LIM protein Ajuba, are required for mitotic commitment in human cells. Cell 2003;114:585–98.
11. Wang X, Zhou YX, Qiao W, et al. Overexpression of aurora kinase A in mouse mammary epithelium induces genetic instability preceding mammary tumor formation. Oncogene 2006;25:7148–58.
12. Carvajal RD, Tse A, Schwartz GK. Aurora kinases: new targets for cancer therapy. Clin Cancer Res 2006;12:6869–75.
13. Harrington EA, Bebbington D, Moore J, et al. VX-680, a potent and selective small-molecule inhibitor of the Aurora kinases, suppresses tumor growth *in vivo*. Nat Med 2004;10:262–7.
14. Gizatullin F, Yao Y, Kung V, Harding MW, Loda M, Shapiro GI. The Aurora kinase inhibitor VX-680 induces endoreduplication and apoptosis preferentially in cells with compromised p53-dependent post mitotic checkpoint function. Cancer Res 2006;66:7668–77.
15. Young MA, Shah NP, Chao LH, et al. Structure of the kinase domain of an imatinib-resistant Abl mutant in complex with the Aurora kinase inhibitor VX-680. Cancer Res 2006;66:1007–14.
16. Cheetham GM, Charlton PA, Golec JM, Pollard JR. Structural basis for potent inhibition of the Aurora kinases and a T315I multi-drug resistant mutant form of Abl kinase by VX-680. Cancer Lett 2007;251:323–9.
17. Giles FJ, Cortes J, Jones D, Bergstrom D, Kantarjian H, Freedman SJ. MK-0457, a novel kinase inhibitor, is active in patients with chronic myeloid leukemia or acute lymphocytic leukemia with the T315I BCR-ABL mutation. Blood 2007;109:500–2.
18. Dokmanovic M, Clarke C, Marks PA. Histone deacetylase inhibitors: overview and perspectives. Mol Cancer Res 2007;5:981–9.
19. Minucci S, Pelicci PG. Histone deacetylase inhibitors and the promise of epigenetic (and more) treatments for cancer. Nat Rev Cancer 2006;6:38–51.
20. Glozak MA, Seto E. Histone deacetylases and cancer. Oncogene 2007;26:5420–32.
21. Nimmanapali R, Fuino L, Bali P, et al. Histone deacetylase inhibitor LAQ824 both lowers expression and promotes proteasomal degradation of Bcr-Abl and induces apoptosis of imatinib mesylate-sensitive or -refractory chronic myelogenous leukemia-blast crisis cells. Cancer Res 2003;63:5126–35.
22. Guo F, Sigua C, Tao J, et al. Cotreatment with histone deacetylase inhibitor LAQ824 enhances Apo-2L/tumor necrosis factor-related apoptosis inducing ligand-induced death inducing signaling complex activity and apoptosis of human acute leukemia cells. Cancer Res 2004;64:2580–9.
23. Bali P, Pranpat M, Bradner J, et al. Inhibition of histone deacetylase 6 acetylates and disrupts the chaperone function of heat shock protein 90: a novel basis for antileukemia activity of histone deacetylase inhibitors. J Biol Chem 2005;280:26729–34.
24. Fiskus W, Pranpat M, Bali P, et al. Combined effects of novel tyrosine kinase inhibitor AMN107 and histone deacetylase inhibitor LBH589 against Bcr-Abl expressing human leukemia cells. Blood 2006;108:645–52.
25. Fiskus W, Pranpat M, Balasis M, et al. Cotreatment with vorinostat (suberoylanilide hydroxamic acid) enhances activity of dasatinib (BMS-354825) against imatinib mesylate-sensitive or imatinib mesylate-resistant chronic myelogenous leukemia cells. Clin Cancer Res 2006;12:5869–78.
26. Bali P, George P, Cohen P, et al. Superior activity of the combination of histone deacetylase inhibitor LAQ824 and the FLT-3 kinase inhibitor PKC412 against human acute myelogenous leukemia cells with mutant FLT-3. Clin Cancer Res 2004;10:4991–7.
27. Lange BM, Rebollo E, Herold A, González C. Cdc37 is essential for chromosome segregation and cytokinesis in higher eukaryotes. EMBO J 2002;21:5364–74.
28. Park JH, Jong HS, Kim SG, et al. Inhibitors of histone deacetylases induce tumor-selective cytotoxicity through modulating Aurora-A kinase. J Mol Med 2008;86:117–28.
29. Yang J, Ikezoe T, Nishioka C, et al. AZD1152, a novel and selective aurora B kinase inhibitor, induces growth arrest, apoptosis, and sensitization for tubulin depolymerizing agent or topoisomerase II inhibitor in human acute leukemia cells *in vitro* and *in vivo*. Blood 2007;110:2034–40.
30. Chou TC, Talalay P. Quantitative analysis of dose-effect relationships: the combined effects of multiple drugs or enzyme inhibitors. Adv Enzyme Regul 1984;22:27–55.
31. Weisberg E, Manley PW, Cowan-Jacob S, et al. Second generation inhibitors of BCR-ABL for the treatment of imatinib-resistant chronic myeloid leukemia. Nat Rev Cancer 2007;7:345–58.
32. Essafi A, Fernandez de Mattos S, Hassen YAM, et al. Direct transcriptional regulation of Bim by FoxO3a mediates STI571-induced apoptosis in Bcr-Abl-expressing cells. Oncogene 2005;24:2317–29.
33. Jiang X, Saw KM, Eaves A, Eaves C. Instability of BCR-ABL gene in primary and cultured chronic myeloid leukemia stem cells. J Natl Cancer Inst 2007;99:680–93.
34. Deininger MW. Optimizing therapy of chronic myeloid leukemia. Exp Hematol 2007;35:144–54.
35. Chu S, Xu H, Shah NP, et al. Detection of BCR-ABL kinase mutations in CD34+ cells from chronic myelogenous leukemia patients in complete cytogenetic remission on imatinib mesylate treatment. Blood 2005;105:2093–8.
36. Peng C, Brain J, Hu Y, et al. Inhibition of heat shock protein 90 prolongs survival of mice with BCR-ABL-T315I-induced leukemia and suppresses leukemic stem cells. Blood 2007;110:678–85.

[Cancer Biology & Therapy 8:10, 1-12; 15 May 2009]; ©2009 Landes Bioscience

Research Paper

Panobinostat treatment depletes EZH2 and DNMT1 levels and enhances decitabine mediated de-repression of JunB and loss of survival of human acute leukemia cells

Warren Fiskus,[1] Kate Buckley,[1] Rekha Rao,[1] Aditya Mandawat,[1] Yonghua Yang,[1] Rajeshree Joshi,[1] Yongchao Wang,[1] Ramesh Balusu,[1] Jianguang Chen,[1] Sanjay Koul,[1] Atul Joshi,[1] Sunil Upadhyay,[1] Peter Atadja[2] and Kapil N. Bhalla[1,*]

[1]MCG Cancer Center; Medical College of Georgia; Augusta, GA USA; [2]Novartis Institute for Biomedical Research Inc., Pharmaceuticals Inc.; Cambridge, MA USA

Key words: EZH2, DNMT1, hsp90, HDAC inhibitor, DNA methyltransferase inhibitor

The PRC2 complex protein EZH2 is a histone methyltransferase that is known to bind and recruit DNMT1 to the DNA to modulate DNA methylation. Here, we determined that the pan-HDAC inhibitor panobinostat (LBH589) treatment depletes DNMT1 and EZH2 protein levels, disrupts the interaction of DNMT1 with EZH2, as well as de-represses JunB in human acute leukemia cells. Similar to treatment with the hsp90 inhibitor 17-DMAG, treatment with panobinostat also inhibited the chaperone association of heat shock protein 90 with DNMT1 and EZH2, which promoted the proteasomal degradation of DNMT1 and EZH2. Unlike treatment with the DNA methyltransferase inhibitor decitabine, which demethylates JunB promoter DNA, panobinostat treatment mediated chromatin alterations in the JunB promoter. Combined treatment with panobinostat and decitabine caused greater attenuation of DNMT1 and EZH2 levels than either agent alone, which was accompanied by more JunB de-repression and loss of clonogenic survival of K562 cells. Co-treatment with panobinostat and decitabine also caused more loss of viability of primary AML but not normal CD34$^+$ bone marrow progenitor cells. Collectively, these findings indicate that co-treatment with panobinostat and decitabine targets multiple epigenetic mechanisms to de-repress JunB and exerts antileukemia activity against human acute myeloid leukemia cells.

Introduction

Gene silencing and loss of gene function mediated through epigenetic mechanisms collaborates with genetic mutations and alterations leading to cancer.[1-3] As multiprotein complexes, Polycomb group proteins epigenetically silence gene expression, including tumor suppressor genes (TSGs).[1-3] EZH2 is the catalytic subunit of the polycomb repressive complex 2 (PRC2), which also includes SUZ12, EED and YY1.[1-3] EZH2 acts as a histone lysine methyltransferase (HKMT), which mediates methylation of lysine (K) 27 on the N-terminal tail of histone H3 to silence expression of PRC2 target genes involved in lineage differentiation.[3-5] EZH2 has also been recognized as a senescence preventing gene in embryonic fibroblasts, as well as shown to be abundantly expressed in purified hematopoietic stem cell (HSCs), where it preserves HSC potential and prevents exhaustion.[6] EZH2 regulates cell proliferation by promoting S phase entry and G_2-M transition, and it is highly expressed in tumor versus normal tissue.[7,8] EZH2 mediated cell cycle progression promoted by gene repression also involves histone deacetylation by HDAC1, with which EZH2 interacts through its PRC2 binding partner EED.[9] EZH2 is overexpressed in a variety of malignancies, including prostate, breast and bladder cancers with poor prognosis.[10-12] Knockdown of EZH2 by siRNA has been demonstrated to inhibit breast cancer cell proliferation, while pharmacologic inhibition of EZH2 resulted in apoptosis of breast cancer but not normal cells.[10,13] Recently, EZH2 was shown to directly interact with and regulate the activity of the DNA methyltransferases DNMT1, DNMT3a and DNMT3b.[14,15] DNMTs function to transfer a methyl group from S-adenosyl-methionine to the 5' position of cytosine in the CpG dinucleotides in the promoters of genes, thereby maintaining a consistent pattern of epigenetic gene silencing of TSGs in cancer cells.[16-19] The heritable pattern of cytosine methylation is maintained during DNA replication by DNMT1, which has a preference for hemi-methylated DNA and is regarded as the primary maintenance DNMT.[17-19] DNA methylation by DNMTs also recruits HDAC activity to the promoters of silenced genes.[20,21] Similar to the PRC2 complex, DNMT1 has a direct interaction with histone deacetylases HDAC1 and HDAC2.[22,23] In acute myeloid leukemia (AML) and chronic myeloid leukemia (CML), all three DNMTs are overexpressed and may play a significant role in the pathogenesis of leukemia due to aberrant hypermethylation of TSGs or DNA

*Correspondence to: Kapil Bhalla; M.D.MCG Cancer Center; Medical College of Georgia; 1120 15th Street; CN-2101 Augusta, GA 30912 USA; Tel.: 706.721.0566; Fax: 706.721.0469; Email: kbhalla@mcg.edu

Submitted: 12/31/08; Revised: 02/17/09; Accepted: 02/18/09

Previously published online as a *Cancer Biology & Therapy* E-publication: http://www.landesbioscience.com/journals/cbt/article/8213

repair related genes.[24,25] Treatment with the antisense oligonucleotides against DNMT1 was demonstrated to cause cell cycle arrest in the S-phase of the cell cycle and inhibited DNA replication with loss of DNMT1 at the replication fork.[26,27] Although genes methylated in cancer cells are packaged with nucleosomes containing the trimethylated K27 on the H3 mark, gene silenced in cancer by H3K27 trimethylation has been shown to be independent of promoter DNA methylation.[17,28] Consistent with this, DNA methylation and transcriptional silencing of cancer genes has been shown to persist despite the depletion of EZH2.[29]

In myeloid leukemia, overexpression of DNMT1 has been associated with promoter hypermethylation of a number of genes, including JunB.[30-33] In AML, promoter hypermethylation of E cadherin, ERα and p15 have also been reported.[34] Inactivation of JunB expression in stem cells leads to myeloproliferative disorders, and JunB overexpression and amplification has been associated with failure of differentiation.[32,35] JunB deficient hematopoietic stem cells show concomitant downregulation of $p16^{INK4a}$ and upregulation of Bcl-2 and Bcl-x_L.[32] Indeed, JunB methylation and impaired expression was observed in blast crisis of CML.[31] The DNMT1 inhibitor decitabine inhibits hypermethylation of the promoter DNA of tumor suppressor genes and decreased global methylation, which supports the rationale for the use of decitabine as a therapeutic agent in the treatment of hematologic malignancies.[36,37] Further, co-treatment with a DNMT1 and HDAC inhibitor has been shown to synergistically hypomethylate the promoters of TSGs and significantly inhibit tumor growth.[38,39] Previously, while the pan-HDAC inhibitor trichostatin A (TSA) was shown to downregulate both the mRNA and protein levels of DNMT1 in tumor cells, treatment with panobinostat (LBH589) was shown to release DNMT1 and HDAC1 from the ERα gene promoter, suggesting an association between DNMT1 and the HDACs.[40,41] In a previous report, we had demonstrated that panobinostat treatment inhibits HDAC6 and induces hyperacetylation of the molecular chaperones heat shock protein (hsp) 90, associated with depletion of EZH2 and other PRC2 components.[42-44] This occurred with the concomitant depletion of the transcription factors HOXA9 and MEIS 1 levels, resulting in loss of clonogenic survival of human leukemia cells.[44] Based on these observations we determined the effects of panobinostat on the interaction between the EZH2 and PRC2 complex with DNMT1, as well as on the levels and chaperone association of DNMT1 and EZH2 with hsp 90. Here, we report that treatment with panobinostat or a geldanamycin analogue hsp90 inhibitor (17-DMAG) attenuated the levels of DNMT1 with EZH2 by inhibiting their chaperone association with hsp90 in acute leukemia cells.[45] We further determined that, as compared to treatment with either agent alone, combined treatment with decitabine (DAC) and panobinostat resulted in greater depletion of DNMT1 levels, more derepression of JunB, and induced greater loss of cell viability and clonogenic survival of cultured and primary acute leukemia cells.

Results

Panobinostat treatment disrupts the association of DNMT1 and EZH2 with hsp90, leading to proteasomal degradation of DNMT1 and EZH2. In a previous report we had shown that panobinostat depletes the levels and activity of EZH2.[44] Based on this, and on the reports that EZH2 directly interacts with and regulates the activity of the DNMT1, we first determined the effects of panobinostat treatment on DNMT1 levels, as well as on the binding of EZH2 to DNMT1. Treatment with panobinostat dose-dependently reduced the protein levels of DNMT1 and EZH2 in the CML blast crisis (CML-BC) K562 and LAMA-84 cells (Fig. 1A).[14] This was accompanied by panobinostat-mediated decrease in the mRNA levels of DNMT1 in a time and dose dependent manner in K562 cells (Fig. 1B). Similar effects were seen in LAMA84 cells (Suppl. Fig. 1A). In contrast, panobinostat treatment did not lower EZH2 mRNA levels (Suppl. Fig. 1B and C). We have previously demonstrated that, by inducing hyperacetylation of hsp90, pan-HDAC inhibitors can inhibit the chaperone function and association of hsp90 with its client proteins.[42,43] Based on this, we next determined the effects of panobinostat treatment on the interaction of DNMT1 and EZH2, and whether panobinostat-mediated depletion of DNMT1 and EZH2 was due to inhibition of their chaperone association with hsp90. Figure 1C shows that exposure to panobinostat disrupted the binding of DNMT1 to EZH2, as well as decreased the binding of hsp90 to both EZH2 and DNMT1. Similar findings were observed in LAMA84 cells (Suppl. Fig. 1D). Exposure intervals as short as 2 to 4 hours to panobinostat reduced the binding of hsp90 to EZH2 and DNMT1 (Suppl. Fig. 1E). This was associated with increased accumulation of both DNMT1 and EZH2 in the detergent (NP40) insoluble fraction of the cytosol, suggesting increase in the levels of misfolded DNMT1 and EZH2 following treatment with panobinostat (Fig. 1D). Additionally, co-treatment with the proteasome inhibitor bortezomib significantly increased the levels of DNMT1 and EZH2 in the detergent insoluble fraction, as well as restored the levels in the total cell lysates (Fig. 1D). Co-treatment with bortezomib did not alter or rescue the levels of AKT or Bcl-x_L in panobinostat treated cells (Fig. 1D). Similar findings were observed in panobinostat-treated LAMA84 leukemia cells (Suppl. Fig. 2A). Panobinostat-mediated decline in EZH2 levels was not due to the activity of caspases, since co-treatment with the caspase inhibitor ZVAD did not restore the levels of EZH2 (Suppl. Fig. 2B). Panobinostat treatment also depleted DNMT1 and EZH2 levels in primary AML cells, which were also restored by co-treatment with bortezomib (Fig. 1E). In these studies, the levels of the hsp90 client protein c-Raf served as the control protein that is a well recognized hsp90 client protein.[42,43]

Co-treatment with panobinostat enhances 17-DMAG mediated depletion of DNMT1 and EZH2 in acute leukemia cells. First, to confirm that DNMT1 and EZH2 are hsp90 client proteins, we determined the effects of the geldanamycin analogue hsp90 inhibitor 17-DMAG on the expression of DNMT1 in the K562 cells. Treatment with 17-DMAG depleted DNMT1 protein levels, while it concomitantly induced hsp70 levels (Fig. 2A).[50] Similar findings were noted, following treatment of primary leukemia cells with 17-DMAG (Fig. 2B). We next determined the effects of 17-DMAG treatment on the binding of DNMT1 and EZH2 to hsp90. Similar to the results with LBH589, exposure to

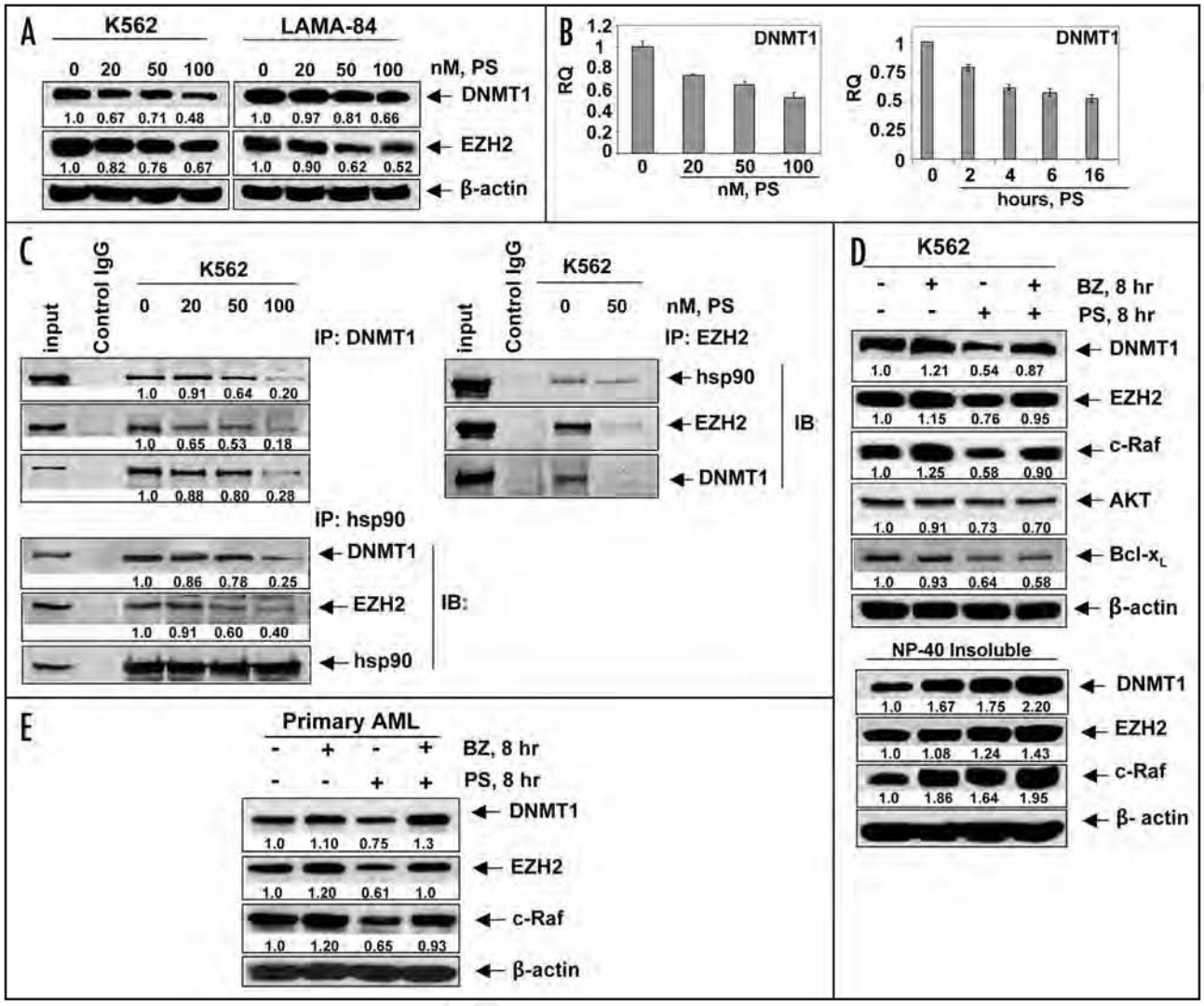

Figure 1. Panobinostat depletes DNMT1 and disrupts its binding to EZH2 and hsp90. (A) Western blot of DNMT1 and EZH2 in K562 and LAMA84 following 24 hours treatment with the indicated doses of panobinostat (PS). The levels of β-actin served as the loading control. (B) K562 cells were treated with the indicated concentrations of panobinostat for 16 hours. Alternatively, cells were treated with 100 nmol/L of panobinostat for the indicated times. Total RNA was isolated and qPCR was performed for DNMT1. The relative quantity (RQ) of DNMT1 mRNA expression was normalized against expression of GAPDH. (C) K562 cells were treated with the indicated doses of panobinostat for 8 hours and DNMT1 (left), EZH2 (right) and hsp90 (bottom) were immunoprecipitated from the cell lysates. The immunoprecipitates were immunoblotted for hsp90, EZH2 and DNMT1. (D) K562 cells were treated with 100 nmol/L of panobinostat and/or 100 nmol/L of bortezomib (BZ) for 8 hours. Following treatment, total cell lysates or NP-40 detergent insoluble fractions were immunoblotted for DNMT1, EZH2 and c-Raf, AKT and Bcl-x_L. The levels of β-actin served as the loading control. (E) Primary AML cells were treated with 100 nmol/L of panobinostat and/or 100 nmol/L of bortezomib for 8 hours. Following treatment, total cell lysates were immunoblotted for DNMT1, EZH2 and c-Raf. The levels of β-actin in the lysates served as the loading control.

17-DMAG reduced the binding of DNMT1 and EZH2 to hsp90 (Fig. 2A), increased the binding to hsp70, as well as attenuated the binding of DNMT1 with EZH2 (Fig. 2C). Additionally, co-treatment with bortezomib restored 17-DMAG induced depletion of DNMT1 and EZH2 (data not shown). We next determined the combined effects of panobinostat and 17-DMAG on the levels of DNMT1 and EZH2. Notably, co-treatment with panobinostat significantly increased 17-DMAG mediated depletion of DNMT1 and EZH2 in K562 cells (Fig. 2D).

Panobinostat treatment induces JunB and enhances decitabine (DAC)-mediated induction of JunB. We next determined the effect of panobinostat on the mRNA expression JunB, a gene that is known to be silenced by promoter hypermethylation in CML cells.[31,32] Treatment with panobinostat dose-dependently upregulated the mRNA levels of JunB, with 2.67 fold increase seen following treatment with 100 nmol/L of panobinostat (Fig. 3A). JunB mRNA induction was observed following exposure interval to panobinostat as short as two hours (Fig. 3B). As noted above for panobinostat, treatment with decitabine (DAC) dose-dependently attenuated DNMT1 protein levels and upregulated JunB mRNA and protein levels (Fig. 3C and D). However, exposure to DAC did not lower the levels of EZH2 (Fig. 3C). We next determined the effect of co-treatment with panobinostat and DAC on EZH2, DNMT1 and JunB levels. Figure 4A demonstrates that as

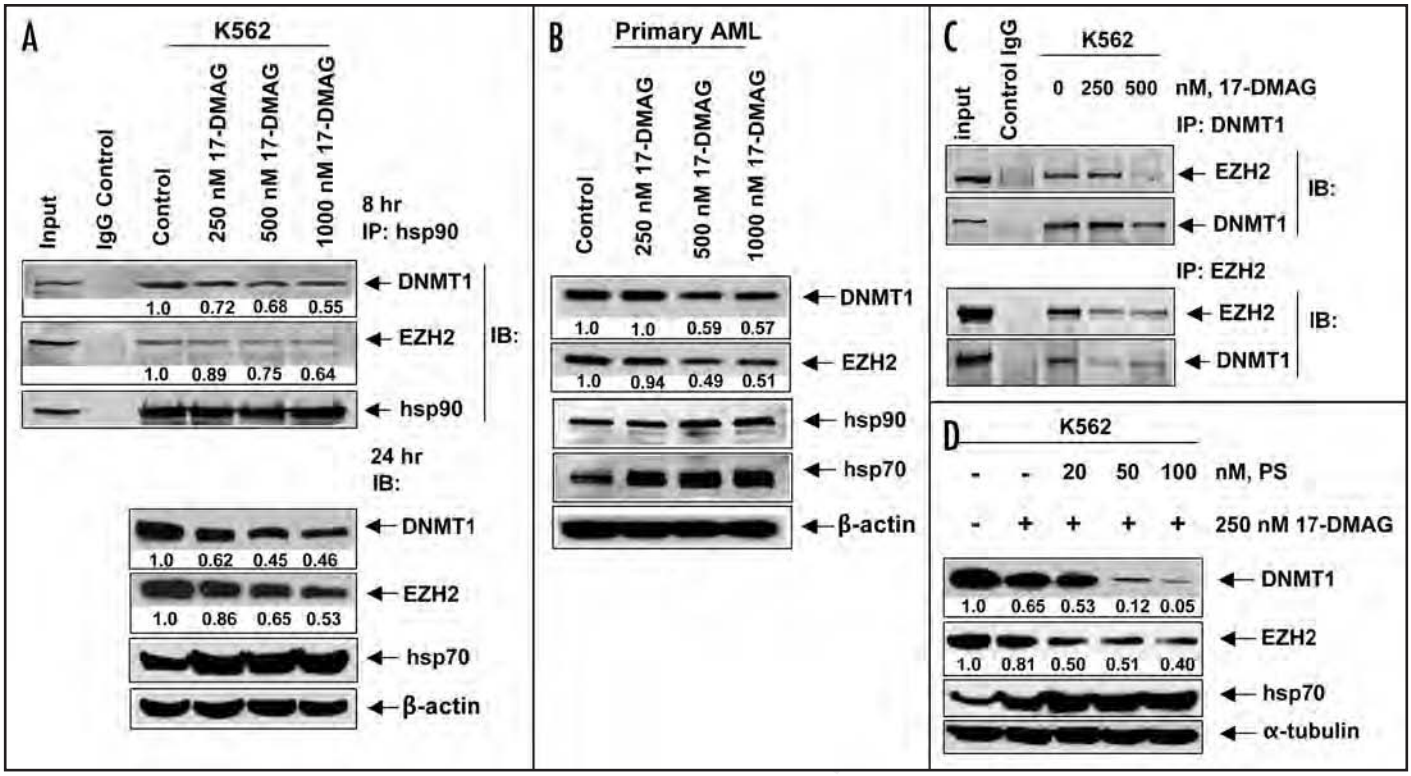

Figure 2. 17-DMAG depletes the levels of DNMT1 and EZH2 by inhibiting their chaperone association hsp90 in acute leukemia cells. (A) K562 cells were treated with the indicated does of 17-DMAG for 8 hours and hsp90 was immunoprecipitated. Immunoblot analysis was performed for DNMT1, EZH2 and hsp90 on the immunoprecipitates. Alternatively, K562 cells were treated with the indicated concentrations of 17-DMAG for 24 hours and immunoblot analysis was done for DNMT1, EZH2 and hsp70. The expression levels of β-actin in the lysates served as the loading control. (B) Primary acute leukemia cells were treated with the indicated concentrations of 17-DMAG for 24 hours. Total cell lysates were harvested and immunoblot analysis was performed for DNMT1, EZH2 hsp90 and hsp70. The levels of β-actin in the lysates served as the loading control. (C) K562 cells were treated with the indicated doses of 17-DMAG for 8 hours and DNMT1 (top) and EZH2 (bottom) were immunoprecipitated. Immunoblot analysis was performed for EZH2 and DNMT1 in the immunoprecipitates. (D) K562 cells were treated with the indicated concentrations of panobinostat and 17-DMAG for 24 hours. Immunoblot analysis was performed for DNMT1, EZH2 and hsp70. The expression levels of α-tubulin in the lysates served as the loading control.

compared to treatment with either agent alone, co-treatment with DAC and panobinostat caused greater attenuation of the levels of DNMT1 and EZH2 levels, while concomitantly inducing more JunB levels. Combined treatment with DAC and panobinostat also had a similar effect on EZH2, DNMT1 and JunB levels in primary AML blasts (Fig. 4B). Consistent with previous reports, sequential treatment with DAC followed by panobinostat induced more JunB mRNA and protein levels than treatment with the reverse schedule of administration of panobinostat followed by decitabine (Fig. 4C).

Decitabine and panobinostat induce JunB expression through different mechanisms. We next determined the mechanism by which DAC and panobinostat de-repress JunB in K562 cells. As shown in Figure 5A, treatment with as little as 0.5 μmol/L DAC for 16 hours caused demethylation of the JunB promoter as demonstrated by methylation specific PCR performed on bisulfite-treated DNA. DAC also demethylated the promoter of the E-cadherin and ERα genes, which are known to be silenced by methylation in hematologic malignancies (Fig. 5A).[41] In contrast, although it de-repressed JunB similar to DAC, panobinostat treatment did not alter the methylation status of JunB in K562 cells (Fig. 5B). Panobinostat also did not affect the methylation status of ERα (Fig. 5B) and E-cadherin (not shown). We next determined whether the panobinostat mediated derepression of JunB was due to chromatin alterations in the JunB promoter. Figure 5C shows a schematic representation of four regions in the CpG island of the JunB promoter. To perform ChIP analyses involving these regions in the JunB promoter, primers sets were tiled: four across the CpG island and one pair 2 kb upstream of the transcription start site (TSS) in another 80% GC rich region. As demonstrated in Figure 5D, ChIP analyses of untreated K562 cells confirmed that EZH2, DNMT1 and Suv39H1 were bound to the JunB promoter in region 3 (-378 to -218 relative to TSS) and DNMT1 and the histone methyltransferase Suv39H1 were bound to region 5 (-174 to +9 relative to TSS) nearest the transcriptional start site. EZH2 did not bind to region 5 of the JunB promoter. The repressive histone marks, tri-methlyated lysine 27 and tri-methylated lysine 9 were present in the untreated chromatin of region 3, corresponding to the localization of EZH2 and Suv39H1 (Fig. 5D). In contrast, only the tri-methylated lysine 9 mark was detected in region 5 corresponding to the localization of Suv39H1 to this region (Fig. 5D). Treatment with panobinostat dose-dependently depleted EZH2 and the tri-methlyated lysine 27 mark from region 3, and DNMT1 and Suv39H1 from region 5 of the JunB

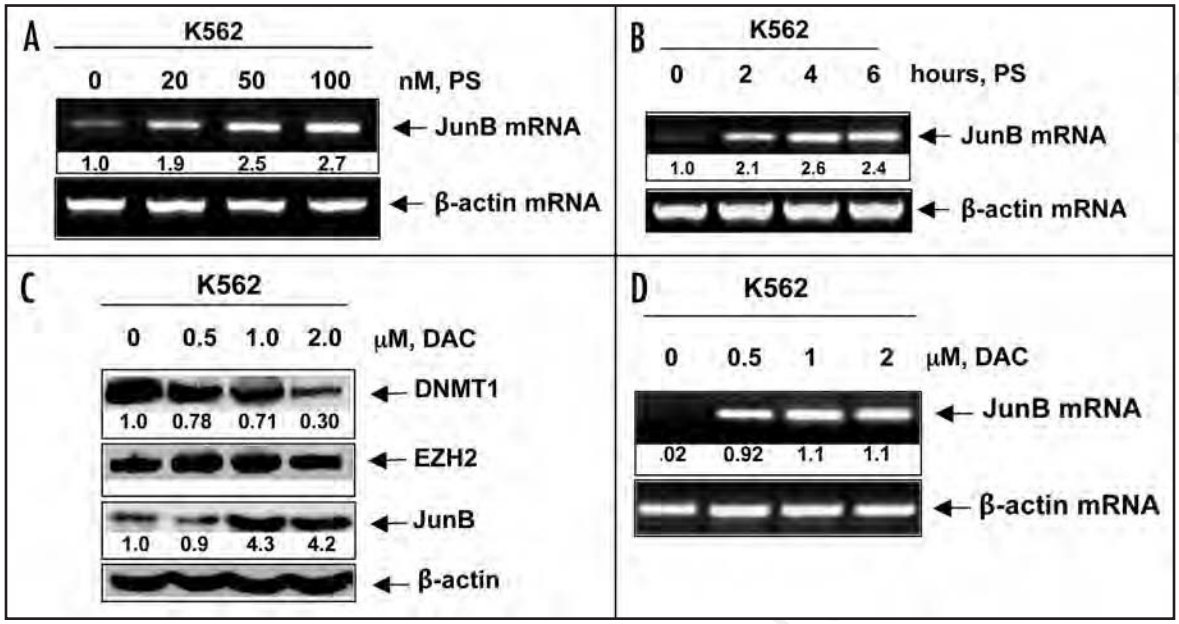

Figure 3. Panobinostat induces JunB mRNA in a dose and time dependent manner. (A) K562 cells were treated with the indicated concentrations of panobinostat for 16 hours. Total RNA was isolated and RT-PCR was performed for JunB mRNA expression. A β-actin specific PCR reaction and expression levels served as the loading control. (B) K562 cells were treated with 100 nmol/L of panobinostat for the indicated times. Following this, RT-PCR analysis was performed for JunB mRNA expression. A β-actin specific PCR reaction and expression levels served as the loading control. (C) K562 cells were treated with the indicated concentrations of decitabine (DAC) for 24 hours. Following this, total cell lysates were harvested and immunoblot analysis was performed for DNMT1, EZH2 and JunB. The levels of β-actin in the lysates served as the loading control. (D) K562 cells were treated with the indicated concentrations of decitabine (DAC) for 16 hours. Following this, total RNA were isolated and RT-PCR analysis was performed for JunB mRNA expression. A β-actin specific PCR reaction and expression served as the loading control.

promoter (Fig. 5D). Panobinostat-mediated depletion of the trimethylated lysine 9 and lysine 27 marks were also accompanied by increase in acetylation of histone H3 associated with the JunB promoter (Fig. 5D). These findings clearly show that panobinostat mediated de-repression of JunB is accompanied by depletion of the repressive chromatin marks but not by demethylation of the CpG dinucleotides in the promoter DNA of JunB.

Co-treatment with decitabine enhances panobinostat and 17-DMAG-mediated anti-leukemia activity in cultured and primary leukemia cells. We next determined the effects of DAC alone and in combination with panobinostat or 17-DMAG on the clonogenic survival of leukemia cells. Treatment with DAC alone for 48 hours only modestly decreased the colony growth of K562 cells (Fig. 6A). Treatment with panobinostat alone caused more inhibition of colony growth than DAC, whereas co-treatment with DAC and panobinostat mediated significantly greater loss of clonogenic survival than either agent alone ($p = 0.04$ and $p = 0.007$, respectively) (Fig. 6A). The combined treatment also induced more apoptosis of K562 cells (data not shown). Treatment with 17-DMAG alone dose dependently inhibited colony growth of K562 cells (Fig. 6B). Co-treatment with DAC and 17-DMAG also induced greater loss of clonogenic survival of K562 cells than treatment with either agent alone ($p = 0.04$) (Fig. 6C). Additionally, co-treatment with panobinostat and 17-DMAG significantly inhibited more colony growth of K562 cells than either agent alone ($p = 0.0001$) (Fig. 6D). We next determined the anti-leukemia activity of DAC and/or panobinostat and/or 17-DMAG against primary AML cells from 8 patients and primary CML-BC cells from 4 patients. Figure 7 demonstrates that treatment with clinically achievable concentrations of panobinostat >17-DMAG >DAC mediated significant loss of viability in all samples tested. Notably, co-treatment with DAC significantly enhanced panobinostat or 17-DMAG-mediated loss of viability in the primary AML and CML cells ($p = 0.008$ and $p = 0.0002$; $p = 0.04$ for panobinostat and DAC in CML). Co-treatment with DAC and panobinostat or 17-DMAG caused significantly lower loss of viability of normal bone marrow progenitor cells (Fig. 7).

Discussion

Findings presented here demonstrate for the first time that both DNMT1 and EZH2 are hsp90 client proteins, and that treatment with pan-HDAC inhibitor panobinostat and the hsp90 inhibitor 17-DMAG disrupt the chaperone association between hsp90 and DNMT1 and EZH2, promoting their misfolding and depletion by the proteasome. Parenthetically, panobinostat-induced activities of caspases were not involved in degrading DNMT1 and EZH2. Although hsp90 is predominantly cytosolic, DNMT1 and EZH2 should now be included in the growing list of nuclear client proteins of hsp90.[51] This highlights the involvement of molecular chaperones such as hsp90 not only in the DNA damage repair pathway but also in the epigenetic regulation of gene expression.[52] Specifically, by regulating DNMT1 and EZH2, and also histone deacetylases, panobinostat regulates dual epigenetic mechanisms of DNA methylation and chromatin modifications

through modulating hsp90 chaperone function.[43,44] Previous reports have implicated hsp90 chaperone function and its regulation by panobinostat in the binding and action of nuclear hormone receptors with their co-activators and co-repressor in modulating the expression of hormone responsive genes.[53] Collectively, these findings suggest that panobinostat treatment could influence multiple epigenetic mechanisms through its effects on HDAC and hsp90 functions.

Although the mechanism is not clear, panobinostat treatment also depleted the mRNA levels of DNMT1. This may further contribute toward panobinostat-mediated overall decline in the levels of DNMT1 in human leukemia cells. Despite the effect on DNMT1 levels, treatment with panobinostat had no effect on DNA methylation of JunB promoter. Panobinostat treatment also did not alter the mRNA levels of EZH2, but significantly depleted the protein levels of EZH2. We had previously reported that this was accompanied by disruption of the PRC2 complex and decline in the levels of SUZ12 and EED.[44] Consistent with this, treatment with panobinostat markedly reduced the recruitment of EZH2 and DNMT1 to the promoter of JunB, as well as modified the epigenetic marks on the promoter chromatin of JunB. Specifically, panobinostat reduced the trimethylated K27 and K9 marks on histone H3. This was associated with significant de-repression of JunB. Therefore, collectively, panobinostat treatment appears to mediate its epigenetic effects by modifying lysine acetylation and methylation on histone proteins and by inhibiting DNMT1 recruitment on gene promoters without modifying promoter gene methylation. These data are in agreement with a previous report in which panobinostat was shown to induce expression of epigenetically silenced ERα through alteration of a multi-protein complex at the ERα promoter rather than through demethylation of the ERα promoter.[41] In contrast, decitabine solely depletes DNMT1 and induces demethylation and de-repression of genes, e.g., JunB, ERα and E-cadherin. Hence, it is not surprising that the combination of DAC and panobinostat, by engaging separate and multiple epigenetic mechanisms, de-represses more JunB than treatment with either agent alone. Based on previous reports which had documented that JunB inactivation promotes leukemogenesis, accentuated derepression of JunB due to co-treatment with DAC and panobinostat could explain the loss of clonogenic survival and cell death of acute leukemia cells.[31,32]

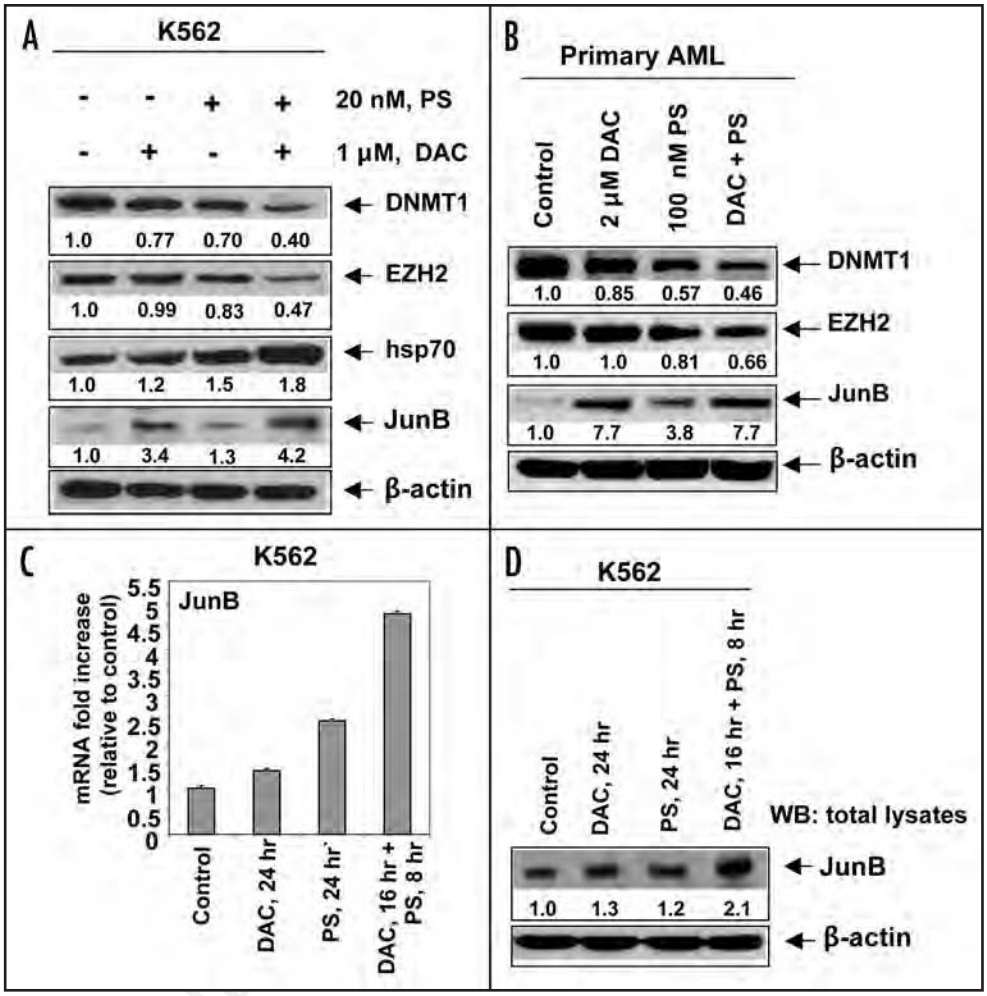

Figure 4. Co-treatment with decitabine and panobinostat enhances DNMT1 depletion and JunB induction. (A) K562 cells were treated with the indicated concentrations of DAC and panobinostat for 24 hours. Immunoblot analysis was performed for DNMT1, EZH2, hsp70 and JunB on the total cell lysates. The expression levels of β-actin in the cell lysates served as the loading control. (B) Primary acute leukemia cells were treated with the indicated concentrations of DAC and panobinostat for 24 hours. Immunoblot analysis was performed for DNMT1, EZH2 and JunB on the total cell lysates. The levels of β-actin in the cell lysates served as the loading control. (C) K562 cells were treated with 20 nmol/L of panobinostat and 1 μmol/L of decitabine in the manner indicated for 24 hours. Following this, total RNA were isolated and qPCR analysis was performed for exon 1 of JunB mRNA. Expression of JunB mRNA was normalized against GAPDH. Alternatively, western blot analysis was performed for JunB on the total cell lysates. The expression levels of β-actin in the lysates served as the loading control.

Previous reports have shown that methylated genes in cancer cells are often packaged in nucleosomes containing H3 with trimethylated K27, which results from the activity of the EZH2 containing PRC2 complex recruiting DNMTs to the gene promoters.[15] For example, PRC2 is required for the repression of E-cadherin by the Snail transcription factor.[54] PRC2 is known to silence Hox and other differentiation program genes, thereby promoting self renewal of embryonic stem (ES) cells or of the cancer stem cells.[3,43] Permanent silencing of tumor suppressors by acquisition of DNA

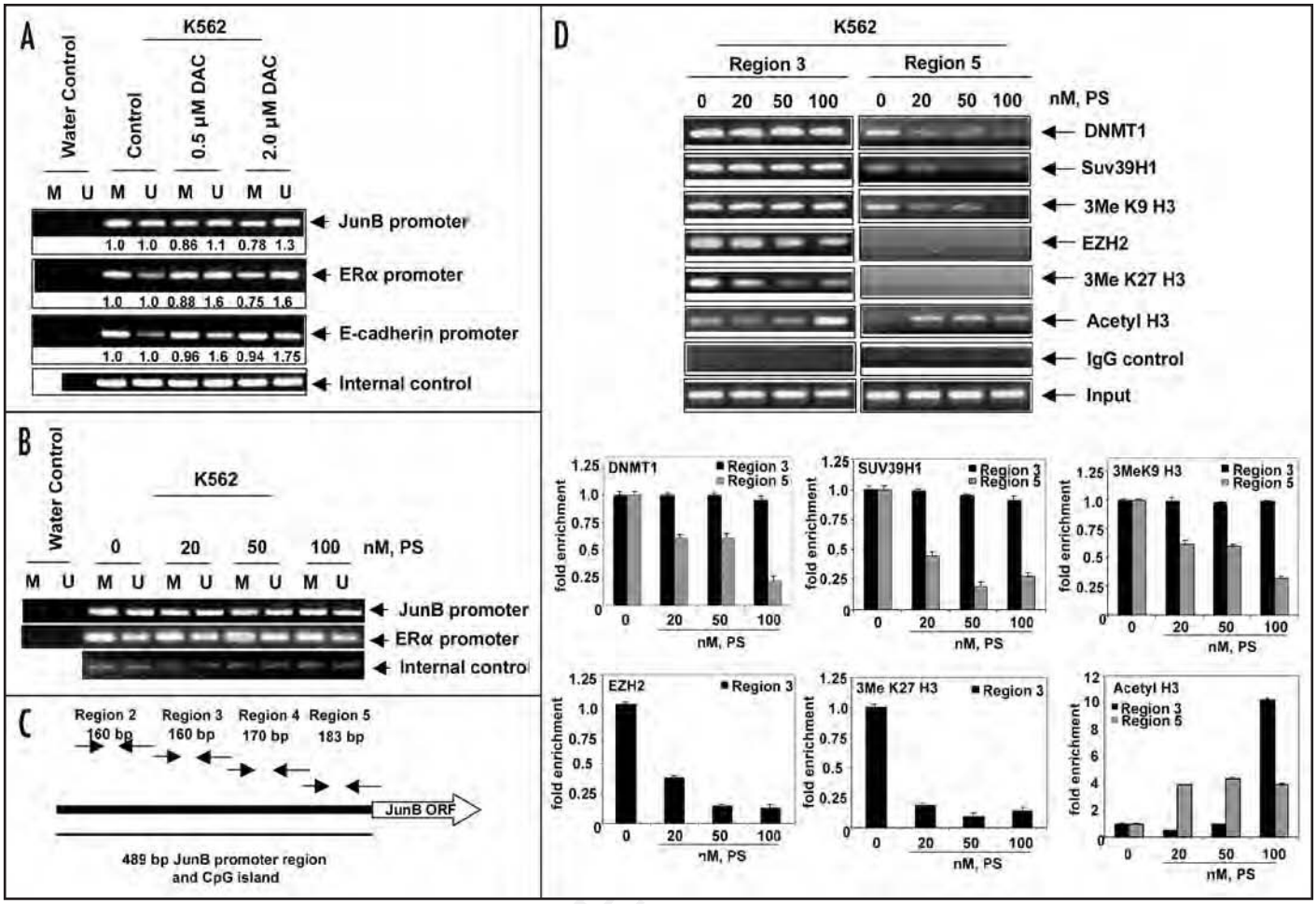

Figure 5. Decitabine and panobinostat alter the JunB promoter through different mechanisms. (A and B) K562 cells were treated with the indicated doses of DAC or panobinostat for 16 hours. Genomic DNA was isolated and bisulfite modified. PCR analysis was performed for the JunB, ERα and E-cadherin promoters using primer sets for methylated and unmethylated DNA. Internal control primers for the amplification of bisulfite modified DNA regardless of methylation status were used to ensure equal loading. (C) Schematic representation of the JunB promoter and CpG island with relative locations of primer sets used for ChIP PCR. (D) K562 cells were treated with the indicated concentrations of panobinostat for 16 hours. Chromatin immunoprecipitations were performed with antibodies to DNMT1, SUV39H1, EZH2, 3MeK27 Histone H3, 3MeK9 Histone H3 and Acetyl H3. Normal mouse IgG was used as a control. PCR products were obtained for region 3 and region 5 on the chromatin immunoprecipitates. Quantitative assessment of the chromatin immunoprecipitates was also determined by qPCR. The bar graphs represent fold enrichment of the chromatin in each region of the promoter relative to the input chromatin.

methylation through DNMTs could be a specific feature of leukemogenesis.[2,5] It appears that in cancer cells, the DNA methylome undergoes characteristic changes including genome wide loss of methylation and aberrant local gain of methylation, resulting in loss of TSG function.[19,21] However, in addition to silencing due to DNA methylation, PRC2 may also be involved in downregulation of INK4A-ARF locus.[7,55] Taken together, a picture of the epigenetic landscape in cancer is emerging that contains silenced genes that have a repressive trimethylated histone H3K27 mark and/or DNA methylation of TSGs.[28,29] This is consistent with the observations, that selective downregulation of EZH2 restored the expression of trimethylated H3K27 marked genes, without affecting promoter DNA methylation or de-repressing genes silenced by DNA hypermethylation.[28] The repressive trimethylated histone H3K27 along with trimethylated H3K4 mark represents the 'bivalent mark', which is a feature of the 'bivalent domains' in the silenced differentiation genes in ES and cancer stem cells.[2,5] Thus, panobinostat treatment could erase the bivalent mark and de-repress the silenced differentiation genes in cancer stem cells. By depleting EZH2 levels and disrupting the PRC2 complex, as well as attenuating the DNMT1 levels, panobinostat treatment could also subsequently disrupt the localization of the PRC1 complex containing BMI1 and RING1 which contribute to the epigenetic silencing of differentiation genes in ES and cancer stem cells.[3,5,56] Recently, activation of the ES cell transcriptional program by c-Myc has also been demonstrated to pathologic self-renewal characteristic in cancer stem cells.[57] Whether panobinostat treatment alone or in combination with DAC also affects this program, remains to be elucidated.

Our data demonstrating greater de-repression of JunB and superior antileukemia efficacy of the combination of DAC and panobinostat are in agreement with previous reports showing

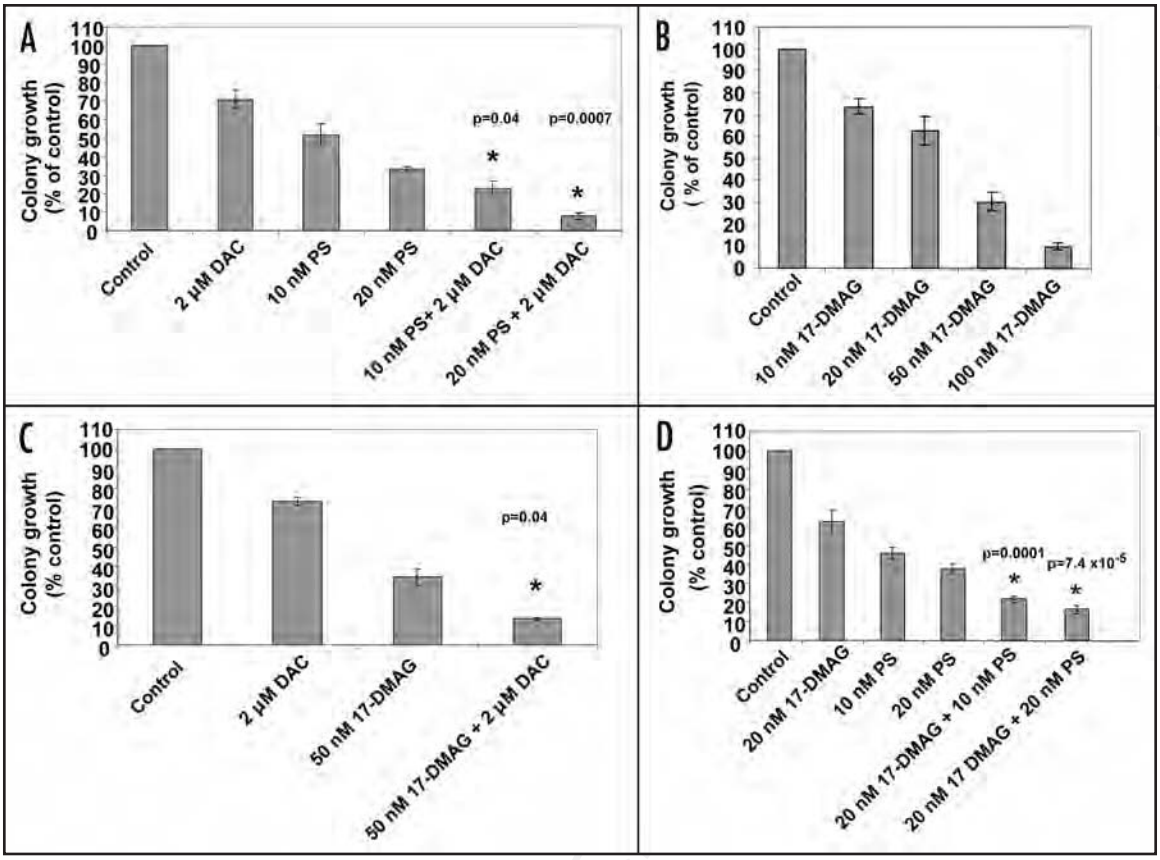

Figure 6. Co-treatment with decitabine and panobinostat, or 17-DMAG inhibits clonogenic survival greater than treatment with the single agents alone. (A) K562 cells were treated with the indicated doses of DAC and/or panobinostat for 48 hours. Following treatment the cells were washed and plated in methocult media for 7 days. (*) represents values significantly less than those following treatment with either agent alone at the indicated concentrations (p = 0.04 and p = 0.007, respectively). (B and C) K562 cells were treated with the indicated doses of DAC and/or 17-DMAG for 48 hours. The cells were washed and plated as before. (*) represents values significantly less than those following treatment with either agent alone at the indicated concentrations (p = 0.04). (D) K562 cells were treated with the indicated concentrations of panobinostat and/or 17-DMAG for 48 hours. Following treatment the cells were washed and plated in methocult media for 7 days.

robust re-expression of silenced genes when their promoters are de-methylated prior to HDAC inhibition.[37,38] Increased anti-leukemia activity has also been demonstrated following treatment with the combination of DNMT and HDAC inhibitors.[58] Recently, the combination of decitabine and valproic acid was reported to induce clinical responses in patients with advanced leukemia.[59] In our studies, although co-treatment with DAC and panobinostat mediated greater loss of survival than either agent alone, how much of this is mediated by more pronounced attenuation of EZH2 and de-repression of JunB is not clear and remains to be established. It is noteworthy that induction of JunB in patients has been used as a prognostic marker for predicting clinical response to imatinib treatment in CML, and patients with increased JunB expression following treatment have been shown as more likely to achieve a clinical response than those with lower junB expression.[60] Genetic or pharmacologic inhibition of EZH2 has also been shown to inhibit growth of transformed cells.[10,13,61] Additionally, co-treatment with the HDAC inhibitor trichostatin A with pharmacologic inhibition of EZH2 has been shown to result in massive apoptosis of transformed cells.[62] It should be noted that pan-HDAC inhibitors, such as panobinostat, induce apoptosis of acute leukemia cells through epigenetic and a variety of other mechanisms.[63-65] Therefore, epigenetic targeting and de-repression of silenced genes is likely to be mechanistically only partially responsible for the enhanced antileukemia efficacy of the combination of DAC and panobinostat. Nevertheless, because of the relevance of the activity of EZH2 and PRC2 for the survival and self-renewal of leukemia stem cells, the combined epigenetic therapy with DAC and panobinostat represents an attractive strategy for the treatment of acute leukemia, especially in the minimal residual disease state.

Materials and Methods

Reagents. Panobinostat (PS) and 17-DMAG were kindly provided by Novartis Pharmaceuticals Inc., (East Hanover, NJ) and Kosan Biosciences (Hayward, CA), respectively. Decitabine was acquired from Sigma-Aldrich (St. Louis, MO). Bortezomib was kindly provided by Millennium Pharmaceuticals (Cambridge, MA). Monoclonal anti-DNMT1 antibody was purchased from Abcam (Cambridge, MA). Anti-EZH2 monoclonal antibody was purchased from BD Transduction labs (San Jose, CA). Rat monoclonal anti-hsp90 and rabbit polyclonal anti-hsp70 were

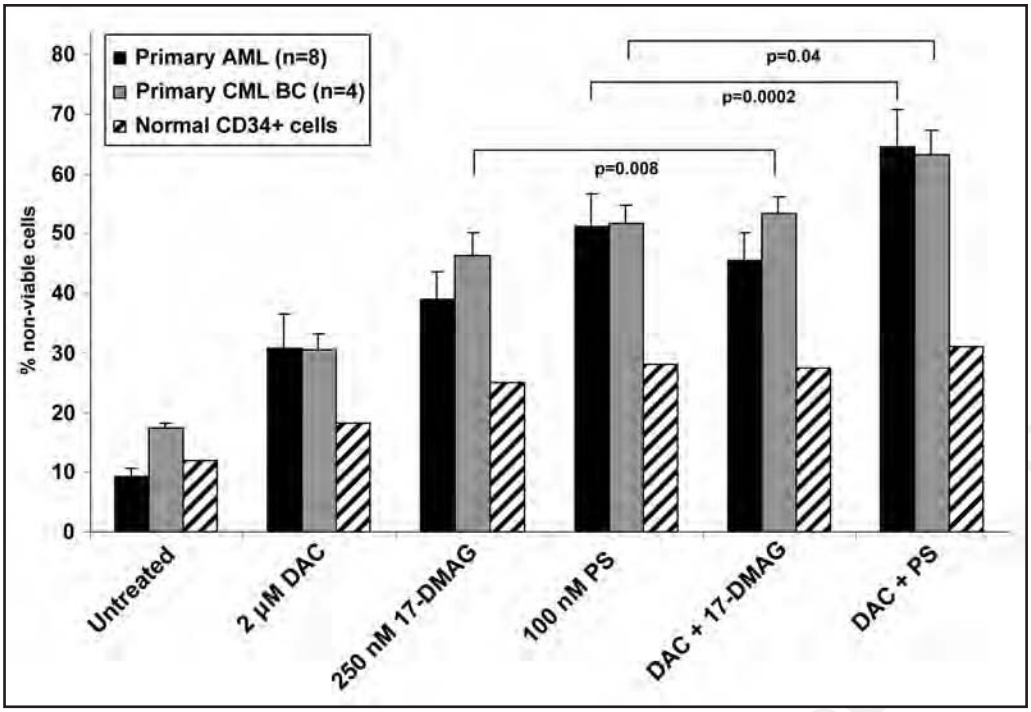

Figure 7. Co-treatment with panobinostat and decitabine exerts superior anti-leukemic activity against primary AML and CML cells than treatment with either agent alone. Peripheral blood or bone marrow from 8 AML, 4 CML-BC and 2 normal CD34+ patients were treated with the indicated doses of 17-DMAG or panobinostat and DAC for 48 hours. Then, the percentages of non-viable cells for each drug alone or drug combination were determined by trypan blue uptake in a hemocytometer. Values represent the percentage of non-viable cells from each condition as compared to the untreated cells.

purchased from Stressgen (Ann Arbor, MI). Anti-β-actin was purchased from Sigma Aldrich (St. Louis, MO). Monoclonal anti-JunB was purchased from Santa Cruz Biotechnologies (Santa Cruz, CA). Monoclonal anti-ubiquitin was purchased from Covance Biologicals (Berkeley, CA). Suv39H1, Trimethyl-lysine 9 H3 and acetyl H3 were acquired from Upstate biotechnologies (Charlottesville, VA). Normal mouse IgG and normal rat IgG were acquired from Santa Cruz (Santa Cruz, CA).

Cell culture. K562 and LAMA-84 cells were cultured in complete RPMI-1640 medium and incubated at 37°C with 5% CO_2 as previously described.[46] Growth media was changed every 2–3 days and cells were maintained at a density of 250,000 cells/mL. Exponentially growing cell cultures were used for all experiments described below.

Leukemia blast and normal CD34+ hemopoietic progenitor cells. Primary acute myeloid leukemia (AML) cells were obtained with informed consent as part of a clinical protocol approved by the Institutional Review Board of the Medical College of Georgia. As previously described, peripheral blood samples were collected in heparinized tubes, or were obtained from leukophoresis units, and mononuclear cells were separated using Lymphoprep (Axis-Shield, Oslo, Norway), washed once with complete RPMI-1640 media, resuspended in complete RPMI-1640 and counted to determine the number of cells isolated prior to their use in the various experiments.[47] The purity of the blast population was confirmed to be 80% or better by morphologic evaluation of cytospun cell preparations stained with Wright stain. Banked, de-linked, and de-identified donor peripheral blood CD34+ mononuclear cells procured for recipients who had since died were purified by immunomagnetic beads conjugated with anti-CD34 antibody prior to use in the cell viability assay (StemCell Technologies).[47]

Cell lysis and protein quantitation. Untreated or drug treated cells were centrifuged and the cell pellets were re-suspended in 200 μL of lysis buffer, then centrifuged and protein concentrations determined, as previously described.[46-48]

Immunoprecipitation of hsp90, DNMT-1 and EZH2 and immunoblot analysis. Following designated treatments, cells were lysed with the lysis buffer as described above. Five hundred micrograms of cell lysate was mixed gently with 5 μg of rat monoclonal anti-Hsp90 or 5 μg of mouse monoclonal anti-DNMT1 or 5 μg of mouse monoclonal EZH2 and incubated at 4°C for 1–2 hours on a rotator. Pre-washed protein-G beads were added to the lysate-antibody mixture and incubated overnight at 4°C on a rotator. The immunoprecipitates were washed 4 times with lysis buffer and eluted from the agarose beads by boiling with 6X SDS sample buffer before SDS-PAGE and western blot analysis, as previously described.[42]

Preparation of detergent soluble and insoluble lysates. Following drug treatment with bortezomib (BZ) and panobinostat, cells were separated into detergent soluble and insoluble fractions as previously described.[42] Briefly, cells were lysed with TNSEV buffer (50 mmol/L Tris-HCl, pH 7.5, 2 mM EDTA, 100 mmol/L NaCl, 1 mmol/L sodium orthovanadate, 1% Nonidet P-40 containing 20 μg/ml aprotinin, 20 μg/ml leupeptin, 1 mmol/L PMSF, 25 mmol/L NaF and 5 mmol/L *N*-ethylmaleimide). The insoluble fractions (pellet) were solubilized with SDS buffer (80 mmol/L Tris, pH 6.8, 2% SDS, 100 mmol/L dithiothreitol and 10% glycerol). Fifty μg of proteins from the Nonidet P-40-soluble and insoluble fractions were separated on 7.5% SDS-polyacrylamide gel and analyzed by western blotting.

SDS-PAGE and western blotting. One hundred micrograms of total cell lysate was used for SDS-PAGE. Western blot analyses of EZH2, DNMT1, hsp70, hsp90, ubiquitin and JunB were performed on total cell lysates or immunoprecipitates using specific antisera or monoclonal antibodies, as previously described.[46-48] The expression level of β-actin or α-tubulin was used as the loading control for the western blots.

RNA isolation and RT-PCR. RNA was extracted from the cultured cells using the Trizol method (Invitrogen, Carlsbad, CA) as previously described.[44,48] Purified RNA was quantified and reverse-transcribed using Superscript II according to the manufacturer's protocol (Invitrogen, Carlsbad, CA). Resulting cDNAs were used in subsequent PCR reactions for JunB (sequences available upon request). PCR reactions for β-actin were used as an internal loading control. PCR reactions were carried out in a gradient Mastercycler (Eppendorf, Westbury, NY) and consisted of a 3-minute denaturation at 95°C followed by 35 cycles of 95°C (30 sec), 52°C (30 sec) and 72°C (30 sec) with a final extension at 72°C (10 min). Amplified products were resolved on a 2% agarose gel and recorded with a UV transilluminator. Horizontal scanning densitometry was performed with ImageQuant 5.2 and the band intensity of each PCR product was compared to that of β-actin. For quantitative assessment of DNMT1 and JunB, qPCR was performed with TaqMan probes against the exon 38–39 boundary for DNMT1 and the exon 1 boundary for JunB. Expression levels were normalized to a TaqMan probe against GAPDH.

Colony culture assay. Following the designated treatments, cells were harvested and washed twice with 1X PBS and approximately 300 cells were plated in complete Methocult (StemCell Technologies, Vancouver, British Columbia) and cultured for 7–10 days at 37°C in a 5% CO_2 environment. Colony growth was measured as a percentage of the control cell colony growth, as previously described.[44]

Bisulfite modification and methylation specific PCR. Following treatment with either decitabine or panobinostat, the genomic DNA was isolated from K562 cells using a DNeasy kit (Qiagen, Valencia, CA). One microgram of genomic DNA was subjected to bisulfite modification with a kit from Chemicon (Temecula, CA) according to the manufacturer's protocol. DNA was eluted in 25 μL of TE Buffer. Methylation-specific PCR reactions were set up using a Hotmaster mix (Eppendorf, Westbury, NY). Primers were designed according to within a CpG island of the JunB promoter and consisted of the following sequences, JunBMF 5'-GAT AGG GTT TTT GCG TAT AGT TGT C-3', JunB MR 5'-TAT TCC ATT TTA ATA CAC ATC CGA A-3' and JunBUF 5'-TAG GGT TTT TGT GTA TAG TTG TTG G-3', JunBUR 5'-CTA TTC CAT TTT AAT ACA CAT CCA AA-3'.[49] Primers were also designed against the E-cadherin and ER alpha promoters and consisted of sequence EcadMF 5'-TAA TTT TAG GTT AGA GGG TTA TCG C-3', EcadMR 5'-CTC ACA AAT ACT TTA CAA TTC CGA C-3', EcadUF 5'-ATT TTA GGT TAG AGG GTT ATT GTG T-3', EcadUR 5'-CAA ACT CAC AAA TAC TTT ACA ATT CCA-3', ERαMF 5'-TAA ATA GAG ATA TAT CGG AGT TTG GTA CG-3', ERαMR 5'-AAC TTA AAA TAA ACG CGA AAA ACG A-3', ERαUF 5'-TAA ATA GAG ATA TAT TGG AGT TTG GTA TGG-3' and ERαUR 5'-AAC TTA AAA TAA ACA CAA AAA ACA AA-3'. Internal loading control primers were designed to recognize the JunB promoter regardless of methylation status. These primers consisted of sequence JunBBSFor 5'-GAG TTA GTA GGG AGT TGG GAG TTG-3' and JunBBSRev 5'-AAC TAT TCC ATT TTA ATA CAC ATC C-3'. PCR reactions were carried out in an Eppendorf Gradient Mastercycler (Westbury, NY) and consisted of a 95°C hold followed by a 2-minute denaturation at 95°C and 30 cycles of 95°C (30 sec), 55°C (30 sec) and 72°C (30 sec) with a final extension at 72°C (10 min). PCR products were resolved on a 2% agarose gel and visualized with a UV-transilluminator. Horizontal scanning densitometry was performed with ImageQuant 5.2 and the band intensity of each PCR product was compared to that of the internal loading control.

Chromatin immunoprecipitation and PCR. K562 cells were treated with panobinostat for 16 hours. Following drug exposure, the chromatin in the cells was crosslinked with formaldehyde for 10 minutes at 37°C. The crosslinking reaction was quenched with 1/20 volume of 2.5 M glycine for 5 minutes at room temperature, then the cells were washed twice for 5 minutes in ice-cold 1X PBS. Cell lysis, sonication and chromatin immunoprecipitation was performed according to the manufacturer's protocol (Upstate Biotechnologies, Charlottesville, VA), and as previously described.[48] Primers for the amplification of the JunB promoter were synthesized by IDT (Coralville, IA). Sequences are available upon request. For quantitative assessment of JunB in the chromatin immunoprecipitates, a SYBR Green mastermix from Applied Biosystems was used (Foster City, CA). Relative enrichment was normalized against GAPDH in the input samples.

Statistical analysis. Significant differences between values obtained in a population of leukemia cells treated with different experimental conditions were determined using the Student's t-test.

Acknowledgements

Co-author P.A. is an employee of Novartis Institute for Biomedical Research Inc., and the corresponding author, K.N.B., has received clinical and laboratory research support from Novartis Institute for Biomedical Research Inc.

W.F., K.B., R.R., A.M., Y.Y., R.J., Y.W., and performed the in vitro biochemical and molecular studies with the cultured leukemia cells. R.B., J.C., S.K., A.J. and S.U. performed the in vitro biologic studies with primary leukemia and normal $CD34^+$ normal bone marrow progenitor cells. P.A. provided reagents for the study. K.N.B. planned and supervised the in vitro and in vivo studies and prepared the report.

Note

Supplementary materials can be found at:
www.landesbioscience.com/supplement/FiskusCBT8-10-Sup.pdf

References

1. Schuettengruber B, Chourrout D, Vervoort M, Leblanc B, Cavalli G. Genome regulation by polycomb and trithorax proteins. Cell 2007; 128:735-45.
2. Bernstein B, Meissner A, Lander E. The Mammalian Epigenome. Cell 2007; 128:669-81.
3. Sparmann A, van Lohuizen M. Polycomb silencers control cell fate, development and cancer. Nature Rev Cancer 2006; 6:846-56.
4. Cao R, Zhang Y. The functions of E(Z)/EZH2-mediated methylation of lysine 27 in histone H3. Curr Opin Genet Dev 2004; 14:155-64.
5. Simon JA, Lange CA. Roles of the EZH2 histone methyltransferase in cancer epigenetics. Mutat Res 2008.
6. Kamminga LM, Bystrykh LV, de Boer A, Houwer S, Douma J, Weersing E, et al. The Polycomb group gene Ezh2 prevents hematopoietic stem cell exhaustion. Blood 2006; 107:2170-9.
7. Bracken AP, Pasini D, Capra M, Prosperini E, Colli E, Helin K. EZH2 is downstream of the pRB-E2F pathway, essential for proliferation and amplified in cancer. EMBO J 2003; 22:5323-35.

8. Otte AP, Kwaks TH. Gene repression by Polycomb group protein complexes: a distinct complex for every occasion?. Curr Opin Genet Dev 2003; 13:448-54.
9. van der Vlag J, Otte AP. Transcriptional repression mediated by the human polycomb-group protein EED involves histone deacetylation. Nat Genet 1999; 23:474-8.
10. Varambally S, Dhanasekaran SM, Zhou M, Barrette TR, Kumar-Sinha C, Sanda MG, et al. The polycomb group protein EZH2 is involved in progression of prostate cancer. Nature 2002; 419:624-9.
11. Kleer CG, Cao Q, Varambally S, Shen R, Ota I, Tomlins SA, et al. EZH2 is a marker of aggressive breast cancer and promotes neoplastic transformation of breast epithelial cells. Proc Natl Acad Sci USA 2003; 100:11606-11.
12. Bachmann IM, Halvorsen OJ, Collett K, Stefansson IM, Straume O, Haukaas SA, et al. EZH2 expression is associated with high proliferation rate and aggressive tumor subgroups in cutaneous melanoma and cancers of the endometrium, prostate and breast. J Clin Oncol 2006; 24:268-73.
13. Tan J, Yang X, Zhuang L, Jiang X, Chen W, Lee PL, et al. Pharmacologic disruption of Polycomb-repressive complex 2-mediated gene repression selectively induces apoptosis in cancer cells. Genes Dev 2007; 21:1050-63.
14. Viré E, Brenner C, Deplus R, Blanchon L, Fraga M, Didelot C, et al. The Polycomb group protein EZH2 directly controls DNA methylation. Nature 2006; 439:871-4.
15. Schlesinger Y, Straussman R, Keshet I, Farkash S, Hecht M, Zimmerman J, et al. Polycomb-mediated methylation on Lys27 of histone H3 pre-marks genes for de novo methylation in cancer. Nat Genet 2007; 39:232-6.
16. Ting AH, Jair K, Suzuki H, Yen R-W C, Baylin SB, Schuebel KE. Mammalian DNA methyltransferase 1: inspiration for new directions. Cell Cycle 2004; 3:1024-6.
17. Jeltsch A. On the enzymatic properties of Dnmt1: specificity, processivity, mechanism of linear diffusion and allosteric regulation of the enzyme. Epigenetics 2006; 1:63-6.
18. Svedruzic ZM. Mammalian cytosine DNA methyltransferase Dnmt1: enzymatic mechanism, novel mechanism-based inhibitors, and RNA-directed DNA methylation. Curr Med Chem 2008; 15:92-106.
19. Teodoridis JM, Hardie C, Brown R. CpG island methylator phenotype (CIMP) in cancer: causes and implications. Cancer Lett 2008; 268:177-86.
20. Robertson K. DNA methylation and chromatin—unraveling the tangled web. Oncogene 2002; 21:5361-79.
21. Jones PA, Baylin SB. The epigenomics of cancer. Cell 2007; 128:683-92.
22. Fuks F, Burgers WA, Brehm A, Hughes-Davies L, Kouzarides T. DNA methyltransferase Dnmt1 assoicates with histone deacetylase activity. Nat Genetics 2000; 24:88-91.
23. Rountree MR, Bachman KE, Baylin SB. DNMT1 binds HDAC2 and a new co-reporessor, DMAP1, to form a complex at replication foci. Nat Genetics 2000; 25:269-77.
24. Mizuno S, Chijiwa T, Okamura T, Akashi K, Fukumaki Y, Niho Y, Sasaki H. Expression of DNA methyltransferases *DNMT-1, 3A* and *3B* in normal hematopoiesis and in acute and chronic myelogenous leukemia. Blood 2001; 97:1172-9.
25. Melnick AM, Adelson K, Licht JD. The theoretical basis of transcriptional therapy of cancer: Can it be put into practice? J Clin Oncol 2005; 23:3957-70.
26. Unterberger A, Andrews SD, Weaver ICG, Szyf M. DNA methyltransferase 1 knockdown activates a replication stress checkpoint. Mol Cell Biol 2006; 26:7575-86.
27. Milutinovic S, Zhuang Q, Niveleau A, Szyf M. Epigenomic stress response. Knockdown of DNA methyltransferase 1 triggers an intra-S-phase arrest of DNA replication and induction of stress response genes. J Biol Chem 2003; 278:14985-95.
28. Kondo Y, Shen L, Cheng AS, Ahmed S, Boumber Y, Charo C, et al. Gene silencing in cancer by histone H3 lysine 27 trimethylation independent of promoter DNA methylation. Nat Genet 2008; 40:741-50.
29. McGarvey KM, Greene E, Fahrner JA, Jenuwein T, Baylin SB. DNA methylation and complete transcriptional silencing of cancer genes persist after depletion of EZH2. Cancer Res 2007; 67:5097-102.
30. Melki JR, Vincent PC, Clark SJ. Concurrent DNA hypermethylation of multiple genes in acute myeloid leukemia. Cancer Res 1999; 59:3730-40.
31. Yang MY, Liu TC, Chang JG, Lin PM, Lin SF. *JunB* gene expression is inactivated by methylation in chronic myeloid leukemia. Blood 2003; 101:3205-11.
32. Passegué E, Wagner EF, Weissman IL. JunB deficiency leads to a myeloproliferative disorder arising from hematopoietic stem cells. Cell 2004; 119:431-43.
33. Furukawa Y, Sutheesophon K, Wada T, Nishimura M, Saito Y, Ishii H, et al. Methylation silencing of the Apaf-1 gene in acute leukemia. Mol Cancer Res 2005; 3:325-34.
34. Shimamoto T, Ohyashiki JH, Ohyashiki K. Methylation of $p15^{INK4b}$ and E-cadherin genes is independently correlated with poor prognosis in acute myeloid leukemia. Leukemia Res 2005; 29:653-9.
35. Mariani O, Brennetot C, Coindre JM, Gruel N, Ganem C, Delattre O, et al. JUN oncogene amplification and overexpression block adipocytic differentiation in highly aggressive sarcomas. Cancer Cell 2007; 11:361-74.
36. Issa JP. Decitabine. Curr Opin Oncol 2003; 15:446-51.
37. Issa JP, Gharibyan V, Cortes J, Jelinek J, Morris G, Verstovsek S, et al. Phase II Study of Low-Dose Decitabine in Patients With Chronic Myelogenous Leukemia Resistant to Imatinib Mesylate. J Clin Oncol 2005; 23:3948-56.
38. Cameron EE, Bachman KE, Myöhänen S, Herman JG, Baylin SB. Synergy of demethylation and histone deacetylase inhibition in the re-expression of genes silenced in cancer. Nature Gen.1999; 21:103-7.
39. Belinsky SA, Klinge DM, Stidley CA, Issa JP, Herman JG, March TH, et al. Inhibition of DNA methylation and histone deacetylation prevents murine lung cancer. Cancer Res 2003; 63:7089-93.
40. Januchowski R, Dabrowski M, Ofori H, Jagodzinski PP. Trichostatin A downregulate DNA methyltransferase 1 in Jurkat T cells. Cancer Lett 2007; 246:313-7.
41. Zhou Q, Atadja P, Davidson NE. Histone deacetylase inhibitor LBH589 reactivates silenced estrogen receptor alpha (ER) expression without loss of DNA hypermethylation. Cancer Biol Ther 2007; 6:64-9.
42. Bali P, Pranpat M, Bradner J, Balasis M, Fiskus W, Guo F, et al. Inhibition of histone deacetylase 6 acetylates and disrupts the chaperone function of heat shock protein 90: a novel basis for antileukemia activity of histone deacetylase inhibitors. J Biol Chem 2005; 280:26729-34.
43. Yang Y, Rao R, Shen J, Tang Y, Fiskus W, Nechtman J, et al. Role of acetylation and extracellular location of heat shock protein 90alpha in tumor cell invasion. Cancer Res 2008; 68:4833-42.
44. Fiskus W, Pranpat M, Balasis M, Bali P, Estrella V, Kumaraswamy S, et al. Histone deacetylase inhibitors deplete EZH2 and associated Polycomb Repressive Complex 2 proteins with attenuation of HOXA9 and MEIS1 and loss of survival of human acute leukemia cells. Mol Cancer Ther 2006; 5:3096-104.
45. Drysdale MJ, Brough PA, Massey A, Jensen MR, Schoepfer J. Targeting Hsp90 for the treatment of cancer. Curr Opin Drug Discov Devel 2006; 9:483-95.
46. Nimmanapalli R, O'Bryan E, Huang M, Bali P, Burnette PK, Loughran T, et al. Molecular characterization and sensitivity of STI-571 (Imatinib Mesylate, Gleevec)-resistant, Bcr-Abl positive, human acute leukemia cells retain sensitivity to SRC kinase inhibitor PD180970 and 17-allylamino-17-demethoxygeldanomycin (17AAG). Cancer Res 2002; 62:5761-9.
47. Fiskus W, Wang Y, Joshi R, Rao R, Yang Y, Chen J, et al. Cotreatment with vorinostat enhances activity of MK-0457 (VX-680) against acute and chronic myelogenous leukemia cells. Clin Cancer Res 2008; 14:6106-15.
48. Guo F, Sigua C, Tao J, Bali P, George P, Li Y, et al. Cotreatment with histone deacetylase inhibitor LAQ824 enhances Apo-2L/tumor necrosis factor-related apoptosis inducing ligand-induced death inducing signaling complex activity and apoptosis of human acute leukemia cells. Cancer Res 2004; 64:2580-9.
49. Herman JG, Graff JR, Myöhänen S, Nelkin BD, Baylin SB. Methylation-specific PCR: A novel PCR assay for methylation status of CpG islands. Proc Natl Acad Sci USA 1996; 93:9821-6.
50. Guo F, Rocha K, Bali P, Pranpat M, Fiskus W, Boyapalle S, et al. Abrogation of heat shock protein 70 induction as a strategy to increase antileukemia activity of heat shock protein 90 inhibitor 17-allylamino-demethoxy geldanamycin. Cancer Res 2005; 65:10536-44.
51. Dezwaan DC, Freeman BC. HSP90: the Rosetta stone for cellular potein dynamics?. Cell Cycle 2008; 7:1006-12.
52. Camphausen K, Tofilon PJ. Inhibition of Hsp90: a multitarget approach to radiosensitization. Clin Cancer Res 2007; 13:4326-30.
53. Fiskus W, Ren Y, Mohapatra A, Bali P, Mandawat A, Rao R, et al. Hydroxamic acid analogue histone deacetylase inhibitors attenuate estrogen receptor alpha levels and transcriptional activity: a result of hyperacetylation and inhibition of chaperone function of heat shock protein 90. Clin Cancer Res 2007; 13:4882-90.
54. Herranz N, Pasini D, Díaz VM, Francí C, Gutierrez A, Dave N, et al. Polycomb complex 2 is required for E-cadherin repression by the Snail1 transcription factor. Mol Cell Biol 2008; 28:4772-81.
55. Kotake Y, Cao R, Viatour P, Sage J, Zhang Y, Xiong Y. pRB family proteins are required for H3K27 trimethylation and polycomb repression complexes binding to and silencing $p16^{INK4a}$ tumor suppressor gene. Genes Dev 2007; 21:49-54.
56. Schwartz YB, Pirrotta V. Polycomb silencing mechanisms and the management of genomic programmes. Nat Rev Genet 2007; 8:9-22.
57. Wong DJ, Liu H, Ridky TW, Cassarino D, Segal E, Chang HY. Module map of stem cell genes guides creation of epithelial cancer stem cells. Cell Stem Cell 2008; 2:333-44.
58. Gore SD, Baylin S, Sugar E, Carraway H, Miller CB, Carducci M, et al. Combined DNA methyltransferase and histone deacetylase inhibition in the treatment of myeloid neoplasms. Cancer Res 2006; 66:6361-9.
59. Garcia-Manero G, Kantarjian HM, Sanchez-Gonzalez B, Yang H, Rosner G, Verstovsek S, et al. Phase 1/2 study of the combination of 5-aza-2'-deoxycytidine with valproic acid in patients with leukemia. Blood 2006; 108:3271-9.
60. Liu YC, Hsiao HH, Chang JG, et al. Usefulness of quantitative assessment of JunB gene expression as a marker for monitoring chronic myeloid leukemia patients undergoing imatinib therapy. Int J Hematol 2006; 84:425-31.
61. Chen Y, Lin MC, Yao H, Wang H, Zhang AQ, Yu J, et al. Lentivirus-mediated RNA interference targeting enhancer of zeste homolog 2 inhibits hepatocellular carcinoma growth through downregulation of stathmin. Hepatology 2007; 46:200-8.
62. Jiang X, Tan J, Li J, Kivimäe S, Yang X, Zhuang L, et al. DACT3 is an epigenetic regulator of Wnt/beta-catenin signaling in colorectal cancer and is a therapeutic target of histone modifications. Cancer Cell 2008; 13:529-41.

63. George P, Bali P, Annavarapu S, Scuto A, Fiskus W, Guo F, et al. Combination of the histone deacetylase inhibitor LBH589 and the hsp90 inhibitor 17-AAG is highly active against human CML-BC cells and AML cells with activating mutation of FLT-3. Blood 2005; 105:1768-76.
64. Fiskus W, Pranpat M, Bali P, Balasis M, Kumaraswamy S, Boyapalle S, et al. Combined effects of novel tyrosine kinase inhibitor AMN107 and histone deacetylase inhibitor LBH589 against Bcr-Abl expressing human leukemia cells. Blood 2006; 108:645-52.
65. Dokmanovic M, Clarke C, Marks PA. Histone deacetylase inhibitors: overview and perspectives. Mol Cancer Res 2007; 5:981-9.